UNIVERSITY OF SOUTHAMPTON

Tight junction biogenesis in the mouse preimplantation embryo

by

Fay Christina Thomas

A thesis submitted for the degree of PhD

School of Biological Sciences

Division of Cell Sciences

Supervisor: Prof T.P.Fleming

September 2002

UNIVERSITY OF SOUTHAMPTON

ABSTRACT

FACULTY OF SCIENCE

BIOLOGICAL SCIENCES

Doctor of Philosophy

TIGHT JUNCTION BIOGENESIS IN THE MOUSE PREIMPLANTATION EMBRYO

By

Fay Christina Thomas

The mouse preimplantation embryo is a valuable model for investigating de novo formation of an epithelium. During early development, the trophectoderm differentiates and forms the wall of the blastocyst from the 32-cell stage. The tight junction (TJ) becomes fully functional at this time, resulting in blastocoel formation. Occludin, claudins and junctional adhesion molecule 1 (JAM-1) are TJ transmembrane proteins. It has previously been shown that occludin is expressed at the mRNA and protein levels throughout cleavage and, following post-translational modification in the morula stage, assembles at the TJ site during the early 32-cell stage, facilitated by cytoplasmic association with the newly expressed TJ plaque protein, ZO-α^+.

Here, I have analysed the expression profile of claudin-1, claudin-3 and JAM-1 by RT-PCR, immunoblotting and immunoconfocal microscopy. Claudin-3 and JAM-1 mRNA was detected from the 2-cell stage onwards. However, claudin-1 mRNA did not appear to be expressed in the mouse preimplantation embryo. Claudin-3 protein is first evident during cleavage at perinuclear Golgi-like sites in 16-cell embryos, followed shortly by membrane assembly at the TJ at the 32-cell stage. In contrast, JAM-1 is detectable from the early 8-cell stage, earlier than any other TJ protein studied in our model. JAM-1 membrane assembly precedes E-cadherin adhesion at compaction. During compaction, JAM-1 localises predominantly to the apical microvillous pole before accumulating at cell-contact sites during later cleavage. Use of a JAM-1 neutralising antibody (BV11) in mouse embryo culture medium indicated that this protein could play an important role in blastocyst formation.

This study provides further evidence that TJ biogenesis is a multi-step process in the early embryo, driven by a temporally regulated expression programme, which regulates blastocyst formation. Moreover, these data indicate that JAM-1 may have a unique role in the early stages of epithelial polarity.

List of contents

List of Figures

List of Tables

Acknowledgements

I would like to thank my Supervisor Prof Tom Fleming for his advice and support during my undergraduate and postgraduate studies. Not only has he been a helpful mentor but also a valued friend. I would also like to thank the whole lab for their help and encouragement, especially Bhav, Judith and Lydia who have not only kept me entertained and full of dim sum, tea and chocolate but also given up a lot of their time to help me with my experiments. I would also like to show my appreciation to Dr. Arthur Wild whose poems, jokes and laughter will be missed greatly. I wish him all the best in his retirement. Thanks also to Dr. Tom Papenbrock for his time and patience when demonstrating the joys of web-based sequence analysis.

A special thanks to all my friends, especially Faye and Sarah who have been a tremendous source of support over the years that I have known them. I am also very grateful to Richard who saved my skin with the loan of his printer. I feel I owe you a few more pints! Thanks also to Liz, who has kept me sane with salsa, swimming and girlie nights. Thanks also to all members of my home group, especially Karen, Jo, Sue and Keith, whose love and prayers have kept me going. A huge thanks to Robert, who has not only helped with the statistics in this thesis, but also supplied me with copious amounts of anchovies, apple juice, "nearly perfect" risotto and generally made me a very happy girl.

The biggest thanks are for my family, whose love and support has been limitless. I am eternally grateful!

List of Abbreviations

2C	– 2-cell embryo
4C	– 4-cell embryo
8C	– 8-cell embryo
AJ	– Adherens Junction
AJC	– Apicolateral Junction Complex
AQP	– Aquaporin
C8	– Compact 8-cell embryo
ConA	– Concanavalin A
CPE (-R)	– Clostridium Perfringens Enterotoxin (Receptor)
DHR	– Discs-large homology region
dsRNA	– double stranded RNA
EB	– Early Blastocyst
Ebs	– Embryoid bodies
EC	- ExtraCellular
ECL	– Enhanced Chemiluminescence
EM	– Early Morula
FE	– Fertilised eggs
hCG	– Human Chorionic Gonadotrophin
HRP	– Horse Radish Peroxidasse
ICM	– Inner Cell Mass
IgSF	– Immunoglobulin Super Family
JAM	– Junctional adhesion molecule
JEAP	– Junction- Enriched and associated protein
LB	– Late blastocyst
LM	– Late Morula
MAGI	– Membrane Associated Guanylate kinase with an Inverted arrangement of protein-protein interaction domains
MAGuK	– Membrane-Associated guanylate kinase
MDCK	– Madain-Darby Canine Kidney
MUPP1	– Multi-PDZ domain Protein 1

NLS	– Nuclear localisation sequence
PBS	– Phosphate Buffered Saline
PDZ	– Post-synaptic density/Discs-large/ZO-1
PLL	– Poly-L-Lysine
PMS	– Pregnant Mares Serum
r.t	– room temperature
RNA*i*	– RNA interferrance
RT	– Reverse Transcriptase
RVP1	– Regressing Ventral Prostate
SH3	– *src* Homology 3
siRNA	– short interfering RNA
ssRNA	– single stranded RNA
TC	– Tissue control
TE	– Trophectoderm
TEM	– TransEndothelial Migration
TER	– Transepithelial Electrical Resistance
TJ	– Tight Junction
TMVCF	– TransMembrane protein deleted in Velo-Cardio Facial/DiGeorge syndrome
UF	– UnFertilised eggs
ZA	– *Zonula Adherens*
ZGA	– Zygotic Genome Activation
ZO	– *Zonula Occludins*
ZONAB	– ZO-1 associated nuclei acid-binding protein

Chapter 1

Introduction

1.1 Epithelia

Epithelial cells are vital to the functioning and survival of multicellular organisms as they line all the cavities and free surfaces of the body, providing both a barrier between different biological compartments and a means to regulate the vectorial transport of ions and solutes between these compartments. Cell polarity is an important feature in the function of this tissue type and is reliant upon specialised adhesion contacts, such as the zonula adherens (ZA) and tight junction (TJ), between neighbouring cells of an epithelium (Diamond, 1977, Volk & Geiger, 1984; Figure 1.1). All of these junctional contacts comprise one or more transmembrane protein that is linked to the cell cytoskeleton via a complex of cytoplasmic proteins.

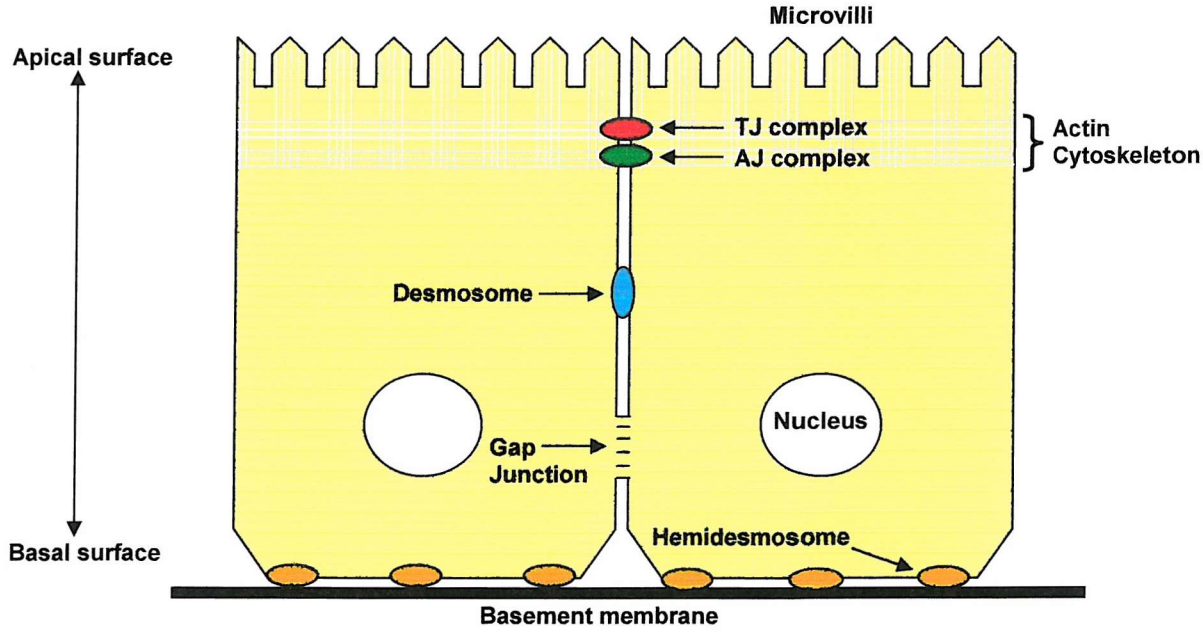

Figure 1.1 Organisation of the cell junctions in a typical epithelial cell layer (adapted from Alberts *et al.*, 1994).

1.2 The zonula adherens junction

Before a fully polarised phenotype is established, cadherin-containing adhesion contacts are associated uniformly along the lateral plasma membrane at the adherens junction (AJ). In polarised epithelial cells this uniform expression becomes apically localised forming a continuous adhesion belt, now called the ZA, around the apex of each epithelial cell. Holding the neighbouring cells together is a calcium-dependent transmembrane protein, called E-cadherin that is linked to the cell cytoskeleton via a complex of cytoplasmic proteins, called the catenins (Figure 1.2).

1.2.1 E-cadherin

E-cadherin (otherwise known as uvomorulin/L-CAM) is the transmembrane glycoprotein component of the ZA. As with the other members of the cadherin protein family (P-, N- and VE-cadherin), E-cadherin has:

i. a cytoplasmically located carboxyl-terminus that binds to cytoplasmic ZA proteins, e.g. β-catenin and γ-catenin (plakoglobin), which in turn, is linked to the actin cytoskeleton through another cytoplasmic protein, α-catenin, binding to β-catenin (Ozawa *et al.*, 1989; Nagafuchi & Takeichi, 1988).

ii. a single transmembrane domain (Takeichi *et al.*, 1988).

iii. an extracellular (EC) amino-terminus comprising a HAV motif, five cadherin repeats and four Ca^{2+} -binding sequences (Blaschuk *et al.*, 1990).

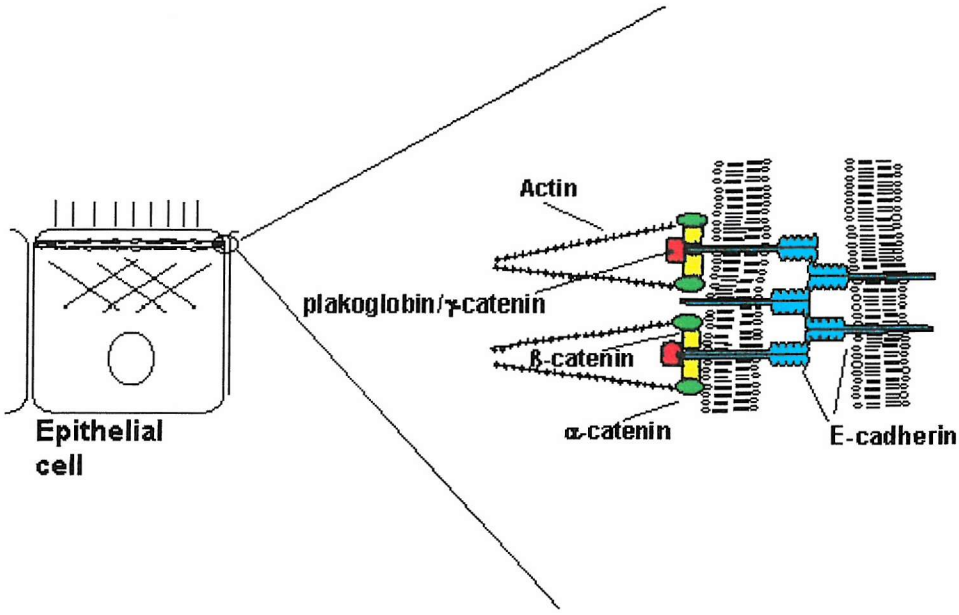

Figure 1.2 The zonula adherens junction (adapted from Collins & Fleming, 1995). Diagramatic representation of the main cytoplasmic ZA proteins and how they link the transmembrane protein, E-cadherin, with the actin cytoskeleton.

The majority of cadherin superfamily members belong to the type I classical cadherins. The EC segment of type I cadherins comprises variable numbers of cadherin repeat domains, each being approximately 110 amino acids in length (reviewed by Aberle, 1996). Each classical cadherin subtype has a unique (usually homophilic) binding specificity that provides distinct adhesive properties within specific cell types (Takeichi, 1990). Due to the preferential homophilic binding of the classical cadherins, cells expressing the same subtype of cadherin will aggregate together, whereas cells expressing different cadherins segregate into specific adhesive clumps (Steinberg & Takeichi, 1994). In addition, cells expressing the same cadherin subtype but in different amounts will also preferentially segregate (Steinberg & Takeichi, 1994). It is these binding properties that may therefore, regulate tissue segregation and differentiation during development (reviewed by Ranscht, 1994).

In the mature classical cadherin, after proteolytic cleavage (see section 1.4.3), there are five cadherin repeats between which are four calcium binding regions. The

binding of Ca^{2+} to the EC domain of the classical cadherins is essential for their function and has been shown to protect these domains from degradation via exogenous proteases (Takeichi, 1977; Hyafil *et al*, 1981; Yoshida & Takeichi, 1982). In epithelial cells, removal of extracellular calcium from the medium causes E-cadherin EC domains to lose their rigidity and so junctional contacts with adjacent cells cannot be maintained (Shapiro *et al.*, 1995).

Located in the distal region of the cadherin N-terminus, is the HAV (His-Ala-Val) motif. This sequence provides an important role in cadherin adhesion, as disruption of ZA can occur with addition of HAV peptides to embryo culture media (Blaschuk *et al.*, 1990). The HAV motif is therefore, part of the adhesive interface between cadherins of adjacent cells. However, several other residues may also contribute to this adhesive interaction (Overduin *et al.*, 1995). Moreover, crystal structure analysis of classical cadherins indicates that cadherin dimers from adjacent cell plasma membranes may aggregate in a linear zipper-like structure, possibly providing strength to the relatively weaker interactions of only two adhesive monomers (Shapiro *et al.*, 1995; reviewed by Aberle *et al.*, 1996).

The cellular remodeling of E-cadherin has been implicated as an important feature in the role of the ZA in epithelial cells (Le *et al.*, 2002). It has been well documented that cadherin-mediated adhesion is important in the growth, development and repair of an epithelium (Reviewed in Yap *et al.*, 1997). Moreover, the expression of constitutively activated Rac1 (a Rho family GTPase) has been shown to regulate the assembly of cadherins and catenins with the actin cytoskeleton (Braga *et al.*, 1999). The link between known regulators of the actin cytoskeleton and ZA assembly further emphasizes the importance of cytoskeletal stability in regulating cell-cell adhesion and hence cell polarity (Hall, 1998; Braga *et al.*, 1999; Ridley *et al.*, 1995). Indeed, the dynamic nature of E-cadherin mediated adhesion has been demonstrated with Ca^{2+} depletion experiments, as mentioned earlier, and the evidence that E-cadherin is not only endocytosed but also recycled within a cell under different physiological conditions and appears to be regulated by PKC (Le *et al.*, 1999, 2002).

1.2.2 The cytoplasmic components of the zonula adherens junction

Many proteins are associated with the cytoplasmic tail of E-cadherin, such as α-, β- and γ- (plakoglobin) catenin and p120. Some of these cytoplasmic proteins are also capable of binding to non-AJ components such as the adenomatous polyposis gene product (APC; Rubinfeld *et al*, 1993; Su *et al.*, 1993), desmosomal proteins (Witcher *et al*, 1996; Wahl *et al*, 1996) and the epidermal growth factor receptor (EGFr; Hoschuetzy *et al.*, 1994). The catenins appear important in cell signalling processes, as they are targets for tyrosine kinases and phosphatases, and are vital in the mechanism of ZA junction formation in both the embryo and in mature tissues (Matsuyoshi *et al.*, 1992; Paria *et al.*, 1991, Hazan & Norton, 1998).

α-catenin (102 kD) binds to both β-catenin and the cortical cytoskeleton (Hirano *et al.*, 1987) and shares sequence homology with vinculin, a component of focal contacts (Geiger, 1979). α-catenin, as with vinculin, appears to have actin binding properties (Rimm *et al.*, 1995), and is necessary for ZA adhesiveness. Without it, E-cadherin cellular adhesion cannot occur (Hirano *et al.*, 1992). In fact, in human oesophageal cancer tissue, it is the loss of α-catenin that appears to coincide with the downregulation of ZA adhesion and thus result in the metastasis of the cancer (Kadowaki *et al.*, 1994). Moreover, in mouse preimplantation embryos, a mutation whereby the C-terminal third of α-catenin is deleted, results in a lethal phenotype similar to that found in E-cadherin mutant embryos (Torres e*t al.*, 1997).

β-catenin (88kD) is the vertebrate homologue of the Drosophila segment polarity gene, *armadillo* (Wieschaus *et al.*, 1984). In addition to its role in cell-cell adhesion, it is also an important component in signal transduction events during development and in *Xenopus* is required for the maintenance of the structural organisation in ectoderm and mesoderm tissue during gastrulation (Heasman *et al.*, 1994). The levels of β-catenin within a cell are as a result of an intricate balance between its transcriptional activation, via the Wnt signalling pathway, and its degradation in the cell cytoplasm (As reviewed in Peifer & Polakis, 2000). β-catenin has 60% sequence homology with the desmosomal protein plakoglobin and together they form a complex with a tumour suppresser gene

product, APC, found in the colon (Rubenfeld *et al.*, 1993; Su *et al.*, 1993). Indeed, disruption of the intricate balance between β-catenin synthesis and degredation has been implicated in the progression of some cancers (Cadigan & Nusse, 1997; Peifer *et al.*, 1997).

γ-catenin /plakoglobin (80kD; Coein *et al.*, 1986;Ozawa *et al.*, 1989) binds to both classical and desmosomal cadherins and is thought to be important in the sorting of desmosomal and ZA junction components (Ruiz *et al.*, 1996; reviewed by Barth *et al.*, 1997). This protein is highly homologous to β-catenin and to the *Drosophila* armadillo protein and may, therefore, also be involved in cell signalling pathways (Butz *et al.*, 1992; Bierkamp *et al* 1996; reviewed in Zhurinsky *et al.*, 2000). Indeed, Plakoglobin null-mutant mice embryos died from embryonic day 10.5 to birth (depending on the genetic background of the particular embryos) and demonstrated that the protein was essential for desomosome function. Interestingly, unlike with β-catenin, plakoglobin did not seem to be necessary for embryonic patterning or basic morphogenetic events during pre-implantation and early post-implantation stages (Haegel *et al.*, 1995; Bierkamp *et al.*, 1996). However, despite the differences between β-catenin and plakoglobin in the knockout studies, there is increasing evidence that plakoglobin may have a unique role in the Wnt signalling pathway (reviewed Zhurinsky *et al.*, 2000).

p120 binds directly to E-cadherin in both E-cadherin-β-catenin and E-cadherin-plakoglobin complexes (Daniel, 1995). p120 is a major *src* substrate which is phosphorylated in response to ligand stimulation of receptor tyrosine kinases and so it is thought that p120 may have a role in regulating signalling pathways in cadherin mediated adhesion (reviewed by Aberle., 1996; Barth *et al*, 1999).

p205 (l-afadin), a novel F-actin binding protein, is also associated with the AJ (Mandai *et al.*, 1997) and co-precipitates with a 190kD protein (s-afadin, p190). S-afadin/p190 is a p205 splice variant and has 90% sequence homology with the human, tight junction (TJ) associated ras-binding protein, AF-6 (discussed later in section 1.3.3.2; Takai *et al.*, 1997; Prasad *et al.*, 1993).

1.3 The tight junction

The TJ is the apical-most intercellular contact between adjacent epithelial cells. This junction has two main roles, both of which are vital to the functioning of an epithelium. Firstly, it acts as a barrier that regulates the diffusion of particular ions and molecules via the paracellular route (Cereijido *et al.*, 1989; Stevenson *et al.*, 1988). Indeed, the integrity of the TJ seal can be examined by measuring the electrical resistance across an epithelium, otherwise known as the transepithelial electrical resistance (TER). Secondly, the TJ prevents the mixing of plasma membrane components of the outer leaflet lipids between the apical and basal surfaces of epithelial cells, enabling membrane polarity to be maintained (Van Meer & Simons, 1986).

1.3.1 The structure of tight junctions

TJs are composed of several interacting proteins localised as a belt around the apex of each epithelial cell (Figure 1.3). In freeze fracture replicas, TJs appear as many strands that are thought to be composed of intramembraneous proteins (Staehelin, 1973; Claude 1978, Morita *et al.*, 1999). The various components of TJs can be subdivided into two main types: 1) transmembrane and 2) cytoplasmic. Since 1993, three groups of transmembrane proteins have been discovered called occludin (Furuse *et al.*, 1993), JAM (junctional adhesion molecule, of which there are now three known types; Martin-Padura *et al.*, 1998, Cunningham *et al*, 2000, Arrate *et al,* 2001) and a protein family called the claudins (Furuse *et al.*, 1998b; Morita *et al.*, 1999).

Analysis of hydrophobicity plots has indicated that both the claudins and occludin have four transmembrane domains with two extracellular loops. However, despite the structural similarity of these proteins, the claudins do not demonstrate any sequence similarity to occludin (Furuse *et al.*, 1998a). It is thought that the extracellular domains of these proteins function as the TJ seal (Furuse *et al.*, 1998a). JAM, on the other hand is a member of the immunoglobulin super family (IgSF) and therefore is quite different to that of occludin or the claudins (Figure 1.4). It has only one putative trans-membrane sequence with two domains within the extracellular portion being similar to the V (variable) regions of immunoglobulins (Martìn-Padura *et al.*, 1998).

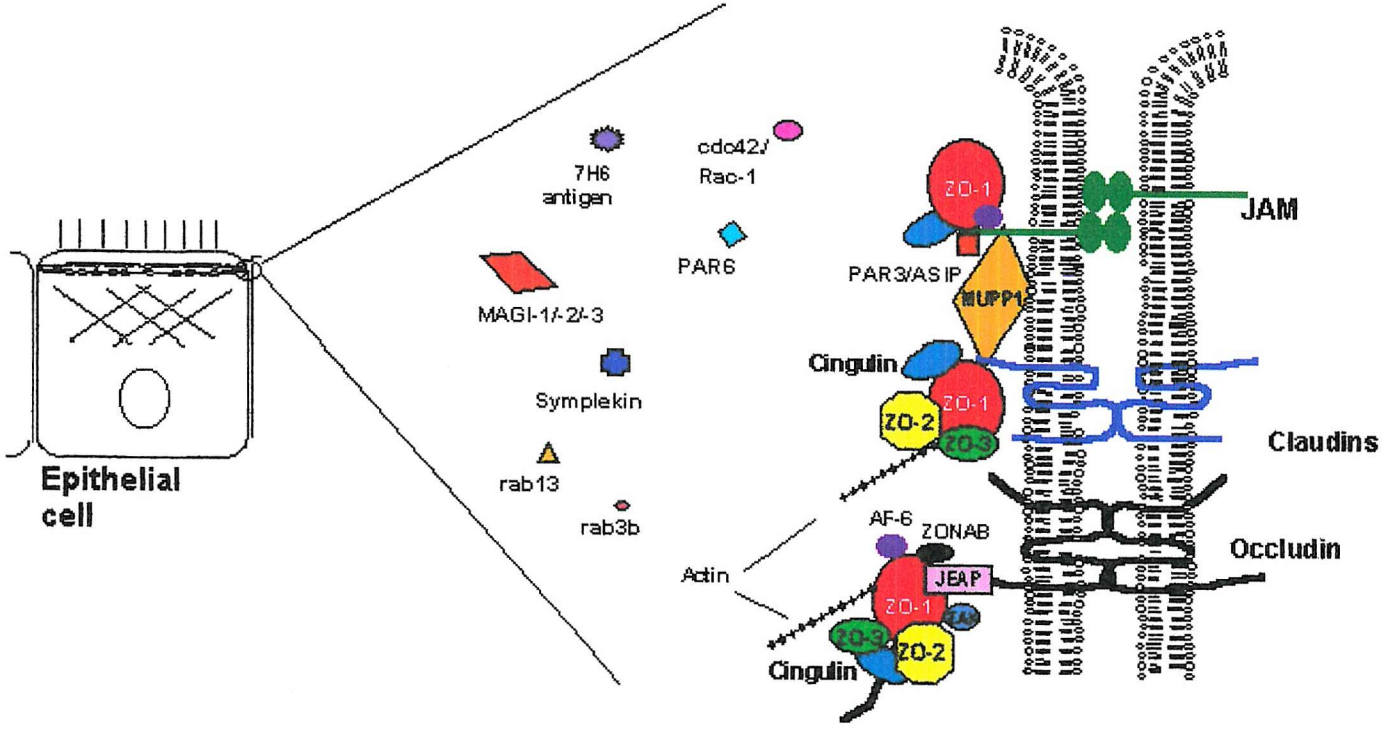

Figure 1.3 The tight junction. The TJ comprises three main types of transmembrane protein (occludin, claudins and JAM) and numerous cytoplasmicly localised proteins. The exact organisation of the TJ complex is only speculative and the structure and function of many of the molecular components contained within it is still uncertain.

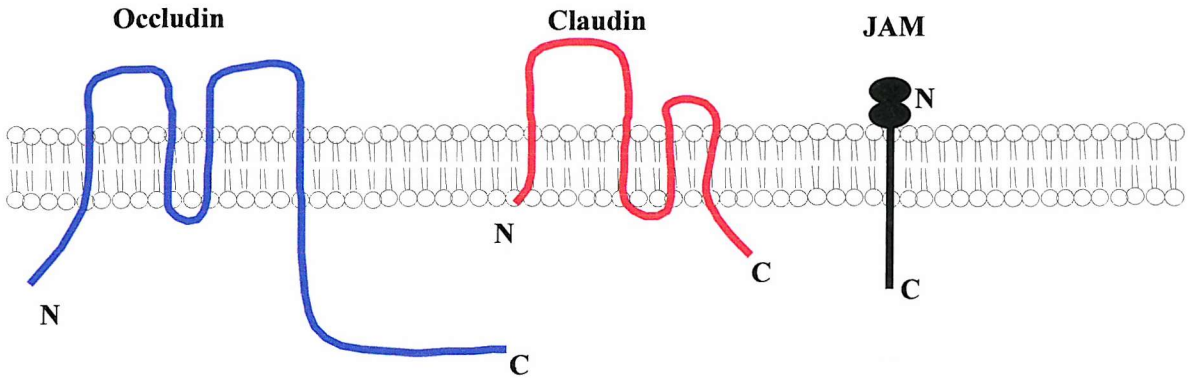

Figure 1.4 Comparison of the theoretical structures of three types of TJ transmembrane protein.

Numerous cytoplasmic proteins have been found localised at the TJ in various epithelia; ZO-1 (Stevenson *et al.,* 1986), ZO-2 (Gumbiner *et al.,* 1991), ZO-3 (Haskins *et al.*, 1998), cingulin (Citi *et al.,* 1988), 7H6 (Zhong *et al.,* 1993), symplekin (Keon *et al.*, 1996), 19b1 (Merzdorf & Goodenough, 1997), AF-6 (Yamamoto *et al.*, 1997), MAGI –1/-2/-3 (Dobrosotskaya *et al.,* 1997; Ide *et al.,* 1999; Wu *et al.,* 2000a and b), MUPP1 (Ullmer *et al.*, 1998; Simpson *et al.*, 1999), ZONAB (Balder and Matter, 2000) and JEAP (Nishimura *et al.*, 2002). Not only do some of these proteins interact with each other but also a number of them are capable of linking transmembrane proteins with the actin cytoskeleton (Reviewed in D'Atri & Citi *et al.*, 2002). Various protein kinases, heterotrimeric G proteins and small GTP-binding proteins are also known to associate with the TJ complex (De Almeida *et al.*, 1994; Denker *et al.*, 1996; Zaharaoui *et al.*, 1994; Dodane & Kachar, 1996; Tsukita *et al.*, 1991 and Anderson & Van Itallie, 1995).

1.3.2 The transmembrane proteins of the tight junction

1.3.2.1 Occludin

Occludin (65kDa) was originally discovered using three rat monoclonal antibodies to a protein found in a junctional membrane fraction from chicken liver (Furuse *et al.*, 1993). This antigen could not be extracted from the plasma membrane without

detergents, indicating that it was an integral membrane protein. Occludin has a long C-terminus (in the cytoplasm), a short N-terminus (also cytoplasmic), two large extracellular loops and one small intracellular turn.

The two extracellular loops of occludin are characteristically hydrophobic in nature with a 25% tyrosine and 36% glycine content in the first loop. Unlike the cytoplasmic domains, the extracellular regions are mainly uncharged apart from one positive and three negative side chains, which are immediately adjacent to the cell membrane. The lack of charged residues within the extracellular loop domains indicates that occludin in one cell could adhere to another occludin loop in an adjacent cell through hydrophobic contacts (Furuse *et al.*, 1993). The non-polar nature of the extracellular domain amino acid sequences appears to have been conserved between human, mouse, dog, chick and rat-kangaroo occludin (Ando-Akatsuka, 1996) indicating its possible evolutionary importance.

Another important domain in occludin is the C-terminus. This region of occludin (~150 amino acids) has been shown to be necessary for the localisation of this protein to the TJ (Furuse *et al.*, 1994). In addition, contained within this region is the ZO-1 binding sequence, indicating that ZO-1 may be a determinant of occludin localisation to the TJ. However, Balda *et al.*, (1996) demonstrated that while C-terminally truncated chicken occludin transfected into MDCK cells was able to localise to the TJ, immunofluorescent staining of the mutant occludin showed it to be discontinuous at the TJ. One possible explanation for this apparent discrepancy is that mutant occludin can be targeted effectively to TJs by associating with endogenous, full-length, occludin molecules (Chen *et al.*, 1997). The C-terminus may also be important in basolateral sorting of occludin, as chimeras of the occludin C-terminal domain with a reporter protein enabled its basolateral targeting (Matter & Balda, 1998). The phosphorylation of occludin is also indicated as an important regulator of its assembly to the TJ and is discussed in further detail in section 1.3.5 (Sakakibara *et al.*, 1997; Howarth *et al.*, 1994).

1.3.2.2 The role of occludin

Numerous studies indicate occludin as an important component of TJs. Firstly, overexpression of occludin in insect cells (by recombinant baculovirus infection) induced the formation of multilamellar structures within the insect cell cytoplasm. These lamella structures were TJ-like in appearance, with the outer leaflets of opposing membranes fused together without gaps (Furuse *et al.*, 1996). Immunofluoresence analysis of these structures showed that they were rich in occludin, indicating that this protein has a role in TJ sealing (Furuse *et al.*, 1996).

Occludin has been shown to correlate specifically with TJ sealing as demonstrated in over-expression studies using Madin-Darby Canine Kidney (MDCK) cells (McCarthy *et al.*, 1996). Western blotting revealed that overexpression of transfected chicken occludin correlated with an increase in TER. These effects were shown to be specific only to occludin protein, as levels of E-cadherin and ZO-1 were unchanged. In addition, an increase in the width and number of TJ strands was also observed, suggesting that occludin may also contribute to the formation of the aqueous pores within these strands (McCarthy *et al.*, 1996). In another study, full length or C-terminally truncated (mutant) chicken occludin expressed in MDCK cells has also been shown to be incorporated into TJ strands (Balda *et al.*, 1996). Both types of transfected occludin induced an increase in TER but surprisingly they also caused an increase in the paracellular flux of small molecular weight tracers across the monolayer. These results indicate that electrical resistance and paracellular flux of tracers (which are commonly used as indicators of the sealed state of TJs) are two independently controlled processes (Balda *et al.*, 1996).

Moreover, a synthetic peptide corresponding to the second extracellular loop of occludin was found to disrupt TER in a reversible manner and increase paracellular tracer flux in the *Xenopus* A6 (epithelial) cell line (Wong & Gumbiner, 1997). Western blotting analysis detected a decrease in the occludin cell content, which appeared to be a result of an increase in protein turnover (as indicated with pulse-chase analysis). This effect appeared specific to occludin and the peptide appeared to have no effect upon other TJ components (e.g. ZO-1, ZO-2 and cingulin) or upon the ZA protein E-cadherin.

The gross epithelial morphology of these cells appeared unchanged (assessed by scanning EM). These findings strongly indicate a role for occludin in the cell-cell sealing at the TJ (Wong & Gumbiner, 1997).

However, in occludin-deficient embryonic stem cells, whereby the two occludin alleles had been specifically disrupted, the ability to form a polarised epithelial layer (embryoid bodies; EBs) was not affected (Saitou *et al.*, 1998). Wild type and mutant EBs also appeared morphologically indistinct from each other (as shown by electron microscopy and freeze fracture). The TJs were still functional (i.e. they were impervious to tracers), indicating the existence of other TJ transmembrane proteins, which may also form epithelial cell-cell contacts (Saitou *et al.*, 1998). Moreover, mice with the null mutation for the occludin gene were born in the expected Mendelian ratios, with no obvious phenotypic abnormalities (Saitou *et al.*, 2000). However, occludin knockout mice were retarded in growth postnatally. Closer histological examination of various tissues and organs from these mice did demonstrate that, although TJ strands appeared normal, the barrier function of some epithelia was disrupted, resulting in chronic inflammation of the gastric epithelium and testicular atrophy (Saitou *et al.*, 2000).

1.3.2.3 The Claudins

Upon reanalysis of chicken liver junctional fractions, two more potential integral membrane proteins, associated with occludin, were identified called claudin-1 and –2 (22kD; Furuse *et al.*, 1998a). After searching a cDNA database, two related mouse proteins were discovered. Localisation of claudins to tight junction strands themselves was established via FLAG$_{TM}$ (Sigma Chemical Co) and GFP (Green fluorescence protein) tagging experiments. Unlike occludin, the claudins only have a short C-terminal domain of either 20 or 40 amino acids depending on whether it was claudin-1 or –2 respectively (Furuse *et al.*, 1998a).

Transfection of claudin cDNA into mouse L fibroblasts (which are known to lack TJs) was found to induce the formation of TJ-like membrane strands, indicating claudin contributed to their formation (Furuse *et al.*, 1998b). Freeze fracture and electron

microscope analysis of the fibroblasts transfected with both occludin and the two claudins indicated that the claudins may be primarily responsible for TJ strands, as, although occludin was found to be concentrated at the strand sites, these strands were fewer and shorter (Furuse *et al.*, 1998b).

Twenty-four members of the claudin family have now been identified (Tsukita *et al*, 2001). Three of these proteins (claudins 3-5 respectively) were previously named Regressing Ventral Prostate (RVP1; Briehl *et al.*, 1991), *Clostridium perfringens* enterotoxin receptor (CPE-R; Katahira *et al.*, 1997), and TransMembrane protein deleted in Velo-Cardio Facial/DiGeorge syndrome (TMVCF; Sirotkin *et al.*, 1997) but nothing was known about their functions. All of these proteins have the same characteristic four transmembrane domains (as demonstrated by their hydrophobicity plots). In contrast to occludin, the two extracellular loops of this protein family are disproportional in size with the first loop being much larger than the second loop (Figure 1.4).

Antibodies have been successfully raised against claudins and Northern blotting has revealed that each claudin member has a distinct tissue expression pattern (Morita *et al.*, 1999). Claudins-1 and –2 are expressed at high levels in liver and kidney. Claudin-3, on the other hand, is primarily expressed in liver and lung. However, Claudins-4, -7 and –8 are mostly expressed in the kidney and lung. Northern blotting could not detect claudin-6 in these tissues, but its cDNA was amplified using RT-PCR in mouse kidney. Claudin-6 was originally identified in an unspecified embryonic source and later detected, using wholemount insitu hybridisation, in embryoid bodies (Ebs; Morita *et al.*, 1999, Turksen & Troy, 2001). Claudin-5/TMVCF, on the other hand has only been detected in endothelial cells (Morita *et al.*, 1999) and claudin-11/OSP is primarily expressed in the testis and brain. The tissue expression patterns of many of these claudins indicate that in many cells there is more than one claudin species (Tsukita & Furuse, 2000). In contrast, there are also some cells that express only one claudin type i.e. the brain, endothelial cells and the testis (Tsukita & Furuse, 2000).

1.3.2.4 Claudins and the barrier function of tight junctions

Claudin-11/OSP deficient mice have recently been generated where the Sertoli cells and myelin sheaths of oligodendrocytes were lacking in TJ strands (Gow *et al.*, 1999). The generation of such a knockout species has thus highlighted the importance of claudins in TJ strand and barrier formation (Tsukita & Furuse, 2000). Another breakthrough in determining the exact functions of claudins arose when the bacterial peptide toxin, *Clostridium perfringens* enterotoxin (CPE), was used (Sonoda *et al.*, 1999). Addition of the carboxyl-terminal half of CPE (C-CPE) was found to bind specifically claudin-4/CPE-R. In MDCK cells (where the two main claudins are claudins–1 and –4), addition of C-CPE was shown to remove specifically claudin-4 from the TJ and also resulted in both a significant decrease in TER and also the number of TJ strands. This is the first piece of conclusive evidence that claudins are involved in the barrier function of the TJ.

Other claudin research has now demonstrated that claudin-1 is also directly involved in TJ barrier function. Indeed, claudin-1 deficient mice illustrated that this protein is vital for the barrier function of skin (Furuse *et al.*, 2002). These mice died within one day of birth, due to excessive water loss through their characteristically wrinkled skin. This was the first evidence that TJs play an important role in mammalian stratified epithelia. Despite the presence of occludin and claudin-4 in the TJs of these transgenic mice, there was no effective compensation response in these cells for the loss of claudin-1. Therefore, this suggests that claudin-1 is crucial to the biogenesis and maintenance of a fully functional epidermal barrier. Overexpression of claudin-6 in the epidermis of newborn mice has also been shown to effect the homeostasis of the other claudin members in this tissue (Turksen & Troy, 2002). Consequently, as in the claudin-1 deficient mice, the epidermal permeability barrier was compromised. These mice died within two days of birth, also largely due to excessive dehydration. In support of this evidence, it is not suprising that overexpression of claudin-1 in MDCK cells results in increased TER and decreased paracellular flux (Inai *et al.*, 1999). Interestingly, claudin-1 overexpression increased expression of ZO-1 but not the expression of occludin or ZO-2, indicating the complexity of the protein interactions at the TJ.

1.3.2.5 Claudins and the formation of aqueous pores within tight junction strands

In hypomagnesemia, an inherited disease of the TJ where the paracellular flux of Mg^{2+} is blocked across the ascending limb of Henle, claudin-16/Paracellin-1 is thought to be responsible (Simon *et al.*, 1999). This particular claudin species is normally found exclusively expressed in the thick ascending limb of Henle. In patients with hypomagnesemia, claudin-16/Paracellin-1 appears to be missing and so Mg^{2+} cannot be resorbed. Thus, it appears that claudin-16/Paracellin-1 is directly involved in selective paracellular flux of Mg^{2+} ions across TJ strands made of claudin protein. It may be that other claudin species can also form the pores of TJ strands or it may be exclusive to claudin-16/Paracellin-1 (Tsukita & Furuse, 2000). It has been suggested that the variable permeabilities of different epithelial cell types (Diamond, 1977; Gumbiner, 1993) may be a result of different claudin species in the TJ strands (Tsukita & Furuse, 2000). Recently, expression patterns of twelve distinct claudin species, out of sixteen tested, demonstrated segment-specific distribution in the mouse nephron (Kiuchi-Saiskin *et* al., 2002). As is discussed below, homotyptic and heterotypic association, among and between these claudin species, may have great significance upon the leakiness of these cell layers. Concomitantly, as with claudin-16, these may then have an effect upon the transport of particular ions, i.e. resorption of certain metabolites in the kidney.

1.3.2.6 Heterotypic binding of claudin species

It has now been discovered that two claudin species can form co-polymers when transfected into fibroblast cells (Furuse *et al.*, 1999). When two fibroblast cultures, singly expressing either claudin-1, -2 or –3, were cultured together claudin-3 was found to bind heterotypically to either claudin-1 or claudin-2. However, claudin-2 and claudin-1 never formed heterotypically paired strands (Furuse *et al.*, 1999). In light of this discovery, it was proposed that where cells express more than one type of claudin, pores could be created within TJ strands where claudins that do not bind heterotypically with each other are forced together (Figure 1.5). It still remains unclear how occludin associates with claudin and whether it only binds homotypically to other occludin molecules.

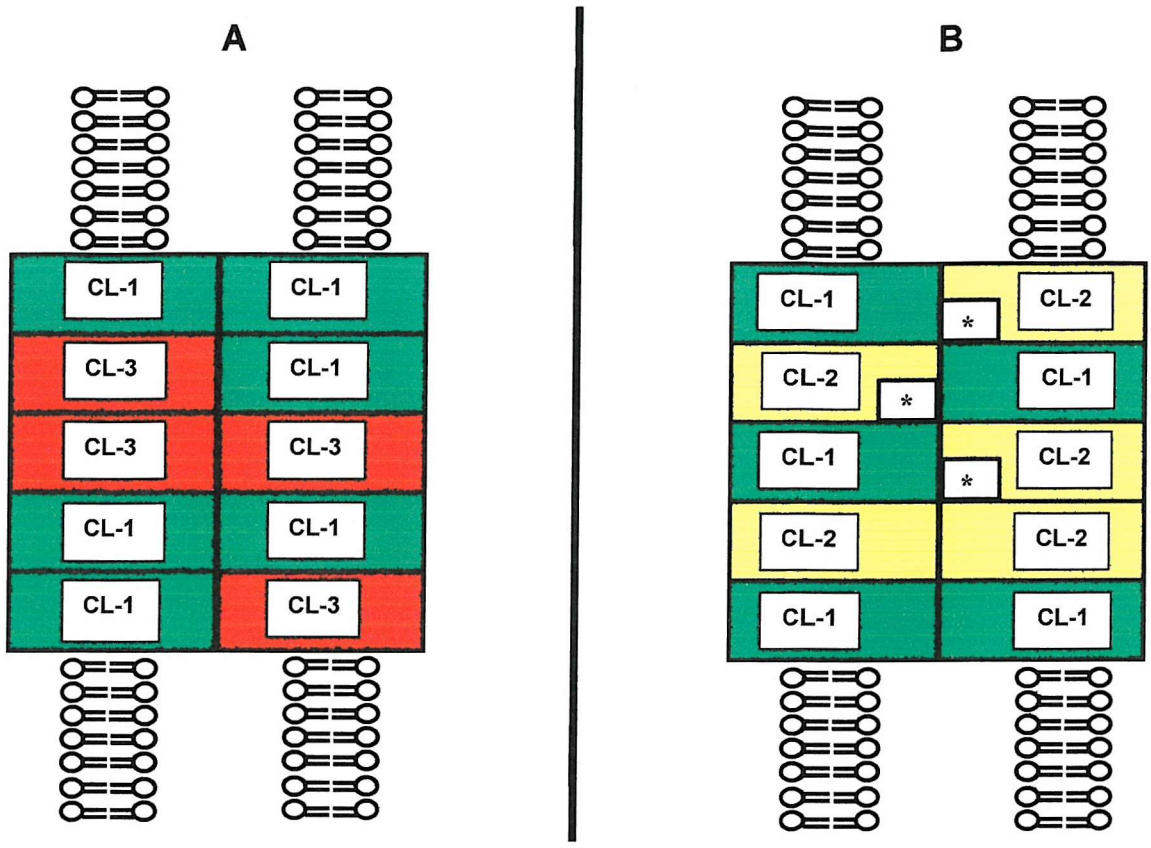

Figure 1.5 Examples of two types of tight junction (Adapted from Tsukita & Furuse, 2000). A) Schematic representation of TJs comprising claudin –1 and –3 forming a tight seal due to heterotypic and homotypic interactions. B) Schematic representation of TJs comprising claudin -1 and -2 forming a comparatively more "leaky" seal compared with A (due to the inability of these claudins to bind heterotypically), thus creating putative pores within TJ strands (*).

Multiple sequence alignments of claudins-1 to -8 indicate that the first and fourth transmembrane domains and the two extracellular loops are quite conserved (Morita *et al.*, 1999; Figure 1.6). The second and third transmembrane domains, on the other hand, are more diverse. Interestingly, all the claudins have a -YV motif at their C-termini and may interact with PDZ binding domains of other TJ proteins such as ZO-1 (Morita *et al.*, 1999; Figure 1.6).

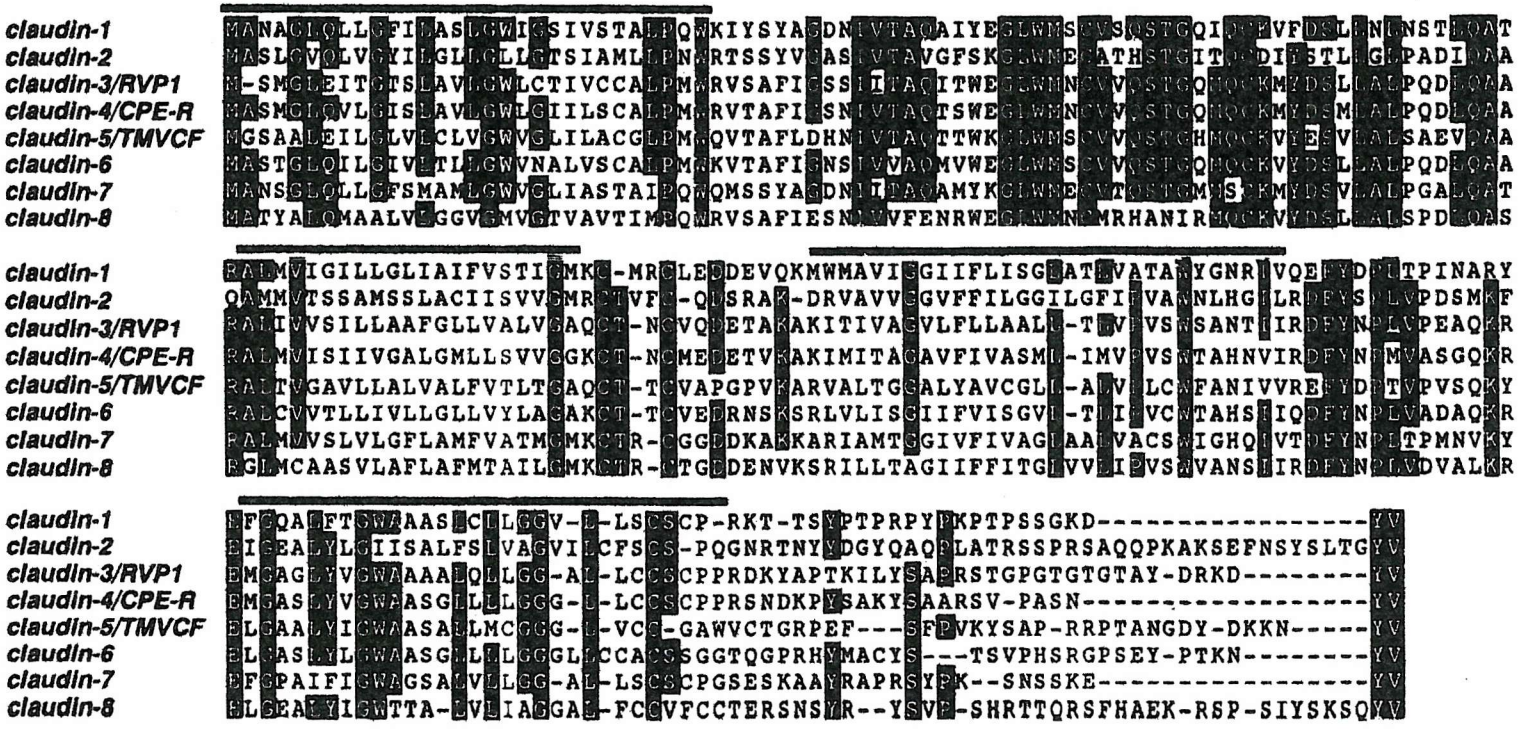

Figure 1.6 Amino acid sequence alignment of claudins 1-8. Shaded areas depict regions of homology. Bars correspond to the four transmembrane regions (Taken from Morita *et al.*, 1999).

1.3.2.7 JAM

Junctional adhesion molecule (JAM; 36-41kDa) was discovered after screening of antigens found at mouse endothelial cell contacts (Martìn-Padura *et al.*, 1998). This adhesion molecule appears to be selectively concentrated at the intercellular junctions of both mouse endothelial and epithelial cells (Martìn-Padura *et al.*, 1998). Confocal and immunoelectron microscopy data suggest that JAM co-distributes at the TJ with ZO-1 and occludin (Martìn- Padura *et al.*, 1998). A monoclonal antibody (BV11) directed against JAM was found to inhibit both spontaneous and chemokine-induced monocyte transmigration through endothelial cell monolayers *in vitro*, thus indicating that JAM may be a key component in regulating such events *in vivo* (Martìn-Padura *et al.*, 1998). Interestingly, expression of JAM cDNA transfected into CHO (Chinese hamster ovary) cells was found to cause a reduction in the paracellular permeability of tracers across confluent monolayers, thus implying that JAM may also be a sealing component of TJs (Martìn-Padura *et al.*, 1998).

1.3.2.7 Human JAM and the JAM protein family

A human orthologue to murine JAM has now been identified (Williams *et al.*, 1999), the protein structure and sequence of which is highly conserved. However, unlike murine JAM, human JAM appears to be constitutively expressed on circulating monocytes, neutrophils, lymphocytes and platelets. Recently, two more IgSF proteins have been discovered, JAM-2/VE-JAM (vascular endothelial JAM) and JAM-3 (36-41kD and 43kD respectively; Cunningham *et al.*, 2000; Palmeri *et al,* 2000; Arrate *et al.*, 2001). As with JAM-1 (previously referred to as JAM), JAM-2 is localized at cell-cell borders, although it's predominant expression is in the heart and high endothelial venules (Palmeri *et al.*, 2000). JAM-3, however, appears to be a counter receptor for JAM-2 that mediates JAM-2 adhesion to T, Natural killer and dendritic cells (Arrate *et* al., 2001; Liang *et al.*, 2002).

The expression of human JAM proteins on immune cells and at endothelial junctions is similar to that of CD31 (PECAM-1), another IgSF molecule (Ohto *et al.*,1985; Stockinger *et al.*, 1990; Muller *et al.*, 1989) Interestingly PECAM-1 has also

been shown to be involved in the transendothelial migration of leukocytes (Muller *et al.*,1993; Vaporciyan et al.,1993; Bogan *et al.*, 1994; Wakelin *et al.*, 1996). In addition to this, a combination of proinflammatory cytokines (TNF-α and INF-γ) applied to human endothelial cells caused JAM-1 and also PECAM-1 to change their protein organisation, from the intercellular junctions to subcellular positions on the apical and basolateral sides, respectively (Ozaki *et al.*, 1999). It has also been shown that JAM-1 is phosphorylated by PKCs upon platelet activation (Ozaki *et al.*, 2000) thus indicating another important role for JAM-1 in immunological processes. In addition to the above, expression cloning has revealed that JAM-1 acts as a receptor for reovirus as it could permit viral infection in cells not usually permissive to reovirus (Barton *et al.* 2001). Moreover, the subsequent infection and intracellular signaling processes, required for an apoptotic response by the infected cell, is also mediated by the viral interaction with JAM-1 (Barton *et al.* 2001).

Interestingly, human JAM-1 has now been shown to regulate TJ resealing in epithelia (Liu *et al.*, 2000). Specific monoclonal antibodies, generated against the extracellular domain of human JAM-1, were shown to significantly inhibit TER recovery in T84 cell monolayers after TJ disruption by transient removal of extracellular calcium. This inhibition appeared to occur in the absence of JAM-1 or occludin redistribution. Reassembly of ZO-1 to the TJ and E-cadherin to the ZA junction did not appear to be affected. Not only do these results indicate a possible role for JAM-1 in regulating TJ barrier function but also that JAM-1 may interact with occludin during TJ reassembly (Liu *et al.*, 2000). Indeed, JAM-1 has now been demonstrated to interact specifically with the cell polarity protein ASIP/PAR-3 (Ebnet *et al.*, 2001). It has been proposed that JAM-1 has an important role in recruiting ASIP/PAR-3 to cell contacts and therefore, is important in TJ formation and cell polarity (Ebnet *et al.*, 2001).

1.3.2.8 Interactions between JAM-1 and other tight junction proteins

There is now increasing information on TJ components that may interact with or bind to JAM-1. Immunoprecipitation of endothelial extracts have shown that the TJ cytoplasmic proteins ZO-1 and AF-6 can be co-precipitated with JAM-1 (Shultz *et al.*,

2000). Interestingly, JAM-1 contains a type II PDZ domain-binding motif. Analysis of JAM-1 constructs indicated that the protein interacts with the second and third PDZ domains of ZO-1 (Shultz *et al.*, 2000). In addition to this, full-length murine JAM-1 appears to co-distribute with AF-6 in human Caco-2 cells, independent of any JAM-1 being present in the adjacent cells. On the other hand, JAM-1 constructs lacking the C-terminus and PDZ domain did not co-localise with AF-6 but were restricted to cell contacts between cells expressing mouse JAM-1 (Shultz *et al.*, 2000). It appears that recruitment of JAM-1 to the intercellular junctions may be due to its interactions with AF-6 and possibly ZO-1 via its PDZ domain. Other immunoprecipitation experiments have indicated that JAM-1 may bind to cingulin and ZO-1 at the TJ (Bazzoni *et al.*, 2000). Therefore, it is thought that JAM-1 could stabilise occludin connection with the actin cytoskeleton by binding both cingulin and ZO-1 (Bazzoni *et al.*, 2000).

1.3.3 The cytoplasmic proteins

1.3.3.1 *Zonula occludins* –1, -2 and –3 (ZO-1, ZO-2 and ZO-3)

ZO-1 (220kDa), ZO-2 (160kDa) and ZO-3 (130kDa) are members of the MAGuK (membrane associated guanylate kinase homologue) protein family as they are membrane associated and contain guanylate kinase (GuK) homology domains (Furuse *et al.*, 1994; Haskins *et al.*, 1998). The GuK homology domain may give these proteins signaling roles but little is really known about its precise function within the *zonula occludins* (ZO) protein. (Anderson *et al.*, 1995). The MAGuK proteins also contain two other domains; 1) the DHR (discs-large homology region); also known as the PDZ (Post-synaptic density/Discs-large/ZO-1) domain and 2) the SH3 (src homology 3) domain (Anderson *et al.*, 1995). The DHR/PDZ and SH3 domains appear to be important in enabling sequence specific binding with other proteins and thus are important in the formation and functioning of the TJ complex (Anderson *et al.*, 1995).

ZO-1 was the first TJ-associated protein found to localise at both epithelial and endothelial TJs (Stevenson *et al.*, 1986; Anderson *et al.*, 1988; Kurihara *et al.*, 1992; Balda & Anderson, 1993). ZO-1 has an alternatively spliced domain, the α-domain (80 amino acids; Willott *et al.*, 1992), the expression of which correlates with TJ activity and

is developmentally regulated (Balda & Anderson, 1993; Sheth *et al.*, 1997). In *vitro* and *in vivo* binding assays indicate that both ZO-2 and occludin bind to domains within the N-terminal half of ZO-1 (Fanning *et al.*, 1998). The C-terminal half of ZO-1, on the other hand, appears to interact with F-actin (Fanning *et al.*, 1998; Itoh *et al.*, 1997). Thus, ZO-1 may be important in organising the components of the TJ and linking them to the cortical actin cytoskeleton (Fanning *et al.*, 1998). In addition to occludin and ZO-2, ZO-1 is known to bind or associate with claudins (Itoh *et al.*, 1999a), the Ras target AF-6 (Yamamoto *et al.*, 1997), the two GTP-ases, rab3b and rab13 (Zaharoui *et al.*, 1994), and the cytoskeletal components, F-actin and α-spectrin (Fanning *et al.*, 1998).

ZO-2 also has splice variants, ZO-2β^- and ZO-2β^+, whereby the β-domain is a 36 amino acid motif (Beatch *et al.*, 1996). Full length canine ZO-2 cDNA had a predicted molecular weight of 132kDa rather than 160kDa and it is presumed that this difference in molecular weight may be due to post-translational modifications (Beatch *et al.*, 1996). ZO-2 can bind occludin, the claudins, ZO-1 and α-catenin and in the absence of TJs will associate with ZA components in fibroblasts, neural retina and cardiac muscle cells (Itoh *et al* 1999a & b; Collins & Rizzolo, 1998).

ZO-3, on the other hand, has no known splice variants. Although ZO-3 contains similar MAGuK domains to ZO-1 and ZO-2, the position of the proline rich domain is different (Haskins *et al.*, 1998). ZO-3 binds directly to occludin, the claudins and ZO-1 but not with ZO-2 (Haskins *et al.*, 1998; Itoh *et al.*,1999b).

1.3.3.2 Other cytoplasmic tight junction proteins

The remaining TJ plaque proteins appear important in connecting the TJ to the actin cytoskeleton and also in signaling events between the TJ and various G proteins. The exact organisation of the TJ complex is only speculative and the structure and function of many of the molecular components contained within it is still uncertain (Figure 1.3).

Cingulin, an acidic elongated 140kDa protein, is found in most, but not all, TJ forming cells. The structure of cingulin appears to resemble a coiled-coil domain whereby two peptides are intertwined with each other (Citi *et al.*, 1988, 1989). It is thought that this protein interacts with actin filaments at the TJ via a myosin-like domain (Ballard *et al.*, 1995).

7H6 (155kDa) is a phosphoprotein found in the TJs of epithelia, endothelia and hepatocytes. This protein appears to have a role in TJ barrier function, as treatment of MDCK cells with metabolic inhibitors (antimycin A and 2-deoxyglucose) causes its redistribution away from the TJ, corresponding with a drop in TER and an increase in lanthanum permeability across the monolayer. This effect is reversible and does not affect the organisation of ZO-1 to the TJ and hence is specific (Satoh *et al.*, 1996).

Symplekin (127kDa) is also localised to the cytoplasmic side of the cell membrane at the TJ region. The expression of this protein appears to be much wider than just in epithelial cells (Zhong *et al.*, 1994; Satoh *et al.*, 1996), as it can be found in the nucleoplasm of non-epithelial cells (Keon *et al.*, 1996).

19B1, found co-localised with ZO-1 in Xenopus A6 cells, is thought to be a maternal protein found in early stages of *Xenopus laevis* development (Merzdorf *et al.*, 1998).

AF-6, originally discovered as a fusion protein with human acute lymphoblastic leukemia-1 (ALL-1), is also found to be co-localised with ZO-1 in cultured epithelial cells (Prasad *et al.*, 1993; Kuriyama *et al.*, 1996). Interestingly, AF-6 has been shown to contain a PDZ domain, two Ras-binding domains, and a myosin V- and a kinesin-like binding domain (Kuriyama *et al.*, 1996). ZO-1 appears to interact with this Ras-binding domain, and activated Ras can inhibit this interaction. In addition to this, afadin (a rat homologue of AF-6) has been characterised as a junctional protein that contains an F-actin binding domain. So AF-6 may also link the TJ with the cell's actin microfilaments (Mandai *et al.*, 1997).

Membrane-associated guanylate kinase with an inverted arrangement of protein-protein interaction domains (MAGI) –1/-2/–3 (122-148kDa, 160kDa, 125kDa, respectively), as the name suggests, are members of the MAGUK protein family. However, these proteins have some distinct differences compared with the more typical MAGUKs. MAGI proteins have the GuK domain at the NH2 terminus (instead of the COOH terminus). In place of the SH3 domain these proteins have two WW domains (named after the conserved tryptophan residues contained within these domains). In addition to the above differences, instead of the usual 1-3 PDZ domains these proteins have multiple PDZ domains (Dobrosotskaya *et al.*, 1997; Wu *et al.*, 2000). MAGI-1 has been shown to interact with β-catenin and E-cadherin in MDCK cells (Dobrosotskaya & James, 2000) and can also be recruited to TJs with ZO-1 (Ide *et al.*, 1999).

Multi-PDZ Domain Protein 1 (MUPP1; 250kDa) has 13 PDZ domains and is found concentrated at TJs. Yeast two-hybrid system identified JAM-1 and claudin-1 as potential MUPP1 binding partners. Claudin-1 appears to bind to the ninth PDZ domain on MUPP1, whereas JAM-1 binds PDZ 10. It is proposed that MUPP1 may act as a scaffold protein at the TJ and may recruit various components of the TJ complex. (Hamazaki, 2002).

ZO-1-associated nucleic acid-binding protein (ZONAB; 47-55kDa) is a Y-box transcription factor that binds to the SH3 domain of ZO-1. This protein is found both in the nucleus and at TJs of epithelial cells (Balda & Matter, 2000). It is thought that together ZO-1 and ZONAB function in the regulation of epithelial cell differentiation.

Junction-enriched and associated protein (JEAP; 98kDa) was found after a screen for novel TJ proteins (Nishimura *et al.*, 2002). JEAP, is specifically expressed in exocrine cells and contains a polyglutamic acid repeat at the NH2-terminus followed by a coiled–coil domain and finally a PDZ binding motif at its COOH-terminus. In experiments where JEAP was exogenously expressed in MDCK cells, it was found to co-localise with ZO-1 and occludin (Nishimura *et al.*, 2002).

1.3.4 The associated signalling molecules of the tight junction

There are a number of cellular signal transduction proteins that may be involved in the regulation and maintenance of the TJ. These proteins include a group of small G-proteins, such as Rab13 and Rab3B, and a group of heteromeric G proteins ($G\alpha_{I-2}$ and $G\alpha_{12}$; De Almeida *et al.*, 1994; Denker *et al.*, 1996; Zahraoui *et al.*, 1994; Dodane & Kachar, 1996). In addition, c-Yes (a tyrosine proto-oncogene) and p120 (a Src substrate) have been speculated to be involved in the maintenance of the TJ (Tsukita *et al.*, 1991; Anderson & Van Itallie, 1995).

Heteromeric guanine nucleotide-regulatory (G) proteins, found at the TJ, are involved in signal transduction. In order to attach to membranes the $G\alpha_I$ subunit needs to be myristoylated (Mumby *et al.*, 1990). In MDCK cells, $G\alpha_{I-2}$ overlaps with ZO-1 at the TJ along the lateral membrane with some intracellular staining, indicating a potential role for $G\alpha$ subunits early in TJ biogenesis (Denker *et al.*, 1996).

The Rab proteins are a large family of small GTPases, whose primary role is to regulate SNARE (Soluble NSF attachment protein receptor) pairing in vesicular transport. Rabs, therefore, regulate vesicle docking processes and aid in the targeting of components in polarised cells (Novick & Zerial, 1997; Chavrier & Goud, 1999). Little is known about the role of Rab3B at the TJ, however Rab13, another TJ associated Rab, seems to be important in TJ biogenesis (Zahraoui *et al.*, 1994; Sheth *et al.*, 2000a). As found in Ras/Rho proteins, Rab13 also contains a CaaX (C, cys; a, mostly aliphatic; X, any amino acid) motif at its C-terminus, a motif thought to be involved in membrane attachment (Hancock *et al.*, 1991). In addition, Rab13 is isoprenylated *in vivo* (Rabs must be prenylated in order to bind membranes; Joberty *et al.*, 1993). Rab13 membrane association and disassociation also appears to be regulated by its binding to the rod cGMP phosphodiesterase δ subunit (δ-PDE; Marzesco *et al.*, 1998). Interestingly δ-PDE contains two sequences at its C-terminus which are required for binding to PDZ domains which, as previously mentioned, are found in other TJ associated proteins such as the ZO proteins (Marzesco *et al.*, 1998).

In recent years, mammalian homologues to partitioning-defective proteins (PAR3/ASIP and PAR6) have been discovered (Izumi *et al.*, 1998; Qiu *et al.*, 2000). In metazoan species, such as *Caenorhabditis elegans,* PAR proteins, in response to sperm cues, are involved in cell polarity in oocytes (Bowerman & Shelton, 1999). Since the discovery of these proteins in mammals, a number of reports have identified a protein complex comprising PAR3/ASIP, PAR6, aPKC and cdc42/Rac-1 (a small GTPase; Joberty *et al.*, 2000; Johansson *et al.*, 2000). Together these proteins are implicated in signalling pathways linked to the regulation of cell polarity and epithelial biogenesis (Lin *et al.*, 2000; Qiu *et al.*, 2000; Yamanaka *et al.*, 2001; Ebnet *et al.*,2001; Gao *et al.*, 2002).

1.3.5 Other tight junction regulatory mechanisms

The barrier function of TJs is highly sensitive to extracellular calcium levels. As seen from TER experiments, removal of this ion causes reversible changes in TJ permeability (Cereijido *et al.*, 1981; Martinez-Palomo *et al.*, 1980; González-Mariscal *et al.*, 1985; Garrod & Collins, 1992). Calcium removal does not appear to affect the synthesis of TJ components but prevents their translocation from the Golgi and storage vesicles to the correct region of the cell's surface membrane (Balda *et al.*, 1993).

Calcium dependence has also been associated with E-cadherin at the ZA junction (Gonzalez-Mariscal *et al.*, 1985; Gumbiner *et al.*, 1988). In low extracellular calcium, extracellular domains of E-cadherin loose their adhesiveness and are unable to maintain junctional contacts with adjacent cells (Gumbiner & Simons, 1986; Gumbiner *et al.*, 1988). These findings suggest that E-cadherin is at the beginning of an important signal transduction pathway that regulates the maintenance of the TJ and hence the epithelial state of cells (Balda *et al.*, 1993).

Protein kinases are also known to be important in the signal transduction pathway between the ZA and the TJ, as indicated by the ability of protein kinase inhibitors to maintain functional TJs despite low extracellular calcium (Citi, 1992). Addition of a PKC agonist, 1,2-dioctanoylglycerol (diC8), to MDCK cell culture medium results in 1)

the translocation of ZO-1 to the TJ region, 2) the reorganisation of actin filaments, 3) the formation of TJ strands and 4) an increase in the control over the paracellular flux of solutes (Balda *et al.*, 1993).

Occludin phosphorylation has been shown to be an important part of assembly and maintenance of the TJ complex (Sakakibara *et al.*, 1997; Howarth *et al.*,1994). Occludin is phosphorylated on Ser and Thr residues (Sakakibara *et al.*, 1997; Cordenonsi *et al.*, 1997) and the phosphorylated state of these residues appears important in regulating TJ biogenesis (Sakakibara *et al.*, 1997; Cordenonsi *et al.*, 1997; Wong, 1997). Monoclonal antibodies with the ability to detect different phosphorylated forms of occludin, used in MDCK calcium-switching experiments, indicate that the phosphorylation of this protein is needed for TJ assembly (Sakakibara *et al.*, 1997). However, in *Xenopus* blastomeres, phosphorylation appears to have the opposite function (Cordenonsi *et al.*, 1997). It is possible that *de novo* TJ biogenesis in embryos is regulated differently to *in vitro* MDCK low calcium systems. However, there may also be other maternal effects in the *Xenopus* embryo that are complicating the analysis. In further support for the role of phosphorylation in TJ assembly, experiments in human intestinal cell lines showed that an increase in TER was concomitantly linked to an increase in occludin phosphorylation (Nishiyama *et al,* 2001).

1.4 Mouse preimplantation development

In this study, the mouse preimplantation embryo has been used to develop an understanding of how recently discovered TJ protein components, JAM-1 and claudin-1, fit into our current interpretation of epithelial differentiation and TJ biogenesis. Although epithelial cell lines are a useful scientific tool, the preimplantation embryo has some important advantages in this context and are easily cultured *in vitro*. In contrast to cell lines, the embryo has not been virally transformed nor is it derived from a tumour. The first epithelium made in animal development is called the trophectoderm (TE), which is an indigenous tissue and thus has a direct relevance to understanding normal processes in epithelial differentiation. In addition to this, the early embryo has relatively long cell cycles (the first two divisions being 20-24hrs, and subsequent ones occurring

every 12hrs) enabling analysis of TJ and epithelial biogenesis mechanisms to be easily observed.

After fertilisation, the mouse egg undergoes five reduction cleavage divisions to form a blastocyst (32-64 cells; Figure 1.7; reviewed in Fleming *et al.*, 2001; Watson & Barcroft, 2001). This comprises two distinct cell types: 1) an outer, differentiated and polarised epithelial layer, the TE (from which extra-embryonic lineages, such as the placenta, are derived) and 2) an inner cell mass (ICM; from which the foetus is derived after implantation). The TE displays epithelial adhesiveness, intercellular junctions and a basally polarised Na^+/K^+-ATPase and therefore is a good developmental model for investigating epithelial differentiation and the assembly *de novo* of various cell-cell adhesion systems (reviewed in Fleming *et al.*, 2000 & 2001).

For the purpose of researching epithelial biogenesis there are five key components of early embryo development that need to be understood and will be discussed further. Prior to and key in the formation of the blastocyst, the embryo must:

i. Resume progression through the first cell-cycle post fertilisation.
ii. Switch gene expression from maternal to zygotic control by the mid-2-cell stage.
iii. Undergo specialised adhesion events (compaction) at the 8-cell stage.
iv. Form two distinct cell populations at the 16-cell stage.
v. Have fully matured epithelial junctional complexes by the 32-cell stage.

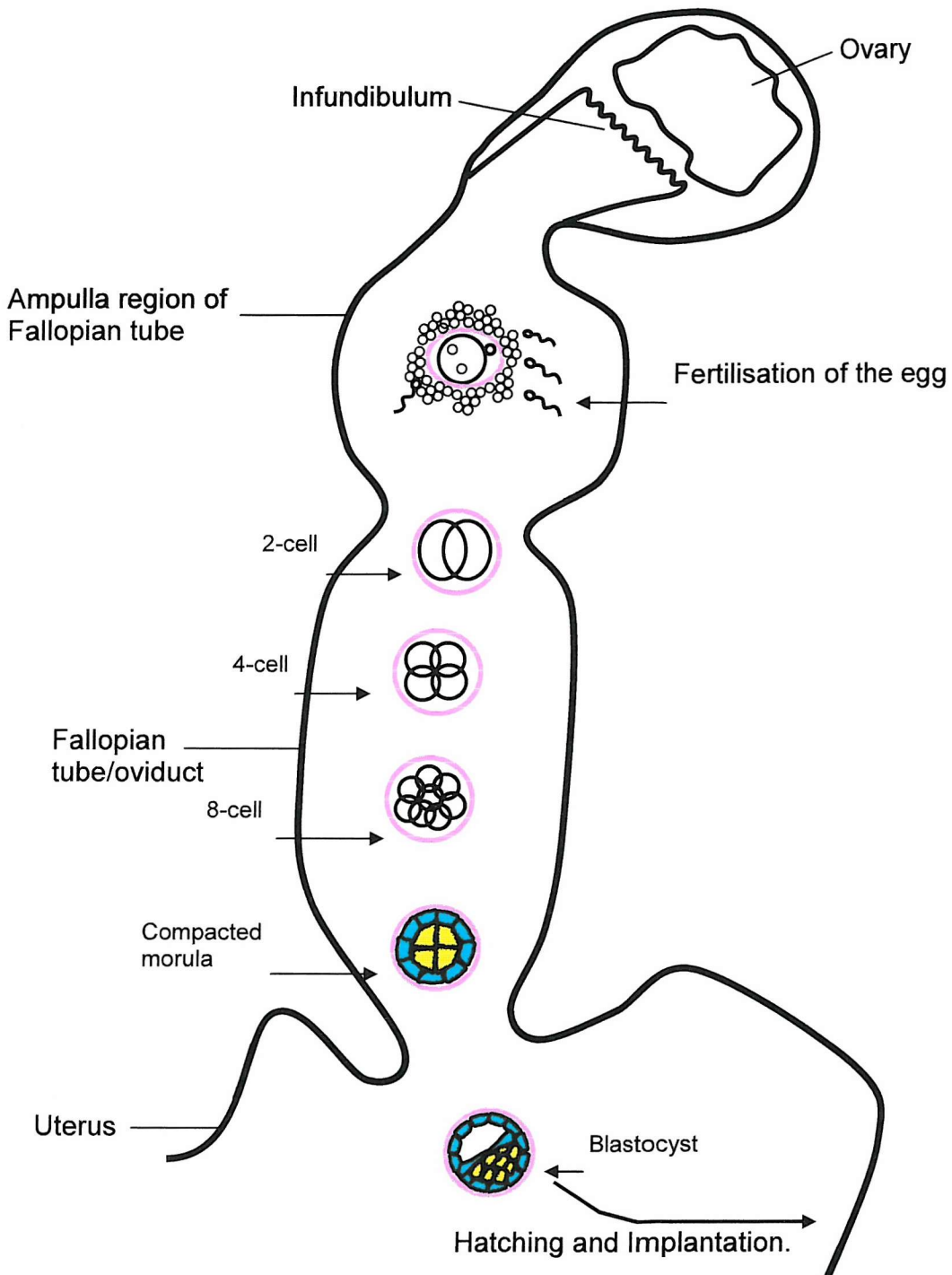

Figure 1.7 Development of a mouse embryo from 1-cell to blastocyst *in vivo* (adapted from Hogan *et al.*, 1994). After fertilisation, the mouse egg undergoes five cleavage divisions to form a structure called the blastocyst at the 32-cell stage of development. The Blastocyst comprises two cell types 1) an outer differentiated and polarised epithelial cell layer ( ), called the trophectoderm (TE; forms the placenta), and 2) inner non-polarised cells ( ), called the inner cell mass (ICM; forms the embryo proper). At the 32-cell stage, fully matured junctional complexes are formed and the TE, is generated. The tight seal between the cells of the TE enables a barrier to form between the internal and external environment of the embryo. Polarised within the basolateral cell membrane, Na^+/K^+-ATPase initiates vectoral fluid transport into the blastocyst to form a cavity called the blastocoel. The expanded blastocyst then "hatches" from its zona pellucida ( ) and implants into the uterine wall, where the embryo continues its development.

1.4.1 The onset of embryogenesis

For several hours post fertilisation, the mouse oocyte undergoes a series of Ca^{2+} oscillations (Cuthbertson & Cobbold, 1985; Kline & Kline, 1992). It is this increase in intracellular Ca^{2+} that results in the resumption of the oocyte cell cycle and signifies the switch from oogenesis to embryogenesis (Jaffe, 1983, Kline & Kline, 1992). In mammals, the resumption of the oocyte cell cycle and its associated changes in intracellular Ca^{2+} levels appear to be largely due the phopholipase C (PLC) mediated hydrolysis of phosphatidylinositol 4,5-bisphosphate (PtdIns(4,5)P_2; Berridge, 1993). Whether the source of PLC is sperm or egg derived has been of much debate (reviewed in Carroll, 2001). Recently, a novel sperm-specific phospholipase C, PLCζ, capable of influencing Ca^{2+} oscillations in mouse eggs has been discovered and is believed to be the "sperm factor" that initiates egg actiation (Saunders *et al.*, 2002). Ca^{2+} release at fertilisation can be inhibited by specifically disrupting InsP3R function (Parrington *et al.*, 1998; Fissore *et al.*, 1999). Considering these experiments and the fact that InsP3R is the most common intracellular Ca^{2+} channel in mouse oocyte, InsP3R is a likely candidate for modulating Ca^{2+} after fertilisation (Parrington *et al.*, 1998).

However, it is also apparent that there are many other factors involved in the control of Ca^{2+} oscillations (reviewed in Carroll, 2001). Indeed, the developmental transition initiated at fertilisation in mammals is a complex signal transduction pathway involving the mitotic kinases, maturation promoting factor (MPF) and MAP kinases (Deng & Shen, 2000; Liu & Yang, 1999). The majority of the evidence from experiments in both mammals and ascidians indicate a central role for MPF in regulating Ca^{2+} oscillations. However the exact interplay between sperm-oocyte membrane fusion, the progression through the cell cycle and the activation of calcium channels and mitotic kinases, resulting in a distinct pattern of Ca^{2+} oscillations, is still a complex process still needed to be unravelled (reviewed in Carroll, 2001).

1.4.2 The transition from maternal to embryonic control of gene expression

During oogenesis, the developing mammalian oocyte synthesizes and accumulates mRNAs and proteins that are vital for supporting and directing early embryonic

development. In the mouse degradation of maternal mRNAs begins prior to ovulation and by the mid-two cell stage the majority of remaining maternal transcripts are degraded (Bachavara *et al.*, 1985; Paynton *et al.*, 1988; Piko & Clegg, 1982). Thus, successful development beyond the early stages of cleavage is dependent upon zygotic gene activation (ZGA) and later the maintenance of appropriate zygotic transcription (reviewed by De Sousa *et al.*, 1998; Latham & Schultz, 2001). The onset of ZGA is one of the first critical events in embryo development and appears to depend upon maternally inherited proteins and their post-translational modifications (Howlett, 1986; Van Blerkom, 1981).

ZGA is characterised by three main events (Telford *et al.*, 1990):

i. The loss of maternally derived mRNA,
ii. The initiation of transcription from the embryonic genome,
iii. The significant alteration in patterns of protein synthesis between one developmental stage and the next.

The timing of ZGA varies between mammalian species (see Table 1.1) but all share the features described above. In the mouse and rat, ZGA was first thought to occur at the 2-cell stage (Flach *et al.*, 1982; Bensuade *et al.*, 1983; Braude *et al.*, 1979). However, evidence has now accumulated that ZGA is a multi-stage progression of gene induction beginning, in the mouse, at the G_2 phase of the 1-cell embryo, continuing up to the 8-cell stage (Bouniol *et al.*, 1995; Latham *et al.*, 1992; Temeles *et al.*, 1994; Tanaka *et al,* 2001; reviewed by Latham & Shultz, 2001). ZGA is now characterised by 1) an initial minor degree of embryonic transcription (at the late 1-cell stage), followed by 2) a major phase of genome activation by the 2-cell stage (coincident with the "block" stage during *in vitro* culture of mouse preimplantation embryos; Whittingham, 1974) and 3) a progressive expression of other genes, including housekeeping genes, being dramatically upregulated at the 8-cell stage (reviewed in Latham & Shultz, 2001).

Table 1.1

Timing of ZGA in mammals

Species	Stage of development
Cow and sheep	8/16- cell
Human	4/8-cell
Rabbit and Pig	4-cell
Mice, rat and hamster	1/2-cell

Maternally inherited proteins, required for early embryonic development, are transcribed and translated from maternal effect genes. Until recently, such genes had not been discovered in mammals. *Mater*, originally identified as an autoantigen implicated in autoimmune ovarian failure, is now known to be vital for early embryonic mouse development beyond the 2-cell stage (Tong & Nelson, 1999; Tong *et al.*, 2000a, b). The exact role of *mater* in early murine development has not yet been established, although it has been inferred that maternal null expression for this gene may cause abnormalities in the embryonic transcriptional machinery (Tong *et al*, 2000b).

Regulation of embryonic transcription appears to be by a variety of mechanisms (including post-translational modifications and the requirement for transcription enhancer sequences) co-ordinated by cell-cycle dependant changes in DNA structure (Howlett, 1986; Van Blerkom, 1981; Wiekowski *et al.*, 1991; Martinez-Salas *et al.*, 1982; Rothstein *et al.*, 1992; reviewed by Latham & Shultz, 2001). Chromatin structure and the types of histones associated with the DNA appear to have a pivotal role both in regulating mRNA recruitment and the stage dependant expression or activation of essential transcription factors (reviewed in Latham & Shultz, 2001).

1.4.3 Compaction and adherens junction formation

Compaction (a calcium dependent process mediated by E-cadherin) is the first adhesion event of the developing embryo and in the mouse begins at the 8-cell stage

(Ducibella & Anderson, 1975). The loosely associated blastomeres of the early 8-cell embryo become adhesive, due to the redistribution and functional activation of E-cadherin (Vestweber *et al.*, 1987). The blastomeres flatten against each other and begin to polarise in their morphology. E-cadherin appears to be an essential component of TE differentiation as embryos null for E-cadherin, although capable of undergoing compaction due to the presence of maternal E-cadherin, are unable to generate a fully functional epithelium and die prior to blastocyst formation (Larue *et al*, 1994; Riethmacher *et al.*, 1995). This phenotype is also seen in null mutant embryos for α-catenin, another component of the cadherin complex (Torres *et al.*, 1997).

In unfertilised and fertilised eggs, E-cadherin is both expressed as 135kDa precursor (Pro-E-cadherin) and as mature 120kDa protein forms (Peyieras *et al.*, 1983; Sefton et al., 1992; Clayton, *et al.*, 1995). E-cadherin, α- and β-catenin mRNA and protein expression can be detected in all preimplantation embryo stages (Sefton *et al.*, 1992; Ohsugi *et al.*, 1996). At the 2-cell stage, E-cadherin expression decreases, corresponding with the degradation of maternal transcripts (Sefton *et al.*, 1992). After the 2-cell stage, E-cadherin mRNA and protein expression increases in accordance with ZGA (Sefton *et al.*, 1992).

The onset of compaction does not appear to be regulated purely by the expression of the AJ proteins, as all AJ components are both expressed and associated with the cell membrane throughout cleavage (Vestweber *et al.*, 1987; Johnson *et al.*, 1986; Fleming *et al.*, 1991; Sefton *et al.*, 1992; Ohsugi *et al.*, 1996). Moreover, if protein synthesis is inhibited, using anisomycin or puromycin, timing of compaction is advanced (*Levy et* al., 1986). Timing of compaction at the 8-cell stage appears to be regulated by post-translational modifications of existing proteins, as neither transcription nor translation is required at this point in embryo development for it to occur (Kidder & McLachlin, 1985; Levy *et al.*, 1986). Protein phosphorylation appears to be an important initiation mechanism of compaction, supported by the evidence that phorbol ester and diacylglycerides (protein kinase activators), and staurosporine or 6-DMAP (kinase

inhibitors) can induce premature compaction in 4-cell embryos (Winkel *et al.*, 1990; O'Sullivan *et al.*, 1993; Aghion *et al.*, 1994).

It is now known that PKCα isoform redistributes to cell contact sites at the onset of compaction, indicating a possible involvement of this isoform with the initiation of this event (Pauken & Capco, 1999). Phosphorylation of E-cadherin is also known to occur immediately prior to compaction (Sefton *et al.*, 1992), thus providing some suggestion that this protein may be a PKC substrate. However, manipulation of compaction timing events does not appear to affect post-translational modification of E-cadherin (Sefton *et al.*, 1996). Recent evidence suggests that β-catenin may be a PKC substrate at compaction as induction of premature compaction also correlates with β-catenin phosphorylation on serine/threonine residues (Pauken & Capco, 1999). However, it has also been proposed that tyrosine phosphorylation of β-catenin is important in regulating a non-functional pool of the E-cadherin-catenin complex prior to compaction thus providing another potential regulation mechanism for compaction (Ohsugi *et al.*, 1996, 1999).

1.4.3.1 Cell polarity at compaction

Blastomere polarisation at compaction occurs by both surface and cytoplasmic components becoming asymmetrically distributed, creating apical and basolateral domains (reviewed by Fleming *et al*, 1998; Gueth-Hallonet & Maro, 1992). Around the time of compaction, microvilli become concentrated at the apical outward-facing membrane surface, polymerised microfilaments and microtubules, along with endosomes and clathrin-coated vesicles, also become localised in the apical cytoplasm (Reeve, 1981; Fleming & Pickering, 1985; Maro *et al.*, 1985). In addition, many actin-associated proteins are found in the apico-lateral region of each blastomere (Sobel, 1983; Lehtonen *et al.*, 1988; Slager *et al.*, 1992), mitochondria become cortically localised (Batten *et al.*, 1987) and the nucleus becomes located in the basal cytoplasm (Reeve & Kelly, 1983). The reorganisation of the actin cytoskeleton, in conjunction with E-cadherin mediated adhesion at compaction, indicates a strong link between adhesion and polarisation and it is now known that these events are mediated by activation of the rho

family of GTPases (Clayton *et al.*, 1999). The cellular reorganisation that occurs at this developmental stage now defines the initiation of TE differentiation and will lead to the formation of the ICM (reviewed by Fleming *et al.*, 2000).

1.4.4 Post compaction development

1.4.4.1 The 16-cell embryo and the generation of two cell lineages

Upon differentiative division of a proportion of 8-cell blastomeres, forming a 16-cell embryo, polar and non-polar cells are created. For instance, the daughter cells inheriting the apical half will retain a polar phenotype and the inheritance of the basal domain by the other daughter cell, will result in an non-polar phenotype (Figure 1.8; Johnson & Ziomek, 1981).

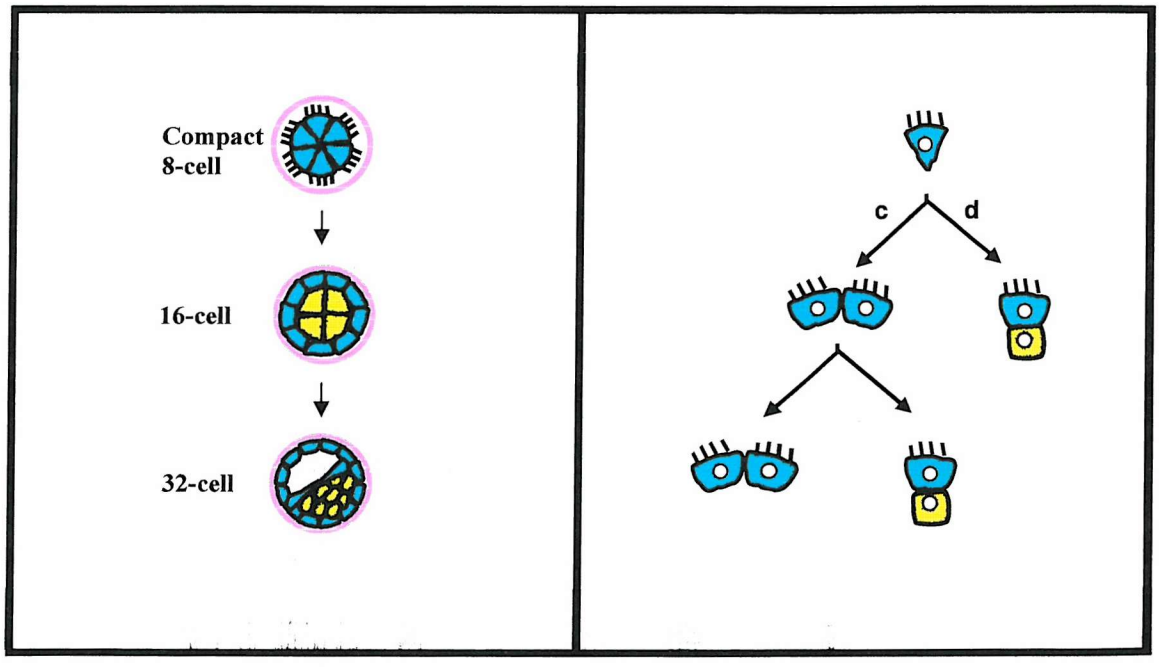

Figure 1.8 Generation of TE and ICM lineages (adapted from Fleming *et al.*, 1998). A schematic representation of cell polarity and cell differentiation in the early mouse embryo. Whole embryos are depicted on the left. TE lineages and ICM lineages are also shown. Conservative (**c**) and differentiative (**d**) cell divisions are illustrated on the right.

Most 8-cell blastomeres divide differentiatively (i.e. along the axis perpendicular to the axis of polarity). However, a small number of blastomeres may divide

conservatively (i.e. parallel to the axis of polarity) and hence both daughter blastomeres will inherit part of the apical pole and therefore both will remain polarised (Figure 1.8; Johnson & Ziomek, 1981b). These two patterns of division are the basis for establishment of the TE and ICM lineages of the blastocyst. The blastomeres of the 16- to 32-cell embryo are still totipotent despite their phenotypic differences (Ziomek *et al.*, 1982), thus providing the embryo with developmental plasticity during blastocyst formation (reviewed by Guth-Hallonet & Maro, 1992). During the fifth cell cycle (16-cell), the outer cells continue to extend their polarised phenotype (gradually maturing into TE) whereas the inner non-polar cells acquire the typical characteristics of the ICM lineage (Figure 1.9; reviewed by Fleming *et al.*, 1998).

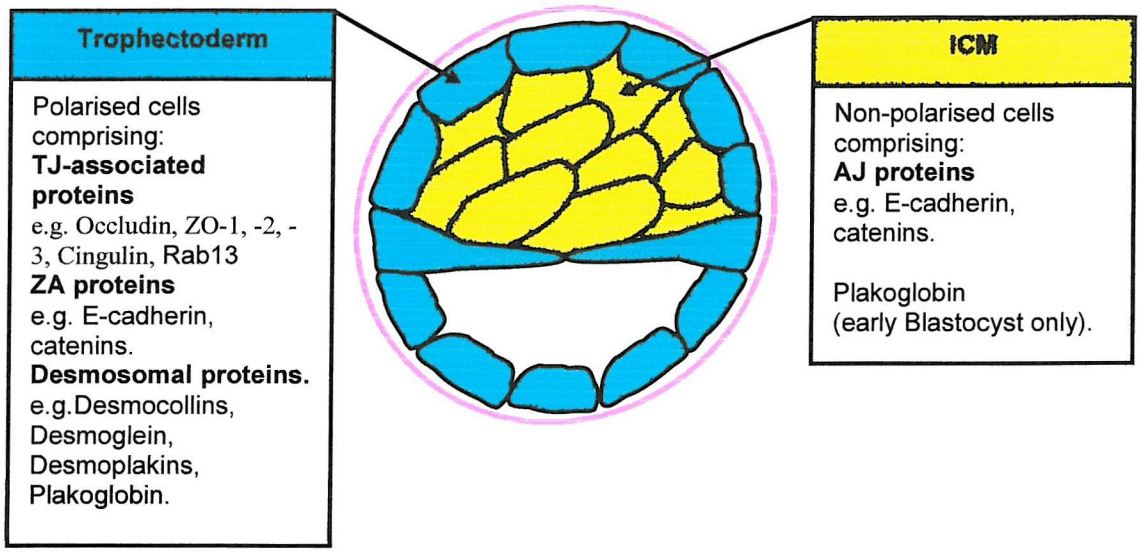

Figure 1.9 Characteristics of TE and ICM cells. Taken from Collins and Fleming, 1995.

The time and stage of development when lineages become unambiguously separated has been analysed with the microinjection of cell lineage tracers (Cruz & Pederson, 1985; Pederson *et al.*, 1986; Dyce *et al.*, 1987). Prior to these studies it was not known whether blastomere pluripotency, during TE maturation, was maintained after the 16- to 32-cell stage transition (Dyce *et al.*, 1987). Indeed, microinjection of horseradish peroxidase (HRP), as a lineage marker, showed that most of the 32-cell

stage TE cells only gave rise to more TE cells (Cruz & Pederson, 1985; Perderson *et al*, 1986). However, ICM cell pluripotency after the 32-cell stage, in the study by Cruz & Pederson (1985), was also shown to contribute to TE lineage. ICM derived TE cells after the 32-cell stage was not supported by other studies (Papaionnou, 1982; Rossant *et al.*, 1983). Indeed, when the entire TE of nascent blastocysts was labelled with fluorescent latex microparticles (Dyce *et al.*, 1987), 80-90% of embryos were found to maintain the distinct lineages acquired at the 32-cell stage, while the remaining embryos were shown to contain one or two cells from the opposite lineage.

1.4.4.2 The 32-cell embryo and completion of epithelial biogenesis

Upon generation of the 32-cell embryo, epithelial integrity increases and the process of blastocoel formation begins. Blastocyst formation is the result of Na^+/K^+-ATPase activity within the TE basolateral membranes (Vorbrodt *et al.*, 1977; Watson and Kidder, 1988). The timing of this developmental process is crucial for ICM development as the blastocoel generates a chemically regulated source of proteins, amino acids, sugars, growth factors and organic and inorganic ions required for further differentiation of the ICM prior to and immediately after implantation.

Na^+/K^+-ATPase is an important component in blastocyst formation comprising three subunit types, α, β and γ. The α-subunit, for which there are four known isoforms, is responsible for ion transport, whereas the β-subunit, for which there are 3 known isoforms, is important in the processing and insertion into the plasma membrane (Herrera *et al.*, 1987; Geering, 1991). The exact role of the γ-subunit has not yet been elucidated (Collins & Leszyk, 1987; Mercer *et al.*, 1993; Jones *et al.*, 1997).

Although the α-subunit of the Na^+/K^+-ATPase is known to be transcribed in early cleavage, the glycosylated β-subunit is expressed much later at the late morula stage and appears to be a key regulator in ATPase activity (Gardiner *et al.*, 1990; Watson *et al.*, 1990). It is now known that multiple subunit isoforms (and potentially multiple isozymes) of Na^+/K^+ ATPase are present in mouse preimplantation embryos (MacPhee *et al.*, 2000). $\alpha_1\beta_1$ appears to be the major isozyme involved in blastocyst formation as it

is the only one found in the plasma membrane of trophectoderm cells. However, it is now known that α_3, β_2 and β_3 isoforms are also present in the early embryo the significance of which is yet to be established (MacPhee *et al.*, 2000).

Jones *et al.*, (1997) have reported that the γ-subunit in mice accumulates from the 8-cell stage up to the blastocyst stage. It is localised to all the surfaces of each blastomere and is not specific to either the TE or ICM lineage. Moreover, inhibition of this subunit, using antisense oligonucleotides, did result in an inhibition of ouabain-sensitive K^+ transport and a concomitant delay in cavitation. However, these effects appeared to be independent of Na^+/K^+-ATPase expression.

Use of the specific inhibitor of Na^+/K^+-ATPase, ouabain, indicates that this ATPase indeed is important in mediating cavitation (DiZio & Tasco, 1977; Wiley, 1984; Manejwala *et al.*, 1989). Moreover, ion exchange experiments in embryo culture medium indicate that it is Na^+ ions that are the major contributors to osmotic gradients across the TE layer and this may involve Na^+ channels and Na^+/K^+ exchangers (Manejwala *et al.*, 1989). In addition to Na^+/K^+ ATPases, a number of the aquaporin (AQP) protein family members have also been detected at the mRNA level during mouse preimplantation development (Offenberg *et al.*, 2000). These proteins belong to a family of membrane-associated proteins involved in the formation of molecular water channels. mRNA for AQPs 1, 3, 5, 6, 7 and 9 have been found expressed throughout cleavage whereas AQP 8 is only detectable from the morula stage onwards (Offenberg *et al.*, 2000). It is therefore possible that some of these proteins, especially AQP 8, may be important in blastocoel fluid accumulation.

Vectorial transport of metabolites required for further development of the ICM may also be regulated by a Na^+-independent glucose cotransporter, GLUT (Hewitson & Leese, 1993; Brison *et al.*, 1993; Pantaleon & Kaye, 1998). From a family of seven isoforms, five are now known to be functional transporters (GLUT1-5). Each transporter has different affinity and kinetic properties and a varied pattern of expression across a range of mature tissues (reviewed in Pantaleon & Kaye, 1998). Early studies into

GLUTs in the mouse preimplantation embryo showed that mRNA encoding GLUT1 could be found in all cleavage stages, whereas GLUT2 was detected from the 8-cell stage onwards (Hogan *et* al., 1994). GLUT2 has been shown to be localised to the basolateral membranes of the TE and could regulate glucose delivery to the blastocoel and ICM (Ahhayan *et al.*, 1992; Hewitson & Leese, 1993; Brison *et al.*, 1993). Interestingly, GLUT3 has also been identified in apical membranes of the TE whereas, GLUT1 has been shown to localise to the basolateral membranes of the TE and uniformly in the ICM membranes. Indeed, GLUT3 has been shown to be vital to blastocyst formation (Pantaleon *et al.*, 1997). In addition to the GLUTs, endocytic activity within the TE cells is also increased at the 32-cell stage. The majority of this endocytosis occurs at the apical surface of these cells, therefore providing additional means of delivery of metabolic components required for further ICM development (Fleming & Pickering, 1985; Fleming & Goodall, 1986; Pemble & Kaye, 1986).

Also at the 32-cell stage, desmosomal components start to assemble (Fleming *et al.*, 1991; Collins *et al.*, 1995). Desmosomes are cell-cell junctions that associate with the cell cytokeratin filaments. The main components of this junction are the transmembrane proteins from the cadherin superfamily, desmocollins and desmogleins and the cytoplasmic proteins plakoglobin, desmoplakin and desmophilins, that link the complex to the cytokeritin network. Desmosome formation occurs at cavitation and it is thought that this junction may stabilise the newly generated epithelium in the process of blastocoel expansion (Fleming *et al.*, 1991).

1.5 Biogenesis of tight junctions in the mouse preimplantation embryo

TJ formation is also an important factor in generating a functional TE epithelium and therefore, is a significant contributor to the initiation of blastocoel formation. The TJ provides a permeability seal and becomes fully functional at the 32-cell stage of mouse embryo development. Maturation of the TJ complex at this stage of development coincides with the polarisation of many membrane proteins required for vectorial transport across the TE.

As seen in the preimplantation embryo, TJ formation occurs in a precise and sequential manner. In the mouse, TJ assembly begins with ZO-1α^-, which assembles at the TJ 1-2 hours post compaction (Fleming *et al.*, 1989; Sheth *et al.*, 1997). ZO-1α^- mRNA and protein can be detected throughout early cleavage and its assembly to the apico-lateral junctional complex (AJC) is dependent on E-cadherin adhesion. If E-cadherin adhesion is blocked using a specific neutralising antibody, ZO-1α^- assembly to the membrane is delayed and its site of localisation is altered (Fleming *et al.*, 1989; Sheth *et al.*, 1997).

Recent evidence suggests that ZO-1α^- co-localises with rab13 from compaction onwards (Sheth *et al.*, 2000a). From this work, immunofluorescence and expression data indicate that rab13 may have a role in the specification of the AJC site and later in the segregation of the TJ from this complex (Sheth *et al.*, 2000a).

During the 16-cell stage (~12 hours after compaction) cingulin localises at the TJ also co-localising with ZO-1α^- (Citi *et al*,.1988; Citi *et al.*, 1989; Fleming *et al.*, 1993). Although cingulin is expressed from both the maternal and zygotic genome, it appears that only the zygotically expressed protein has a role in TJ formation (Javed *et al.*, 1993). High maternal expression in unfertilised eggs indicates that cingulin may have a role in oogenesis, however a particular role has not yet been elucidated.

Finally, at the 32-cell stage, the ZO-1α^+ isoform is expressed *de* novo at the membrane after intracellular association with occludin (Sheth *et al.*, 1997, 2000b). Immediately prior to TJ assembly, ZO-1α^+ can be detected in the Golgi and hence its membrane assembly is sensitive to brefeldin A treatment (an inhibitor of Golgi to cell surface transport; Sheth *et al.*, 1997). It is at the Golgi that ZO-1α^+ and occludin co-localise. Unlike ZO-1α^+, occludin mRNA and protein are detectable throughout cleavage but its membrane assembly appears dependent upon ZO-1α^+ mRNA and protein expression at the late 16- and early 32-cell stage of mouse embryo development (Sheth *et al.*, 2000b).

The sequential assembly at the TJ is known to correlate with the sequential expression of the proteins that form this complex, with the exception of occludin, thus, ZO-1α^- mRNA synthesis is the first to be detected, then cingulin and finally ZO-1α^+ (Javed *et al.*, 1993; Fleming *et al.*, 1998). The membrane assembly of occludin does not appear to be controlled by expression alone but is dependent upon post-translational modifications (Sheth *et al.*, 2000b).

1.5.1 Claudins and JAM in the mouse preimplantation embryo

The majority of the work to date on the claudins and JAM has been conducted on tissues and cell lines. Embryo studies show how this model, unlike cell lines, can reveal substages in epithelial differentiation. Expression patterns for one TJ transmembrane protein, occludin, had already been examined and therefore, it was important to examine how JAM and claudins fitted into our current knowledge of TJ biogenesis.

The aims of my research were:

i. To investigate timing of mRNA transcription for JAM-1, claudin-1 and claudin-3.
ii. To study protein expression and localisation of JAM-1, claudin-1 and claudin-3.
iii. To assess how claudin-1 peptides, JAM-1 neutralising antibodies and RNA*i* for both these components effect mouse preimplantation embryo development.

Chapter 2

Material and methods

2.1 Embryo culture

2.1.1 Superovulation

Four- to five- week old MF1 mice (Olac-derived, Southampton University Animal House) were superovulated by intraperitoneal injections of 5-10 iu/0.1-0.2ml pregnant mares serum (PMS, Folligon, Intervet) and then 5-10iu/0.1-0.2ml human chorionic gonadotrophin (hCG, Chorulon, Intervet) 48 hours later. Immediately following the hCG injection, females were either left to mate with sexually mature males of the same strain or left unmated for unfertilised egg collection. For collection of fertilised eggs and staged embryos, mated females were checked for copulation plugs the morning after hCG injection.

2.1.2 Embryo collection and culture

Females were culled by cervical dislocation and the oviducts were dissected out and placed in pre-warmed sterile 0.85% NaCl solution. Unfertilised or fertilised eggs were collected the morning following hCG injection. Cumulus masses were obtained by tearing the ampulla of the oviduct and eggs were released from the masses by treatment with hyaluronidase (100mM for 10 minutes) followed by washes in H6 plus 4mg/ml BSA (H6-BSA, Whittingham and Fulton, 1978, see Appendix I) and a brief culture in T6 plus 4mg/ml BSA (T6-BSA, see Appendix I). For collection of staged embryos, oviducts were flushed from the infrindibulum using a blunt-ended needle attached to a 1ml syringe containing warm H6-BSA. 2-cell embryos (48hrs post hCG) or 8-cell embryos (72 hrs post hCG) were flushed from dissected oviducts. Flushed embryos continued to develop in vitro in T6-BSA drops covered in light paraffin oil (J.M. Loveridge plc) in sterile culture dishes (Falcon). Cultured embryos were maintained in a 37°C incubator with 5% CO_2 in the air.

2.1.3 Embryo staging

Fertilised eggs were collected 18-20 hours post hCG and were checked for the presence of two pronuclei. 2-cell, 4-cell early and compact 8-cell embryos were

identified using morphological criteria. 16-cell embryos were staged by isolating freshly compacting 8-cell embryos and culturing them for a further 10-12 hours and late morula (~32 cell-stage) were staged by culturing compact 8-cells for 24 hours. Cell number was confirmed using propidium iodide/Hoechst staining described in section 2.9.3.

2.1.4 1/4 - 2/8 couplet experiments for precise blastomere staging

Late 4-cell embryos were treated to remove the zona pellucida (section 2.6.2) and incubated in Ca^{2+} free medium for 15 minutes prior to disaggregation into single blastomeres using a small, heat-polished glass micropipette (section 2.1.6). Groups of five 1/4 blastomeres were cultured in individual drops of T6-BSA in Sterilin dishes and were checked hourly for division into 2/8 couplets. Newly formed 2/8 couplets were then designated as 0 hour 2/8 couplets.

2.1.5 0-hour 8-cell and compact 8-cell embryos

Time course experiments, needed for analysing aspects of epithelial biogenesis, required pools of embryos to be developmentally synchronised. Events leading up to compaction were analysed using recently divided 8-cell embryos. These embryos were observed as they divided from 4-cell to 8-cell (~65 hours post hCG) and at hourly intervals newly developed 8-cell embryos were deemed "0-hour 8-cell embryos". Events leading up to cavitation were analysed in a similar manner using recently compacted 8-cell embryos. Pools of embryos were observed as they entered compaction (~70 hours post hCG) and at hourly intervals newly compacted 8-cell embryos were deemed "0-hour compact 8-cell embryos".

2.1.6 Preparation of heat-polished micropipettes

Glass capillaries (Clark Electromedical, type GC100-15) were pulled over the flame of an alcohol wick lamp and then broken off in the centre to form two micropipettes. Each micropipette was then placed in a microforge (Fonbrune) with the pulled tip placed in contact with a preformed glass bead on the filament. The filament was then heated until the micropipette had fused with the bead. At this point, the filament was turned off and the micropipette was retracted to form a clean break at the tip. The internal bore of the micropipette was made to be approximately

50μM. The tip of the micropipette was then flame-polished by placing it close to the heated filament.

2.2 Isolation of mRNA from preimplantation mouse embryos and mouse tissue

2.2.1 mRNA isolation using messenger affinity paper (mAP)

To prevent DNA contamination of the RNA samples, all solutions used for RNA preparation were pre-treated with 400mJ cm_{-2} UV-irradiation (spectrolinker XL-1000, Scotlab). Single or multiple embryos, cultured to the appropriate stage, were then transferred by mouth pipette from the culture dish onto 2mm squares of mAP paper (Amersham), presoaked in 0.5M NaCl, in a minimal volume of T6-BSA media (Collins and Fleming, 1995b). Poly(A)$^+$ RNA was then prepared by lysing the cells in 10 x 1μl drops of 4M guanidinium thiocyanate in Tris-HCl (pH 7.5) and washed twice in 10 x 1μl drops of 0.5M NaCl. The mAP paper was then placed in 400μl of 0.5M NaCl in a 0.5ml microfuge tube (Advanced Biotechnologies). The mAP paper was washed by vortexing the eppendorf tube and the liquid removed using a sterile pulled pipette and suction tubing. These washes were repeated twice with 0.5M NaCl and then twice again using 400μl 80% ethanol. Samples could be stored at -70°C for up to 14 days (for more information on this method see Collins *et al.*, 1995).

2.2.2 mRNA isolation using Dynabeads Oligo $(dT)_{25}$

As with the mAP method, all solutions used for RNA preparation were pre-treated with 400mJ cm_{-2} UV-irradiation (spectrolinker XL-1000, Scotlab). Single or multiple embryos, cultured to the appropriate stage, were then washed three times in H6-PVP (Appendix I) and then taken in a 1μl drop of sterile phosphate buffered solution (PBS) and snap frozen on dry ice in siliconised 0.5ml microfuge tubes (Costar). Samples were then transferred to a -70°C freezer for storage until required for RT-PCR. Immediately prior to cDNA amplification, embryo samples were removed from the –70°C freezer and placed on dry ice. The Dynabeads mRNA DIRECT Kit (Dynal, UK) was used for isolation of Poly(A)$^+$ RNA according to the manufacturer's instructions with minor modifications (Wrenzycki *et al* 1998 a, b; Eckert and Niemann, 1998).

2.2.3 Isolation of total RNA from mouse tissues

Tissue samples were dissected from freshly culled mice, cut into ~1mm cubes and snap frozen in microfuge tubes. Tissue samples were homogenised in buffer provided in the RNeasy miniprep kit (Qiagen). RNA was isolated using the same kit following the protocol specified for animal tissues. RNA concentration was calculated using a U-2000 spectrophotometer by converting the optical density reading into amount of RNA in the sample (Appendix IV). Samples were treated with DNase enzyme at 37°C for 60 minutes.

2.3 RT-PCR

2.3.1 Primer design

Primers were designed manually with the aid of DNAstar (lazergene), or using a DOS version of Oligo (a primer design program). Nested claudin-1 primers (cld1/7-cld1/10) were adapted for mouse from human claudin-1 primers originally designed by Dr. M. Ghassemifar (University of Southampton). Occludin primers were designed and provided by Dr B. Sheth (University of Southampton). Poly-A-polymerase, JAM and luciferase primers were provided by Dr J. Eckert (University of Southampton). α- catenin sequences were taken from Ohusugi *et al* (1996). See Tables 2.1 and 2.2 for primer details.

2.3.2 Definitions of controls used for RT-PCR

Various controls were used for each RT-PCR experiment to assure that amplification products were not as a result of DNA contamination:

mAP only – Embryonic/Tissue template had not been added to the mAP. The mAP only control was then processed alongside the embryo samples.

Minus RT – RT enzyme was not added to the RT reaction. mRNA template and all other master mix components were present.

Master mix only – Contained all reaction components excluding any template.

Confirmation of negative results was accounted for with one or more of the following controls:

Tissue – RNA isolated from mature mouse tissue was used in place of the embryonic mRNA.

Poly-A polymerase – Highly abundant, endogenous, Poly-A polymerase mRNA was amplified alongside other templates to control for RNA degradation during sample collection.

Luciferase – Exogenously added luciferase mRNA was primed to control against mRNA degradation during dynabead extraction or the RT-PCR procedure.

Table 2.1

RT-PCR primers

	Primer sequences	Optimal annealing temperature (°C)	Fragment size (bp)
claudin-1 (nested)	**sense outer primer (cld1/1)** 5′-atcggctccatcgtcagc-3′ **antisense outer primer (cld1/2)** 5′-actagaaggtgttggctt-3′ **sense inner primer (cld1/3)** 5′-caacatcgtgaccgctca-3′ **antisense inner primer (cld1/4)** 5′-ataaggccgtggtgttg-3′	55 55	563 484
claudin-1	**sense primer (cld1/5)** 5′-tgggtttcatcctggcttctc-3′ **antisense primer (cld1/6)** 5′-tgacagccatccacatcttct-3′	56	336
claudin-1 (nested)	**sense outer primer (cld1/7)** 5′-atcctggcttctctgggatgga-3′ **antisense outer primer (cld1/8)** 5′-gataaggccgtggtgttgggta-3′ **sense inner primer (cld1/9)** 5′-tgctggggacaacatcgtga-3′ **antisense inner primer (cld1/10)** 5′-gaaagtaggacacctcccaga-3′	68 62	564 445
claudin-3	**Sense primer (cld3/1)** 5′-ttttcctgttggcggctctg-3′ **Antisense primer (cld3/2)** 5′-cgtagtccttgcggtcgtag-3′	62	269
JAM-1	**Sense primer (JAM1/1)** 5′-gaggggaaagccgggaggaaactgt-3′ **Antisense primer (JAM1/2)** 5′-caaaggctgtcacggggtcaaagat-3′	60	607

Table 2.2
Primers continued

	Primer sequences	Optimal annealing temperature (°C)	Fragment size (bp)
occludin	**sense outer primer (occ/1)** 5'-agtcaacacctctggtgc-3' **antisense outer primer (occ/2)** 5'-caggcagatgcacctctc-3' **sense inner primer (occ/3)** 5–agtcaacacctctggtgc-3' **antisense inner primer (occ/4)** 5'-caggcagatgcacctctc-3'	55 48	588 512
poly-A polymerase	**5'-sense primer (polyA/1)** 5'-gtttcctcggtggtgtttcctgggctatgc-3' **3'-antisense primer (polyA/2)** 5'-tggagttctgttgtgggtatgctggtgtaa-3'	55	252
α-catenin	**5'-sense primer (Cata/1)** 5'-gccctactgttgggcag-3' **3'-antisense primer (Cata/2)** 5'-gcagcagagtccattag-3'	60	223
luciferase	**5'-sense primer (luc/1)** 5'-acttcgaaatgtccgttcgg-3' **3'-antisense primer (luc/2)** 5'-tccggaatgatttgattgcc-3'	56	600

2.3.3 cDNA synthesis from mAP embryo samples

The mAP paper and bound poly(A)$^+$ RNA were dried at room temperature and the reverse transcriptase reaction master mix was added to the microfuge tube (Advanced Biotechnologies). The RT-reaction was performed as follows: first-strand cDNA synthesis was primed either with random hexamers (Perkin Elmer) or specific 3'-antisense primers (Oswel DNA service) for the mRNA of interest. The 20µl reaction contained either 2.5µM random hexamers or 1µM of the specific antisense primer, 1mM of each deoxynucleotide (Pharmacia), 30U RNAguard ribonuclease inhibitor (Human Placenta derived; Pharmacia) and 200 units M-MLV reverse transcriptase in buffer supplied (Gibco BRL). The reaction was incubated for 10 minutes at room temperature, 45 minutes at 37°C and 5 minutes at 95°C.

2.3.4 Amplification of cDNA of interest – mAP method

All 20μl of the RT reaction was then placed in fresh tubes for amplification of the cDNA. The volume was made up to 50μl by adding 4.5μl x 10 Vent buffer (New England Biolabs), 1μM of the 5'-sense outer primer and 1μM of the 3'-antisense outer primer (Tables 2.1 and 2.2) and either diethylpyrocarbonate (DEPC)-treated (Sigma) milli-Q (Millipore) or Analar water (Anachem). False priming was prevented by using "hot start" with Ampliwax PCR gems (Perkin Elmer) following the manufacturer's protocol. 1U Vent DNA polymerase (New England Biolabs) in 5μl of 1 x Vent buffer was added above the re-solidified wax. For amplification temperatures and times see individual results chapters.

For nested PCR, a second DNA-amplification reaction was set up similar to the first but using inner primers and 2-5μl of the first stage PCR reaction as the template. Hot start and amplification steps were carried out as before, with the appropriate annealing temperatures used for the inner primer pairs (Tables 2.1 and 2.2).

A typical PCR program was carried out for 30-40 cycles of:

1) 95°C for 30 seconds
2) specific annealing temperature for 30 seconds
3) 72°C for 30-40 seconds (depending on the length of the amplification product)

2.3.5 cDNA synthesis from embryo samples after Dynabead extraction

RNA was eluted in either 9μl or 4μl Analar water with no further dilution of the mRNA prior to addition to a 20μl or 10μl RT reaction, respectively. cDNA synthesis was primed either with random hexamers (Perkin Elmer) or with specific 3'-antisense outer primers (Oswel DNA service). The 10μl and 20μl reactions consisted of 1x RT buffer (Perkin-Elmer), 5mM $MgCl_2$, 1mM of each dNTP (Amersham), 2.5 μM random hexamers or 1μM specific antisense primer, 10 U Rnase inhibitor (Perkin-Elmer) and 25U MMLV reverse transcriptase (Perkin-Elmer). The reaction was incubated for 10 minutes at 25°C, 60 minutes at 42°C and 5 minutes at 99°C and then cooled to 4°C. Alternatively, superscript II (Gibco BRL),

or Sensiscript$^{(TM)}$ (Qiagen), reverse transcriptase were used to amplify cDNA following the maufacturer's instructions.

2.3.6 Amplification of a cDNA of interest- Dynabead method

For the 20µl RT reactions, 2-20µl was then transferred to a 50µl PCR reaction as a template. In the case of the 10µl RT reactions, all of the volume was transferred into a 100µl PCR reaction. In both PCR reactions, 1x PCR buffer (Gibco BRL), 1.5mM MgCl, 200µM of each dNTP and 1µM of each sequence specific primer (Tables 2.1 and 2.2) were used. During the hot start (99°C for 5 minutes and 72°C for 2 minutes), 2U *Taq* DNA polymerase (Gibco) were added at 72°C.

Amplification was carried out for 35-40 cycles of:

1) 95°C for 30 seconds
2) specific annealing temperature for 30 seconds
3) 72°C for 30-40 seconds

Followed by a 5 minute final extension at 72°C.

2.4 Visualisation of amplification products

Reaction products (10µl) from all PCR methods were run on 0.5 x TBE 1-2% agarose gels stained with ethidium bromide.

2.5 Cloning

Recently amplified PCR products were ran on a 1% agarose gel and subsequently purified, using the QIAquick gel extraction kit (Qiagen). Purified PCR products were ligated into a pGEM-T Easy vector (Promega), according to the manufacturer's protocol. Ligation products were then ethanol precipitated (section 2.5.1), resuspended in sterile water and transfected into DH5α cells via electroporation (section 2.5.2).

Electroporated DH5α cells were then transferred to a 15ml falcon tube and incubated for an hour at 37°C and 200 rpm, on a shaker (Jencons; Labline incubator shaker). 10µl, 50µl and 100µl of cells were then transferred to agar-ampicillin plates

coated with IPTG and X-gal (Appendix II) and were incubated for ~20 hours at 37°C. Individual white colonies were picked and grown in 5ml LB-ampicillin media in 50ml Falcon tubes, overnight on a shaker at 37°C and 250 rpm. Meanwhile, a stock agar-ampicillin plate, containing all potential clones, was cultured and kept at 4°C for up to 1 week.

Ligated plasmids were then isolated from the DH5α cells using a Hybaid recovery™ plasmid mini prep kit. Plasmids were digested with the appropriate restriction enzyme, chosen to cut both the insert and the plasmid at one site only. Appropriate clones were chosen after running the digested plasmid products on an agarose gel and observing the molecular weights of the cut products. The nucleotide sequence of the cDNA inserts was confirmed by sequencing (section 2.7). Cloned cells containing a plasmid of interest were then grown, from the stock plate, in 50ml Falcon tubes, overnight on a shaker at 37°C and 250 rpm and either frozen as stock cells or used for double stranded RNA (dsRNA) synthesis (section 2.6).

2.5.1 Ethanol precipitation method after ligation

The ligation reaction was precipitated in the presence of the following components:

1µl - 3M sodium acetate
25µl - 100% ethanol
1µl - pellet paint (Novagen)

Ligation samples were then incubated at -80°C for 15 minutes and were then centrifuged at maximum speed for 10 minutes. The supernatant was then discarded and the pellet was then washed in 200µl of 70% ethanol and centrifuged for a further 10 minutes. All liquid was removed and the pellet was then dried at r.t. for 30 minutes and subsequently resuspended in 6µl of sterile mili-Q water.

2.5.2 Electroporation

2.5µl of DNA from the resuspended ligation reaction (2.5.1) was added to 40µl of DH5α cells in an eppendorf (on ice). The DNA/cell mixture was mixed and transferred to an electroporation cuvette (Genepulser cuvette, 0.1cm electrode gap, Biorad). A 1.8KV pulse was delivered to the cuvette using a Biorad *E.coli* pulser and Gene pulser (Capacitance 25µFD, Resistance 800 Ω). Cells were then immediately resuspended in 1ml SOC/Mg/glucose medium (Appendix I).

2.6 Synthesis of dsRNA for RNA*i*

Plasmids were isolated from cloned cells, as described previously, using the Hybaid recovery™ plasmid mini prep kit. An appropriate restriction enzyme, which cuts only the pGEM-T easy vector at one site (close to, but downstream of the transcription start site and cloned insert), was used to linearise the plasmid prior to RNA transciption. This was done for upper and lower strands of the plasmid in separate reactions.

Linearised plasmids were protein digested in the following reaction and incubated at 50°C for 50minutes:

1µl – Proteinase K (10mg/ml stock; Melford)
1µl - 1M Tris-Cl (pH8; Sigma)
1µl 0.2M $CaCl_2$
5µl 10% SDS
92µl DNA digest

The reaction mix was then phenol/chloroform extracted, back extracted in 1x Tris-EDTA buffer, chloroform extracted and then ethanol precipitated. The dried pellet was then resuspended in 4µl of Analar water and assembled into a transcription reaction. Transcription was accomplished, following the manufacturer's protocol, using a Riboprobe® *in vitro* transcription kit (Promega), using either a T7 or SP6 polymerase enzyme for upper and lower strand synthesis, respectively. Reactions were then incubated in 1µl of DNAase enzyme for 20 minutes at 37°C.

ssRNA was then Phenol/chloroform extracted (section 2.6.1) and resuspended in 25µl Analar water. ssRNA was then annealed to create a dsRNA by adding equal amounts of sense and antisense RNA, heating for 5 minutes at 95°C and then leaving to cool at room temperature (overnight) prior to cooling further to 4°C. 1µl dsRNA was run on a RNAase free gel, alongside 0.5µl ssRNA, prior to aliquoting and storing at ¯20°C.

2.6.1 Phenol/chloroform extraction of ssRNA

The following components were added together:

18µl – transcription reaction

75µl – 1M ammonium acetate, 100mM EDTA

117µl – Analar water (Anachem)

To the above mixture, 150µl of phenol/chloroform and the aqueous fraction was removed and kept separate. The phenol/chloroform reaction was then back extracted with 50µl of analar H_2O and again the aqueous fraction was removed and pooled with the previously collected fraction. To the pooled aqueous fraction, an equal volume of isopropanol was added and the mixture was then incubated at ¯20°C for 1 hour. The mixture was centrifuged for 30 minutes at 13000g at 4°C. The isopropanol was then discarded and the pellet was dried at r.t prior ro resuspension in analar H_2O.

2.7 Sequencing

Claudin-1 was sequenced directly from the 2nd stage PCR product (Oswel DNA service). JAM-1 and claudin-3 and all other products were sequenced after cutting out the product from agarose gel using the QIAquick gel extraction protocol (Qiagen). Purified product was then prepared for sequencing using BigDye cycle sequencing protocols. Dried sample pellets were then sequenced using an ABI377 (Applied biosystems, School of Biological Sciences service).

2.7.1 Sequence analysis

Sequences were analysed using the computer package Chromas and then identified with a basic Blast search on the NCBI website (http://www.ncbi.nlm.nih.gov/BLAST/).

2.8 Microinjection

Glass microinjection needles (Clark electromedical instrumements, 1mm external diameter, 0.75 internal diameter) were prepared using a microelectrode puller (Flaming Brown micropipette puller, model P97; Sutter instrument and Co). Pulled needles back-filled with dsRNA solution (using capillary action) and inserted into a microinjector holder (Narishige). Microinjection of either dsRNA or Tris-EDTA buffer was achieved using a constant flow system (Narishige). Each embryo was injected with ~10pl dsRNA in a concaved slide containing H6-BSA media. Injected embryos were cultured in T6-BSA media as with the usual culture procedure.

2.9 Imunofluorescence and confocal microscopy

For this procedure embryos were attached to coverslips in the well of "chambers". Chambers were made of a coverslip glued to a metal washer thus enabling solutions to be changed without a meniscus disturbing the attached embryos during immunofluorescence processing (Figure 2.1).

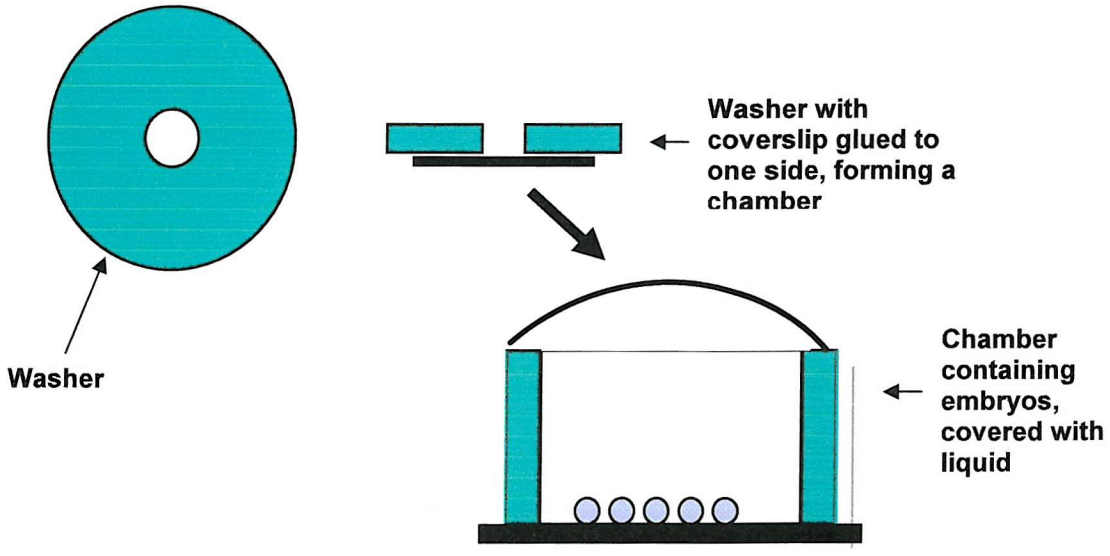

Figure 2.1. The chamber set up for immunofluorescent staining of embryo proteins

2.9.1 Chamber preparation

The chambers were made using stainless steel washers, 1mm thick, 25mm wide with a 5mm hole (UK suppliers: Glenwood, Unit 3, Hadstock Rd, Linton, Cambridge, CB1 6NR). The washers were first cleaned with 100% alcohol and dried with lint free tissue paper. Coverslips (22mm diameters No 0) were glued to the flat base of these washers using RS Cyanoacrylate Adhesive (School stores, cat. No. 567-171) making sure that no glue covered the central well and left to dry for 30 minutes and stored in a 50ml syringe tube.

First the chamber wells were checked for leaks and washed with a small drop of PBS. The PBS was then removed using a needle and syringe. For formaldehyde fixed embryos, chambers were coated with 1.5mg/ml poly-L-Lysine hydrobromide (PLL; Sigma) in PBS for 15 minutes. In the case of methanol fixed embryos, chambers were coated for 15mins with 0.1mg/ml concanavalin A (Con-A; Sigma) in PBS. Chamber wells were washed three times with PBS (formaldehyde fixation) or with H6-PVP (for methanol fixation) immediately prior to transferring the embryos to the wells.

2.9.2 Embryo preparation and fixation

Removal of the zona pellucida was achieved by incubation of the embryos in acid Tyrode's solution for a few seconds (Nicolson *et al.*,1975). After dissolution of the zonas, embryos were washed and left to recover in pre-warmed H6-BSA. Recovery time depends on embryo stage. 1- to16-cell embryos ideally need an hour to recover, however, blastocysts only require a few minutes (to avoid cavity collapse).

After recovery, embryos were fixed in 1-4% formaldehyde for 10-15minutes at room temperature and loaded onto PLL coated chambers. For methanol fixation, embryos were washed three times in H6-PVP after acid Tyrodes recovery and then transferred to Con-A coated chambers. Once embryos were transferred, chambers were sealed with a coverslip and centrifuged for 10minutes at 1500 rpm.

After centrifugation, the coverslips were removed from the top of the chambers. For methanol fixation, chambers were submerged in -20°C methanol and kept at this temperature for 7-20 minutes. After methanol fixation, samples were rehydrated with PBS (3 x 5minute washes). For formaldehyde fixed embryos, chambers were briefly washed in PBS, permeabilised in 0.25% Triton X-100 in PBS for 15minutes, washed 3 times in PBS, incubated in 2.6 mg/ml NH_4Cl solution for 10 minutes and again washed 3 times in PBS.

2.9.3 Processing of fixed embryos for immunofluorescent staining

Primary antibodies were diluted in an appropriate amount of PBS containing 1:1000 Tween-20 (Table 2.3). 30µl diluted antibody was added to each chamber well (for negative controls only PBS:Tween-20 was added) and left to incubate overnight at 4°C. After primary incubation, chambers were washed 3 times over 30 minutes and 30µl appropriately diluted secondary antibody was then added to the chambers for 1 hr at room temperature. Chambers were then washed a further three times over 30 minutes in PBS:Tween-20. Samples were then mounted in PBS-Citifluor (City University, London), covered with another coverslip and sealed with nail varnish.

For nuclear staining either Hoechst or propidium iodide staining was used. For Hoechst nuclear stain (Sigma), 50µg/ml was used in the final PBS:Tween-20 wash. For propidium iodide (Sigma), 1mg/ml was diluted 1:2000 in the second PBS:Tween-20 wash.

Rhodamine phalloidin was for staining of actin filaments. 6.6µM stock in methanol was diluted 0.5µl/ml in PBS:Tween-20 (Molecular Probes) and added to the second PBS:Tween-20 wash after secondary antibody incubation.

Table 2.3

Working antibody dilutions for immunocytochemistry

Antibody	Dilution	Fixative
Polyclonal Rabbit anti-mouse **claudin-1** (Zymed)	1:300	1% Formaldehyde
Polyclonal Rabbit anti-human **Claudin-1** (Zymed)	1:30	1% Formaldehyde
Polyclonal Rabbit anti-mouse **Claudin-3** (Zymed)	1:30	1% Formaldehyde
Monoclonal Rat anti-mouse **E-cadherin** (DECMA; Sigma).	1:1000	7mins Methanol or 1-4% Formaldehyde
Monoclonal Rat anti-**JAM-1** (BV12; Dr G.Bazzoni, Instituto di Recerche Farmacologiche Mario Negri, Milan).	1:24000	7mins Methanol or 4% Formaldehyde
Monoclonal Rat anti-**JAM-1** (BV20; Dr G.Bazzoni, Instituto di Recerche Farmacologiche Mario Negri, Milan).	1:700	4% Formaldehyde
Purified Guinea Pig anti-mouse **ZO-1** α^+ (Dr.B.Sheth, University of Southampton)	1:100	1% Formaldehyde (no more than 10 mins)
Alexa 488/546 anti-mouse/rabbit/rat/guinea pig (Molecular Probes).	1:500	Formaldehyde/ Methanol

2.9.4 Double labelling

The two antibodies being used for double labelling of embryos were diluted together in accordance with single labelling concentrations (Table 2.3). The chambers were processed as per usual. To ensure that there was no cross-reaction between primary and secondary antibodies under double labelling conditions a number of controls were analysed. Inappropriate secondary antibodies were tested upon the primary antibodies of interest and a combination of secondary antibody only controls were also examined.

2.9.5 Confocal microscopy

Embryos were visualised using x63 oil-immersion objective on a Nikon inverted microscope linked to a Bio-Rad MRC-600 series confocal imaging system, equipped with a Krypton-Argon laser. Laser light penetration (neutral density) through the embryo sample was fixed at either 10 or 100%. K1/K2 filter sets were used to visualise Fluorescein (FITC), Rhodamine (TRITC), Alexa 488 and Alexa 546.

2.10 Collection and analysis of protein samples

2.10.1 Tissue lysate preparation

Mouse tissues were removed from freshly culled female mice and snap frozen in isopropanol using liquid nitrogen. Tissue blocks were then ground into powder with a pestle and mortar on dry ice and immediately rehydrated in boiling PBS/1%SDS. Tissue lysates were then boiled for 5 minutes followed by centrifugation for 10 minutes at 10,000 rpm. The liquid phase was then removed and stored at -70°C until needed for protein assays or Western blotting.

2.10.2 Collection of embryo protein samples

For Western blotting, numerous precisely-staged embryos were collected for each sample. These embryos were first washed three times in H6-PVP and then, taken up in minimal volume of H6-PVP, and placed in either 2x sample buffer (Appendix II) or 4x Novex sample buffer. Samples were then boiled for 3-5 minutes, centrifuged at 10,000 rpm, and stored at -70°C.

2.10.3 Determination of protein content in mouse tissues

Protein concentration of tissue samples was determined using the Lowry method (DC protein Assay, BioRad). Standard solutions of 0.15, 0.25, 0.5, 0.75, 1.0, and 1.5 mg/ml were made from a 2 mg/ml stock solution of BSA in PBS/1%SDS. 5µl of the standards and different dilutions of the protein solution being tested (e.g. neat, 1:5, 1:10) were loaded onto a 96 well microtitre plate in the following way:

	1	2	3	4	5	6	7	8	9
A	0.15	0.25	0.5	0.75	1.0	1.5			
B	0.15	0.25	0.5	0.75	1.0	1.5			
C									
D	Test 1	Test 2	Test 3		Test 4	Test 5	Test 6		
E	Test 1	Test 2	Test 3		Test 4	Test 5	Test 6		
F									

25µl of solution A' (20µl reagent S + 1ml reagent A) was added to each standard and test sample followed by 200µl of reagent B. The plate was then left for 15 minutes and then read on a microplate reader at 750nm (Dynatech, MR5000).

2.11 Electrophoresis and immunoblotting

2.11.1 Gel percentages and resolution of proteins

As JAM-1 and Claudin-1 are both low molecular weight proteins, a high percentage acrylamide gel was used. For both proteins, either a 12 or 15% polyacrylamide gel was used for tissue blots. Gels were cast in a Hoeffer 220 minigel system and run in a Hoeffer electrophoresis tank with electrode buffer (Appendix II). For embryo blots pre-cast 4-12% gradient TB buffered gels (Novex) were used and run with Novex equiptment with MOPS buffers (Novex). Both gel types were blotted for 2-3 hours in a Hoeffer blotting tank with standard transfer buffer (Appendix II).

2.11.2 SDS-PAGE and blotting

Embryo and tissue samples were diluted to a 1x solution with 4x or 6x buffer (Appendix II) and boiled at 95°C for 5 minutes and briefly centrifuged at 10,000 rpm prior to loading on the gels. Gels were run on 150v constant current through the stacker gel and at 200v at constant current through the resolving gel until sufficient separation of the markers of interest had occurred. Gels were blotted onto Hybond-C nitrocellulose (Amersham) in transfer buffer (Appendix II) for 2-3 hours at 300mA.

2.11.3 Western blotting

Blots were blocked with 5-10% non-fat dried milk powder in PBS: 0.05%-0.1% Tween before incubation in specific primary antibody at appropriate concentrations (Table 2.4) in blocking buffer. Blots were washed three times in 30 minutes on a "belly dancer" machine (Stovall Life Science), prior to and after primary antibody incubation. Blots were then incubated in the appropriate HRP-conjugated secondary antibody for 1 hour. After an additional three washes in PBS: 0.05%-0.1% Tween, blots were developed with either an enhanced chemiluminesence (ECL; Amersham) or the SuperSignal® West PICO (Pierce) kit and visualised on ECL film.

Table 2.4

Antibodies for Western blotting

Antibody	Dilution
Rabbit anti-mouse **claudin-1** (Zymed; 71-7800)	1:178
Rabbit anti-human **claudin-1** (Zymed; 51-9000)	1:100
Rabbit anti-mouse **claudin-3** (Zymed; 34-1700)	1:100
Rat anti-mouse **E-cadherin** (DECMA; sigma)	1:1600
Rat anti-mouse **JAM-1** (BV12; G.Bazzoni, Instituto di Recerche Farmacologiche Mario Negri, Milan)	1:240
Rat anti-mouse **JAM-1** (BV20; G.Bazzoni, Instituto di Recerche Farmacologiche Mario Negri, Milan)	1:140
Rabbit anti-human **occludin** (J.M.Anderson, Yale University).	1:1000
HRP-conjugated donkey **anti-rabbit** (Amersham).	1:10000
HRP-conjugated rabbit **anti-rat** (Sigma)	1:12000

2.11.4 Coomassie blue and Ponceau red staining

Gels were checked for efficient transfer or the presence of proteins by staining with coomassie blue (ICN) for a minimum of 30 minutes and then washed and destained to produce the desired contrast with strong and then weak destain solutions (Appendix II).

Prior to or post Western blotting, blots were stained with 2% Ponceau red (Raymond Lamb) in 3% trichloroacetic acid for 20 minutes followed by a 10 minute wash in Mili-Q water to visualise the proteins on the blot and check for efficient protein transfer.

2.11.5 Blot stripping of antibodies

Blots were incubated in 50 ml 1x stripping buffer (Appendix II) mixed with 0.35ml ß-mercaptoethanol for 30 minutes at 65°C in a shaking water bath. Blots were washed in PBS-0.05%-0.1 Tween in a fume cupboard and then washed three times over 30 minutes with PBS-0.05%-0.1 Tween. Blots were then blocked with PBS:0.05%-0.1 Tween:10% milk for 30 minutes and then normal blotting procedures were followed therein.

2.12 Peptide design

A peptide (Cld1-K15; 8.8kDa, Appendix III), corresponding to the first extracellular loop of claudin-1, was made by Dr R.Sharma (University of Southampton). Due to the hydrophobicity of this relatively large peptide, 15 lysines were added to the C-terminus to decrease its aggregation in solution. As a control, a scrambled version of this peptide was also made, also containing a 15 lysine C-terminus (Appendix III).

2.13 Cell culture

CMT64/61 cells, derived from a mouse lung carcinoma, were provided by Dr Jane Collins (Faculty of Medicine, University of Southampton). A 1ml vial of the cells was thawed and cultured in Falcon petri dishes in Waymouth's medium (MB 752/1) supplemented with 2mM glutamine and 1% Penicillin / Streptomycin. Cells were cultured in fresh medium every two to three days. Cells were kept under sterile conditions at 37°C and 4.5% CO_2 in a Grant Gow–Mac controlled CO_2 incubator. Once stock plates had been established, stock viles were made to maintain cell numbers in the liquid nitrogen freezer. For the precise freezing and thawing technique see section 5.13.1

2.13.1 Cell freezing and thawing

1ml stock ampuoles containing 1 x 10^6 cells were made up as follows: Culture medium was removed and the cells were washed twice with PBS. Once confident that all traces of the culture medium had been washed from the cells, the PBS was removed and replaced with 2.5ml trypsin EDTA and left in the incubator for 10 minutes. A 10ml pipette was then used to flush off any cells still stuck to the bottom of the plate. When satisfied that most of the cells had lost their attachment to the petri dish the trypsin EDTA-cell solution was added to the Sterilin universal and ¾ diluted with PBS to prevent the trypsin EDTA from damaging the cells and mixed thoroughly. An aliquot of this solution was taken to establish the amount of cells in the universal and the remainder was then spun in a centrifuge (5 minutes at 1000rpm) to form a cell pellet. The count was determined using a haemocytometer under a light microscope. The cells were mixed with trypan blue so to stain up any dead cells. The following formula was used to calculate a total cell number:

N^o viable cells $^{-ml}$ = (N^o cells counted / N^o triple rule squares) x25 x10^4 x original dilution

Once the cells had formed a solid pellet, the PBS and trypsin EDTA solution was removed. Using fresh Waymouths medium, containing 10% DMSO, cells were diluted to obtain 1 x 10^6 cells per ml and were transferred to 1ml ampuoles, frozen at $^-$70°C for two hours and then transferred to a liquid nitrogen freezer.

When thawing cells, frozen ampuoles were brought to room temperature and then transferred to a 20ml universal. 10ml of culture medium (warmed to 37°C in the incubator) was added drop wise to the cells and then mixed using a 10ml pipette (Sterilin). Cells were then centrifuged and resuspended in a further 10ml of medium. 2.5ml of the cell solution was then placed in a Falcon tissue culture petri dish (100 x 20 mm) and 12.5ml of medium (37°C) was added to make a total volume of 15ml.

2.13.2 Transepithelial electrical resistance (TER)

Cells were grown on Falcon cell culture inserts (polyethylene terepthalate membrane, 3μm pore size Cat number 35-3096) in a 24 well titre plate. 0.4ml culture medium containing 0.08 x 10^6 cells was added above each insert and 0.8ml of media (without cells) was added to each well below the insert. TER measurements were obtained using an epithelial voltohmmeter (World Precision instruments), as per the manufacturers instructions.

2.13.3 Ca^{2+} switch

Confluent cells were transferred to Ca^{2+} free medium until TER was reverted to baseline values (i.e prior to cell-cell contact formation). Once TER had been disrupted, the Ca^{2+} free medium was replaced with normal culture medium.

Chapter 3

Expression of JAM-1 in the mouse preimplantation embryo

3.1 Introduction

Junctional adhesion molecule (JAM-1) was first discovered as a transmembrane protein concentrated at tight junctions (TJs) in endothelial and epithelial cells (Martìn-Padura *et al.*, 1998). In order to elucidate the function of JAM-1 in the mouse preimplantation embryo the pattern of JAM-1 transcription and protein expression from egg to implantation was examined. Information regarding the transcription and translation of JAM-1 in combination with protein localisation data hopefully will provide valuable insight into the role of JAM-1 in TJ biogenesis.

The presence of mRNA can be detected with RT-PCR or Northern blotting. For the purpose of this study, RT-PCR was considered the optimal method for establishing mRNA expression patterns in the preimplantation embryo, as it is a sensitive method that can detect low abundance mRNAs in single embryos due to its amplification capabilities. In addition, the expression and localisation of murine JAM-1 protein in unfertilised eggs and 1-cell to blastocyst stage embryos has been investigated. Western blotting was used to analyse JAM-1 protein expression. Membrane localisation of JAM-1 protein was determined using indirect immunofluorescence and confocal microscopy.

3.2 Materials and methods

3.2.1 Primers

Sequence data for JAM-1 was obtained from Genbank, the European Molecular Biology Laboratory, and the DNA database of Japan under the accession code U89915. Murine JAM-1 cDNA is 2029bp in length of which 903bp comprise the coding region (bases 71-973). JAM-1 primers were designed in our laboratory by Dr Judith Eckert. The priming region targeted is within the coding sequence and the cDNA encodes the majority of the extracellular region of murine JAM-1 protein (Figure 3.1).

(A)

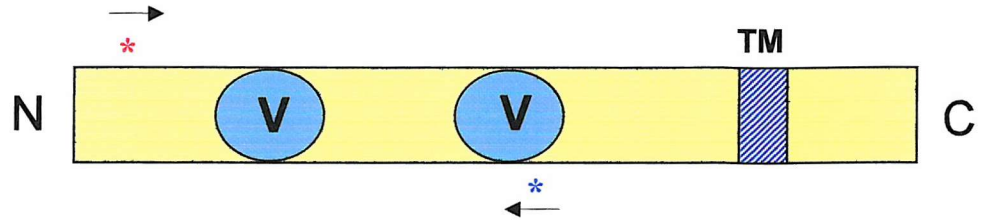

(B)

Primer name	Primer sequence	Position on cDNA sequence
JAM1/1	5′-gaggggaaagccgggaggaaactgt-3′	* **80-104**
JAM1/2	5′-caaaggctgtcacggggtcaaagat-3′	* **686-662**

Figure 3.1. Murine JAM-1. (A) Position of primers in relation to the structural model of murine JAM-1. (B) Primer sequences and position on cDNA sequence.

3.2.2 JAM-1 RT-PCR

JAM-1 RNA was isolated from mouse liver tissue, as described in section 2.2.3. However, mRNA from embryo samples was isolated, as described in section 2.2.2, using the Dynabeads mRNA DIRECT kit (Dynal, UK). For full details of RT-PCR methods used see sections 2.3.5 and 2.3.6.

Amplification was carried out for 35 cycles of:

1) 95°C for 30 seconds.

2) 60°C for 30 seconds.

3) 72°C for 40 seconds.

After these cycles, a 5 minutes 72°C final extension step was added.

3.2.3 Sequencing

Sequencing and analysis was carried out as described in sections 2.7 and 2.7.1. The RT-PCR amplification product was a 100% match to the 607bp murine JAM-1 sequence targeted by these primers (Appendix III).

3.2.4 JAM-1 Antibodies

Anti-murine JAM-1 monoclonal antibodies (mAbs), BV11 and BV12, were provided by Dr G. Bazzoni (Instituto di Recerche Farmacologiche Mario Negri, Milan, Italy), the production of which are discussed in detail in Martín-Padura *et al.*, (1998). These two antibodies appear to bind slightly different epitopes, as BV12 is unable to inhibit BV11 binding (Martín-Padura *et al.*, 1998). Subsequent analysis of mAbs BV11 and BV12 has demonstrated that they may bind similar, overlapping but non-identical epitopes around amino acids 24-31 (Figure 3.2; Bazzoni *et al.*, 2000a). In addition to BV11 and BV12, two more anti-JAM-1 monoclonal antibodies were provided by Dr G. Bazzoni, BV19 and BV20. The exact region of JAM-1 to which these bind is not yet known.

A)

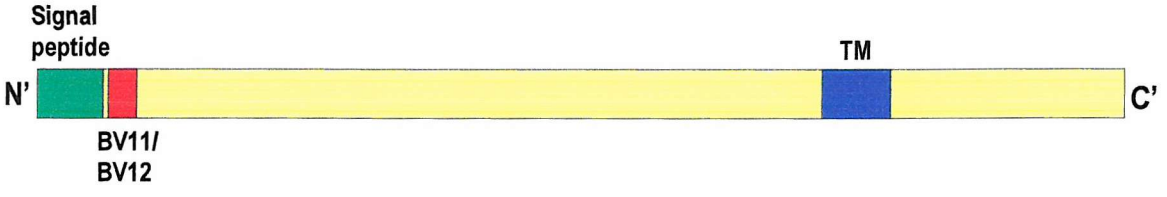

B)

MGTEGKAGRKLLFLFTSMILGSLVQGKGSVYTAQSDVQVPENESIKLTCTYSGFSS
PRVEWKFVQGSTTALVCYNSQITAPYADRVTFSSSGITFSSVTRKDNGEYTCMVSEEGG
QNYGEVSIHLTVLVPPSKPTISVPSSVTIGNRAVLTCSEHDGSPPSEYSWFKDGISMLTAD
AKKTRAFMNSSFTIDPKSGDLIFDPVTAFDSGEYYCQAQNGYGTAMRSEAAHMDAVELN
VGGIVAAVLVTLILLGLLIFGVWFAYSRGYFETTKKGTAPGKKVIYSQPSTRSEGEFKQTSS
FLV

Figure 3.2 Amino acid sequence of murine JAM-1. A) Demonstrates a schematic overview and B) the amino acid sequence of murine JAM protein (accession code U89915), illustrating the putative hydrophobic signal peptide, the BV11/BV12 binding domain and the transmembrane (TM) domain.

3.2.5 Western blotting

For full details on Western blotting procedures and antibody concentrations used see section 2.11.3 and Table 2.4. Western blots were visualised with either an

enhanced chemiluminescence kit (ECL; Amersham) or with SuperSignal® west PICO (Pierce), following the manufacturer's protocol.

3.2.6 Immunofluorescence and Confocal microscopy

Using the conditions described by Martín-Padura *et al.*, (1998), late blastocysts were fixed in methanol for 3 minutes and were incubated in one of three concentrations of BV12 primary antibody; 10μg/ml, 1μg/ml or 0.1μg/ml in PBS:Tween 20 buffer. For further details on embryo preparation for immunofluorescence see section 2.9. Longer methanol incubations, and 1% and 4% formaldehyde were also tested for an optimal fixation method. Subsequently, 0.1μg/ml BV12 and 4% formaldehyde was used as the preferred immunofluorescence procedure. Rhodamine phalloidin (Molecular probes) was used to stain the actin filaments in compacting 8-cell embryos (see sections 2.9.3 and 3.3.5.4).

The main JAM-1 immunofluorescence data were obtained using BV12. However, Western blotting was only successful using the anti-murine JAM-1 antibody BV20. Therefore, confirmation of the BV12 immunofluorescence data using BV20 was also necessary. BV20 was used at 1μg/ml on embryos fixed in 4% formaldehyde.

3.2.6.1 Analysis of precisely timed 8-cell embryos

JAM-1 localisation patterns were examined more precisely in the 8-cell stage mouse preimplantation embryo. Late 4-cell embryos were collected and at hourly intervals recently divided 8-cell and transitional 8-cell embryos (i.e. between 4-7 cells) were removed and either fixed immediately (0-hour group) or cultured for 3-hour, 6-hour or 9-hour periods post cleavage before fixation (4% formaldehyde), immunostaining and confocal microscope analysis.

3.2.6.2 Analysis of JAM-1 localisation patterns in 1/4 - 2/8 couplets

As there is considerable asynchrony in blastomere division in the mouse embryo, late 4-cell embryos were treated to remove the zona pellucida, disaggregated to single cells (1/4 cells; see section 2.1.4) and observed every hour for division into

8-cell couplets (named 2/8 couplet). Then, as with the intact embryo experiment (section 3.3.5.4), 2/8 couplets were fixed, stained and analysed for JAM-1 protein localisation patterns.

3.3 Results

3.3.1 cDNA amplification of JAM-1 from mouse tissue RNA

JAM-1 cDNA (expected product size 607bp) was successfully amplified from 160pg of mouse liver RNA following RT-PCR (Figure 3.3). The annealing temperature recommended by the primer design program oligo (58°C) plus three more annealing temperatures (60, 62 and 64°C) were tested and all successfully amplified JAM-1. These products were not from DNA contamination as the minus RT and master mix controls showed no product amplification. All annealing temperatures tested were suitable for further use on embryo samples. However, 60°C appeared to give a marginally better signal than the other temperatures tested.

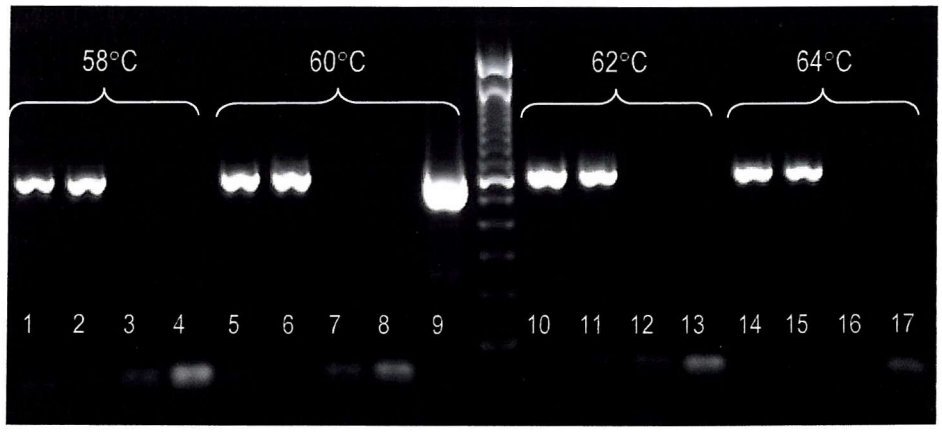

Figure 3.3 Amplification of JAM-1 in tissue. JAM-1 amplification from 160ng (lane 9) and 160pg (lanes 1, 2, 5, 6, 10, 11, 14 and 15) of mouse liver RNA was successful at all annealing temperatures tested. All –RT controls (lanes 3,7,12 and 16) and master mix controls (lanes 4,8,13 and 17) showed no product amplification.

3.3.2 Analysis of JAM-1 from unfertilised egg to late blastocyst stages

Samples of multiple embryos (5x) were collected for a variety of preimplantation stages. JAM-1 mRNA expression was not detected in unfertilised or fertilised eggs but was found to be expressed in all subsequent embryo stages up to and including late blastocysts (Figure 3.4). RT-PCR for JAM-1, at each stage, was

repeated on at least one more occasion. This pattern of expression suggests that JAM-1 mRNA is not expressed maternally, but only zygotically. The negative result for both unfertilised and fertilised eggs was repeated in 10x embryo samples and the number of PCR cycles was increased from 35 to 40 cycles (data not shown). Again, JAM-1 was not amplified from these stages. Although this RT-PCR is only a qualitative analysis of JAM-1 mRNA expression, there does appear to be a weak expression of JAM-1 in 2-cell (2C) and 4-cell (4C) embryos in comparison to the later preimplantation stages. This signal appears to increase at the eight-cell (8C) stage through to blastocyst.

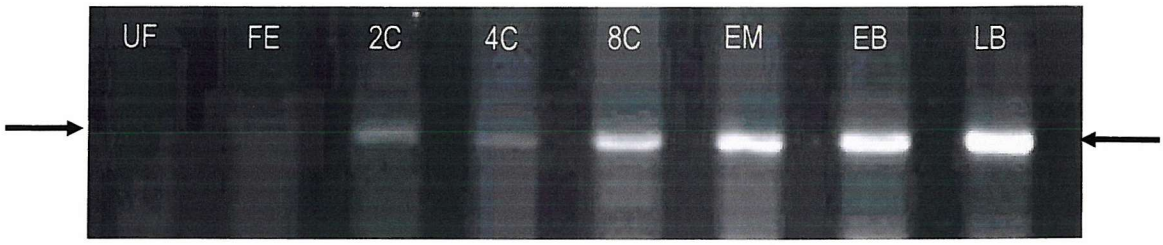

Figure 3.4 Analysis of the presence of JAM-1 mRNA in unfertilised mouse eggs and from 1-cell to late blastocyst embryo stages. A 600bp (arrows) JAM-1 product was not detected in unfertilised (UF) and fertilised eggs (FE) but was found in all subsequent embryo stages (2C – LB).

3.3.3 Detection of JAM-1 protein in mouse lung lysates

Four anti-murine JAM-1 antibodies (BV11, BV12, BV19 and BV20) were tested upon mouse lung tissue lysates. Only BV20 detected a protein at the approximate molecular weight for JAM-1 (37-41kD; Figure 3.5).

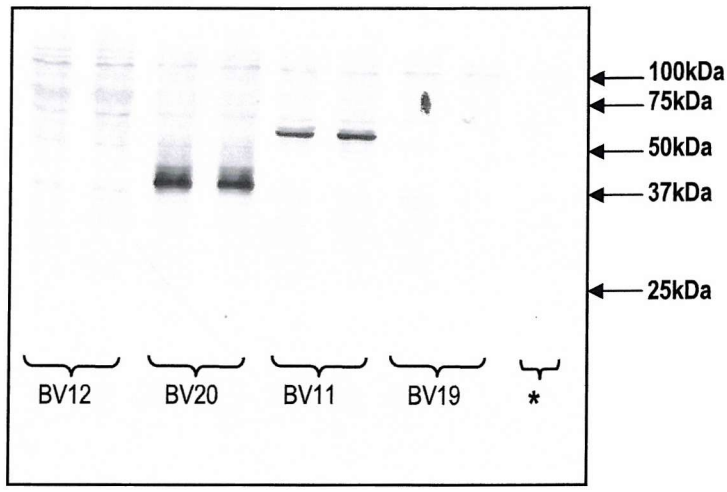

Figure 3.5. JAM-1 Western blotting with mouse lung tissue lysates. Only BV20 detected a protein at the expected molecular mass for JAM-1 (37-41kD). The BV11 antibody appeared to detect a protein at an approximate molecular weight of 65-70kDa. The secondary only control (*) picked up a weak banding pattern which could be seen in all other gel lanes. However, none of the bands were the same size as the expected JAM-1 product.

Since a single mouse blastocyst contains approximately 25ng of protein (Brinster, 1967), the amplification signal for JAM-1 needed further optimisation upon tissue samples to improve detection sensitivity before use on embryo samples. Two signal amplification kits were used, ECL (Amersham) and SuperSignal® west PICO (Pierce) picogram. The SuperSignal® kit gave much stronger amplification of the proteins of interest. The SuperSignal® kit also detected less non-specific bands, as seen in the secondary antibody only control lanes (Figure 3.6).

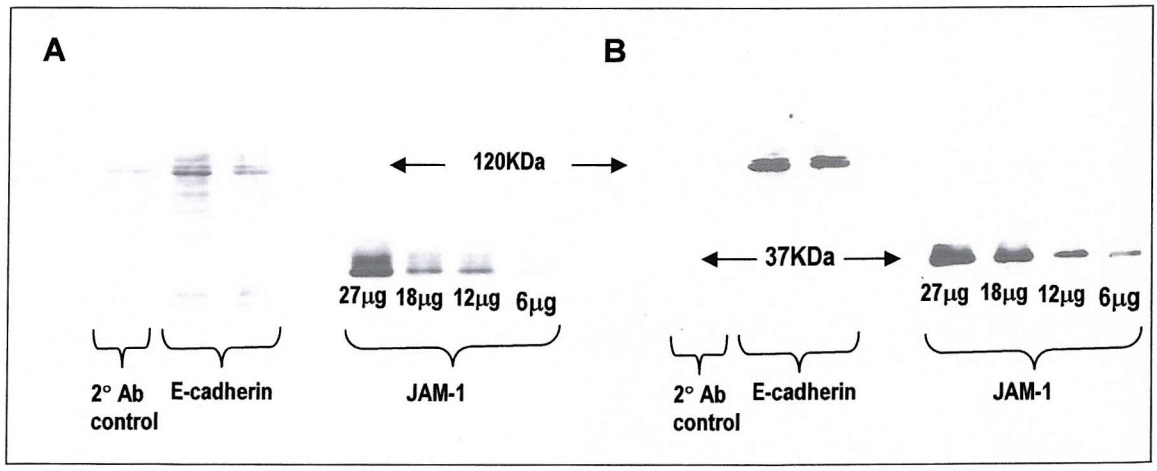

Figure 3.6 Sensitivity of JAM-1 Western blotting with BV20. Both the Amersham (A) and the Pierce (B) kits were able to detect JAM in protein samples as low as 6µg. The Pierce SuperSignal® Kit gave a stronger and more specific amplification of JAM-1. In both kits the +ve control was the E-cadherin antibody DECMA (Sigma).

3.3.4 Detection of JAM-1 protein expression in embryos

Using the Supersignal kit described above, JAM-1 protein expression from fertilised oocytes up to late blastocysts was examined (Figure 3.7). Each embryo sample contained approximately 500 eggs or embryos. JAM-1 protein was not detected in samples up to and including the pre compact 8-cell embryo. Weak expression of JAM-1 was first detected in compact 8-cell embryos and increased in all subsequent stages examined.

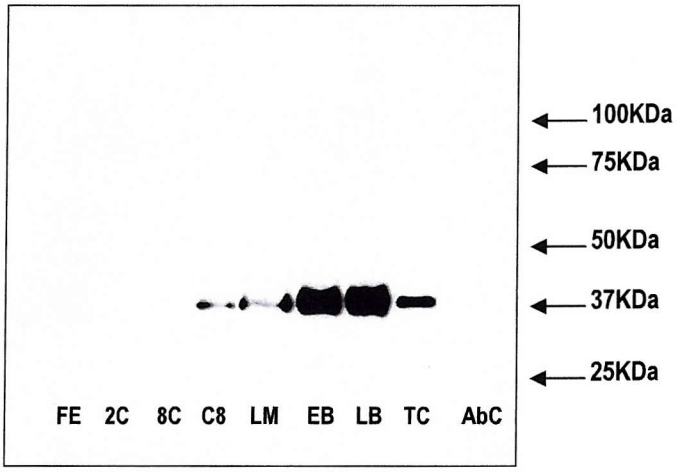

Figure 3.7 JAM-1 protein expression in embryos. All samples contained approximately 500 eggs or embryos. JAM-1 protein was undetected, using BV20 antibody, in fertilised eggs, 2-cell or 8-cell embryos. JAM-1 expression was weakly detected in compact 8-cell embryos and increased in intensity in each subsequent developmental stage (C8-LB). 18μg protein from a mouse lung tissue lysate was used as a positive control (TC). Non-specific bands were undetected in the secondary antibody only control (AbC).

3.3.5 Immunofluorescence and confocal microscopy

3.3.5.1 Analysis of optimal BV12 antibody concentrations

Using 3 minutes methanol fixation (see section 3.2.6), 0.1μg/ml BV12 detected JAM-1 most effectively in comparison with the other concentrations (Figure 3.8). Under these conditions, clear junctional staining at points of cell-cell contact and some TE basal membrane localisation of JAM-1 protein was observed. Using BV12 at higher concentrations (1μg/ml and 10μg/ml) the results obtained were inconsistent. BV12 was used at 0.1μg/ml for all subsequent JAM-1 immunofluorescence.

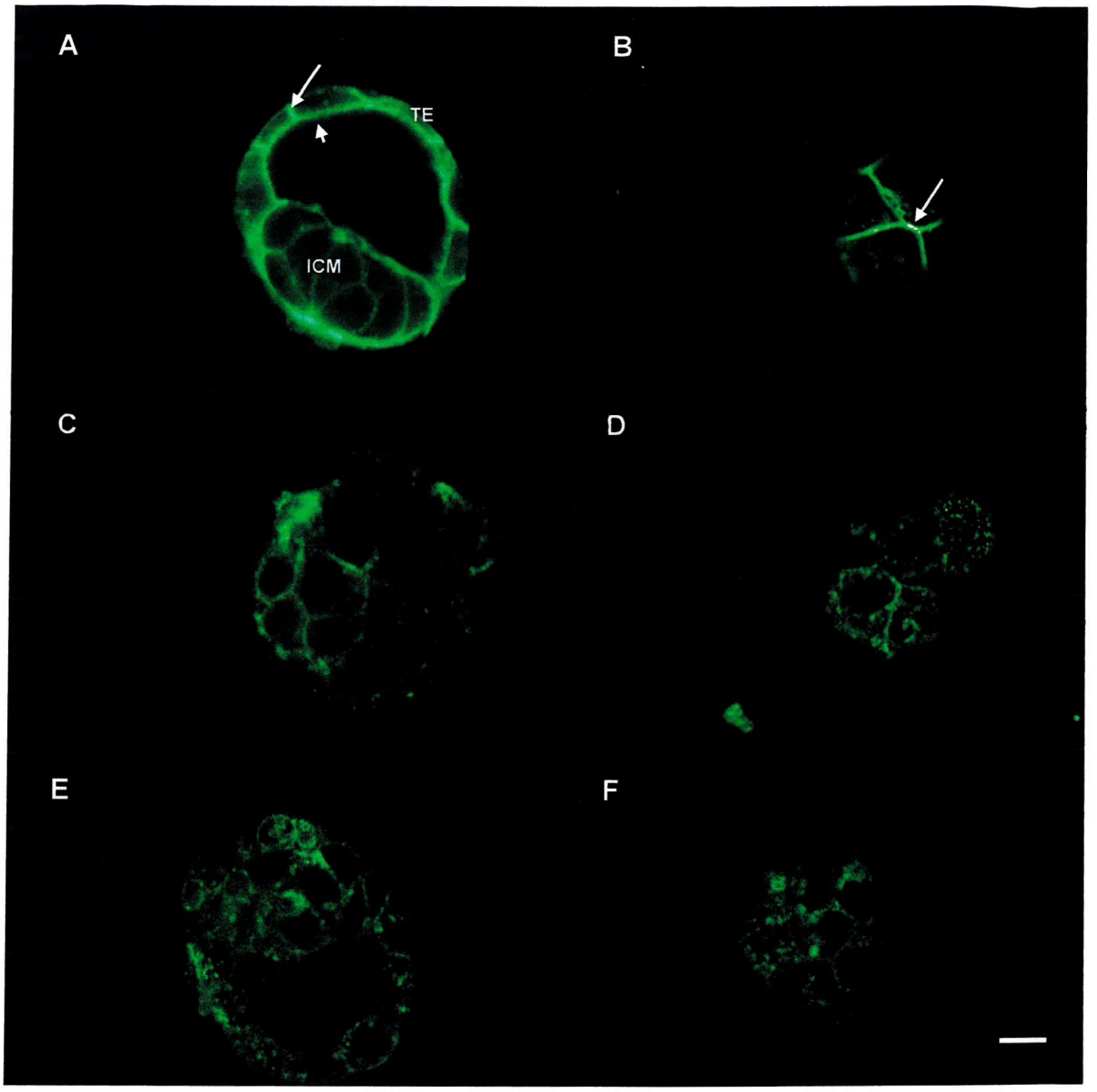

Figure 3.8 Analysis of three different concentrations of JAM-1 (BV12) antibody in immunofluorescence analysis of mouse early blastocysts. 0.1μg/ml BV12 produced good junctional/cell contact staining of JAM-1 protein, both in TE and in the ICM cells (Images A and B). At higher concentrations of BV12, (1 μg/ml C+D; 10 μg/ml, E+F), JAM-1 staining was weaker and inconsistent. Arrows depict junctional staining. Arrowhead shows TE basal membrane localisation of JAM-1. Scale bar, 20 μm

3.3.5.2 Optimal fixation for BV12

Although 3 minutes methanol fixation was suggested to be suitable for detecting JAM-1 in tissue sections (Martín-Padura *et al.*, 1998), the results obtained under these conditions in early blastocysts were inconsistent. Longer incubations in methanol were tested and 7 minutes methanol fixation appeared to improve the consistency of results (data not shown). In addition, formaldehyde fixation was tested (1% and 4%: 15 minutes). 4% formaldehyde gave sharper junctional staining in comparison with methanol fixation and a stronger fluorescent signal than 1% formaldehyde (Figure 3.9).

3.3.5.3 Embryo stages

Using 0.1μg/ml BV12 and formaldehyde fixation (4% for 15 minutes), unfertilised eggs to late blastocyst stages of mouse development were analysed for potential JAM-1 localisation patterns (Figure 3.10). As a positive control for each embryo stage examined, the E-cadherin antibody, DECMA (Sigma), was used on embryos alongside those stained for JAM-1. The n-numbers for these experiments are tabulated below (Table 3.1). Unfertilised (UF) eggs, 2-cell and 4-cell embryos showed no JAM-1 protein staining, despite the presence of E-cadherin protein in embryos of the same developmental stage. Junctional staining at cell-cell contacts was first detected in pre-compact 8-cell embryos (arrows; Figure 3.10a). At the onset of compaction, 8-cell embryos also revealed JAM-1 localisation at the apical, outward facing microvillous poles (arrowheads; Figure 3.10b). At the morula stage, JAM-1 was again localised along the lateral cell-cell contacts. The lateral membrane localisation of JAM-1 was also seen in early (E) and late (L) blastocysts, in both TE and ICM lineages, the pattern of which was very similar to the E-cadherin staining. However, midplain sections did reveal an apical concentration of JAM-1 between TE cells (arrowheads; Figure 3.10b).

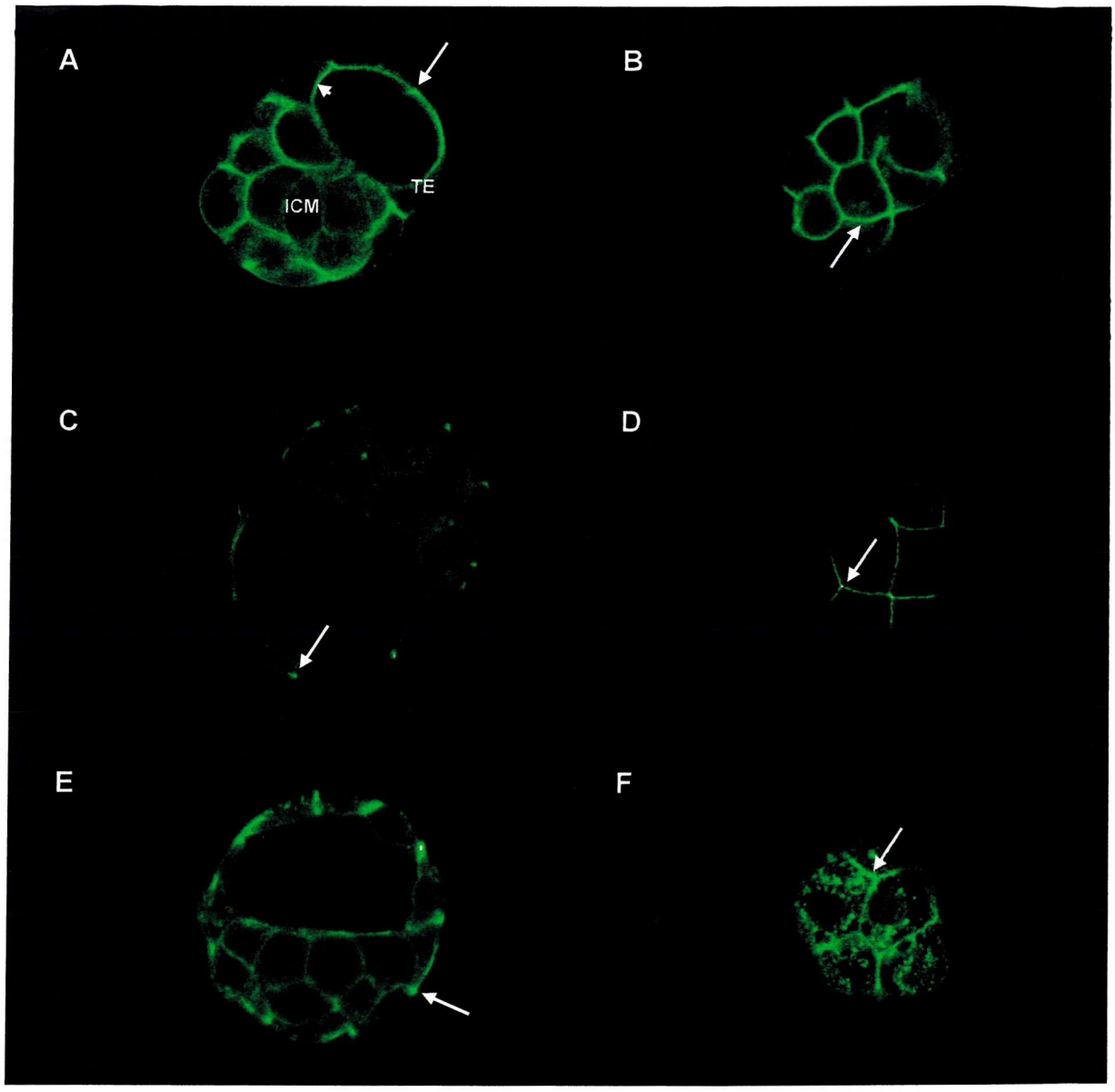

Figure 3.9 The effect of different fixations on BV12 staining in early blastocysts.
Immunofluorescence and confocal microscope analysis of EBs fixed in 4% formaldehyde (images A + B), 1% formaldehyde (images C + D) or 7 minutes in -20°C methanol (images E + F). In all cases, JAM-1 protein was localised at contact sites between cells both in the TE and ICM. 4% formaldehyde stains JAM-1 more efficiently than 1% formaldehyde and with less cytoplasmic artefacts than methanol fixation. Arrows depict junctional staining. Arrowhead shows basal membrane localisation of JAM-1. Scale bar, 20μm.

Table 3.1

Numbers of stages investigated for JAM-1 protein localisation

Embryo stage investigated	Numbers examined	
	JAM-1	**E-cadherin**
Unfertilised eggs	16/16 negative	7/7 positive
mid 2-cell	22/22 negative	9/9 positive
mid 4-cell	8/8 negative	3/3 positive
8-cell	6/6 positive	4/4 positive
Compact 8-cell	14/14 positive	8/8 positive
Early morula	9/9 positive	3/3 positive
Early blastocyst	11/11 positive	4/4 positive
Late blastocyst	11/11 positive	11/11 positive

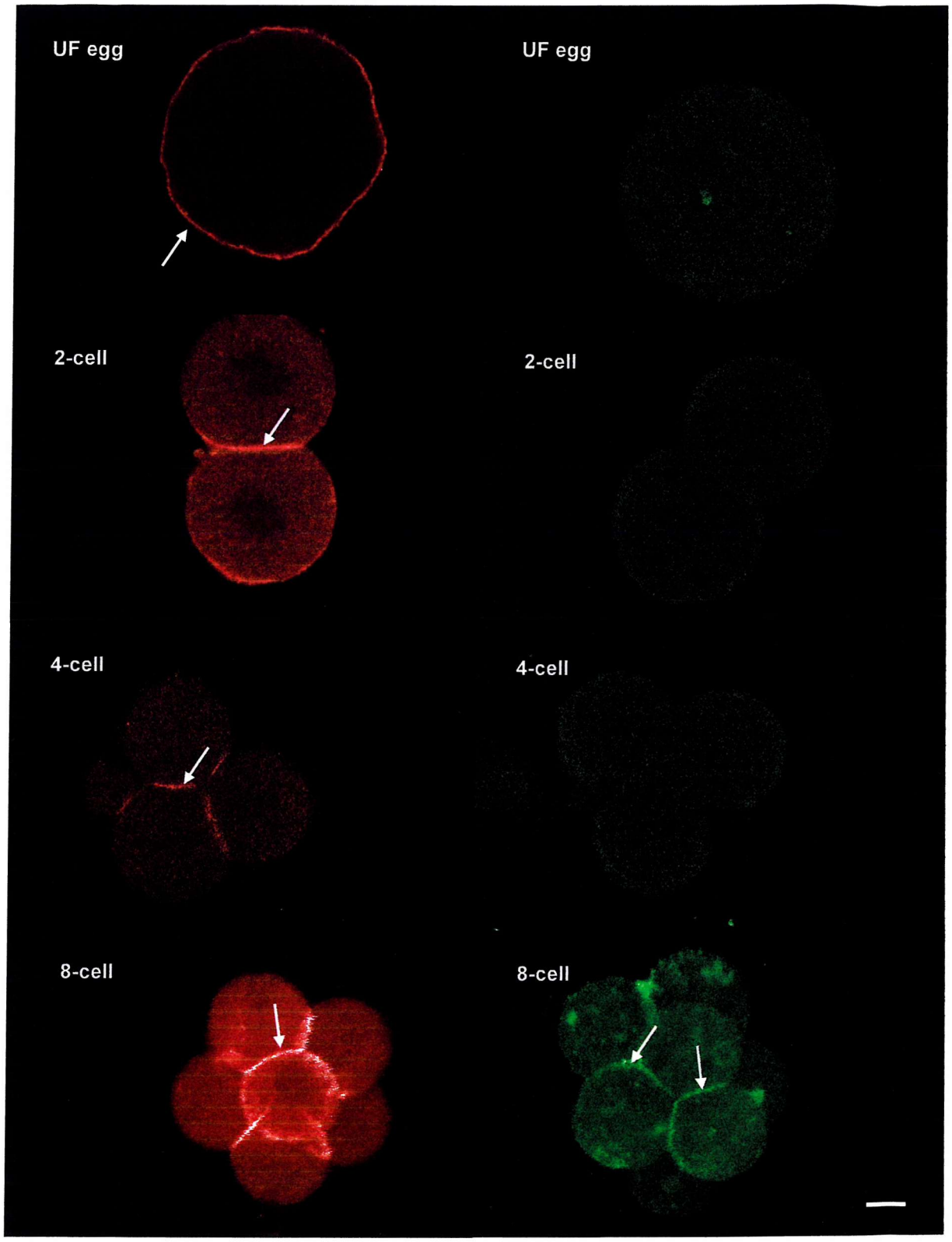

Figure 3.10.a. Confocal microscope midplane (UF egg to 4-cell) and projected z-series (8-cell) images of E-cadherin (red) and JAM-1 staining (green) in unfertilised eggs, and early cleavage stages. Cell-cell contact staining for JAM-1 and E-cadherin is indicated by the arrows. Scale bar, 20μm

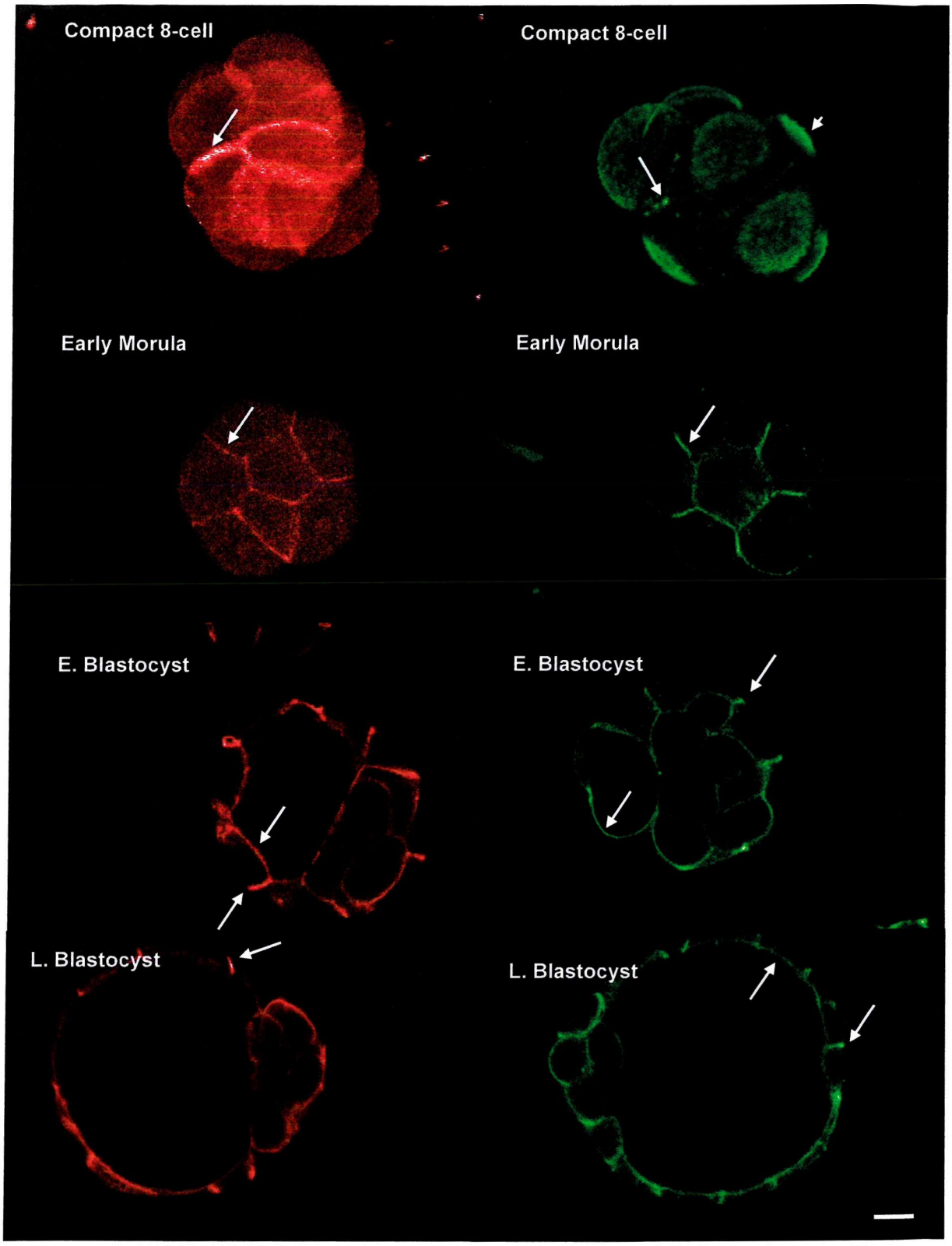

Figure 3.10.b. Confocal microscope projected z-series (compact 8-cell) and midplane (early morula to late blastocyst) images of E-cadherin (red) and JAM-1 staining (green) from compaction to blastocyst stages. Cell-cell contact staining for JAM-1 and E-cadherin is indicated by the arrows. Polar staining for JAM-1 is depicted by an arrowhead. Scale bar, 20μm

3.3.5.4 Polar membrane staining of JAM-1

Verification of polar membrane localisation of JAM-1 was achieved by double labeling actin filaments present in compacting 8-cell embryos with phalloidin, enabling visualisation of the microvillous pole (see sections 2.9.3 and 3.2.6). Merged images showed that JAM-1 was found at the blastomere poles around the time of compaction (Fig 3.11; arrows).

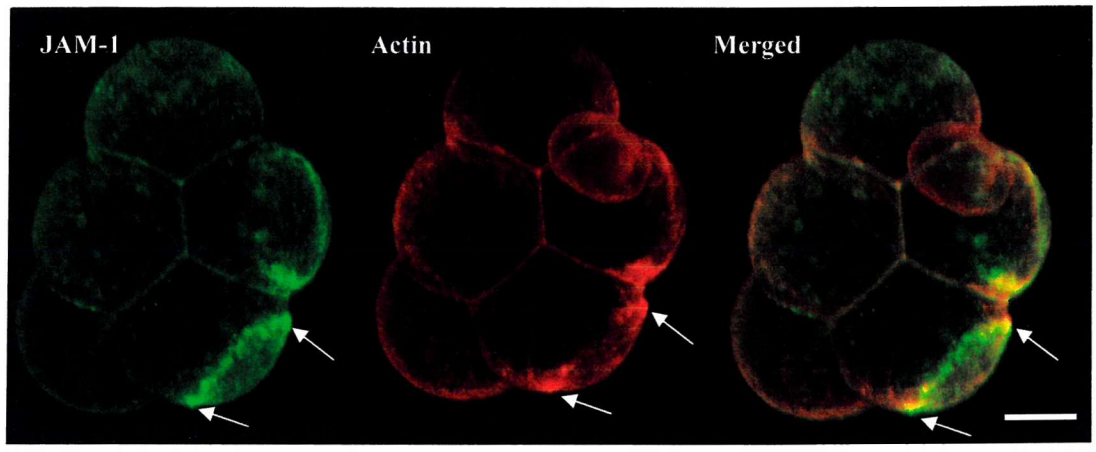

Figure 3.11. Verification of JAM-1 localisation at the blastomere poles of compact 8-cell embryos double labelled for actin n = 5. Arrows denote the polar localisation of both JAM-1 and actin. Scale bar, 20μm

To further investigate the polar membrane staining, embryos were cultured and fixed at 0, 3, 6 and 9-hours post cleavage into 8-cell (see section 3.2.6.1). Two main criteria were examined; 1) the presence or absence of JAM-1 staining at sites of cell-cell contact and 2) the presence or absence of JAM-1 at the blastomere poles (Figure 3.12 and 3.13). Some trends in the membrane localisation patterns were observed. At 0-hours and 3-hours, most but not all 8-cell embryos had cell-cell contact staining however at 6-hours and 9-hours, all 8-cells had JAM-1 protein localised at cell-cell contacts (Figure 3.13). There were also apparent trends in the polar localisation of JAM-1 at the time points investigated. In all 0-hour 8-cell embryos, there was no apparent localisation of JAM-1 protein to the apical surface of any blastomeres. Three hours into the third cleavage division, polar staining increased becoming more consistent over the following six hours (6-hours and 9-hours respectively). This appeared to be coincident with the onset of compaction and the development of the microvillous pole (Figure 3.12).

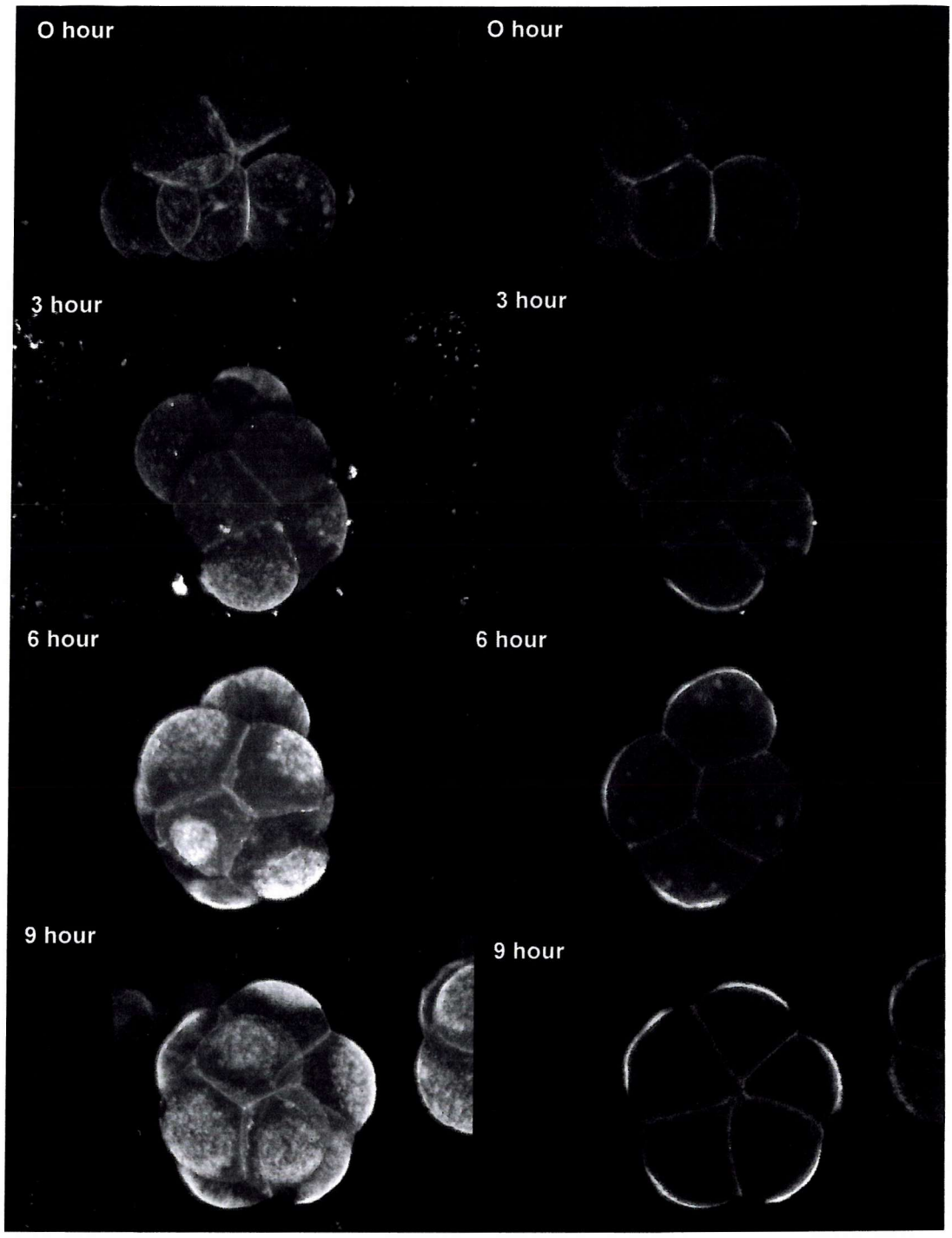

Figure 3.12. Typical staining patterns for JAM-1 in timed 8-cells. On the left all confocal microscope images are projected z-series. On the right, all images are approximate midplane sections of an 8-cell embryo. Note the progressive appearance of JAM-1 polar localisation over time, which is coincident with the onset of compaction.

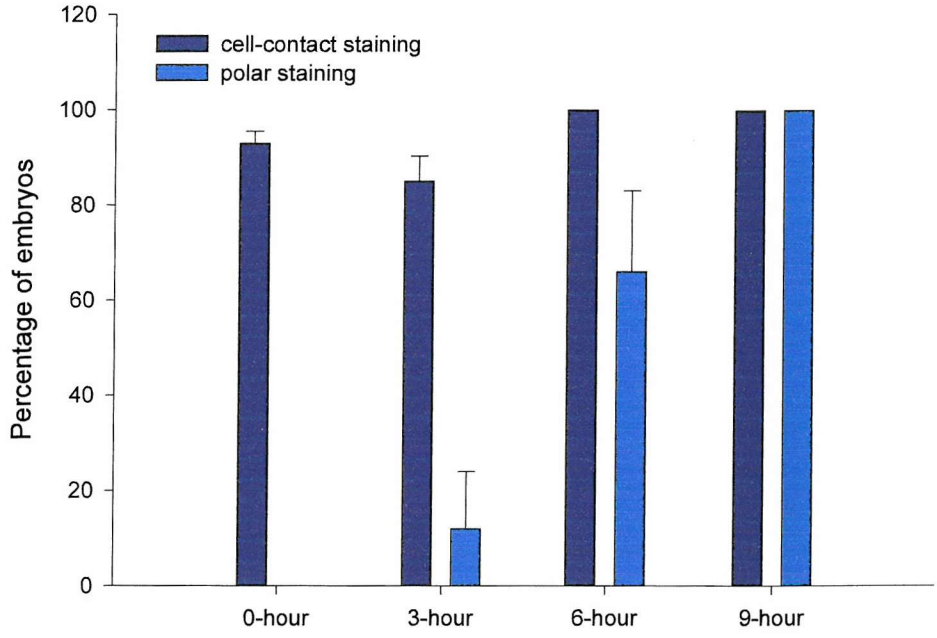

Fig 3.13. Analysis of the presence or absence of cell-cell contact and polar staining of JAM-1 protein in precisely timed 8-cell embryos. n = 4 experiments comprising 150 embryos in total.

3.3.5.5 Analysis of JAM-1 localisation patterns in 1/4 - 2/8 couplets

The presence or absence of JAM-1 staining at cell-cell contact and blastomere poles (Figure 3.14) was also investigated in timed 2/8 couplets. However, it was also apparent that in the couplets the cell contact staining was discontinuous in some embryos, so the continuity of the cell-cell contact staining was also assessed for each time point.

The apparent trend in cell-cell contact localisation for JAM-1 protein in 2/8 couplets did not appear to be as straightforward as the previous whole embryo time course experiments (Figure 3.14). Continuous contact staining decreased progressively between 0-hours and 6-hours post cleavage to 2/8 cells and then subsequently increased at 9-hours. Moreover, a high proportion of 6-hour 2/8 cells had no cell-cell contact staining. Discontinuous cell-cell contact staining was not apparent in 0-hour 2/8 couplets but was increased from 35% to 54% at 3-hours and

6-hours, respectively. At 9-hours the frequency of continuous cell-cell contact staining in 2/8 cell increased. In addition, at 9-hours, the occurrence of discontinuous cell-cell contact staining for JAM-1 was only 42%.

The polar localisation of JAM-1 in the 2/8 couplets was similar to that found in the whole embryo experiments. In all 0-hour couplets, there was no apparent localisation of JAM-1 protein to the apical surfaces of blastomeres. Three hours into the third cleavage division polar staining increased slightly, becoming more consistent over the following six hours (6-hours and 9-hours respectively). However, it was only at 9-hours post 1/4 blastomere division, that the polar localisation was the predominant pattern. Once again the polar localisation was coincident with the onset of compaction and the development of the microvillous pole (Figure 3.15).

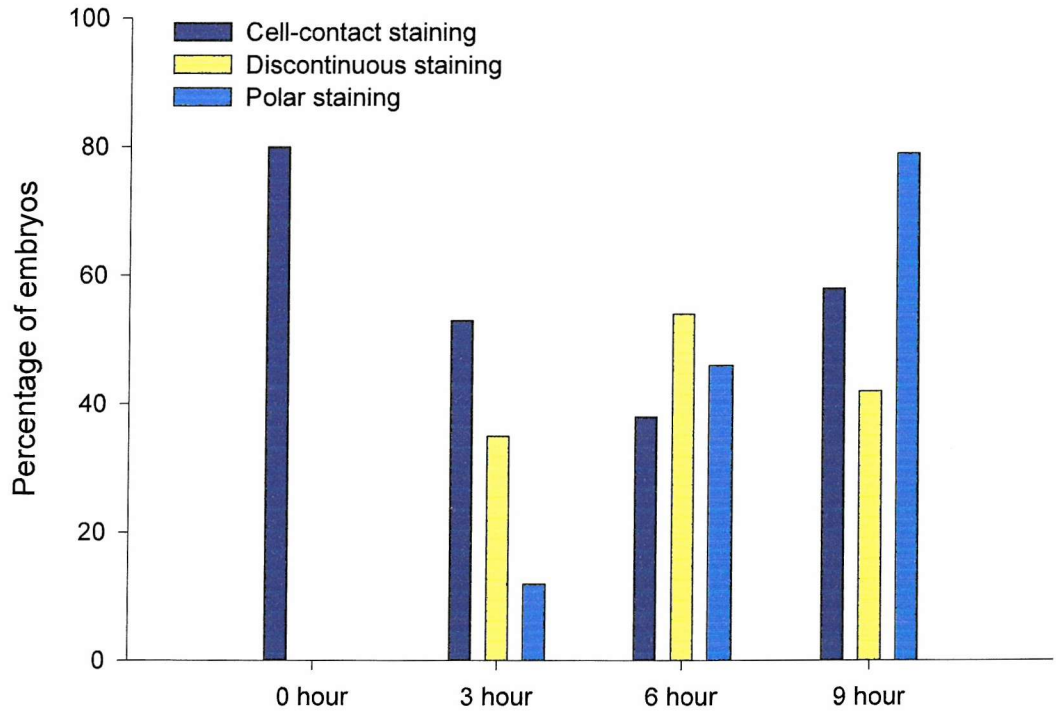

Figure 3.14 Analysis of continuity, presence or absence of cell-cell contact and polar localisation of JAM-1 protein in 2/8 couplets. n = 1 experiment comprising 39 2/8 –cells in total.

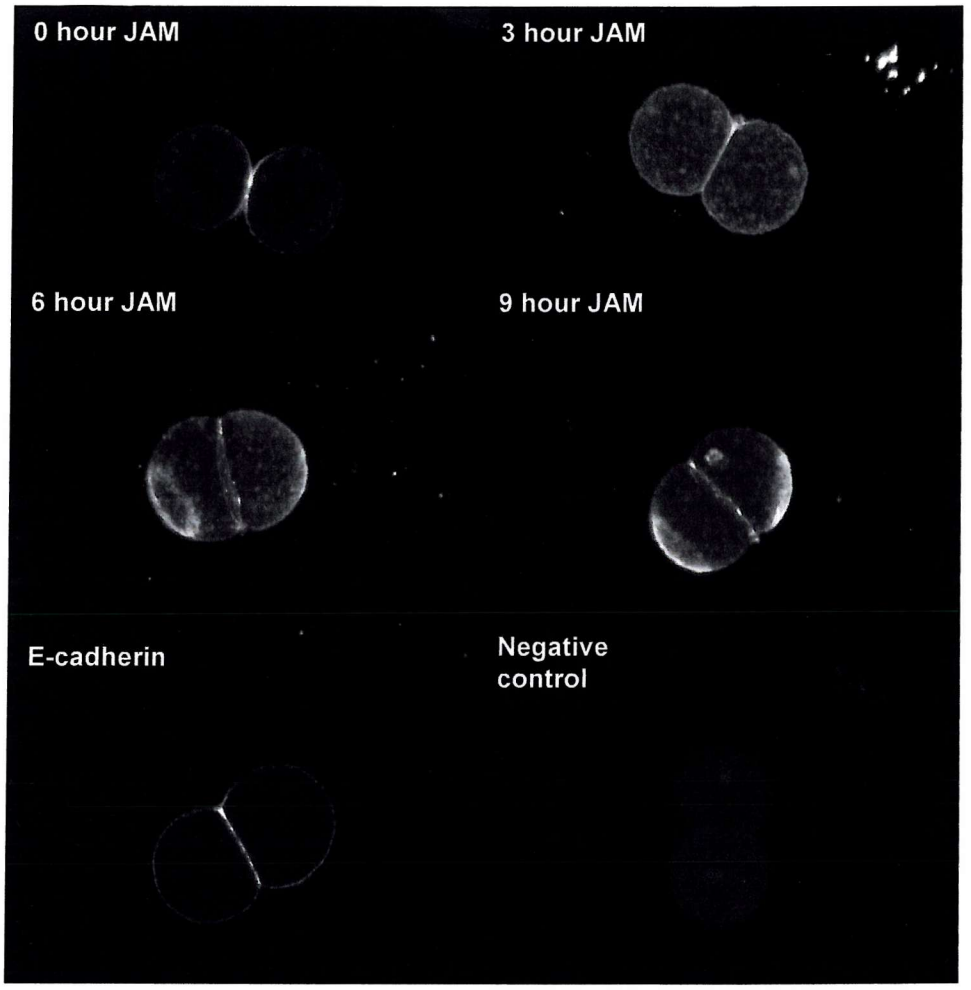

Figure 3.15 Typical staining patterns for JAM-1 in 2/8 couplets. Confocal images of typical JAM-1 localisation at the four different time points compared with E-cadherin and the negative control (no primary antibody).

3.3.5.6 Immunofluorescence with BV20

Since BV20 was the only suitable JAM-1 antibody for Western blotting, verification of the BV12 immunofluorescence data using this antibody was required. Immunofluorescence data using BV20 did not contradict data obtained using the BV12 antibody. JAM-1 expression was not detected in unfertilised eggs through to the 4-cell stage of preimplantation development (data not shown). The weak contact staining in 8-cell embryos, the unusual apical pole localisation at compaction and presence of JAM-1 in both ICM and TE lineages were all exhibited in experiments using BV20 (Figure 3.16). Although BV20 expression patterns were similar to those found with BV12, the staining with this antibody was weaker. Moreover, the intensity of the ICM staining in comparison with the TE was also found to be much

weaker with the BV20 antibody. This staining pattern has been seen with BV12 but mostly when the embryos were treated with 1% formaldehyde.

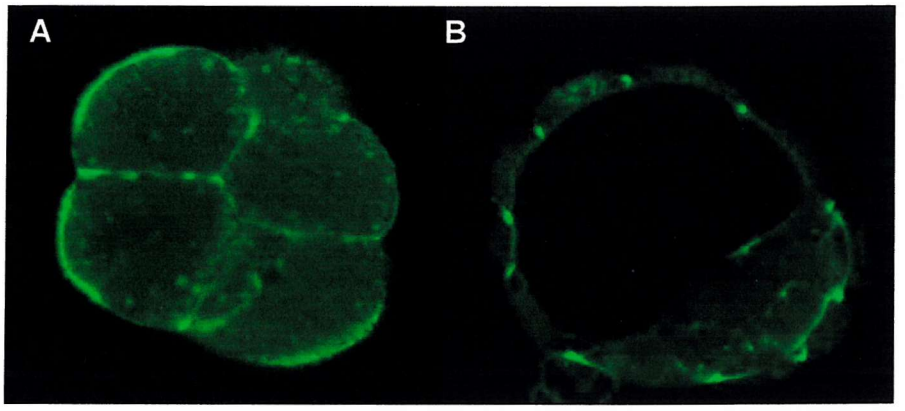

Figure 3.16 Immunofluorescence analysis of JAM-1 using BV20. A) Compact 8-cell embryos immunolabelled with BV20 showed a discontinuous cell-cell contact and bright polar staining. This pattern was similar to embryos immunolabelled with BV12. **B)** In blastocysts, the BV20 staining was similar to that found with BV12. However, although present, the ICM staining was much weaker.

3.4 Discussion

In summary, mRNA for JAM-1 was undetected in either unfertilised or fertilised eggs but was detected in all cleavage and blastocyst stages. The lack of maternal mRNA expression of JAM-1 is unusual for TJ proteins e.g. occludin, Rab13 & ZO-1α^- (Sheth *et al*, 1997, 2000a,b). JAM-1 expression has been detected on some occasions in bovine fertilised eggs (personal communication with D.Miller and J.Eckert) indicating either species variation or a more sensitive detection method. Moreover, the inconsistency in detecting maternally expressed bovine JAM-1 indicates that low abundancy could be the reason for no amplification of JAM-1 from mouse oocytes. However, in agreement with the JAM-1 RT-PCR data, no protein has been detected either by Western blotting or immunofluorescence in oocytes. In fact, the first JAM-1 protein expression is not until the 8-cell stage of development.

In this study, murine JAM-1 mRNA is first detected in 2-cell embryos coinciding with ZGA. Although quantitative RT-PCR was not carried out, the data suggest that 2-cell and 4-cell embryos may have less mRNA expression compared with later embryo stages. In the 8-cell embryo, there appears to be a marked increase

in JAM-1 mRNA expression that possibly increases further in the compacted 8-cell embryo. This potential increase either in transcription or message stability may coincide with a crucial point in JAM-1 protein synthesis and is consistent with a change in JAM-1 localisation (sections 3.3.4 and 3.3.5.3).

Western blotting with the monoclonal anti murine JAM-1 antibody, BV12, was unsuccessful in detecting JAM-1 in mouse tissue lysates. It is possible that BV12 is not a suitable antibody for detecting JAM-1 in its denatured form as it is a monoclonal antibody and therefore has an affinity for only one epitope. Not all monoclonal antibodies are suitable as probes in Western blots and it is possible that the single epitope to which BV12 has an affinity for may have been disrupted upon the unfolding of the protein. Subsequently, three more monoclonal JAM-1 antibodies were tested upon mouse tissue lysates (BV11, BV19 and BV20). All JAM-1 antibodies had not been tested previously in Western blotting.

Out of the four available JAM-1 antibodies only BV20 was suitable for detecting JAM-1 in its denatured state. Data obtained from embryo lysates demonstrated that JAM-1 protein expression is first detectable in compact 8-cell embryos. This protein expression increased in late morulae and again in the early and late blastocysts. This result is in accordance with the mRNA data, where there is an apparent marked increase in mRNA expression in pre-compact 8-cell embryos that increases further after compaction. Immunolocalisation data suggest that JAM-1 protein is first expressed in 8-cell embryos where it is found weakly localised at cell-cell contacts. In addition to this, JAM-1 immunolabeling showed more intense staining post compaction than earlier in cleavage, as depicted by the timed 8-cell experiments (sections 3.3.5.4 and 3.3.5.5). The detection of JAM-1 via immunofluorescence before it can be seen in Western blots is not unexpected since the efficiency of antibody-antigen binding can vary between these techniques depending upon the structure of the epitope of interest. Since the antibodies used are monoclonals it is likely that the efficiency of JAM-1 detection in Western blots was compromised by the target epitope being denatured by the SDS in the Western blotting method.

Expression patterns of JAM-1 in early and late blastocysts indicate that, although JAM-1 is known as a TJ protein (Martín-Padura *et al.*, 1998), this may not be its only point of localisation. Indeed, JAM-1 was expressed both in the TE and the ICM, unlike other TJ proteins, which have only been found expressed in the TE (Sheth *et al.*, 1997, 2000a,b). In addition, the early expression and membrane localization of JAM-1 in the preimplantation embryo is unusual for a TJ protein, in that it occurs prior to compaction. This localization pattern is similar to the expression profile found for adherens junction (AJ) proteins such as E-cadherin (Vestweber *et al.*, 1987; Clayton *et al.*, 1993). These data suggest that JAM-1 may have a role in the early stages of cell adhesion and TJ formation.

Indeed, JAM-1 has been shown to be involved in the recruitment of the cell polarity protein ASIP/PAR-3 to the TJ in epithelial cell lines (Ebnet *et al.*, 2001 and Itoh *et al.*, 2001). In fact, in wound healing assays, JAM-1 recruitment to the wounded regions occurs in the early stages of junction reformation along with E-cadherin and ZO-1. ASIP/PAR-3 is not recruited until JAM-1 is established at the cell-cell contact sites (Ebnet *et al.*, 2001). From these experiments it is proposed that JAM-1 has a role in the generation of cell polarity in epithelial cells. Thus, the presence of JAM-1 in 8-cell embryos and the change in localisation as the embryo undergoes compaction may be indicative of a potential role for JAM-1 in cell polarity and the generation of the TE epithelium. Moreover, it was hypothesized that the relationship between JAM-1, ZO-1, cingulin and occludin may indicate a potential role for JAM-1 in the molecular organisation of the TJ (Bazzoni *et al.*, 2000b). As seen in this chapter, JAM-1 membrane localisation in the mouse embryo precedes all of the above-mentioned TJ proteins, providing support to the notion that JAM-1 may indeed aid in facilitating the early stages of TJ assembly.

Analysis of JAM-1 membrane localisation in compact 8-cell and blastocyst stage embryos indicates that JAM-1 can also be distributed in both the basal and apical membranes of polarised blastomeres (Fig 4.10.b). As discussed in section 1.3.2.4.1, human JAM-1 expression in endothelial cells is very similar to PECAM-1 (CD31). As both these molecules belong to the IgSF (Immunoglobulin superfamily), information regarding the role of PECAM-1 may aid in understanding the functions of JAM-1 (Ohto *et al.*,1985; Stockinger *et al.*, 1990; Muller *et al.*, 1989).

Interestingly, both PECAM-1 and JAM-1 have been shown to have important roles in transendothelial migration (TEM) of leucocytes across the endothelial barrier (Muller *et al.*, 1993; Martín-Padura.*et al.*, 1998). Moreover, the combined use of inflammatory cytokines, TNF-α and IFN-γ, on human endothelial cells causes both PECAM-1 and JAM-1 to alter their protein localisation from the intercellular junctions to subcellular positions on the basolateral or apical sides, respectively. The apical distribution of JAM-1, in endothelia, could provide interesting information into the polar localisation of JAM-1 at compaction and *visa versa.* One hypothesis for the function of JAM-1 is that it binds monocytes and therefore may direct the migration of these cells through the intercellular region of the endothelial layer. PECAM-1, although not involved in the induction of leucocyte binding at the endothelial layer, is vital for their extravasion (Muller *et al.*, 1993). It is therefore, tempting to hypothesise that JAM-1 and PECAM-1 co-operate in the process of TEM by acting in slightly different regions of the intercellular cleft (Martín-Padura *et al.*, 1998). Although the requirement for JAM-1 in the apical and basal membranes of polarized blastomeres is not related to TEM as such, these studies demonstrate that JAM-1 localisation patterns are not exclusive to the TJ and are likely to be part of a dynamic signalling pathway.

The change in JAM-1 localisation, from cell-cell contact to the apical pole and back to cell-cell contact again, in the preimplantation embryo is particularly unusual. It may be that, as with E-cadherin, JAM-1 is not in its functional state prior to the onset of compaction and possibly post-translational modifications to the JAM-1 protein may explain such localisation patterns. It is known that in platelet activation, JAM-1 becomes phosphorylated by PKC (Ozaki *et al.*, 2000) and it is postulated that phosphorylation is a key factor in the functional regulation of JAM-1, at least in this process. Western blot analysis would be particularly useful in determining the role of post-translational modifications upon JAM-1 membrane association and function. Phosphorylation has already been shown to be a key component in AJ and TJ biogenesis. Therefore it is possible that, the phosphorylation state of JAM-1 could have interesting implications for TJ biogenesis in the mouse embryo (Winkel *et al.*,1990; Pauken and Capco,1999 & 2000; Sheth *et al.*, 2000). Indeed, recent data in our laboratory has demonstrated that PKCζ is distributed to the apical pole of

compact 8-cell embryos whereas PKCι/λ does not (Judith Eckert, personal communication). It is therefore tempting to suggest that PKCζ may be involved in JAM-1 polar localization but further experiments our required to ascertain whether this is true.

JAM-1 and actin double labelling in compacted 8-cell embryos was investigated to confirm JAM-1 localisation at the microvillous pole. Indeed, the expression profile of JAM-1 is similar to that found with actin throughout development. Thus, the change in the localization of JAM-1 between cell-cell contacts and the apical pole during compaction may reflect actin-reorganisation of JAM-1. Other TJ proteins, such as occludin, ZO-1 and ZO-3, have been shown to directly bind actin (Itoh *et al.*, 1997; Fanning *et al.*, 1998; Wittehen *et al.*, 1999). Indeed, actin is a key constituent of both TJs and AJs and is an essential component of polarized cells (Madara *et al.*, 1987; Drenckhahn & Dermietzel, 1988; Farquhar & Palade , 1986; Rimm *et al.*, 1995; Yonemura *et al.*, 1995). It is tempting to suggest that the polar localization of JAM-1 at compaction indicates that this protein may have a role in establishing cell polarity and may be regulated by PKCζ. Therefore, investigating the effects of disrupting JAM-1 expression in the early embryo will hopefully provide further insight into the early stages of TJ biogenesis and epithelial polarity.

Chapter 4

Expression of claudin-1 and claudin-3 in the mouse preimplantation embryo

4.1 Introduction

Since the initial cloning of claudin-1 from chicken liver and the discovery of the related protein in mice (Furuse *et al.*, 1998a), no information has been published regarding claudins in the mouse preimplantation embryo. As with JAM-1, in order to study the roles of claudin-1 and claudin-3 in the early embryo, it was first necessary to examine both their mRNA and protein expression from egg to implantation.

Once again, RT-PCR was decided upon as the best method of mRNA expression analysis. Western blotting, indirect immunofluorescence and confocal microscopy were used to examine the protein expression and localisation during preimplantation development.

4.2 Material and methods

4.2.1 Primers

Sequence data for claudin-1 was obtained from Genbank, the European Molecular Biology Laboratory and the DNA database of Japan under the accession code AF072127. Claudin-1 cDNA is 952bp long of which bases 156-791 comprise the coding region. In this study, ten different primers were designed to claudin-1 (Figure 4.1). For further details of the primers used see section 2.3.1.

Sequence data for claudin-3 was obtained from Genbank, the European Molecular Biology Laboratory and the DNA database of Japan under the accession code NM009902. Claudin-3 cDNA is 1090bp long of which 56-715bp comprise the coding region. One primer pair was designed to amplify a 288bp product (Figure 4.2).

4.2.2 RT-PCR

Claudin-1 and Claudin-3 mRNA were isolated using either mAP or Dynabead extraction methods (described in section 2.2.1 and 2.2.2, respectively). RNA was

converted to cDNA after mRNA isolation with mAP or Dynabeads, as described in section 2.3.3 and 2.3.5, respectively. cDNA amplification was carried out according to the protocols outlined in sections 2.3.4 (mAP paper) and 2.3.6 (Dynabeads).

(A)

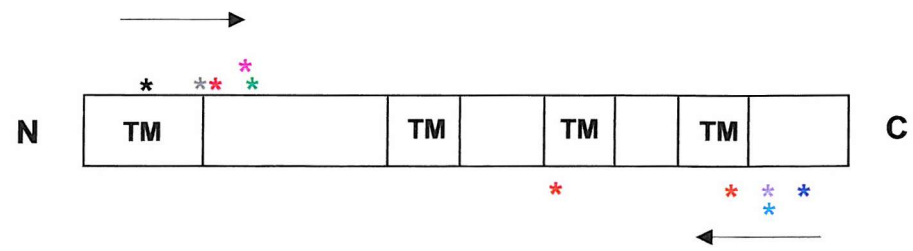

(B)

Primer name	Primer sequence	Position on cDNA sequence
cld1/1	5′-atcggctccatcgtcagc-3′	**210-227**
cld1/2	5′-actagaaggtgttggctt-3′	**773-756**
cld1/3	5′-caacatcgtgaccgctca-3′	**269-286**
cld1/4	5′-ataaggccgtggtgttg-3′	**751-736**
cld1/5	5′-tgggtttcatcctggcttctc-3′	**181-201**
cld1/6	5′-tgacagccatccacatcttct-3′	**516-496**
cld1/7	5′-atcctggcttctctgggatgga-3′	**189-210**
cld1/8	5′-gataaggccgtggtgttgggta-3′	**753-732**
cld1/9	5′-tgctggggacaacatcgtga-3′	**260-279**
cld1/10	5′-gaaagtaggacacctcccaga-3′	**703-683**

Figure 4.1. Primers designed to claudin-1. A) Illustrates the positions of primers used to amplify claudin-1 mRNA from tissue and embryo samples (*) in relation to the transmembrane regions (TM) within the protein structure. B) Shows details of claudin-1 primers and their positions in the claudin-1 cDNA sequence.

(A)

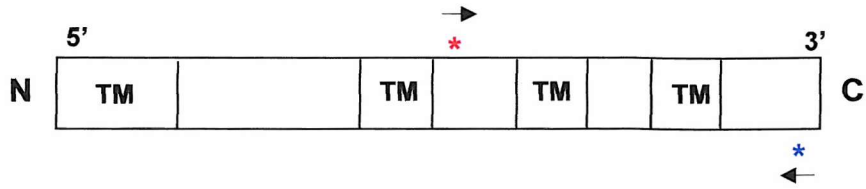

(B)

Primer name	Primer sequence	Position on cDNA sequence
cld3/1	5'-ttttcctgttggcggctctg-3'	* 423-442
cld3/2	5'-cgtagtccttgcggtcgtag-3'	* 710-691

Figure 4.2. Primers designed to claudin-3. A) Illustrates the positions of primers used to amplify claudin-3 mRNA from tissue and embryo samples (*) in relation to the transmembrane regions (TM) within the protein structure. B) Shows details of claudin-3 primers and their positions in the claudin-3 cDNA sequence.

4.2.3 Claudin antibodies

Originally, when the first paper describing claudin-1 was published, it was thought not possible to produce antibodies against either claudin-1 or claudin-2 (Furuse *et al.*, 1998a). The difficulty in producing monoclonal or polyclonal antibodies against these two claudins was attributed to either their small size and/or their low antigenicity (Furuse *et al.*, 1998a). Since then, Zymed have produced, commercially available, polyclonal antibodies for both of these claudins.

For the purpose of this chapter, the polyclonal rabbit anti-claudin-1 antibody (71-7800, Zymed) was used for all protein expression and membrane localisation analysis described. The immunogen is a 25 amino acid synthetic peptide derived from the C-terminus of the human claudin-1 protein (sequence not specified) and reactivity was confirmed with human, mouse, rat and dog claudin-1 by Western blotting and immunofluorescence. Antibody 71-7800 was later reported by Zymed also to cross react with claudin-3. For the purpose of this report this antibody is now referred to as claudin-1/-3. More recently available Zymed antibodies, 51-9000 and 34-1700, specific for claudin-1 and claudin-3 respectively, were used to look at the individual expression of claudin-1 and claudin-3 protein in embryos and tissues.

4.2.3.1 The Claudin-1/-3 antibody (71-7800)

Suitability of the claudin-1/-3 antibody for immunofluorescence had not been examined by Zymed. Working concentrations for the antibody were specified by Zymed as 1-2μg/ml for use with protein extract from tissue in Western blotting and was confirmed to react with mouse, rat, human and dog.

4.2.3.2 The Claudin-1 antibody (51-9000)

Claudin-1 antibody concentrations, recommended by Zymed, ranged between 1-2μg/ml for Western blotting and 5-10μg/ml for immunofluorescence. This antibody had been confirmed to be reactive with human, rat and dog claudin-1 but its reactivity with other species (including mice) had not been determined.

4.2.3.3 The Claudin-3 antibody (34-1700)

Claudin-3 antibody concentrations, recommended by Zymed, ranged between 0.5-3μg/ml for Western blotting. Suitability of this antibody for claudin-3 detection via immunofluorescence had not been tested. This antibody had been confirmed to be reactive with mouse and dog claudin-3.

4.2.4 Western blotting

For full details on Western blotting procedures see section 2.11.3. Concentrations tested for each antibody are described in table 4.1. Some embryo blots were reused after removing any previously bound antibody from the nitrocellulose paper, as described in section 2.11.5.

Table 4.1

Claudin antibody dilutions used for Western blotting

Antibody	Antibody dilutions tested
Claudin-1/-3	0.5-3μg/ml
Claudin-1	2-7μg/ml
Claudin-3	2-7μg/ml

4.2.5 Immunofluorescence and confocal microscopy

As described in section 2.9, immunofluorescence staining for claudin-1/-3 was tested under methanol, 1% and 4% formaldehyde fixation conditions. Primary antibody concentrations ranging from 1/200 (2μg/ml) and 1/1000 (0.4μg/ml) were tested on embryos, the results of which are described in section 4.3.16.

Claudin-1 and claudin-3 antibodies were tested under methanol, 1% and 4% formaldehyde fixation conditions (Section 4.3.18 and 4.3.19; Figures 4.28 and 4.31). Primary antibody concentrations ranging from 1:30 (7μg/ml) to 1:150 (1.3μg/ml) were tested upon embryos (data not shown). 1% formaldehyde and a primary antibody dilution of 1:30 was used for both claudin-1 and claudin-3 to examine expression profiles for both these proteins in mouse preimplantation embryo development (Figures 4.30 and 4.33).

To ensure that staining patterns observed were specific, claudin-1 and claudin-3 peptides (Zymed) were used as specific inhibitors for the corresponding antibodies. Primary antibodies (7μg/ml) were pre-incubated in specific inhibition peptide (35μg/ml), at 4°C overnight, prior to use in normal immunofluorescence protocol. To ensure the specificity of the antibody inhibition, additional embryos were incubated in claudin antibodies that had been pre-incubated with an inappropriate peptide.

4.2.5.1 Embryo staging

Embryos were staged according to the criteria described in section 2.1.3.

4.2.5.2 Double labelling

Double labelling was achieved using the methods described in section 2.9.4. Embryos were fixed in 1% formaldehyde and antibodies were diluted to 1/300 and 1/250 for claudin-1 (Zymed) and ZO-1α^+ (made in house, Sheth *et al.*, 1997), respectively (see table 2.3 for further details). The appropriate anti-rabbit (488) and anti-guinea pig (546) Alexa dyes (Molecular Probes) were used at 1/500. To ensure there was no cross-reaction between primary and secondary antibodies inappropriate secondary antibodies were tested upon the primary antibodies of interest and a combination of secondary only controls were also examined.

4.3 Results

4.3.1 Expression of claudin-1 mRNA in mouse late blastocysts

Using two primer pairs, cld1/-1 with cld/-2 (outer primers) and cld1/3 with cld1/-4 (inner primers), nested RT-PCR was carried out on mRNA, bound to mAP paper, from *in vitro* cultured late blastocysts. Claudin-1 mRNA was amplified on four separate occasions from either multiple (10x and 5x) or single embryo samples. Claudin-1 in the five and tenfold embryo samples was detected using an annealing temperature of 55°C for both first and second stage PCR reactions. In the first PCR (Figure 4.3.A), claudin-1 signal was detected in 5x (lane 4), but not 10x embryos (lane 5). When the RT-PCR was repeated, large amounts of claudin-1 were detected in both 5x and 10x late blastocysts (Figure 4.3.B; lanes 4 + 5). The PCR product was sequenced and upon BLAST searching was found to be 100% identical to *Mus muscularis* claudin-1 (Appendix III).

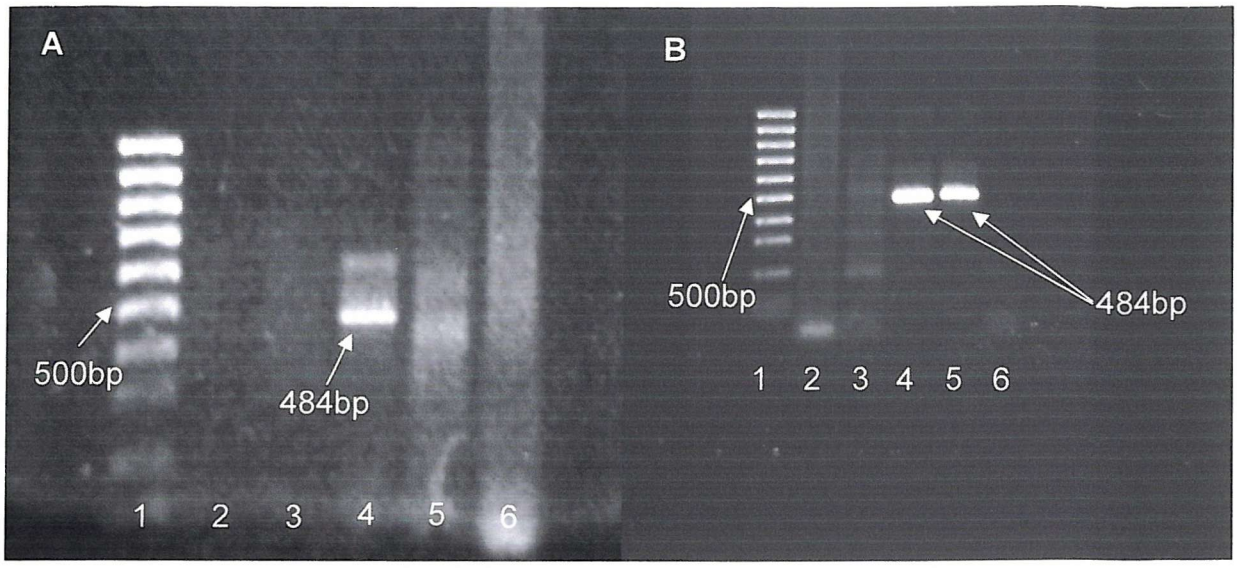

Figure 4.3 Detection of claudin-1 in mouse late blastocysts. Using primers cld1/1 -/2, -/3 and /-4, claudin-1 was detected in mouse late blastocysts (LB; expected product size 484bp). In the first PCR (A) claudin-1 was only detected in the 5x LB sample (lane 4) and not in the single or 10x LB sample (lane 3 and 5, respectively). Master mix and mAP paper only controls were both negative (lanes 2 and 6 respectively). In the second PCR (B) claudin-1 was detected in 5x (lane 4) and 10x (lane 5) LB samples but not in the single LB sample (lane 3). Once again the master mix and mAP paper controls showed no product amplification (lanes 2 and 6, respectively).

4.3.2 Optimisation of claudin-1 primers on mAP using Vent DNA polymerase

In order to see if the RT-PCR signal was optimal for primers cld1/1 to cld1/4, annealing temperatures above and below 55°C were tested on single and 5x late blastocyst samples. At a primer annealing temperature of 53°C, more multiple non-specific bands were amplified (Figure 4.4.A). However, DNA of the correct size was detected in one of the single late blastocyst samples (Figure 4.4.A; lane 4) and in the 5x late blastocyst sample (Figure 4.4.A; lane 5). At a primer annealing temperature of 57°C (Figure 4.4.B), DNA was amplified from a single late blastocyst (Figure 4.4.B; lane 4). However, claudin-1 was not detected in the 5x embryo sample of the same stage (Figure 4.4.B; lane 6). It was decided that an annealing temperature of 55°C should be used for future experiments.

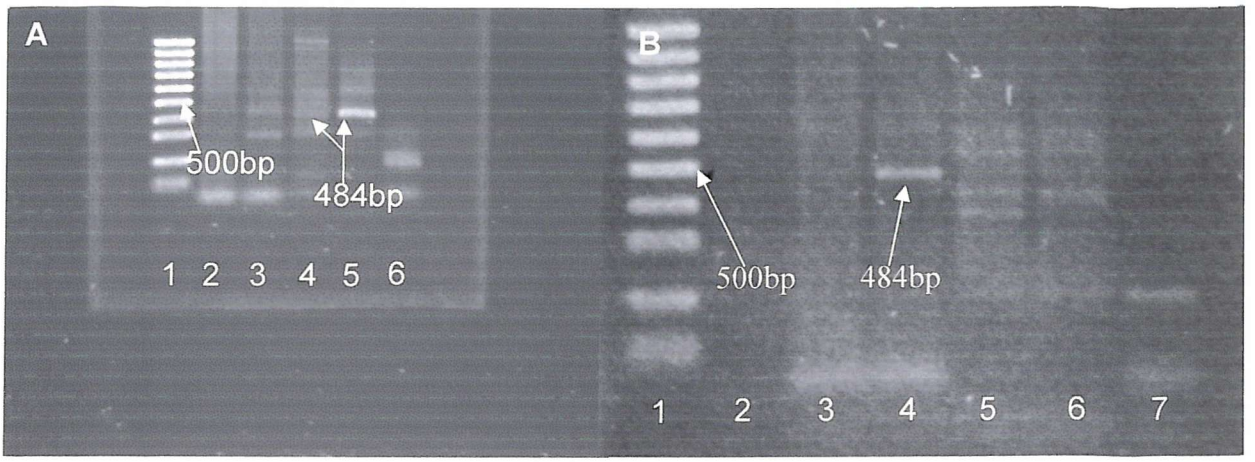

Figure 4.4 Optimisation of claudin-1 primers on mouse late blastocysts (LB) using nested primers (cld1/1 – cld1/4). A) At 53 °C, claudin-1 was detected in one of the two single LB samples (lanes 3 and 4) and the 5x LB sample (lane 5) the master mix and mAP paper controls were negative for claudin-1 (lanes 2 and 6). B) At 57 °C, claudin-1 was only amplified in one of the two single LB samples (lanes 4 and 5) and not in the 5x LB sample (lane 6). Master mix and mAP paper controls showed no amplification of claudin-1 (lanes 3 and 7).

4.3.3 Inconsistency in claudin-1 detection by RT-PCR

After the initial success in amplifying claudin-1 mRNA, problems were experienced with its detection in late blastocysts and earlier developmental stages. Gels were frequently blank and RNase contamination was suspected as the problem. It was thought that the DEPC used to treat our water might have deteriorated. This was replaced but the problem was not resolved. PCR with autoclaved and UV-irradiated water did not solve the problem either. Commercially produced Analar water (Anachem), a different PCR room, thermocycler and stock of RT-PCR enzymes, plus new primer and dNTP aliquots were all tested, however, the problem persisted. Using an Access RT-PCR Kit (Promega) and our RT-PCR reagents, the embryo template and occludin primers (designed by Dr B. Sheth, University of Southampton) were tested. These primers are known to work under a wide range of conditions and the template should be highly abundant in embryos (Sheth *et al.*, 1997). Only the RT-PCR involving our solutions failed (Figure 4.5; lanes 2-4). The experiment was run both on our PCR thermocycler (Figure 4.5) and on an alternative PCR thermocycler (results not shown), both machines gave the same results.

Figure 4.5 Analysis of RT-PCR amplification difficulties. Single stage RT-PCR amplification of occludin (expected product size 588bp) in late blastocysts comparing in-house RT-PCR reagents (lanes 2-4) verses Promega kit RT-PCR reagents (lanes 5-7). Alternative primers (α-catenin) were also tested upon LBs (lanes 9-11; 223bp) to test the embryo template using Promega kit RT-PCR reagents. Kit reagents and the Kit supplied plasmid positive controls (lanes 12-14; 323bp) were also tested. The PCR products were run on a 2% agarose gel. Only when our in-house reagents were used products were not detected (lanes 2-4).

Due to the reagent problems, analysis of claudin-1 expression in the early embryo was continued using the Access RT-PCR kit. However, despite using the kit, no specific mRNA expression could be detected in late blastocysts or any other embryo stage (Figure 4.6). The positive RT-PCR control (Kit plasmid; Figure 4.6; lane 23), and the occludin embryo controls were all positive (Figure 4.6; lanes 20-22).

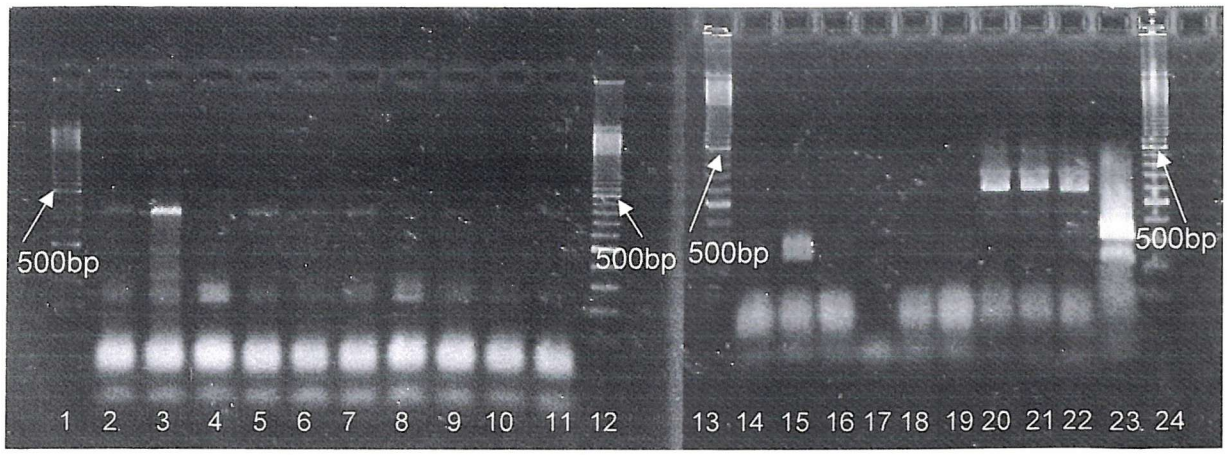

Figure 4.6 RT-PCR for claudin-1 on various embryo stages using the Access RT-PCR Kit. RT-PCR on mouse late blastocysts (LBs), early blastocysts (EBs) and late morulae (LM) using the Access RT-PCR single stage system (Promega). Claudin-1 (expected product size 563bp) could not be amplified from any of the following embryo samples: 5x LBs (lanes 2+3), single LB (lanes 4 and 5), 5 x EBs (lane 6), single EB (lane 7), 5 x LM (lanes 8-10), single LM (lanes 11, 14 and 15), The occludin (588bp; lanes 20-21) and kit (323; lane 23) positive control gave the correct amplification products. The mAP only (lanes 16+17), mAP + media controls (lanes18+19) showed no product amplification.

4.3.4 RNA extraction from tissues

Despite replacing the old RT-PCR reagents, claudin-1 product could still not be amplified reliably. Further analysis into each RT-PCR reagent indicated that the dNTPs were causing the problem. A different dNTP set was used but claudin-1 could no longer be detected in late blastocysts despite amplification of other mRNAs (results not shown). Primers cld1/1, cld1/2, cld1/3 and cld1/4 were tested and subsequently optimised on mouse liver tissue RNA isolated, as described in section 2.2.3, to verify that the primers were capable of detecting claudin-1.

4.3.4.1 Primer optimisation

Testing primers cld1/1 and cld1/2 on liver tissue mRNA revealed that claudin-1 could be detected from 190pg of total RNA. The optimum conditions for using the claudin-1 primers were tested by altering both the temperature and $MgCl_2$ concentration. For these experiments, only one stage PCR was used but with increased cycle numbers than the nested PCR protocols tried previously. Primer annealing temperatures of 53°C, 55°C and 58°C were tested at $MgCl_2$ concentrations of 1mM, 1.5mM and 2mM (Figure 4.7). At 53°C and 55°C, 2mM $MgCl_2$ enhanced the non-specific binding of the primers and thus produced multiple amplification

products. At an annealing temperature of 58°C 2mM $MgCl_2$ specific claudin-1 amplification was apparent. At all three temperatures, 1mM $MgCl_2$ provided little or no signal. On the other hand, all three temperatures amplified claudin-1 at 1.5mM $MgCl_2$.

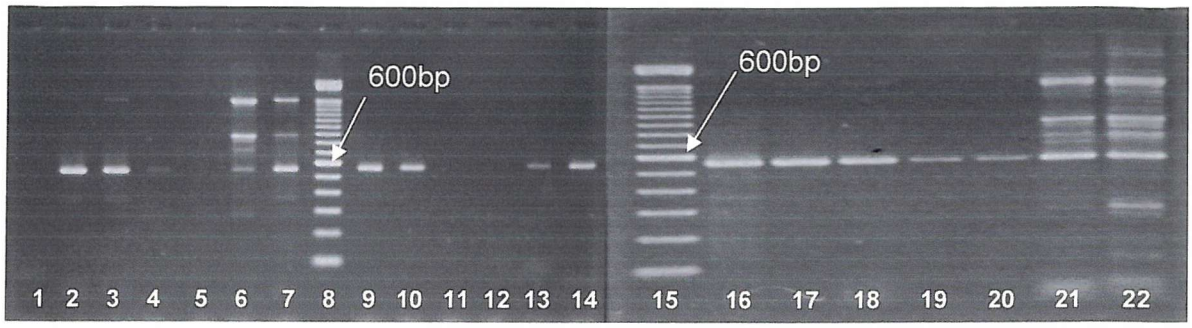

Figure 4.7 Optimisation of cld1/1 and cld1/2 primers on mouse liver total RNA. Claudin-1 (563bp) was amplified with relative specificity at 53°C 1.5mM $MgCl_2$ (lanes 2 and 3) but not with 1mM $MgCl_2$ (lanes 4 and 5). 2mM $MgCl_2$ at 53°C also amplified claudin-1 but was not as specific in its amplification (lanes 6 and7). At 58°C with both 1.5mM (lanes 9 and 10) and 2mM $MgCl_2$ (lanes 13 and 14) gave specific amplification of claudin-1 but once again 1mM $MgCl_2$ (lanes 11 and 12) was unsuccessful. At 55°C 1.5mM (lanes 17 and 18) and 1mM $MgCl_2$ (lanes 19 and 20) claudin-1 mRNA was specifically amplified, with 1.5mM $MgCl_2$ producing greater amplification. However at 55°C 2 mM produced many non-specific products in addition to amplifying claudin-1 (lanes 21 and 22). The master mix control was negative (lane 1). Claudin-1 was also successfully amplified from the 190ng tissue RNA positive control (lane 16).

4.3.5 RT-PCR following Dynabead mRNA extraction and multiple embryo samples

Using optimal conditions (determined using tissue RNA, see section 4.3.4.1; 55°C and 1.5mM $MgCl_2$), claudin-1 RT-PCR was tested again on embryos using Dynabeads to extract the mRNA (as described in section 2.2.2). Two PCR protocols were followed: 1) 20µl RT reaction, of which 5µl was transferred into a 50µl PCR and 2) 10µl RT reaction of which all was transferred into a 100µl PCR reaction. Both RT-PCR methods failed to amplify claudin-1 mRNA using cld1/1 and cld1/2, despite amplification of both occludin and poly-A polymerase (results not shown). Using the 10µl RT and 100µl PCR method, single, 2x, 3x, 4x, 5x and 10x embryos were with primers FT1 and FT2, but still claudin-1 mRNA could not be amplified (Figure 4.8).

Figure 4.8 Primers cld1/1 and cld1/2 on embryo mRNA following Dynabead extraction. Claudin-1 was not detected in 1x (lane 2), 2x (lane 3), 3x (lane 4), 4x (lane 5), 5x (lane 6) or 10x (lane 8) late blastocyst samples but was amplified from 190pg of total RNA (lane 9). The minus RT enzyme control (lane10) did not amplify claudin-1. Some contamination was found in the master mix only control but this was not found in any other sample.

4.3.6 Alternative claudin-1 primers

Due to repeated problems with claudin-1 amplification, primers cld1/1-cld1/4 were analysed further for possible primer hairpin structures and likely primer dimer conformations using the primer design program, Oligo. Primer analysis indicated that cld1/1 – cld1/4 may form hairpins or that they may anneal to each other. New primers (cld1/5 and cld1/6; see section 2.3.1 and Figure 4.1) were designed to eliminate the possibility of inefficient priming as the cause of the claudin-1 amplification problems. The new primers were first tested upon liver tissue total RNA and successfully amplified claudin-1 (Figure 4.9).

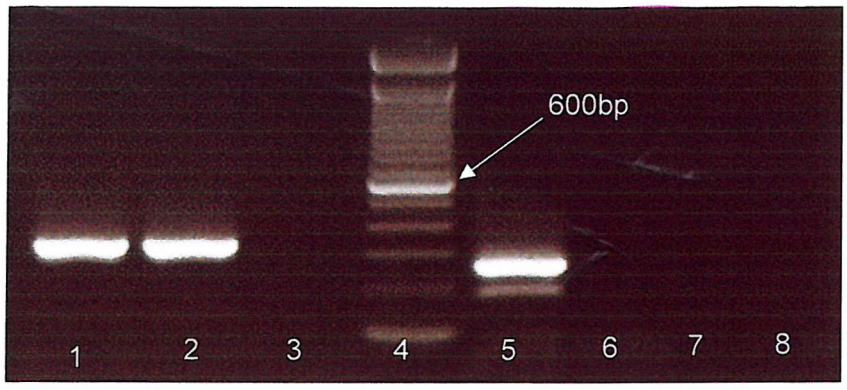

Figure 4.9 Amplification of claudin-1 RNA from mouse liver using primers cld1/5 and cld1/6. Using 2mM MgCl2 and a 60°C primer annealing temperature, claudin-1 RNA was amplified (lanes 1 and 2). Both the minus RT and master mix controls did not amplify claudin-1 (lanes 3 and 7 respectively). Poly-A polymerase was also amplified (lane 5), whereas with both poly-A polymerase minus RT and master mix controls showed no product amplification (lanes 6 and 8 respectively).

4.3.7 RT-PCR on late blastocysts using primers cld1/5 and cld1/6

Primers cld1/5 and cld1/6 were tested upon late blastocysts using the same conditions as with the tissue RNA (section 4.3.6). However, claudin-1 was only amplified in the tissue positive control and not in the embryo sample despite poly-A polymerase being amplified from a small proportion of the same embryo samples (1/20 of the RT reaction). The lack of claudin-1 mRNA in the second late blastocyst (Figure 4.10; lane 4) may have been due to RNA degradation as the poly-A polymerase signal (usually a highly abundant transcript) was very weak (Figure 4.10; lane 5) in comparison with the first late blastocyst (Figure 4.10; lane 3). However, poly-A polymerase transcript was abundant in the first embryo tested and so the lack of claudin-1 expression in this sample appears not to be due to mRNA degradation.

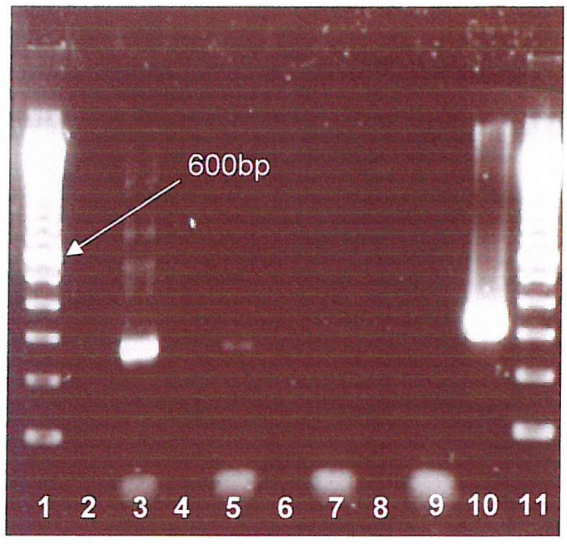

Figure 4.10 RT-PCR upon late blastocysts using primers cld1/5 and cld1/6. In the two late blastocysts (LB) no claudin-1 amplification was achieved (lanes 2 and 4). However, although the the poly-A polymerase positive control was amplified efficiently from one LB (lane 3) the signal was weak for the second LB (lane 5). Minus RT controls (lanes 6+7) and master mix controls were negative (lanes 8 and 9). Claudin-1 was amplified from the tissue RNA control (lane 10).

4.3.8 RT-PCR on tissue with cld1/7, cld1/8, cld1/9 and cld1/10 primers

Although there was relatively little success with the mouse claudin-1 primers, nested human claudin-1 primers for use on human embryos had previously been successful in our laboratory. One possible explanation for the difficulty in amplifying claudin-1 mRNA in the mouse embryo might have been due to a complex secondary structure. The exact positions of the human claudin-1 primers were mimicked on the mouse sequence. The primers were first tested on tissue (Figure 4.11). Claudin-1 was visualised on a 1% agarose gel from both first stage (Figure 4.11; lanes 1 and 2) and second stage RT-PCR reactions (Figure 4.11; lanes 10 and 11).

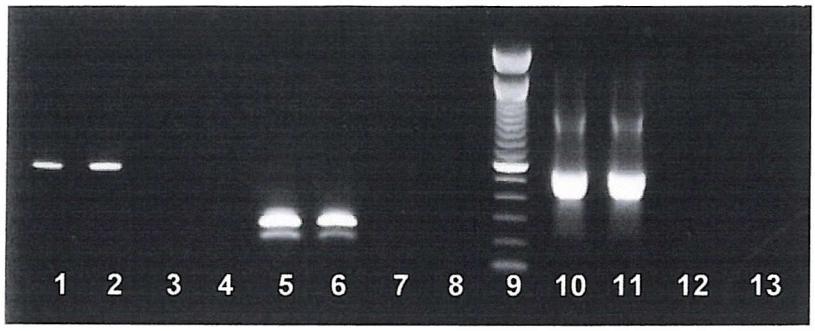

Figure 4.11 Nested RT-PCR upon mouse tissue primers cld1/7, cld1/8, cld1/9 and cld1/10 Claudin-1 was successfully amplified in mouse liver tissue in both single stage (lanes 1 and 2) and nested RT-PCR (lanes 10 and 11). Positive control primers for Poly-A polymerase also successfully amplified their expected product (lanes 5 and 6). Minus RT controls for first stage claudin-1 (lanes 3 and 4), second stage claudin-1 (lanes 12 and 13) and poly-A polymerase (lanes 7 and 8) RT-PCR reactions did not show any product amplification.

4.3.9 RT-PCR on late blastocysts using cld1/7, cld1/8, cld1/9 and cld1/10

Nested RT-PCR was tested upon multiple late blastocyst samples. However, despite all positive controls being successfully amplified, claudin-1 was not detected from either 5x or 20x late blastocysts, despite a high exposure of the gel products with the Alpha imager (Figure 4.12).

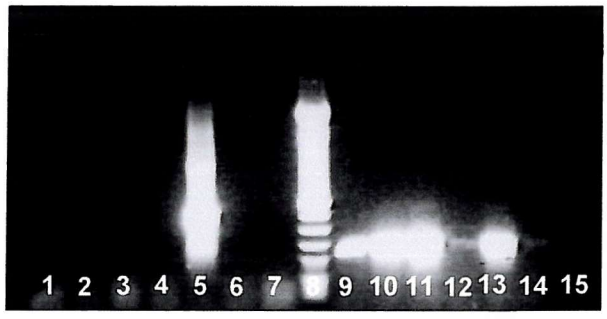

Figure 4.12 Nested RT-PCR upon late blastocysts (LB) using primers cld1/7, cld1/8, cld1/9 and cld1/10. Despite amplification of poly-A polymerase in 5x (lanes 9 and 12) and 20x LB (lanes 10 and 11) claudin-1 was not amplified in equivalent embryos samples (lanes 1 and 4 and lanes 2 and 3 respectively). Tissue positive controls for both Poly-A polymerase and claudin-1 were strongly amplified (lanes 13 and 5 respectively).

4.3.10 mRNA expression of Claudin-3 in embryos

Initially, only claudin-1 mRNA and protein expression was planned to be examined in this study. However, due to the cross reactivity of the claudin-1

antibody (71-7800; claudin-1/-3) with claudin-3, it was thought important also to establish mRNA and protein expression for claudin-3.

Single stage primers (cld3/1 and cld3/2) were designed to amplify claudin-3 mRNA. These primers successfully amplified claudin-3 in tissue (data not shown) and later were shown to amplify claudin-3 in embryo samples (Figure 4.13 and 4.14), the products of which were confirmed by sequencing (see section 2.7). Initially multiple (5x) early and late blastocyst samples were examined for claudin-3 mRNA expression. Claudin-3 was found to be abundant in both early and late blastocysts (Figure 4.13). Upon examination of earlier embryo stages, claudin-3 was found expressed in embryos from the 2-cell stage up to and including late blastocysts (Figure 4.14). In unfertilised eggs, two faint bands were amplified at sizes immediately above and below the expected product height of 288bp. The lower amplification product was also detected in 1-cell embryos and in subsequent stages. Sequencing of this lower product was attempted but no recognisable sequence was obtained. As an external control for the RT-PCR procedure luciferase RNA was added to each embryo sample prior to dynabead extraction. Poly-A polymerase was used as an internal control.

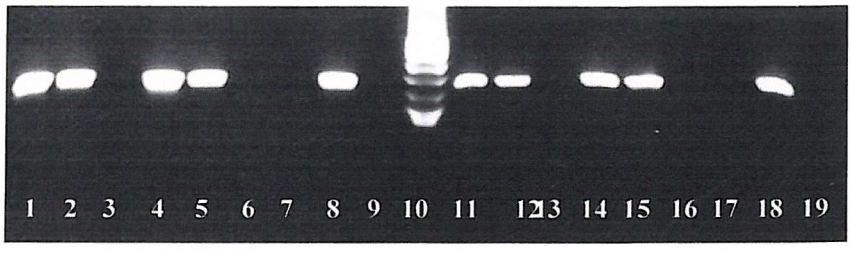

Figure 4.13 Claudin-3 RT-PCR on late (LB) and early (EB) blastocysts and tissue samples. Claudin-3 was successfully amplified from 5x EB (lanes 11 and 12), 5x LB (lanes 14 and 15) and mouse liver tissue (lane 18). Poly-A polymerase positive control were also successfully amplified from 5x EB (lanes 1 and 2), 5x LB (lanes 4 and 5) and mouse liver tissue (lane 8). Both master mix (lanes 17 and 7) and –RT controls (13,16,19,3,6 and 9) were negative.

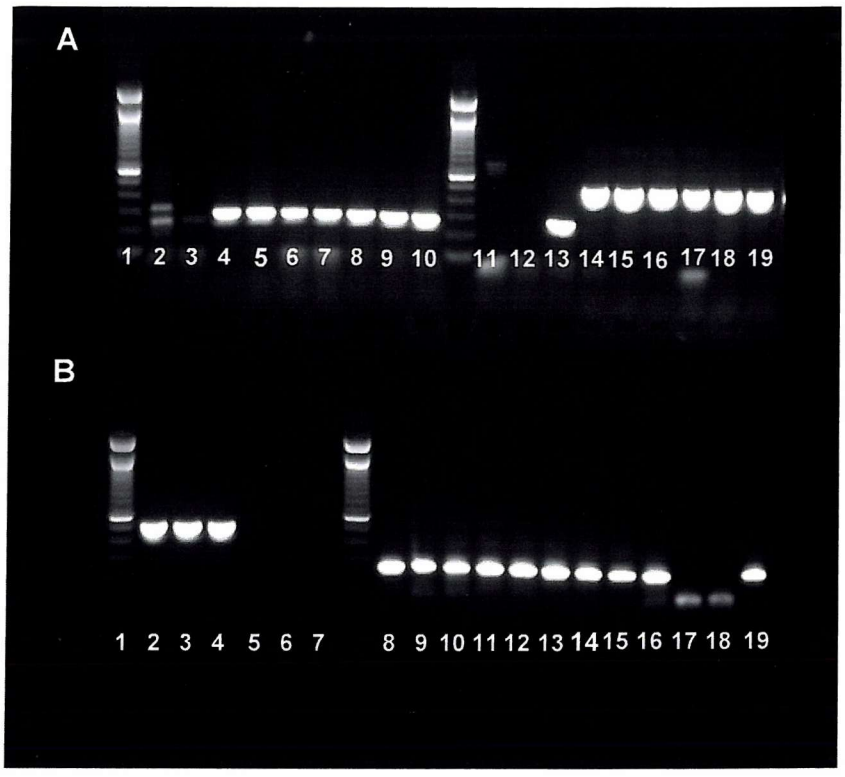

Figure 4.14 Claudin-3 RT-PCR on mouse embryos. Claudin-3 was successfully amplified from 2-cell (lane 4A), 4-cell (lane 5A), 8-cell (lane 6A), compact 8-cell (lane 7A) late morula (lane 8A) and in early (lane 9A) and late blastocysts (lane 10A). The tissue control for claudin-3 was also positive (lane 13A). Two amplification products, neither of which being at the expected size for claudin-3, were found in unfertilised eggs (lane 2A). Fertilised eggs (lane 3A) had faint expression of the lower amplification band found also in unfertilised eggs. All the external control (luciferase RNA; lanes 14-19A and lanes 2-6B) and Poly-A polymerase positive controls (lanes 8-19B) for each embryo stage (loaded in the same order as the claudin-3 samples) had an appropriate amplification signal. All minus RT (lanes 12A, 6B and 18B) and master mix (lanes 11A, 5B and 17B) controls showed no product amplification.

4.3.11 Claudin-1/-3 protein expression in mouse tissue lysates

Firstly, to determine a suitable concentration for use on 31.5μg total protein extracted from mouse liver tissue, claudin-1/-3 antibody was tested at concentrations of 1, 2 and 0.5μg/ml (Figure 4.15). Using Tris 1% Tween, 10% milk powder for blocking and for both primary (overnight; 4°C) and secondary antibody (1-hour; r.t) incubations, bands were detected at the expected mobility for claudin-1/-3 protein (~molecular weight 22kDa). The optimal concentration of claudin-1/-3 antibody appeared to be 2μg/ml, which produced the strongest specific reaction.

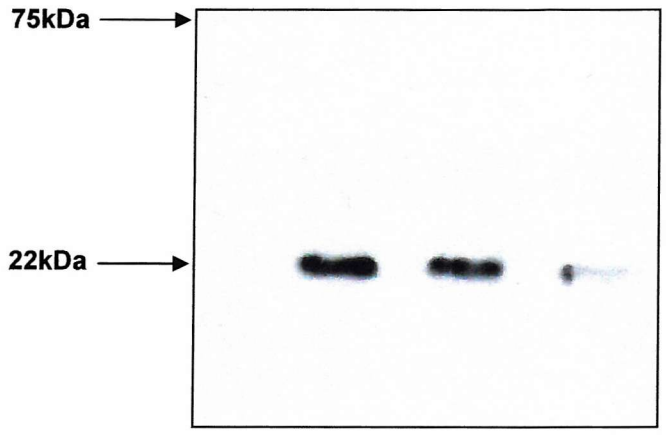

Figure 4.15 Western blot analysis of claudin-1/-3 antibody at concentrations of 2μg/ml, 1μg/ml and 0.5μg/ml, on 31.5μg of total protein from mouse liver tissue.

Although, a clear band corresponding to the molecular weight for claudin-1/-3 was detected under the conditions described above, the ECL signal appeared to be relatively weak. Blocking conditions for the primary antibody incubation were reduced from 10% to 5% milk powder but all other conditions were kept the same. 2μg/ml claudin-1/-3 antibody was used for subsequent blots. In a sample containing 31.5μg of total protein from mouse liver, a much stronger signal, corresponding to a ~22kDa protein was detected (Figure 4.16). A few higher molecular weight bands were detected but these were weak in comparison to the band of interest.

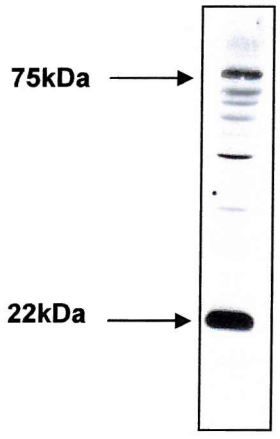

Figure 4.16 Western blot showing claudin-1/-3 detection (used at 2μg/ml in 5% milk in Tris-1% Tween) from 31.5μg protein extracted from mouse liver tissue.

The blotting conditions were now regarded as optimal for claudin-1/-3 detection in 31.5μg mouse liver. However, this amount of protein corresponds to approximately the total protein content of 1260 mouse embryos (~25ng of total protein per embryo; Brinster, 1967). A lower tissue amount, equivalent to 500 embryos was tested using the same conditions. Detection of claudin-1/-3 was still acceptable, producing a bright signal with ECL at the approximate mobility of 22 kDa (Figure 4.17). Some non-specific bands at a higher molecular weight were still apparent.

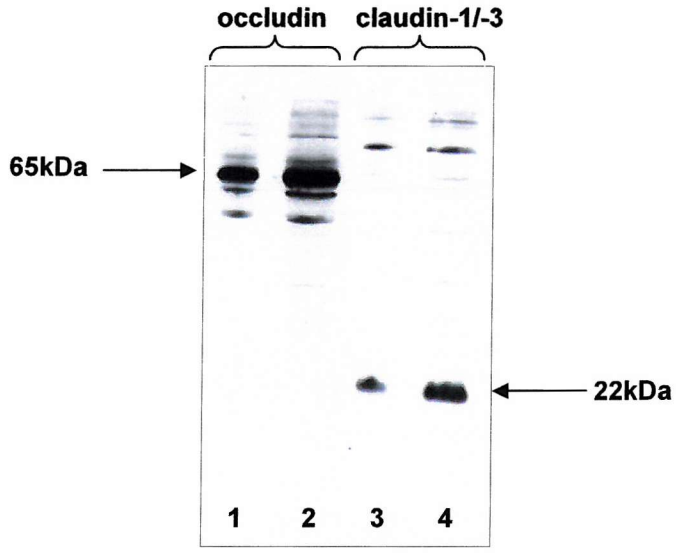

Figure 4.17 Western blot analysis of occludin and claudin-1/-3 protein expression in mouse liver tissue equivalent to the protein content of 500 (lanes 1+3) and 1260 (lanes 2+4) embryos.

Prior to testing embryo samples for claudin-1/-3 expression, 3μg/ml of claudin-1/-3 antibody was tested in comparison with 2μg/ml to see whether a higher antibody concentration than suggested by Zymed would improve detection of claudin-1/-3 (Figure 4.18). There was a slight increase in claudin-1/-3 signal when the primary antibody was used at a concentration of 3μg/ml in 31.5μg of total mouse liver protein, but this increase was almost indistinguishable in 12.5μg of total protein (equivalent to 500 embryos).

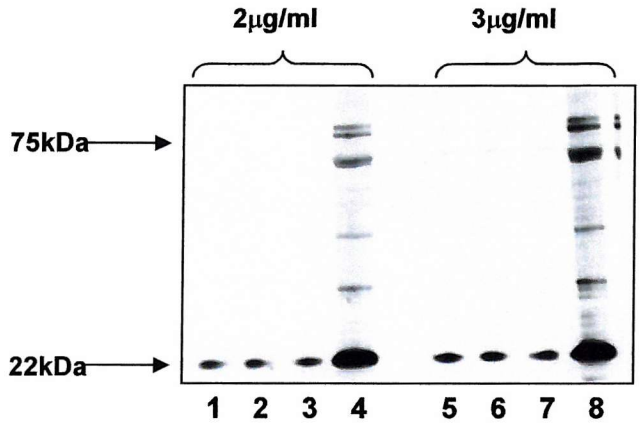

Figure 4.18 Comparison of claudin-1/-3 antibody at concentrations of 2µg/ml and 3µg/ml in Western blot of mouse liver protein. All lanes, except lanes 4+8 are equivalent to 500 embryos. Lanes 4+8 are equivalent to 1260 embryos.

4.3.12 Claudin-1/-3 protein expression in mouse preimplantation embryos

Protein samples isolated from 500 late blastocysts and 500 early blastocysts were tested in comparison to the equivalent total protein extracted from mouse liver tissue (Figure 4.19). A strong signal at ~22kDa weight and at the same mobility as in the tissue sample was detected in the mouse late blastocysts but a much weaker expression was found in early blastocysts.

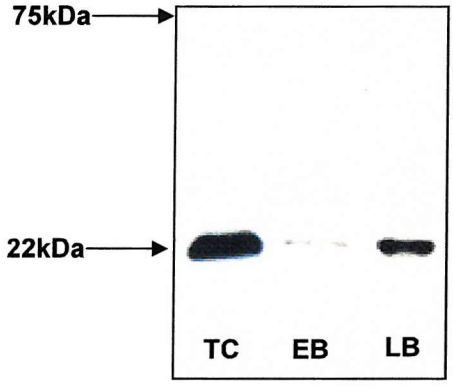

Figure 4.19 Detection of claudin-1/-3 protein expression in early (EB) and late (LB) blastocysts. Primary antibody concentration of 3µg/ml. Positive control is 12.5µg protein from mouse liver (TC).

Earlier embryo stages were collected for protein analysis. However, despite detection of claudin-1 in early blastocyst and liver tissue samples, claudin-1/-3 was not observed in late morulae (LM) or unfertilised eggs (UF; Figure 4.20). However,

these results are in accordance with the immunofluorescence data described in section 4.3.16.

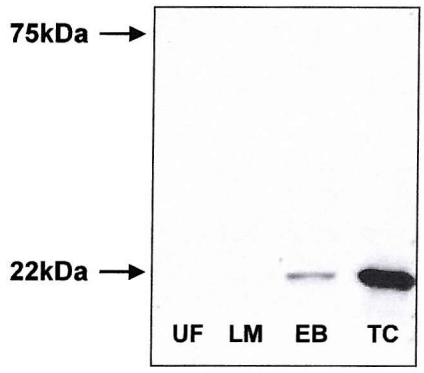

Figure 4.20 Western blot detection of claudin-1/-3 protein expression in earlier embryo stages. Claudin-1/-3 protein was detected in tissue control (TC) and early blastocyst (EB) samples but not in late morulae (LM) or unfertilised eggs (UF).

4.3.13 Claudin-1 and claudin-3 expression in mouse tissue lysates

New specific antibodies against claudin-1 and claudin-3 were tested upon mouse tissue lysates. Both antibodies used on Western blots at three different concentrations (2, 4 and 7µg/ml; Figure 4.21). At each of these concentrations a band of approximately 22kDa was detected. However, other bands were also detected between 50kD and 150kD. The non-specific bands were more predominant with the claudin-1 antibody compared with the claudin-3 antibody.

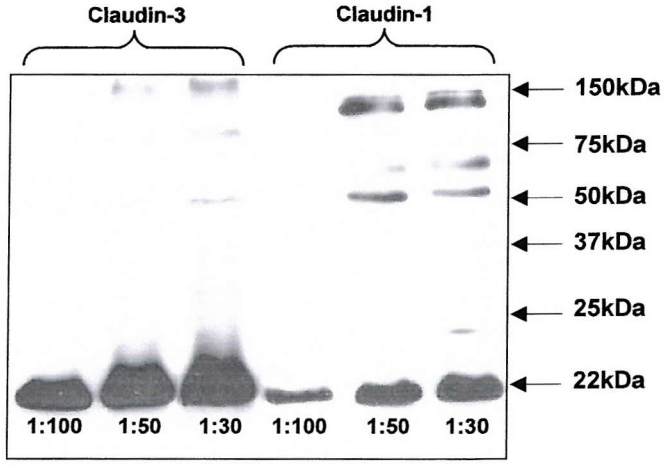

Figure 4.21 Western blot detection of claudin-1 and claudin-3 using the new Zymed antibodies. Claudin-1 and claudin-3 (~22kDa) were detected in mouse liver tissue. However, proteins of a higher molecular weight were also detected with high antibody concentrations.

4.3.14 Claudin-1 and claudin-3 expression in mouse preimplantation embryos

Because of time constraints and the amount of embryos required for Western blotting, an existing embryo blot was stripped and reused to test the new claudin antibodies (see sections 2.11.5 and 4.2.4). Claudin-1 was detected in the liver tissue control equivalent to 1260 embryos but not in the tissue control equivalent to 500 embryos. Moreover, claudin-1 was not detected in any embryo stage (each comprising ~500 embryos). Proteins above 50kDa were also detected in the tissue samples, fertilised eggs, 2-cell embryos and weakly in compact 8-cell embryos but not in any other embryo stage (Figure 4.22).

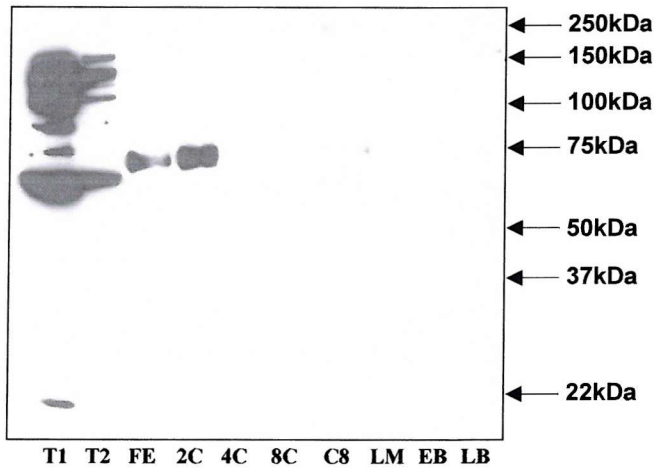

Figure 4.22 Western blot analysis of claudin-1 on embryos using 51-9000 antibody (Zymed). Claudin-1 (~22kDa) was detected in tissue control samples equivalent to 1260 embryos (TC1) but not in tissue equivalent to 500 (TC2) embryos. Claudin-1 was not detected in any of the embryo samples (FE-LB), each comprising ~500 embryos. Proteins above 50kDa were also detected in the tissue samples, fertilised eggs, 2-cell embryos and weakly in compact 8-cell embryos but not in any other embryo stage.

The same blot was stripped (section 2.11.5) and reused for probing with claudin-3 antibody (Figure 4.23). On this occasion, both of the tissue control samples (equivalent to either 1260 or 500 embryos) for claudin-3 were detected. However, despite detection of claudin-3 in the tissue lysates, the protein was not detected in any of the embryo samples. Non-specific bands were not detected in this blot.

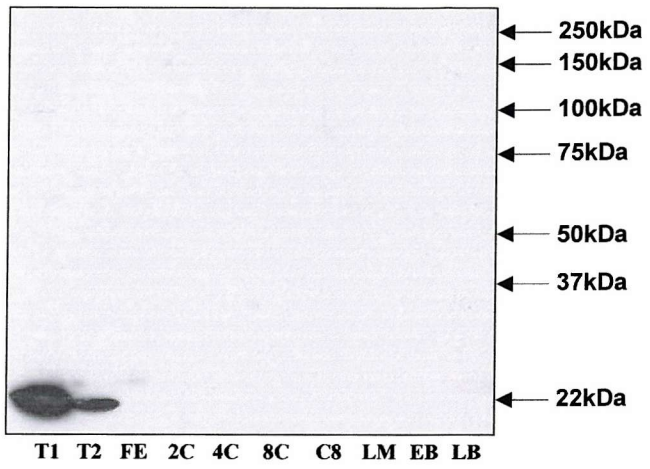

Figure 4.23 Western blot analysis of claudin-3 on embryos using 34-1700 antibody (zymed). Claudin-3 (~22kDa) was detected in tissue control samples equivalent to 1260 (TC1) and 500 (TC2) embryos. However, claudin-3 was not detected in any of the embryo samples (FE-LB).

4.3.15 Optimal conditions for claudin-1 immunostaining

Late blastocysts were fixed in 1% formaldehyde for 15 minutes and claudin-1/-3 primary antibody concentrations of 1/250 (2.5μg/ml), 1/500 (0.8μg/ml) and 1/1000 (0.4μg/ml) were tested for their ability to detect claudin-1/-3 protein localisation in the mouse embryo (Figure 4.24). Claudin-1/-3 antibody at a dilution of 1/1000 was found to be too weak such that junctional staining for claudin-1/-3 was only visible in tangential, and not midplain, confocal sections. Claudin-1 at a 1/500 primary antibody dilution showed improved detection but results were inconsistent from embryo to embryo. However, claudin-1/-3 antibody at a dilution of 1/250 gave good junctional staining and the results were consistent in all late blastocysts tested. However, for all claudin-1/-3 antibody dilutions tested, the nuclei of each blastomere were also stained.

As an alternative to formaldehyde fixation, methanol was also tested on mouse blastocysts (Figure 4.25). Embryos were fixed for 10, 15 or 20 minutes and claudin-1/-3 antibody was used at dilutions of 1/200 (2μg/ml), 1/300 (1.3μg/ml) and 1/400 (1μg/ml). 1/200 and 1/400 dilutions were found to not be suitable for staining claudin-1/-3 but 1/300 gave good junctional staining in tangential planes at 10, 15 and 20 minutes methanol fixation. 10 minutes fixation appeared to give the best images in both tangential and midplain sections. The nuclear staining found in formaldehyde fixed embryos was much less apparent in embryos fixed in methanol.

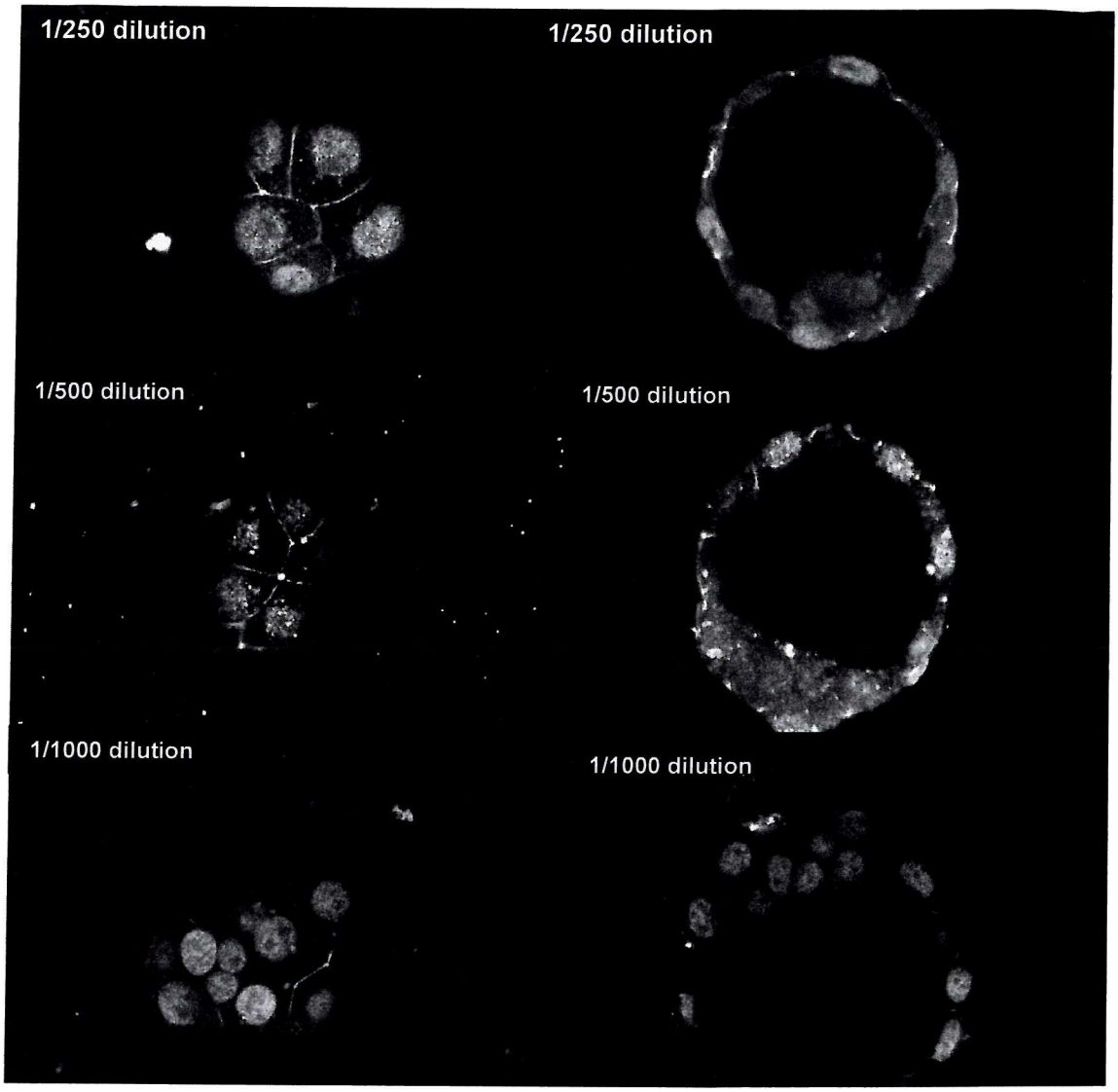

Figure 4.24 Tangential (left) and mid-plane (right) confocal images of claudin-1/-3 immunofluorescent staining of mouse late blastocysts fixed in 1% formaldehyde using different primary antibody dilutions.

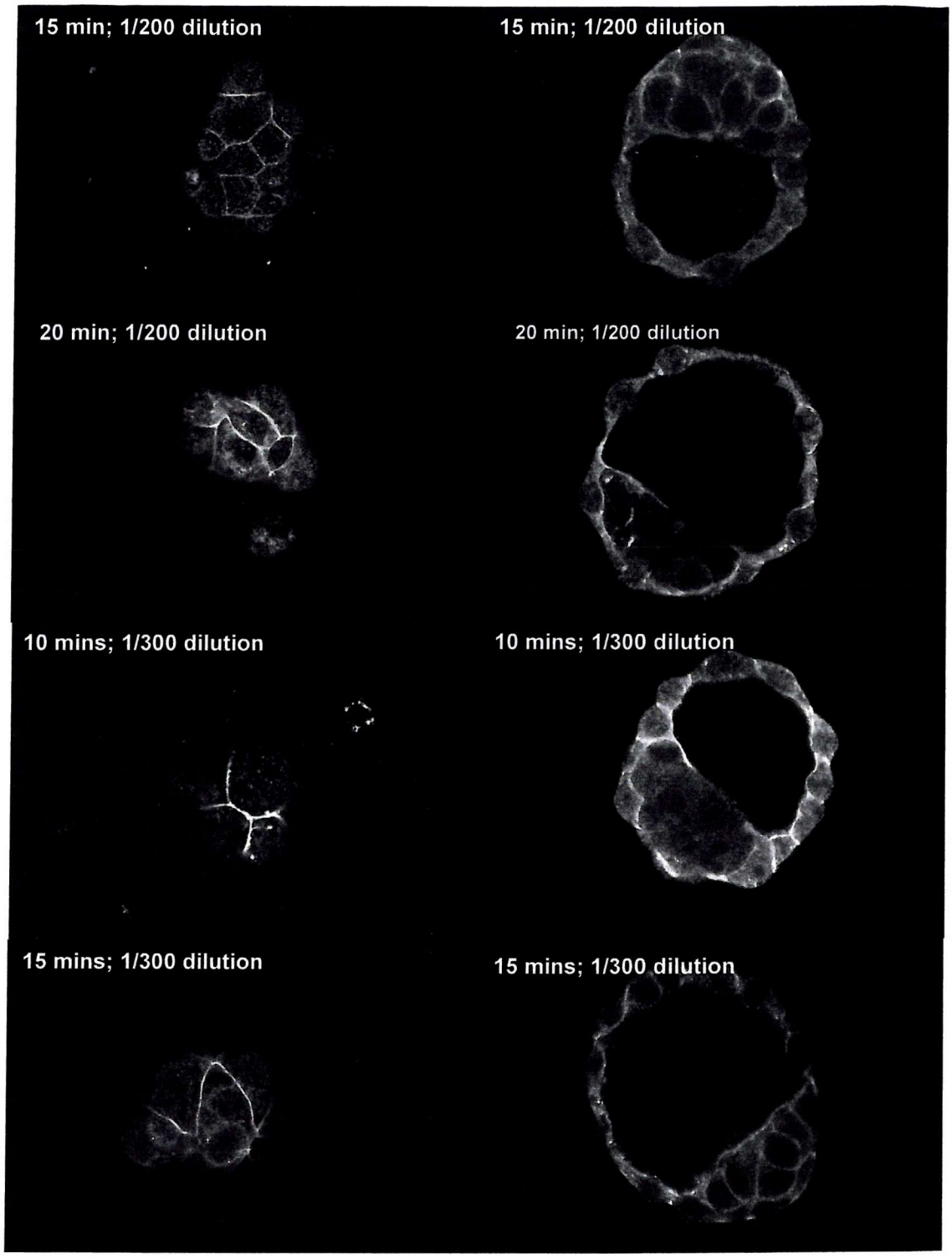

Figure 4.25 Tangential (left) and mid-plane (right) confocal images of claudin-1/-3 immunofluorescent staining of mouse late blastocysts fixed in methanol for 10, 15 or 20 minutes, using three different primary antibody dilutions (also continued on next page).

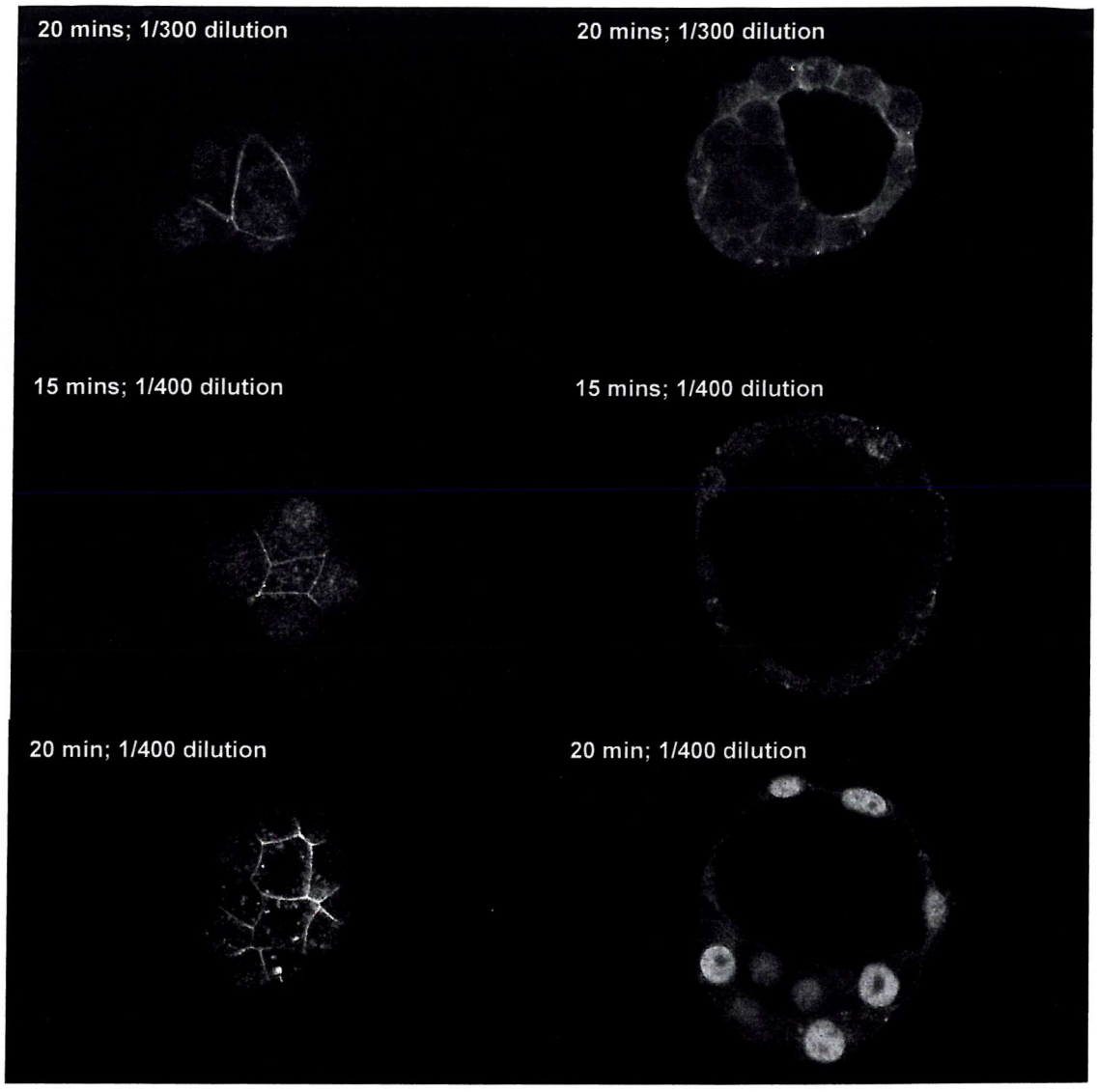

Figure 4.25 cont...

4.3.16 Embryos stages

10 minutes methanol fixation and a primary antibody dilution of 1/300 were subsequently used as the conditions appropriate for analysis of claudin-1/-3 localisation in the early mouse embryo (Figure 4.26). From 2-cell to compact 8-cell stages, embryos were negative for claudin-1 staining. At the 16-cell stage, distinct punctate perinuclear foci (arrowheads) and some cell contact staining (arrows) of claudin-1 were detected at the early (E) morula stage. At the late (L) morula stage, claudin-1 is increasingly evident at cell-cell contact sites. Early (E) and late (L) blastocysts showed claudin-1 staining at TJ sites and was not found in the ICMs.

Table 4.2

The number of stages examined for claudin-1/-3 protein localisation

Embryo stage investigated	Numbers examined
mid 2-cell	10/10 negative
mid 4-cell	8/8 negative
Compact 8-cell	8/8 negative
Early morula	3/10 positive (perinuclear)
Late morula	15/15 positive (junctional)
Early blastocyst	32/32 positive (junctional)
Late blastocyst	53/53 positive (junctional)

4.3.17 Co-localisation of claudin-1/-3 and ZO-1

Immunolocalisation patterns for claudin-1/-3 were similar to those found for another transmembrane TJ protein, occludin. Occludin has been shown to co-localise with ZO-1α^+ prior to its translocation to the TJ and the onset of blastocoel formation. Embryos double labelled for claudin-1/-3 and ZO-1α^+ revealed that these two proteins were co-localised at TJ sites in both late morulae and early blastocysts (Figures 4.27). Attempts to capture embryos at the precise point of claudin-1/-3 and ZO-1α^+ perinuclear localisation, prior to junction formation, were not successful. Double labelling experiments were postponed while the new claudin antibodies were being tested upon embryos.

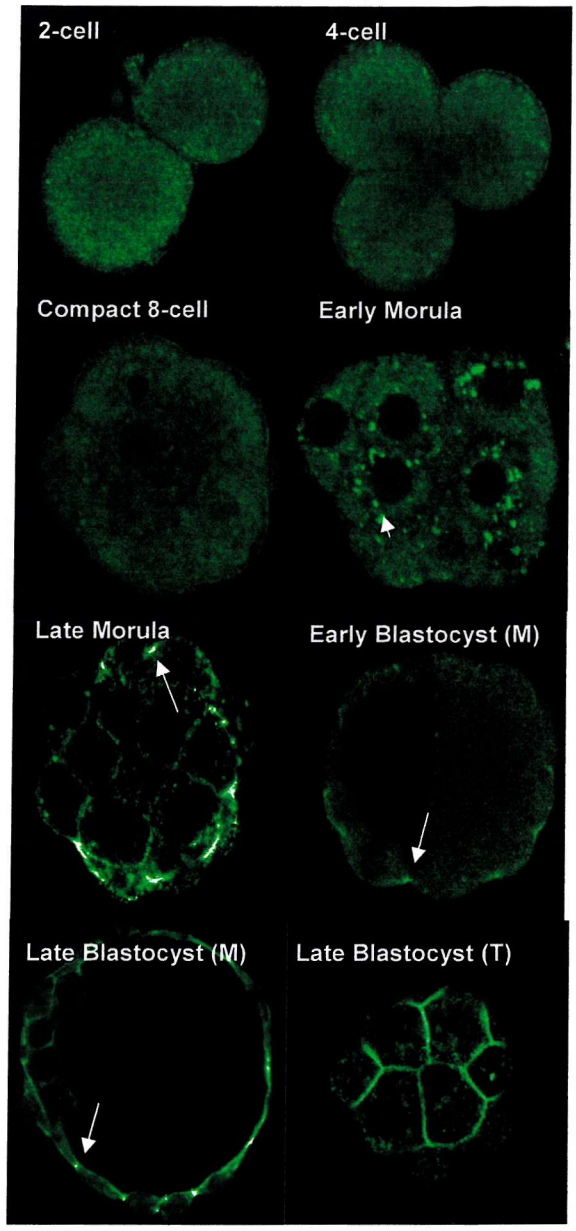

Figure 4.26 Confocal images of claudin-1/-3 immunofluorescence staining from 2-cell to late blastocyst stages of embryo development. Claudin-1/-3 protein was not detected in embryos up to and including compact 8-cell stage. Claudin-1/-3 was first detected in early morulae at perinuclear foci (arrowhead). Junctional localisation was evident as the TJ matured, in late morulae and blastocysts. As seen in the midplane (M) images of early and late blastocysts claudin-1/-3 localisation was found predominantly at cell-cell contacts of the trophectoderm cells (arrows). A tangential (T) image of a late blastocyst demonstates the continuous distribution of claudin-1 at apical contact sites between blastomeres.

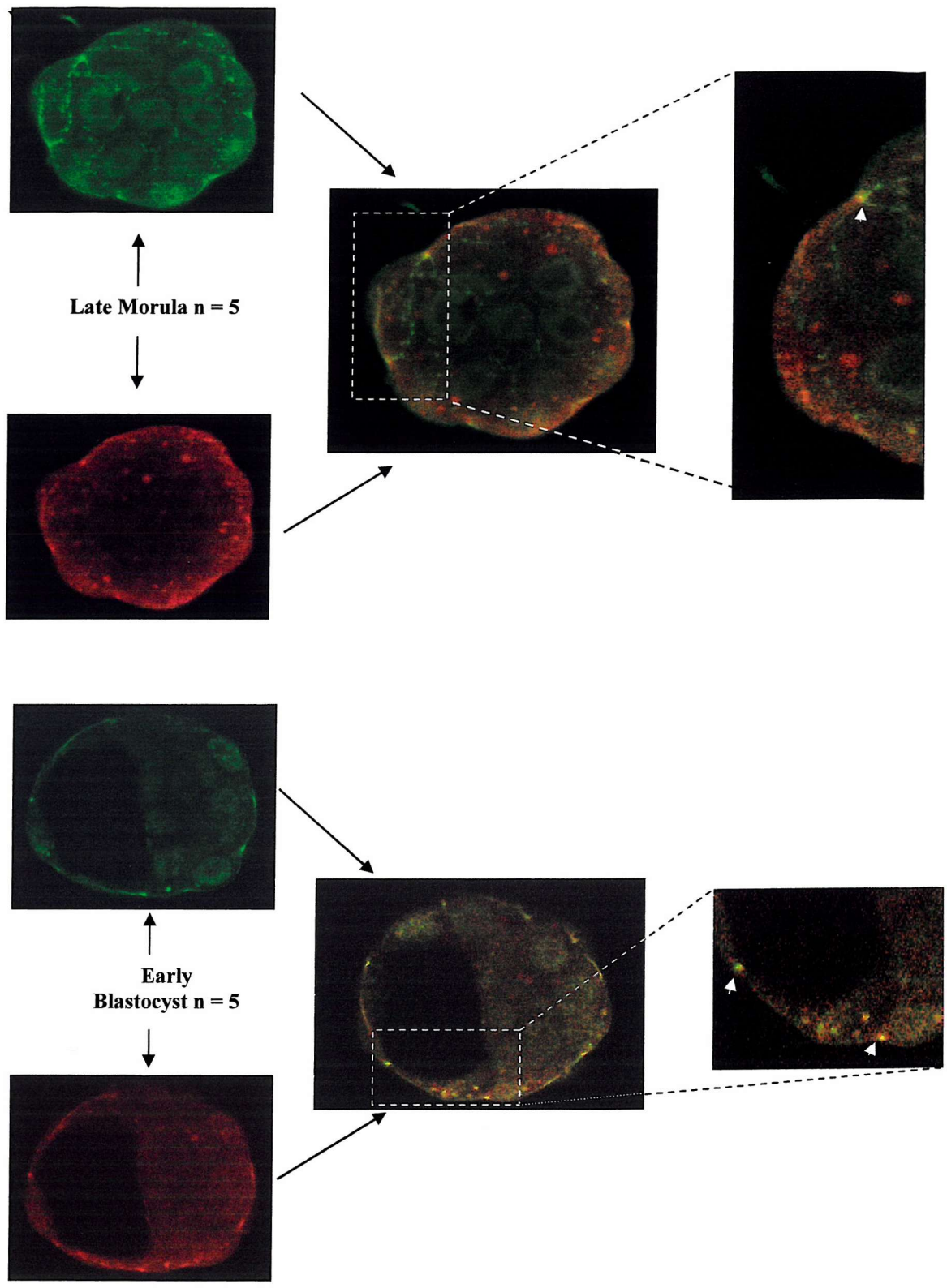

Figure 4.27 Co-localisation of claudin-1/-3 and ZO-1α+. Green images depict claudin-1/-3 localisation and red images depict ZO1α^+ localisation. Merged staining is shown in yellow, with junctional colocalisation highlighted by the arrowheads.

4.3.18 Claudin-1 immunofluorescence using Zymed antibody 51-9000

Claudin-1 immunolocalisation with the new specfic Zymed antibody was tested upon LB after fixation in 1% formaldehyde, 4% formaldehyde and methanol (Figure 4.28). None of the staining patterns from these antibodies were typical for a TJ protein. Although weak contact staining was seen in 1% formaldehyde and 10 minutes methanol samples, it was difficult to visualise any junctional localisation in mid plane confocal images. In fact, the most prominent stain found was localised to the nucleus. 1% formaldehyde was used for all subsequent experiments.

To test the specificity of the antibody staining, claudin-1 antibody was pre-incubated with claudin-1 peptide prior to the samples being incubated in the primary antibody solution (see section 4.2.5). As a control, an inappropriate peptide (corresponding to the claudin-3 antibody) was also used. In both claudin-1 only and claudin-1 plus claudin-3 peptide samples, the prominent nuclear stain was evident (Figure 4.29). Embryos incubated in claudin-1 antibody preincubated in claudin-1 peptide the nuclear stain was blocked. However, these embryos also had a bright antibody localisation at and below the apical surface of all the trophectoderm cells. This unusual localisation was not seen in embryos treated with claudin-1 antibody preincubated with claudin-3 peptide.

The unusual nuclear staining of the new claudin-1 antibody was examined in earlier embryo stages (Figure 4.30). Claudin-1 was not found at blastomere cell contacts in either 2-cell, 4-cell, pre-compact 8-cell and compact 8-cell embryos. However, nuclear staining was evident in 4-cell, pre-compact 8-cell and compact 8-cell embryos. Instead of a bright diffuse pattern within the nucleus (as seen in late morulae, early blastocysts and late blastocysts), the nuclear localisation focused around the nucleolus. Nuclear localisation was not evident in 2-cell embryos.

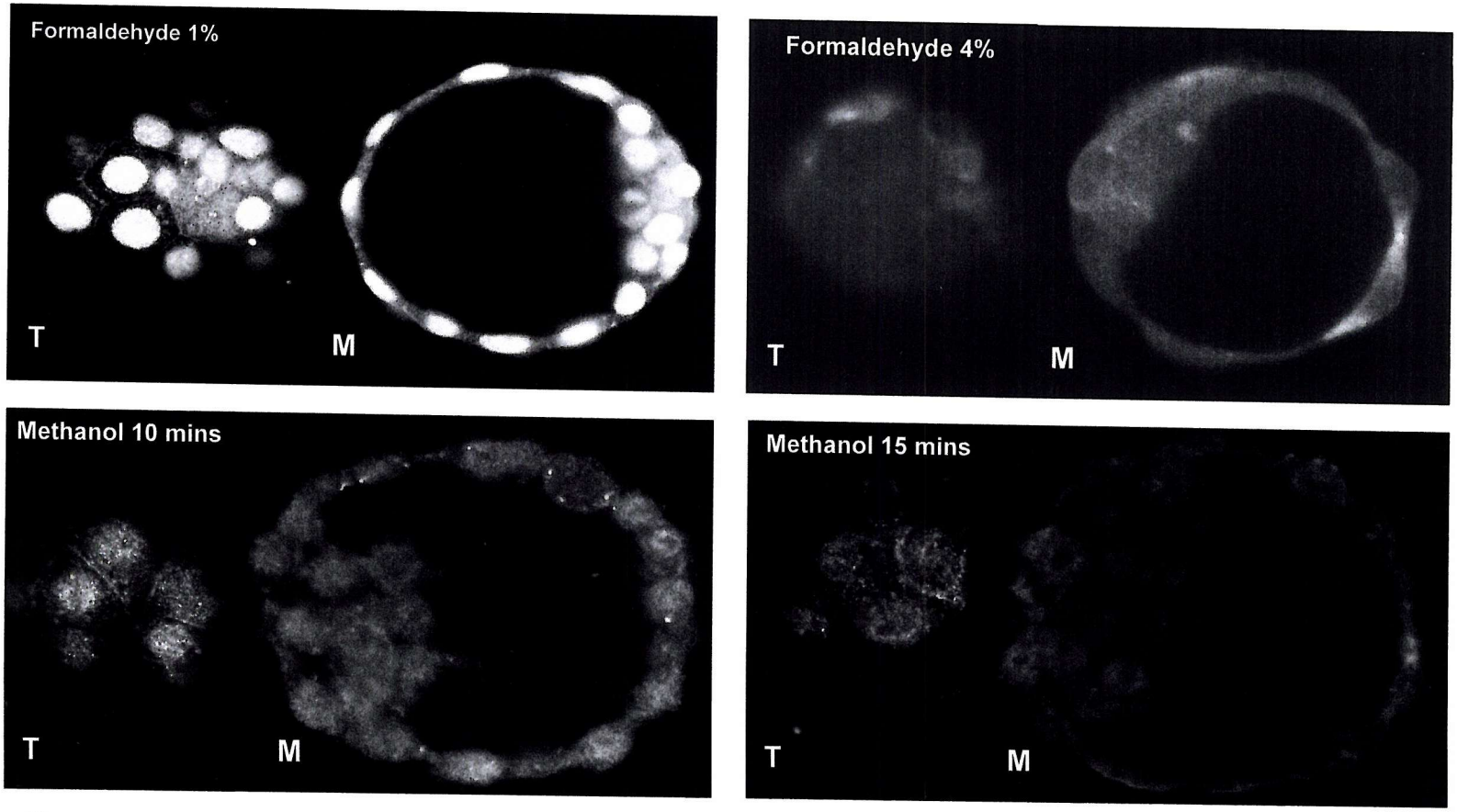

Figure 4.28 Typical claudin-1 staining of late blastocysts. Tangential plane (T) and midplane (M) images of late blastocysts stained for claudin-1 after different fixation methods

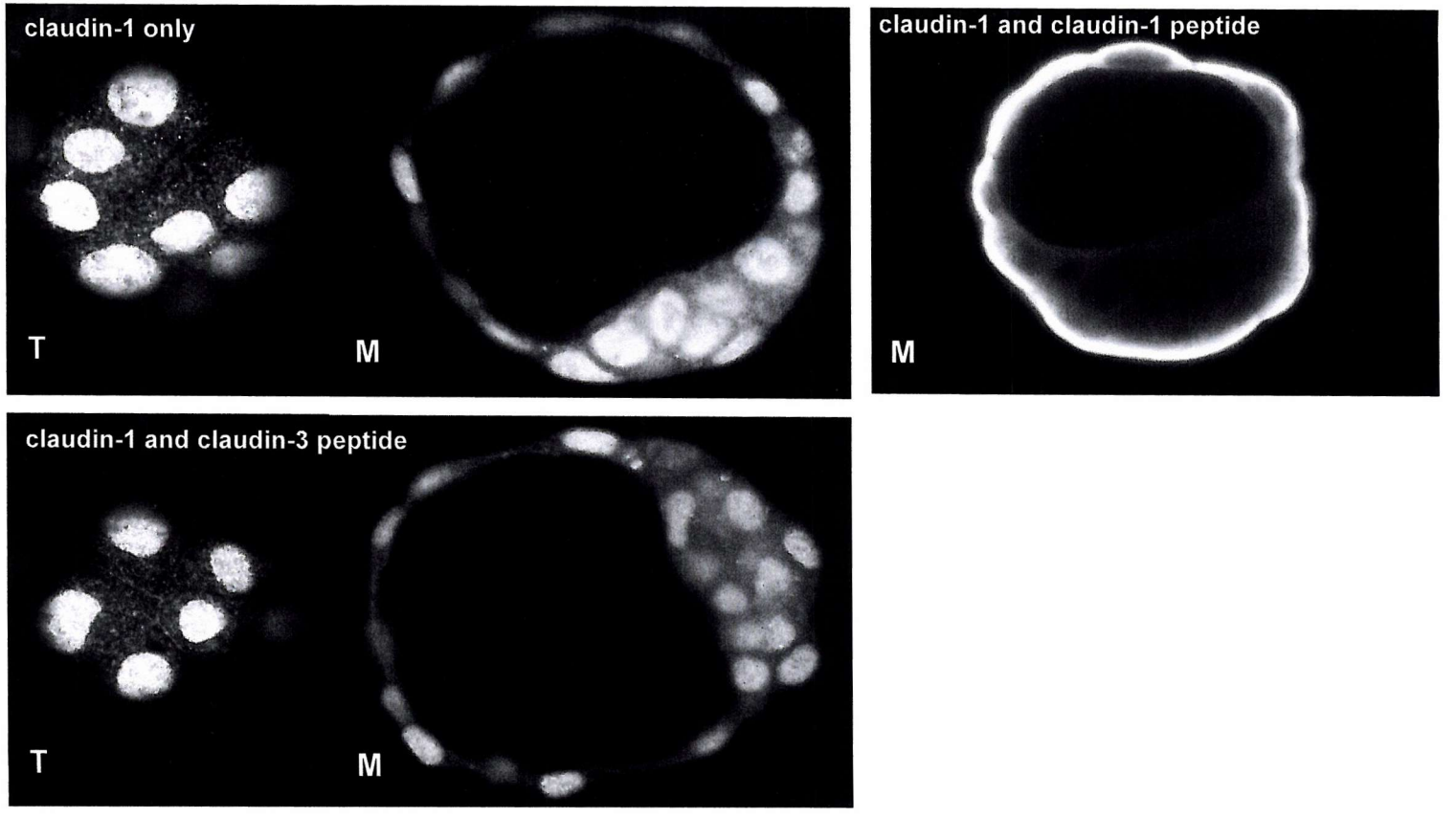

Figure 4.29 Claudin-1 antibody specificity. Embryos fixed in 1% formaldehyde were stained with either claudin-1 antibody only, claudin-1 antibody pre-incubated with claudin-1 peptide or claudin-1 antibody pre-incubated with claudin-3 peptide. The predominant nuclear staining pattern seen in previous experiments was seen in claudin-1 only and cladin-1 antibody pre-treated with claudin-3 peptide treated embryos. Nuclear staining was not seen in claudin-1 antibody pre-incubated with claudin-1 peptide treated embryos

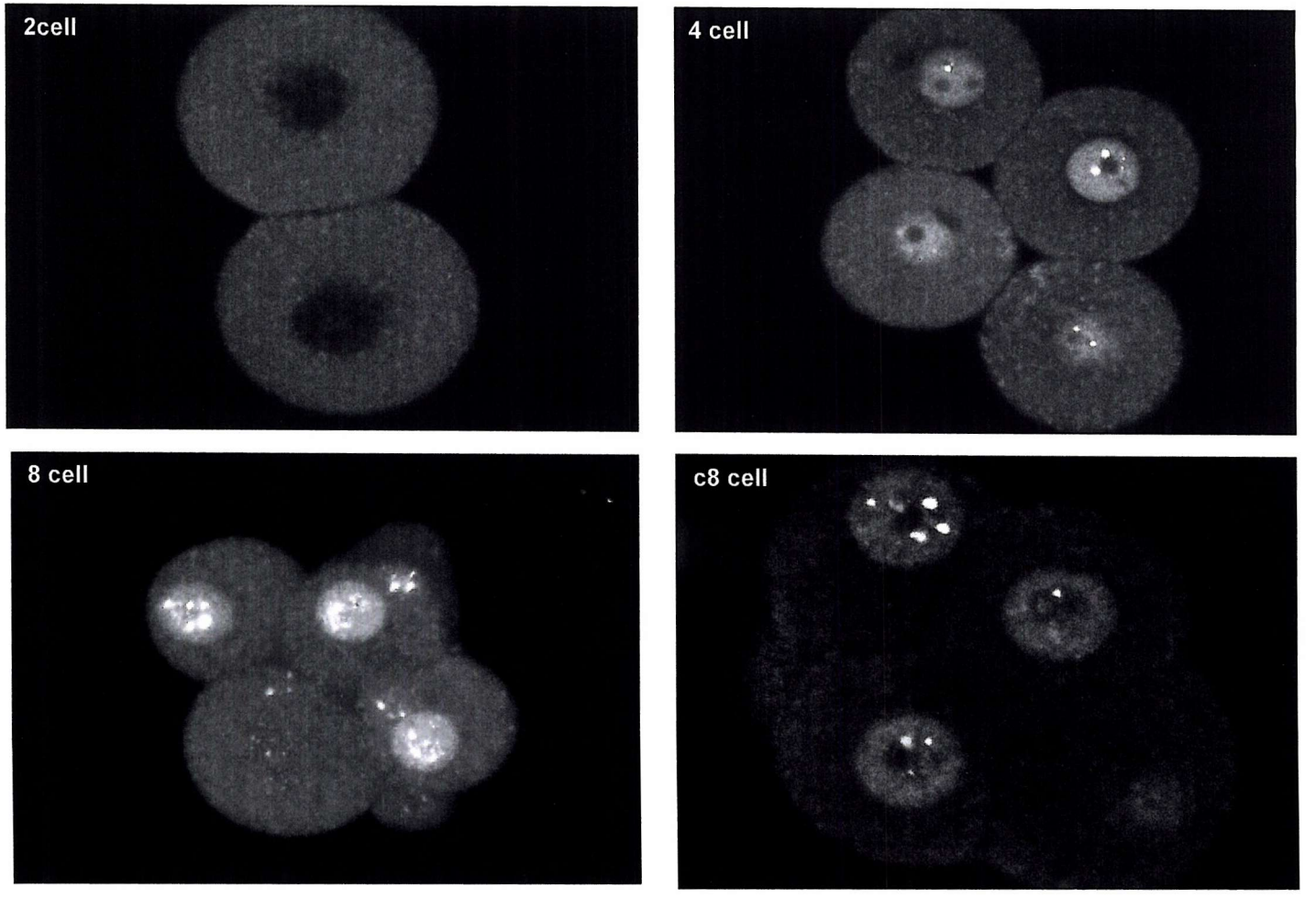

Figure 4.30 Typical claudin-1 staining in early embryo stages. Claudin-1 contact staining was not evident in 2-cell, 4-cell, pre-compact 8-cell and compact 8-cell embryos. However, 4-cell, 8-cell and compact 8-cell had claudin-1 staining in focal regions within the nucleus. 2-cell embryos did not exhibit nuclear staining.

4.3.19 Claudin-3 immunofluorescence using Zymed antibody 34-1700

Claudin-3 immunolocalisation with the new specific Zymed antibody was also tested under different fixations (1% formaldehyde, 4% formaldehyde and methanol; Figure 4.31). Again, none of the staining patterns from these antibodies were typical for a TJ protein. A weak contact stain was seen with all but the 15 minute methanol fixed embryos. Nuclear staining was seen in formaldehyde fixed embryos but was less evident in methanol fixed embryos.

Again, the specificity of the claudin-3 antibody was tested after preincubating it with either its corresponding control peptide (claudin-3) or an inappropriate peptide, corresponding to claudin-1 (Figure 4.32). Embryos incubated in claudin-3 antibody or claudin-3 antibody pre-incubated with claudin-1 peptide showed a nuclear localisation pattern. The nuclear and contact staining was not seen in embryos treated with claudin-1 antibody pre-incubated with claudin-3 peptide.

The nuclear localisation patterns in early preimplantation embryos were also examined (Figure 4.33). Both nuclear and cell-contact localisation of claudin-3 was not evident in 2-cell or 4-cell embryos. But bright diffuse nuclear localisation was evident in 8-cell and compact 8-cell embryos. Amongst the diffuse nuclear stain claudin-3 was found concentrated in areas within the nucleus of some compact 8-cell blastomeres.

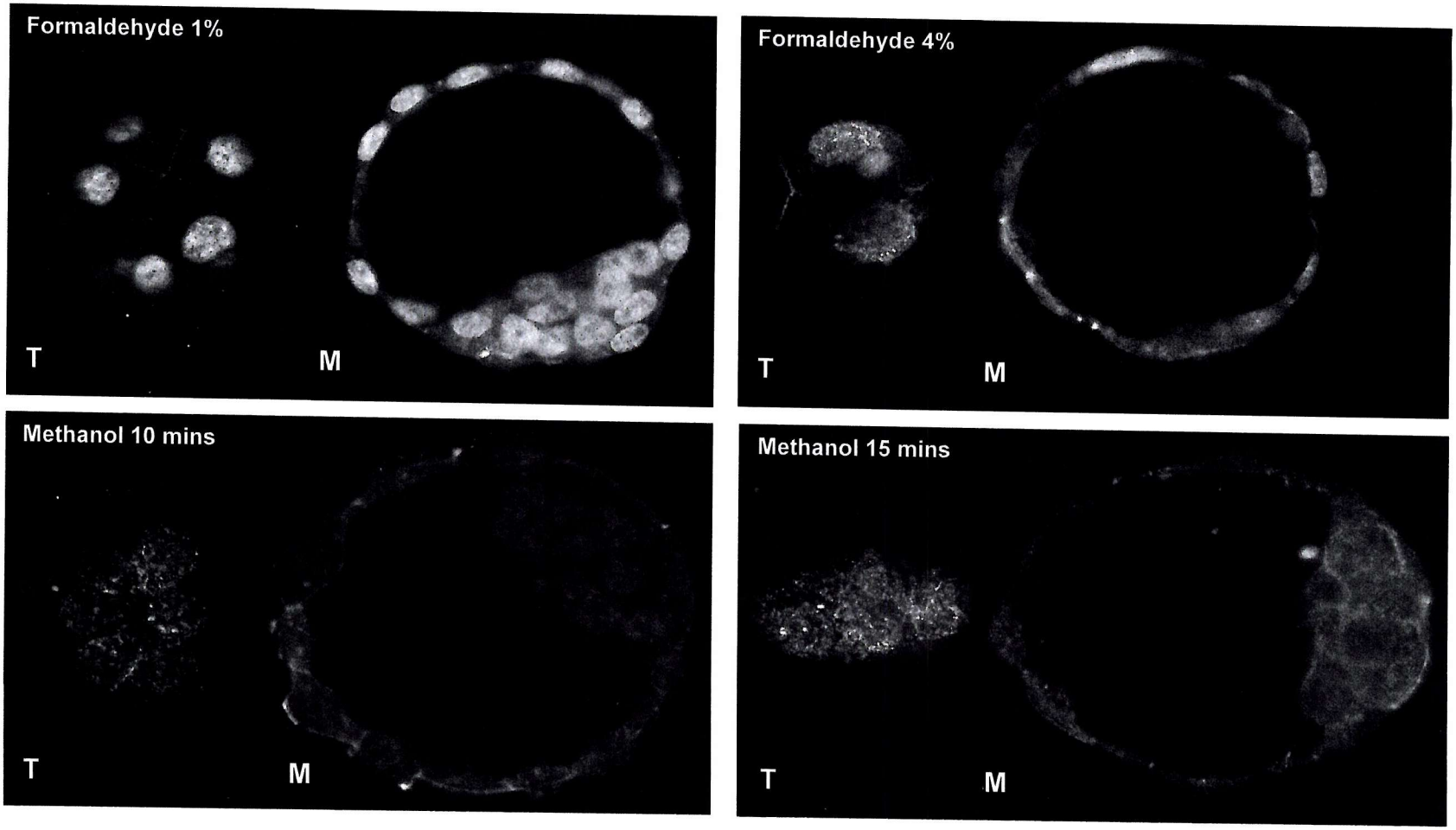

Figure 4.31 Typical claudin-3 staining in late blastocysts. Tangential plane (T) and midplane (M) images of late blastocysts stained for claudin-3 after different fixation methods.

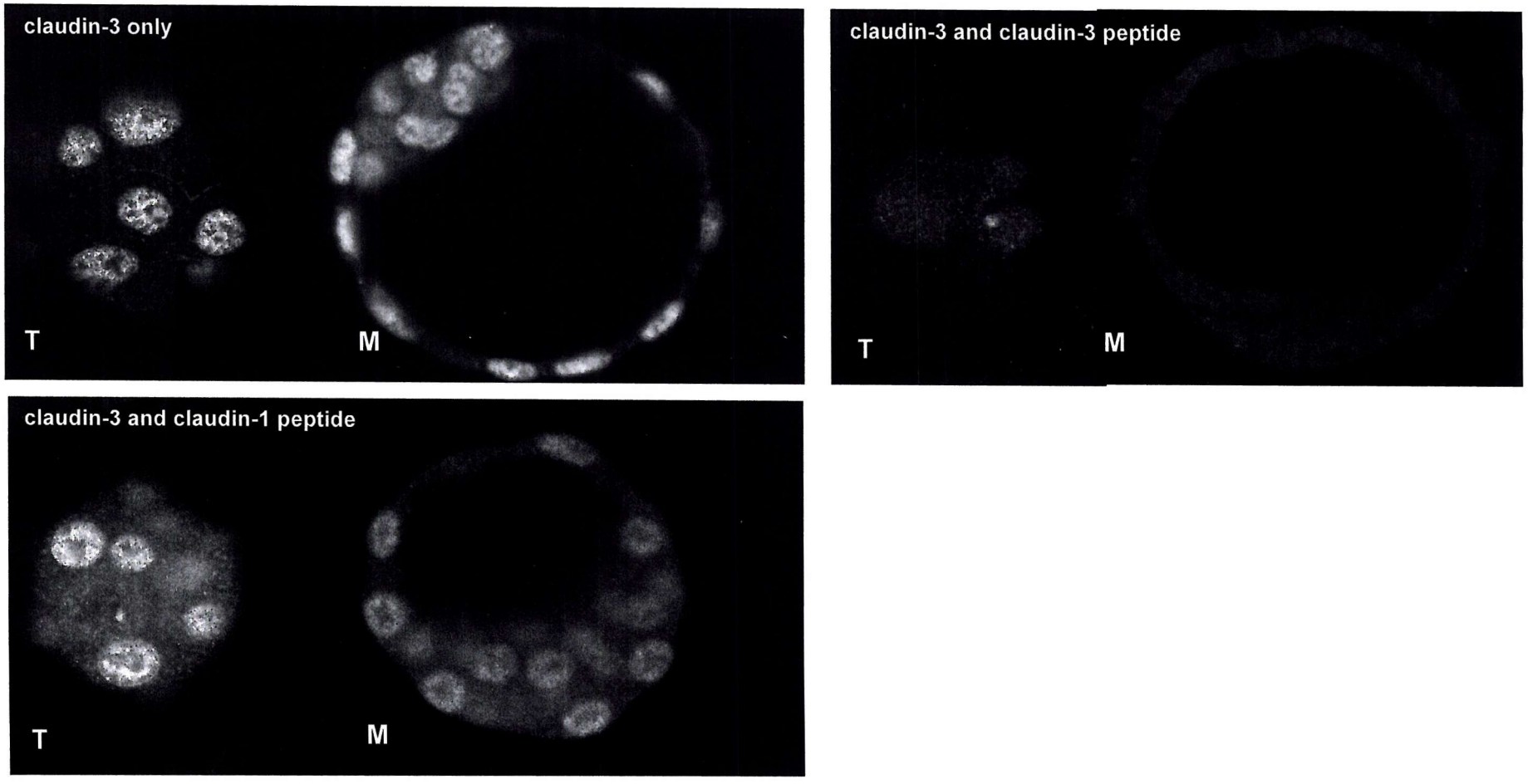

Figure 4.32 Claudin-3 antibody specificity. Embryos fixed in 1% formaldehyde were stained with either claudin-3 primary antibody only, claudin-3 antibody pre-incubated with claudin-1 peptide or claudin-1 antibody pre-incubated with claudin-3 peptide. The predominant nuclear staining patter in previous experiments was seen only in claudin-3 only and claudin-3 antibody pre-incubated with claudin-1 peptide treated embryos. Nuclear staining was not seen in claudin-3 antibody pre-incubated with claudin03 peptide treated embryos.

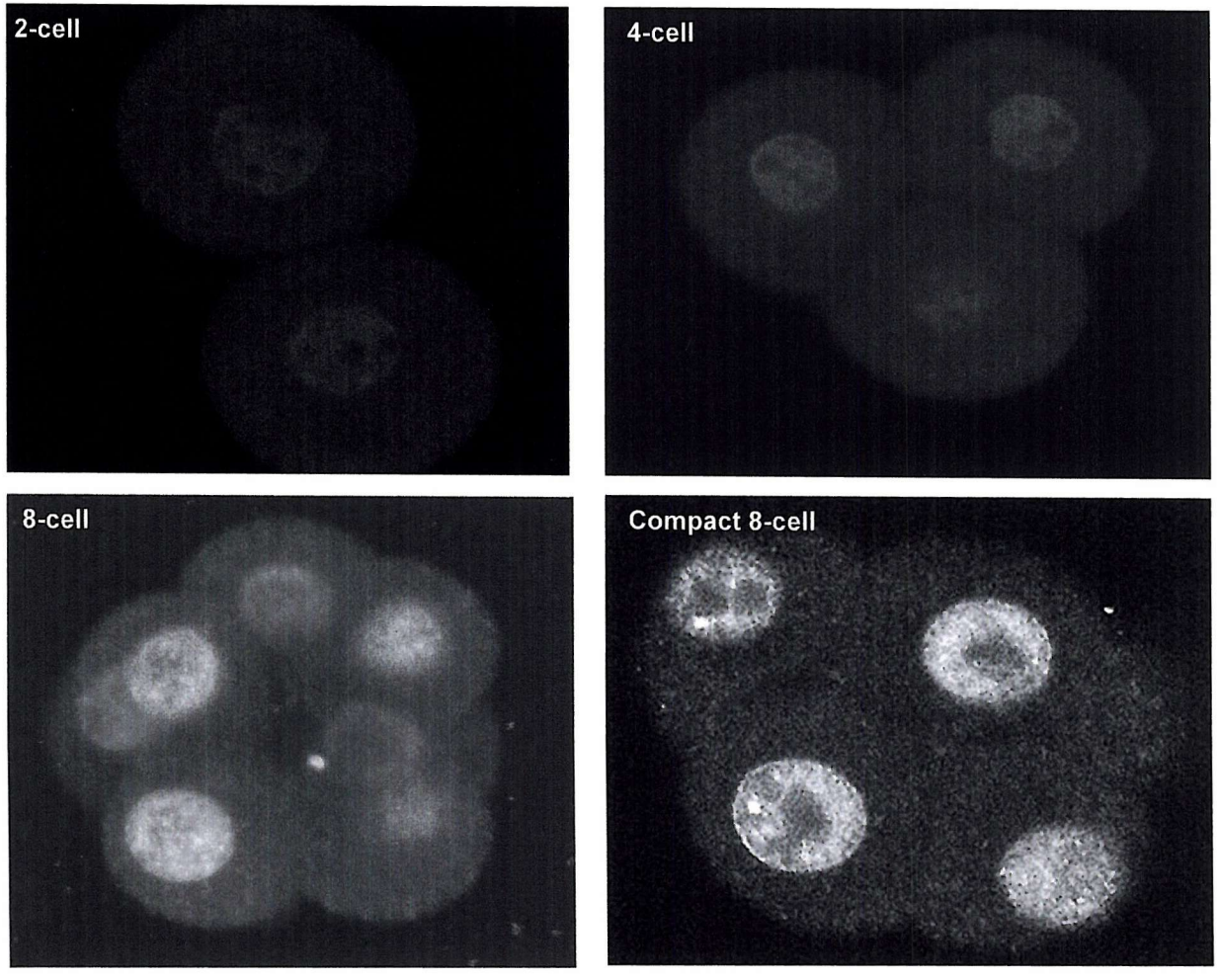

Figure 4.33 Typical claudin-3 staining in early embryo stages. Claudin-3 contact staining was not evident in 2-cell, 4-cell, pre-compact 8-cell embryos. However, 8-cell and compact 8-cell embryos had a diffuse nuclear stain with occasional foci within the nucleus of compact 8-cell embryos. 2-cell and 4-cell embryos did not exhibit nuclear staining.

4.4 Discussion

In summary, claudin-1 mRNA was detected in late blastocysts in four experiments, but since then these results could not be repeated. Despite using two different embryo mRNA isolation techniques, various RT-PCR protocols, multiple primer pairs (previously optimised on tissue RNA) and alternative RNA and DNA polymerase enzymes, claudin-1 could no longer be detected in the preimplantation embryo (despite its amplification from tissue). More PCR cycles and an increased amount of embryonic mRNA (i.e the use of multiple embryos per RT-PCR reaction) also did not enable claudin-1 mRNA to be detected, indicating that the amount of stable claudin-1 mRNA is either too low for our amplification method or non-existent for the particular embryo stages tested.

Further computer analysis of cld1/1 – cld1/4 primers indicates that they may form primer dimers or loop structures. However, primer design does not seem to be the problem, as the primers repeatedly amplify claudin-1 in tissue RNA, even when the starting material from this total RNA sample was 5.9pg. A typical late blastocyst is known to contain approximately 1ng total RNA of which 50pg is mRNA (Heyner *et al.*, 1989). The fact that claudin-1 has been detected in embryos on four separate occasions also indicates that the primers are not the source of the detection problem.

Although a minus RT control was not used in the experiments where claudin-1 expression was detected, amplification from DNA contamination is not suspected. If claudin-1 had been amplified from embryonic DNA rather than mRNA the expected size of the amplification signal would be larger than 488bp. Claudin-1 was amplified using nested primers cld1/1, cldn1/2, cldn1/3 and cldn1/4, both these primer sets flank at least two intron-exon splice sites, as determined using the NCBI blast (www.ncbi.nlm.nih.gov) and ensemble (www.ensemble.org) websites. When claudin-1 signal was amplified in both 5x and 10x embryo samples in the same RT-PCR (Figure 4.3B), amplification products above the expected molecular weight were not observed. It is possible that claudin-1 is not normally expressed, at least at detectable levels, in preimplantation embryos and the occasional detection of its mRNA was as a result of unusual gene expression in a few mice, potentially from the same mother.

Alternate primer pairs designed to amplify claudin-1 also detected claudin-1 mRNA in tissue samples but not in embryo samples. The fact that equivalent human claudin-1 primers can amplify claudin-1 in human embryos (Ghassemifar *et al.*, 2002, submitted) indicated that claudin-1 mRNA secondary structure and inefficient priming are unlikely reasons for the amplification problems. Indeed, since the human embryos used in this work were from IVF patients the claudin-1 mRNA expression detected in these experiments may not have been indicative of a normal expression pattern, as embryos were donated from people with fertility problems. Alternatively, detection of claudin-1 in human and not in mouse embryos may be due to either species variation or a more sensitive detection method.

Claudin-3 mRNA on the other hand, was much easier to detect in embryos indicating that claudin-3 mRNA is more abundant than claudin-1. The strong expression of claudin-3 from the 2-cell stage is most likely to be from zygotic genome activation and not from maternal sources as amplification of the expected product (288bp) was not seen in either unfertilised eggs or 1-cell embryos. The bands amplified prior to the 2-cell stage are unusual. Claudin-3 does not appear to have any introns and since these primers were checked for their specificity to claudin-3 (using the NCBI, BLAST website) the different bands in the unfertilised egg are unlikely to be from DNA contamination or splice variants. Unfortunately sequencing of these bands in the egg was not successful and still needs to be checked in order to determine whether they are specific to claudin-3 expression or as a result of non-specific priming.

Membrane localisation data suggests that claudin-1/-3 is present from the 16-cell stage. As described previously (section 3.4), variations in the sensitivity between immunofluorescence and Western blotting techniques may account for the discrepancies between the protein expression and localisation data in this research. Claudin-1/-3 protein expression was detected in mouse early- and late- blastocysts. However, there is remarkably less claudin-1/-3 protein in early blastocysts compared with late blastocysts. Previous data have shown that maturation of the TJ complex coincides with blastocyst formation (Sheth *et al.*, 2000a). During cavitation the

blastocyst has been shown to become increasingly impermeable to molecular tracers (Sheth *et al.*, 2000a; Ducibella *et al.*, 1975; Magnuson *et* al., 1978). The presence of a fully functional permeability barrier in all late blastocysts compared to 77% of nascent blastocysts in a permeability assay, using FITC-dextran (4kDa) as a molecular tracer, indicate that TJ integrity can vary in the early stages of blastocyst development (Sheth *et al.*, 2000a; personal observations, see chapter 5). Since claudins, like occludin, are an integral part of TJ sealing, (Furuse *et al.*, 1998b; Inai *et al.*, 1999; Furuse *et al.*, 1993; Balda *et al.*, 1996) an increase in its protein expression between early and late blastocysts is not surprising and may be indicative of the maturation of the TJ as the blastocyst becomes established.

Considering the inconsistency in the claudin-1 RT-PCR data and the successful detection of claudin-3 in preimplantation embryos, it is likely that a large proportion, if not all, protein expression detected with the claudin-1/-3 antibody corresponds to claudin-3 protein. Interestingly, claudin-3 mRNA expression is detected much earlier than when the protein is first detected. The apparent delay in claudin-3 mRNA being translated into protein indicates that earlier protein expression is being regulated by other cellular factors. Control over the timing of translation may be due to eukaryotic initiations factors (eIF) as these have been documented to be upregulated in a stage specific manner in the mouse early embryo of which, some members have been implicated in zygotic genome activation (ZGA; De Sousa, *et al.*, 1998). Moreover, the presence of some TJ mRNAs, but not the related protein, in ICM cells also demonstrates translational regulation of TJ components (Sheth *et al.*, 1997; Javed *et al.*, 1993).

Methanol fixation of embryos appeared the best method for staining with claudin-1/-3 antibody. Claudin-1/-3 was first detected at perinuclear foci in early morulae prior to its presence at cell-cell contacts. Interestingly, this expression pattern has also been seen for the structurally similar TJ transmembrane protein, occludin (Sheth *et al.*, 2000b). As mentioned previously, co-localisation studies revealed that occludin membrane localisation appears to be regulated by the late expression of the ZO-1α^+ isoform (Sheth *et al.*, 1997). Therefore, considering that claudin-1/-3 membrane localisation is reminiscent of that found for occludin,

claudin-1/-3 membrane assembly could also be regulated by ZO-1α^+. Double labelling of embryos for both claudin-1/-3 and ZO-1 α^+ confirms the presence of ZO-1α^+-claudin-1/-3 co-localisation at the tight junction in both late morulae and early blastocysts. Unfortunately, co-localisation of claudin-1 and ZO-1α^+ prior to membrane localisation has not yet been demonstrated. Double labelling experiments were attempted in the early morulae but ZO-1α^+ perinuclear localisation was not observed. Co-localisation of these two proteins in late morulae and early blastocysts is not surprising as the direct binding of claudin-1 to ZO-1, ZO-2 and ZO-3, via its C-terminus has already been demonstrated in MDCK cells (Itoh *et al.*, 1999). It would be interesting to see if co-localisation patterns of claudin-1/-3 with ZO-1α^+ were similar to that found with occludin in earlier stages but unfortunately due to various technical problems and time limitations this could not be pursued further.

Since the availability of new, more specific, claudin antibodies it was hoped that the individual expression patterns for both these proteins could be investigated. Although the claudin-1 specific antibody had not been previously tested for reactivity with mouse claudin-1 it had been successfully tested upon rat claudin-1. Western blotting with both the claudin-1 antibodies with mouse tissue samples was successful in detecting claudin-1 and claudin-3. Unfortunately, neither claudin could be detected in the embryo blot for a range of preimplantation stages. Either the individual levels of these claudin proteins were below the detection level of the Western blotting protocol or the embryo blots may have been compromised. It is possible that the latter is true as the blots used for these experiments were not fresh and had been stripped from previous experiments. However, ponceau staining of all the proteins on the gel had not been markedly different from when it was fresh. More time to collect the numbers of embryos required for blotting may eventually elucidate claudin protein expression patterns in the early embryo.

Membrane localisation of claudin-1 and claudin-3, using the new antibodies in blastocysts was much harder to distinguish than with the claudin-1/-3 antibody, suggesting that both claudin-1 and claudin-3 protein levels could be relatively low and that previous results with the old claudin antibody could be a combination of both these claudin types. Indeed, if the problems with detecting junctional

localisation of claudin-1 and claudin-3 individually are largely due to low abundancy, then the absence of detectable protein in Western blots could be indicative of this. In addition to this both antibodies showed a strong, uniform staining in the nuclei of all cells of blastocysts and morulae.

Specific inhibition peptides against these antibodies blocked both the low level of junctional staining and the bright nuclear stain. However, although inhibition peptides for claudin-3 antibody appeared to confirm the specificity of the staining patterns, the preincubation of claudin-1 antibody with its specific peptide showed an unusual fluorescence around the apical surface of the TE. The unusual phenomenon could not be explained, however, the nuclear staining was no longer apparent. In control embryos where claudin-1 antibody was preincubated with claudin-3 peptide the weak junctional and bright nuclear staining still remained, again suggesting that the nuclear localisation of claudins-1 and –3 may be specific. Unfortunately, the sequence to which these antibodies were made was not provided, although Zymed were confident that these antibodies were specific. Searches using claudin-1 and claudin-3 protein sequences do not pick up any known nuclear proteins, however, high molecular weight bands on tissue blots do indicate a potential for this antibody to cross react with other proteins.

Immunolocalisation data using the claudin-1 and claudin-3 antibodies in earlier embryo stages suggests that nuclear staining in blastocysts is not a result of fixation. Indeed, nuclear staining was seen in both methanol and formaldehyde fixed embryos. Moreover, the protein localisation patterns for both these antibodies showed a progressive staining pattern whereby early cleavage stages were not stained. Interestingly, claudin-1 nuclear staining in 2-cell up to 8-cell embryos was not uniformly distributed but clustered around the nucleolus, possibly associated with spliceosomes.

Both ZO-1 and ZO-2 have been shown to be present in the nucleus in cells with diminished cell contact although such activity has not been reported for a TJ transmembrane protein, (Gottardi *et al.*, 1996; Gonzales-Mariscal *et al,* 2001; Islas *et al.*, 2002). Interestingly, ZO-2 is also present in the nucleus of both sub-confluent

and confluent cultures (Islas *et al.*, 2002). However, both ZO-1 and ZO-2 have been shown to contain nuclear localisation sequences (NLS) whereas both claudin-1 and claudin-3 do not contain any NLS discovered to date. Despite the hydrophobic nature of transmembrane proteins other transmembrane proteins, such as epidermal growth factor receptor (EGFR) have shown nuclear localisation patterns (Lin *et al.*, 2001). Moreover, the absence of a known NLS in claudins may also not be reason enough to dismiss the possibility that this localisation pattern is real. Indeed, β-catenin, although not a transmembrane protein, does not contain a conventional NLS and it's nuclear import is thought to be mediated by another protein containing a NLS, probably within the LEF/TCF protein complex (Fagotto *et al.*, 1998; Yokoya *et al.*, 1999). Considering that ZO-2 binds to claudin-1 and its nuclear expression pattern is similar to claudin-1 staining, the nuclear staining could be real.

Indeed, nuclear staining was also found using the claudin-1/-3 antibody mainly in formaldehyde fixed cells. It would seem a big coincidence that all claudin antibodies, raised from different peptides, resulted in a cross reaction with an unrelated protein that localises to the nucleus. Work has been presented at the 40th annual ASCB meeting (2000), by L.Gonzalez-Mariscal demonstrating that the same polyclonal antibody produces nuclear staining for claudin-1/-3 at the leading edge of primary, rabbit kidney, cell cultures. Interestingly, highly confluent cells on the other hand do not demonstrate nuclear staining under the same procedure. Therefore, it is possible that the nuclear staining under formaldehyde fixation is not an artifact and is as a result of new, recently established, TJs. Assuming these results are specific to claudins a whole new aspect to nuclear regulation and cell proliferation could be unravelled.

In conclusion, it appears that claudin-1 mRNA is not usually expressed in the mouse preimplantation embryo, as the initial discovery of claudin-1 mRNA in late blastocysts could not be repeated in this developmental stage or earlier ones. Indeed, due to the apparent abundance of claudin-3 mRNA in the mouse embryo it is most likely that all protein data obtained using the claudin-1/-3 antibody actually corresponded to claudin-3 protein. Although further investigation into the nuclear staining is required, the Western blotting data for both claudin-1 and claudin-3

indicate that these antibodies are detecting a protein unrelated to either of the two claudins.

Chapter 5

Functional analysis of JAM-1 and claudin-1 proteins in mouse embryos

5.1 Introduction

A monoclonal antibody (BV11) specific to mouse JAM-1 extracellular domain has been shown to block monocyte transmigration across endothelial cell layers (Martín-Padura *et al.*, 1998). The same antibody also inhibited leukocyte recruitment in the cerebrospinal fluid of mice with experimental meningitis (Del Maschio *et al.*, 1999). Likewise, a similar monoclonal antibody, specific to the extracellular domain of human JAM-1, has been shown to inhibit recovery of transepithelial electrical resistance (TER) in T84 cell monolayers after disruption of the TJ by transient removal of extracellular calcium (Liu *et al.*, 2000). In light of the ability for BV11 to disrupt JAM-1 function both *in vitro* and *in vivo*, treatment of preimplantation embryos with this antibody was attempted to disrupt JAM-1 during early embryogenesis.

At present, an extracellular domain neutralising antibody has not been raised against claudin-1. However, as described earlier, hydrophobicity plots indicate that both the claudin family members and occludin, although not related in sequence, have similar protein topography (Furuse *et al.*, 1998a). Occludin function has been shown previously to be disrupted using synthetic peptides corresponding to its extracellular loops (Wong and Gumbiner, 1997; Vieira *et al.*, 1999). In both reports, these peptides reversibly inhibited TER in epithelial cell lines. Due to the functional similarities between the claudins and occludin, the use of synthetic peptides specific to the extracellular loops of claudin-1 may also be an effective method to disrupt claudin-1 in the preimplantation embryo.

RNA interference (RNA*i*) is another useful tool to establish the importance of a particular gene. This method has been widely used in *Drosophila melanogaster* and *Caenorhabditis elegans* (reviewed in Maine, 2001; Nishikura, 2001). Double stranded RNA (dsRNA) can inhibit expression of a particular gene of interest in a sequence specific manner. The dsRNA appears to trigger the degradation of the mRNA for the gene targeted. The exact molecular mechanisms behind RNA*i* are

beginning to be understood for *Drosophila* (Lipardi *et al.*, 2001). Firstly, dsRNA is broken down into smaller 21-23mer sequences which form short interfering RNAs (siRNAs; Zamore *et al.*, 2000; Elbashir *et al.*, 2001; Hamilton & Baulcombe, 1999; Parrish *et al.*, 2000). The generation of siRNA is thought to be due to an RNAseIII-like enzyme called Dicer (Bernstein *et al.*, 2001). The siRNAs generated by Dicer then associates with RISC (RNA-induced silencing complex), a multicomponent nuclease, which in turn directs degradation of a specific mRNA (Hammond *et al.*, 2001; Bernstein *et al.*, 2001). The success of RNA*i* in mammalian systems has not been so well documented. However, in recent years there have been increasing reports of RNA*i* being used successfully in some mammalian cell lines and in preimplantation embryos (Billy *et al.*, 2001; Svoboda *et al.*, 2000; Wianny & Zernicka-Goetz, 2000). In this investigation, RNA*i* was used as an alternative method to disrupt JAM-1 and claudin-1 expression in the early embryo.

In this chapter, the use of a neutralising antibody (BV11) and an inhibitory peptide (Cldn1-K15) to disrupt JAM-1 and claudin-1 function respectively, in the mouse preimplantation embryo is reported. Preliminary data for JAM-1 and claudin-1 RNA*i* is also discussed.

5.2 Methods

5.2.1 Murine JAM-1 neutralising antibody, BV11

As with all the JAM-1 antibodies used for this research, anti-murine JAM-1 monoclonal antibody (mAB), BV11 and BV12 were provided by Dr G. Bazzoni (Instituto di Recerche Farmacologiche Mario Negri, Milan, Italy; see chapter 3).

5.2.2 The effects of JAM-1 antibodies upon mouse preimplantation embryo development

Since the timing of expression and localisation of JAM-1 was shown to be similar to that of E-cadherin (Chapter 3), the JAM-1 neutralising antibody BV11 was used alongside an E-cadherin neutralising antibody, ECCD-1. Addition of ECCD-1 to the culture medium of pre- and post-compaction mouse embryos can inhibit or reverse embryo compaction, respectively (Johnson *et al.*, 1986).

In this study, BV11 was added to embryo culture medium of zona intact, precisely timed 0 hour 8-cell embryos or to recently compacted embryos (section 2.1.5). BV11 was used at a concentration previously shown to be effective at neutralising JAM-1 function in endothelial cells (5μg/ml; Martín-Padura *et al.*, 1998). The effect of an alternative JAM-1 antibody, BV12 (used at 5μg/ml), was also tested upon 8-cell and compact 8-cell embryos. Both BV11 and BV12 are IgG2b antibodies. A totally unrelated antibody (directed against human CD21) of the same species and isotype was used as a control (Dr. A.AL-Shamkhani, University of Southampton). CD21 is a complement binding protein found expressed on B-lymphocytes. This antibody was seen as an appropriate control since CD21 expression has not been reported in the mouse preimplantation embryo and its function is unrelated to both JAM-1 adhesion and TJ biogenesis. Functional analysis was attempted in T6 culture medium either in the presence or absence of BSA, using PVP as a replacement for BSA (section 2.1.2 and Appendix I). The majority of the experiments described in this chapter were conducted with T6-BSA medium, as results obtained in either media were comparable. Every 12 hours, embryos were transferred into fresh culture medium with or without antibody. Embryo development was monitored to the blastocyst stage.

5.2.2.1 Statistical analysis of JAM-1 time courses

Statistical analysis of the JAM-1 time course data was carried out by a medical statistician (Robert Hemmings). Data for both compaction and cavitation time courses were analysed using the same statistical method. "Time to event" analysis was conducted using both a proportional hazards model, adjusting for experiment as a covariate, and a Wilcoxon test stratisfied for experiment.

5.2.2.2 Analysis of the integrity of the tight junction seal after antibody treatment

The effect of BV11 upon the paracellular permeability of nascent blastocysts was examined using T6-BSA medium containing FITC-dextran. Following antibody incubation over the period from before compaction to cavitation, embryos that formed blastocysts were removed and placed in control or experimental (T6-BSA plus antibody) medium containing 1mg/ml FITC-dextran of size 4kDa (Sigma).

Embryos were viewed, via confocal microscopy, within 10 minutes of transfer. Each embryo was then scored for the presence or absence of fluorescence within the blastocoel (Figure 5.1).

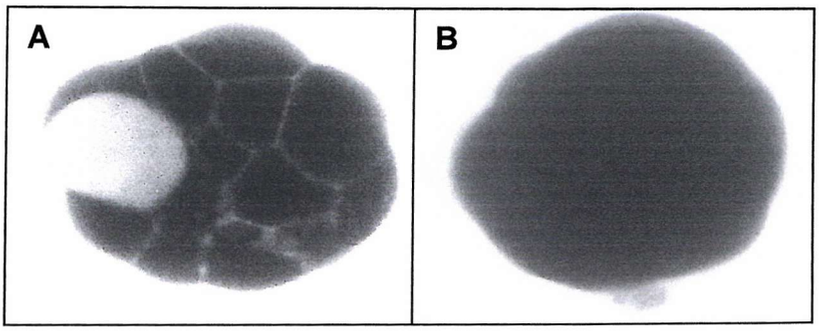

Figure 5.1 Live early blastocysts (A,B) were examined by confocal microscopy in the presence of FITC-dextran 4kDa. Embryos were then categorised as leaky (A) or sealed (B) depending upon their ability to exclude FITC-dextran 4kDa from the blastocoel cavity and between blastomeres.

5.2.3 Peptide design

Claudin-1, 1st EC loop, peptide (Cldn1-K15; 8.86kDa, Figure 5.2) was made in house by Dr R.Sharma (University of Southampton). Due to the highly hydrophobic nature of this relatively large peptide, 15 lysines were added to the C-terminus to decrease its aggregation in solution. Addition of lysine residues has been shown to be effective in causing highly hydrophobic transmembrane peptides to become soluble in aqueous medium, enabling easier delivery to the protein target (Tomich *et al.*, 1998). After preliminary results were obtained with CLDN1-K15 a scrambled version was also made. The scrambled claudin-1 peptide sequence was randomised and checked to ensure no cross-reaction with other known proteins using the Internet based sequence retrieval system (http://srs.embl.heidelberg.de:8000/srs5/). As with the experimental peptide, 15 lysines were added to the C-terminus of the scrambled peptide (see Appendix III for the scrambled sequence).

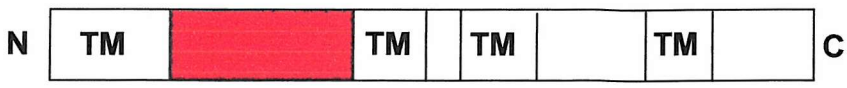


```
1      MANAGLQLLG FILASLGWIG SIVSTALPQW KIYSYAGDNI VTAQAIYEGL WMSCVSQSTG
61     QIQCKVFDSL LNLNSTLQAT RALMVIGILL GLIAIFVSTI GMKCMRCLED DEVQKMWMAV
121    IGGIIFLISG LATLVATAWY GNRIVQEFYD PLTPINARYE FGQALFTGWA AASLCLLGGV
211    LLSCSCPRKT TSYPTPRPYP KPTPSSGKDY V
```

Figure 5.2 Target region of claudin-1 protein to which the Cldn1-K15 is designed to bind (depicted in red).

5.2.4 Analysis of the effect of Cldn1-K15 upon mouse preimplantation embryo development (method 1)

Claudin-1 peptide treatment to embryos was varied in several ways to develop a reliable strategy that would permit optimal activity and access to the peptide (Figure 5.3). Thus, Cldn1-K15 peptide was added to different embryo culture media over a concentration range of 0.1 - 20μM. To optimise Cldn1-K15 peptide access to the interior of blastocysts, additional methods were employed. First, zona-intact blastocysts were treated with CCD (0.5μl/ml) to collapse the blastocoel and open the existing TJ barrier. Then CCD treated embryos were exposed to Cldn1-K15 peptide in the absence of CCD and the rate of recavitation was determined (method 1). This method was also used with occludin peptide G (corresponding to amino acids 226-241 in the second extracellullar loop, see Appendix III). Due to the hydrophobic nature of peptide G, it was diluted initially in DMSO 10mM stock. Stock Cldn1-K15 was 10mM in sterile water.

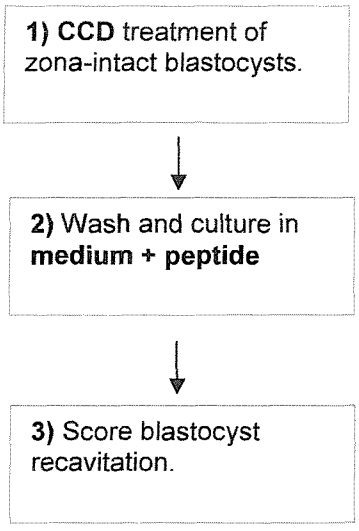

Figure 5.3 Schematic of method 1 for examining the effect of claudin-1 peptide on embryos.

5.2.5 Analysis of the effect of Cldn1-K15 upon mouse preimplantation embryo development (method 2)

In the second set of peptide experiments, another strategy was employed to increase further the accessibility of the peptide to the interior of the embryo (method 2; Figure 5.4). For these experiments, the zona pellucida was removed by acid Tyrodes (see section 2.9.2) and embryos were disaggregated after incubation in CCD for 15 minutes with a small, heat-polished glass micropipette (see section 2.1.6). These embryos were further incubated for 5 minutes in CCD containing medium and then transferred into either control medium or medium containing Cldn1-K15.

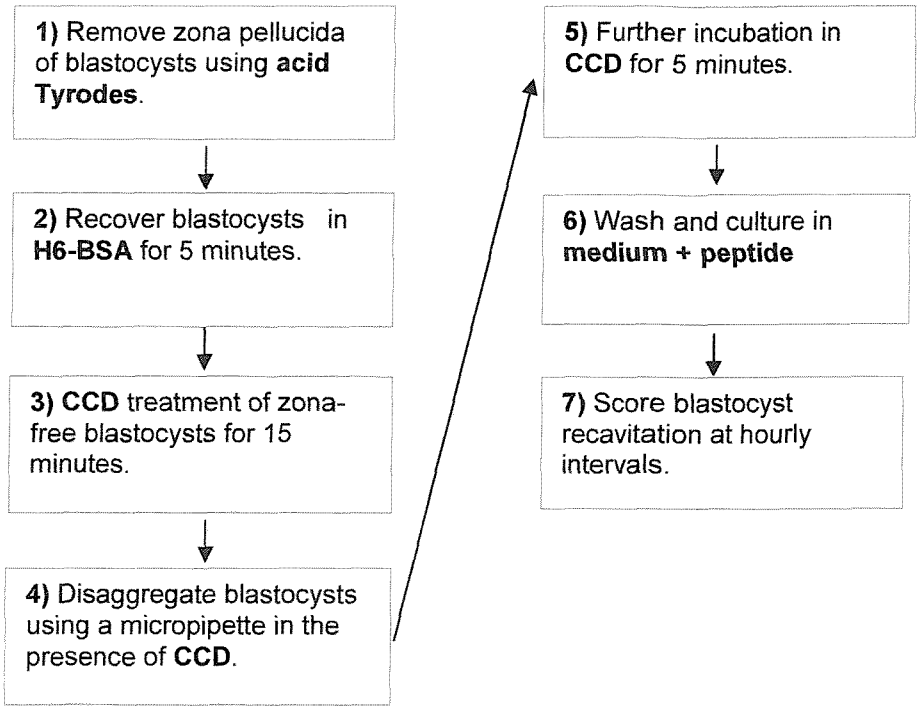

Figure 5.4 Schematic of method 2 for examining the effect of claudin-1 peptide on embryos.

5.2.6 Analysis of the effect of Cldn1-K15 upon mouse preimplantation embryo development (method 3)

Since TJs may begin to reseal soon after removal from CCD containing medium, Cldn1-K15 peptide was also added prior to CCD removal to further improve its access (Figure 5.5). As with methods 1 and 2, disaggregated embryos were removed from the CCD (now containing peptide) medium and their development was observed in culture medium + Cldn1-K15.

In conjunction with improving the peptide experiment protocols, alternative media types were tested. In all methods, the effects of Cldn1-K15 were examined using either early or late blastocysts.

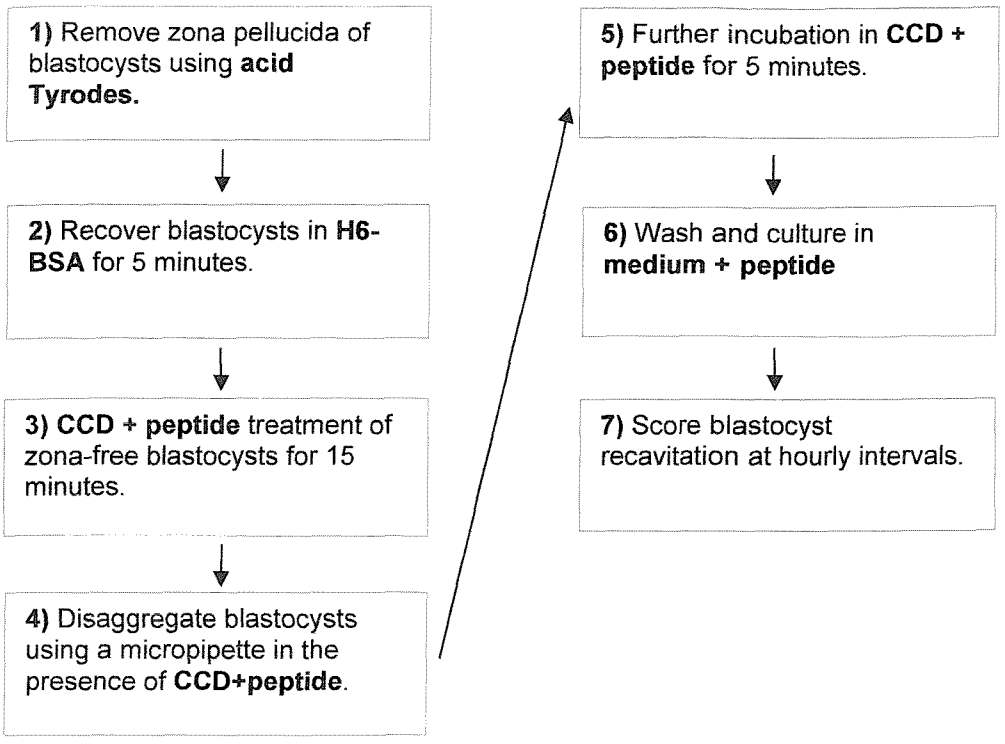

Figure 5.5 Schematic of method 3 for examining the effect of claudin-1 peptide on embryos.

5.2.7 Effect of Cldn1-K15 on the transepithelial electrical resistance (TER) of CMT64 cells

For full details on epithelial cell culture and measurement of TER see section 2.13 and 2.13.3. Effects of Cldn1-K15 were examined in two different ways. Initially, established monolayers of CMT64 cells incubated in either control medium (Waymouth's medium supplemented with 2mM glutamine and 1% Penicillin / Streptomycin) or medium containing Cldn1-K15 peptide. The TER was then measured at hourly intervals and compared to the value taken at "time 0". In later experiments, using a Ca^{2+} switch assay (section 2.13.4) to disrupt pre-established TJs and the effect of Cldn1-K15 upon the TER recovery was investigated.

5.2.8 Synthesis of dsRNA for microinjection

For full details of cloning methods and synthesis of dsRNA see section 2.5 and 2.6. RT-PCR was performed on tissue RNA using either JAM-1 primers (JAM1/1 and JAM1/2) or claudin-1 primers (cld1/1 and cld1/2) using the method described in sections 2.3.5 and 2.3.6. with an annealing temperature appropriate for the primers used (Table 2.1). The PCR products were then gel purified, using the

QIAquick gel extraction kit (Qiagen), to remove components of the PCR reaction. Purified PCR products were ligated into a pGEM-T Easy vector (Promega), re-purified and transfected into DH5α cells via electroporation. DH5α cells were then grown overnight at 37°C on agar-ampicillin plates coated with IPTG and X-gal. Individual white colonies were picked and grown in LB-ampicillin medium overnight at 37°C on a shaker. A stock agar plate of all clones was grown. Meanwhile, potentially ligated plasmids were then isolated from the transfected cells using the Hybaid recovery™ plasmid mini prep kit. Clones were digested with appropriate enzyme chosen to cut both the insert and the plasmid at one site only. Appropriate clones were chosen after running the products on an agarose gel and observing the molecular weights of the cut products (Figure 5.6 and 5.7). Clones were verified by sequencing (Appendix III).

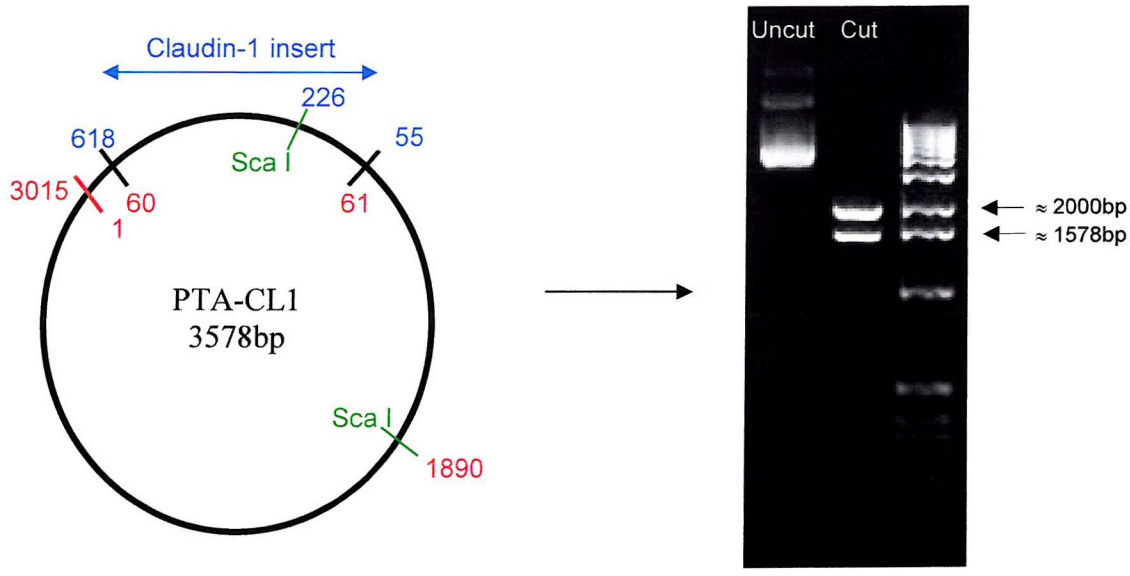

Figure 5.6 Claudin-1 clone (PTA-CL1) picked for RNA synthesis. Red numbers depict base positions on plasmid. Blue numbers depict base positions on the claudin-1 cDNA sequence. Restriction sites for Sca I are shown in Green. Expected product sizes for the two restriction products were 2000 and 1578bp

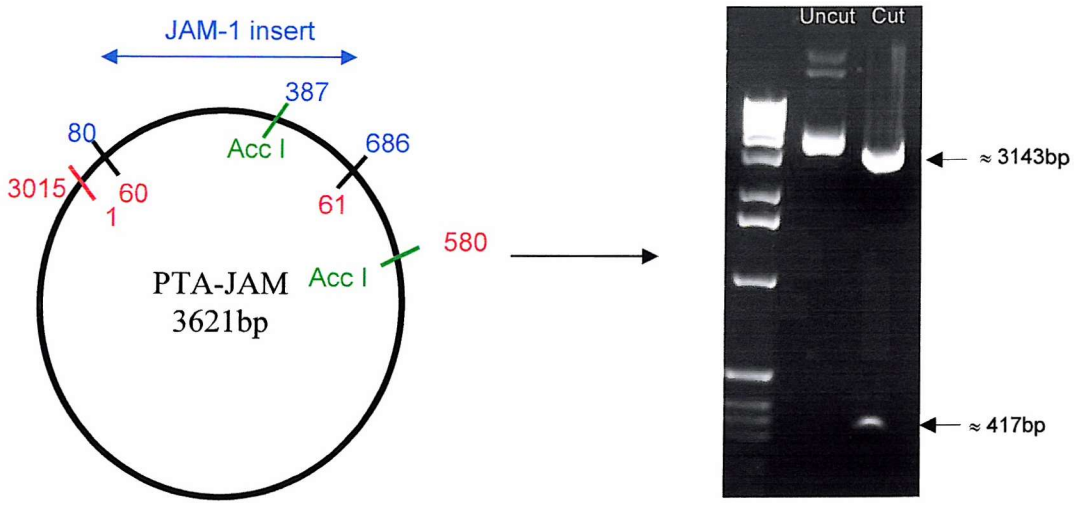

Figure 5.7 JAM-1 clone (PTA-JAM) picked for RNA synthesis. Red numbers depict base positions on plasmid. Blue numbers depict base positions on the JAM-1 cDNA sequence. Restriction sites for Acc I are shown in Green. Expected product sizes 3143 and 417bp.

Clones were then linearised using appropriate restriction enzymes. Plasmids linearised with Sal I were transcribed with a T7 RNA polymerase (Promega). Plasmids linearised with Nco1 were transcribed with the SP6 RNA polymerase (Promega). Prior to transcription RNA samples underwent a protein digest using proteinase K (Melford). ssRNAs were annealed and ran on a gel (Figure 5.8 and 5.9) prior to storage at –20°C until required for microinjection (see sections 2.8 and 5.3.5).

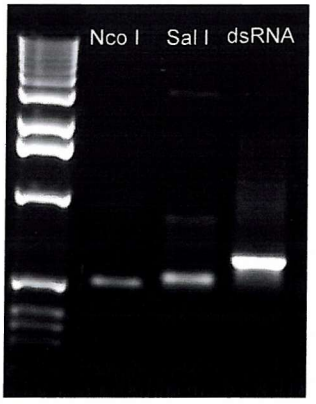

Figure 5.8 Claudin-1 ssRNA and annealed RNA. Plasmids linearised with either Nco I or Sal I were transcribed to create ssRNA of the claudin-1 insert. The linearised products were then annealed to form claudin-1 dsRNA.

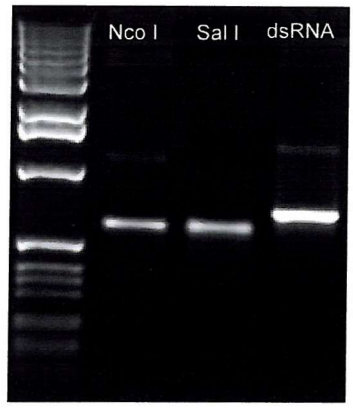

Figure 5.9 JAM-1 ssRNA and annealed RNA. Plasmids linearised with either Nco I or Sal I were transcribed to create ssRNA of the JAM-1 insert. The linearised products were then annealed to form JAM-1 dsRNA.

5.3 Results

5.3.1 Effect of BV11 upon compaction of mouse preimplantation embryos

To assess whether BV11 can reverse compaction in early morulae, compact 8-cell embryos were incubated in either T6-BSA (Figure 5.10) or T6-PVP (Figure 5.11) with or without antibody. Embryos incubated in BV11 and control media were morphologically indistinguishable and remained compacted. In both experiments, ECCD-1 caused the embryos to decompact.

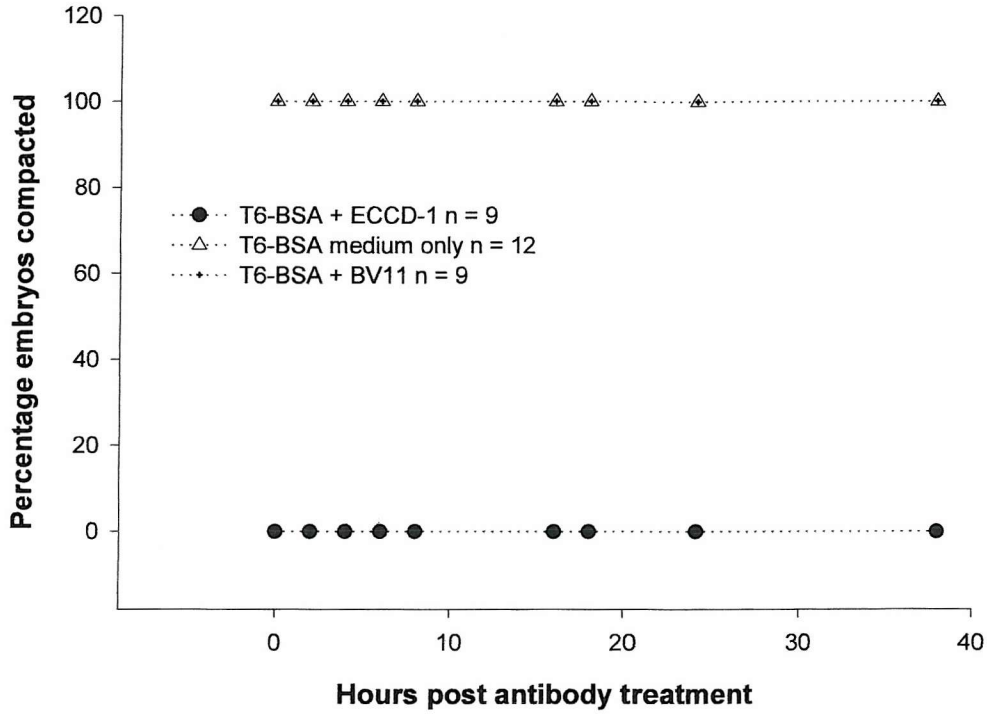

Figure 5.10 Effect of BV11 upon compacted embryos in T6-BSA culture media

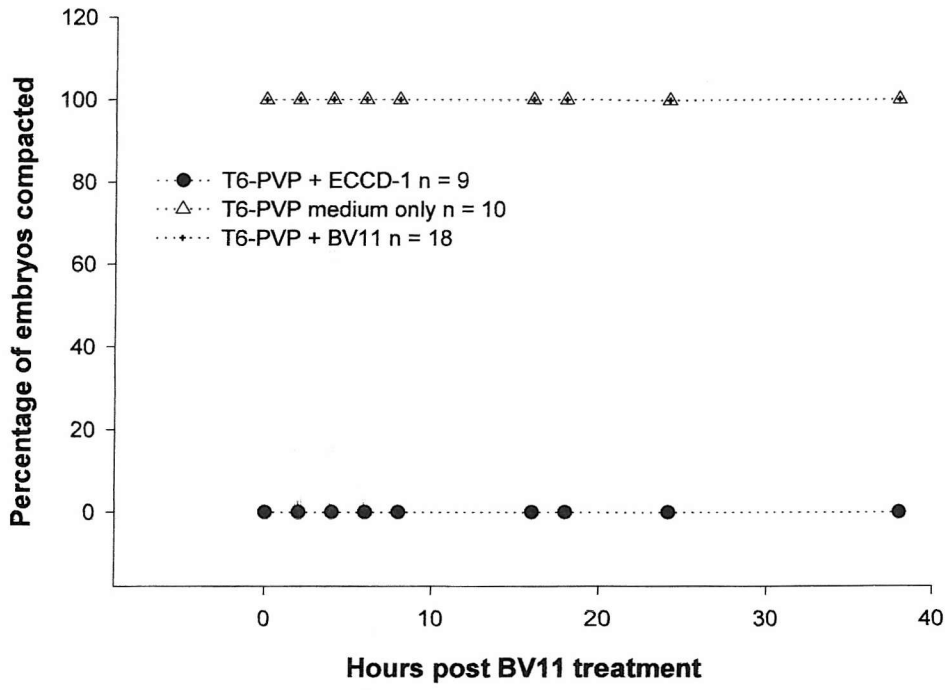

Figure 5.11 Effect of BV11 upon compacted embryos in T6-PVP culture media

To assess whether the rate of compaction was affected by JAM-1 antibodies, precisely timed 0 hour 8-cell embryos were observed at hourly intervals. Pools of embryos were divided between four treatment groups (medium only, IgG2b control, BV11 and BV12). Compaction was scored at each time point and the percentages were plotted over time (Figure 5.12). "Time to event" analysis was carried out on the data (as described in section 5.2.2.1). For both methods of analysis there was a high effect of "experiment", indicating that any conclusions made from the pooled data could be unreliable (also indicated by the large standard error bars in Figure 5.12).

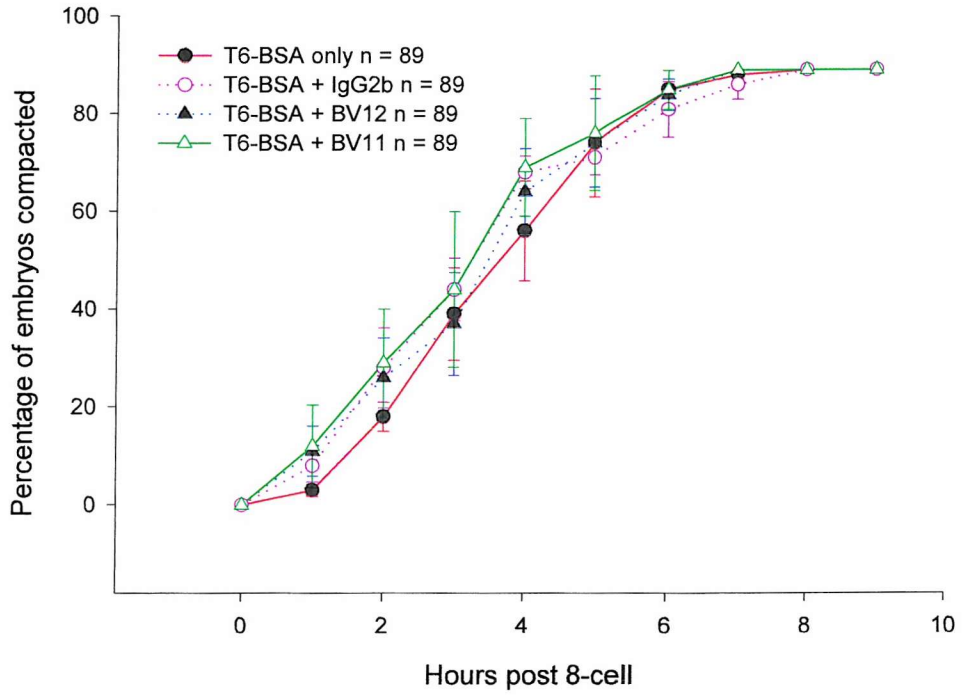

Figure 5.12 Comparison of BV11 and BV12 antibodies with IgG2b and T6-BSA controls upon embryo compaction, n = 4 experiments.

5.3.2 Effects of BV11 upon cavitation of mouse preimplantation embryos

The effects of BV11 and BV12 on precisely timed 0-hour compacted embryos were examined in both T6-PVP (results not shown) and T6-BSA media. Results were similar for both media types tested. Preliminary data suggested that BV11 and BV12 could reduce the rate of cavitation (Figure 5.13). As expected, ECCD-1 control embryos showed a severe delay in cavitation. Medium only, BV11 and BV12 incubated embryos were morphologically indistinguishable from one another. However, as reported in the literature, embryos that managed to cavitate in the presence of ECCD-1 looked abnormal.

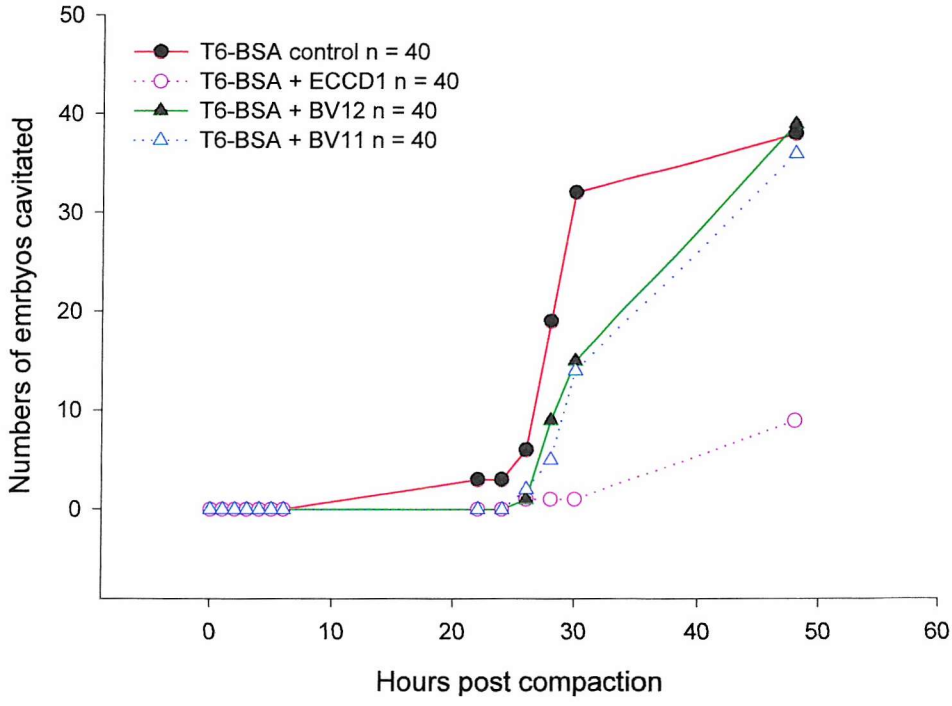

Figure 5.13 Preliminary data comparing the effects of BV11 neutralising antibody with BV12, BSA and ECCD-1 controls upon embryo cavitation, n = 1 experiment.

In time courses where IgG2b controls were used in place of ECCD-1 (Figure 5.14), there was a large decrease in cavitation rates in BV11 embryos compared with the IgG2b control group. However, a difference was also seen (although not as marked) between BV12 and medium only treatment groups versus IgG2b control embryos. "Time to event" analysis indicated that both BV11 and BV12 treated embryos showed a statistically significant decrease in cavitation compared with IgG2b control by 58% ($p = <0.0001$) and 45% ($p = 0.004$), respectively. However, the T6-BSA control embryos also showed a significant decrease in cavitation compared with IgG2b control by 42% ($p = 0.0091$). In comparison with the T6-BSA control group neither BV11 (6%; $p = 0.7916$) nor BV12 (28%; $p = 0.129$) showed a statistically significant decrease in cavitation.

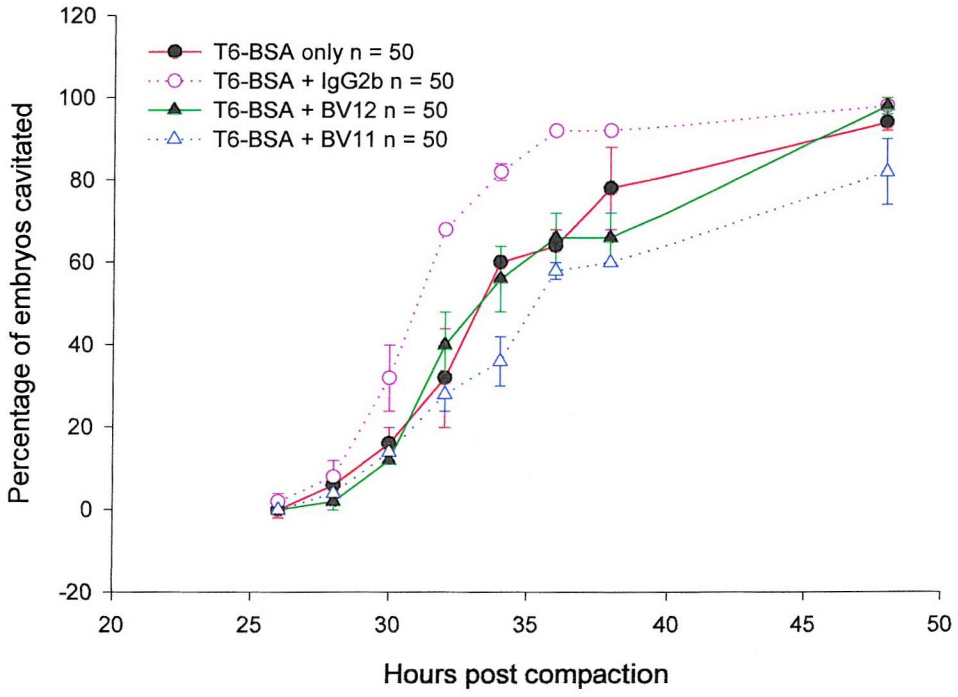

Figure 5.14 Comparison of BV11 and BV12 antibodies with IgG2b and T6-BSA controls upon embryo cavitation n = 2 experiments.

5.3.3 Effects of JAM-1 upon the paracellular permeability of nascent blastocysts

A previous study in the laboratory using FITC-dextran (4kDa) showed that approximately 25% of nascent blastocysts (i.e. blastocysts with the cavity comprising <20% of it's total volume) were still permeable to this tracer (Sheth *et al*, 2000a). However, 100% of larger blastocysts, with a cavity >20% of its volume, excluded FITC-dextran.

In this investigation, precisely timed 2-hour cavitated embryos were incubated in FITC-dextran (4kDa) and observed living, within 10 minutes under confocal microscopy for their permeability to this tracer (section 5.2.2.2). Results were categorised for nascent blastocysts (<20% cavity; Figure 5.15) and blastocysts (>20% cavity; Figure 5.16). Surprisingly, permeability results for control embryos (incubated in medium only) were not consistent with the previous data by Sheth *et al.*, (2000a). for example, on average, 53% of medium only treated embryos were

permeable to FITC-dextran (4kDa). However, the high degree of variation in nascent blastocysts (Figure 5.15) within each treatment group (demonstrated by the error bars), showed that there was no significant difference between embryos incubated in JAM-1 antibodies and the control media. This was also confirmed using a Student's T-test.

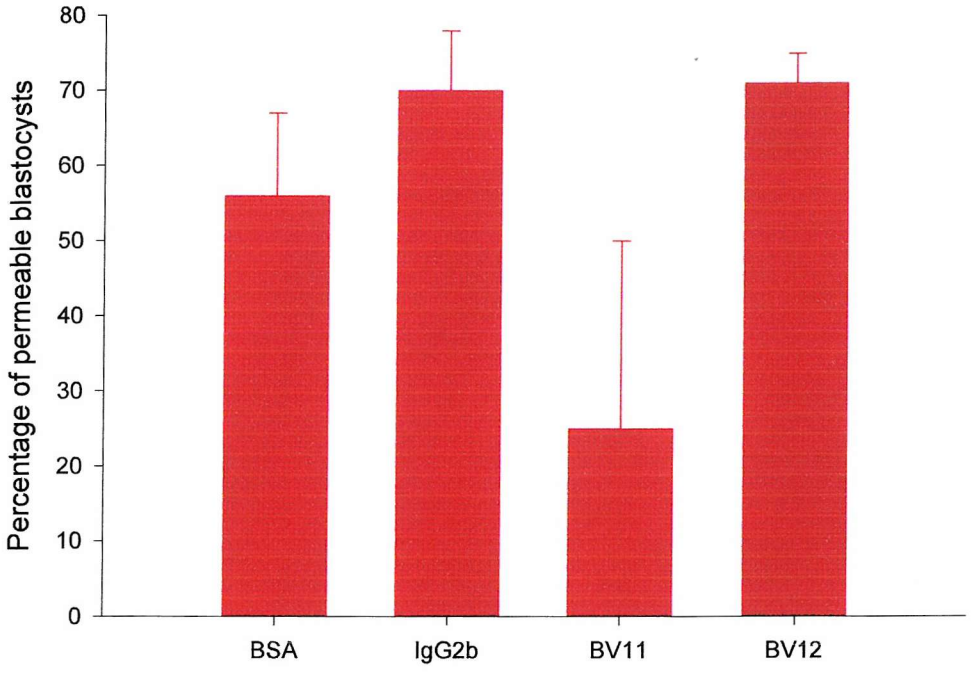

Figure 5.15 Permeability of nascent blastocyst (cavity <20% total volume) to FITC dextran (4kDa) following incubation in either medium or medium plus antibody. n = 2 experiments

As seen in the nascent blastocyst data, permeability of embryos with larger blastocoels was greater than in the ealier study (Sheth *et* al., 2000a; Figure 5.16). However, as in previous data, the IgG2b control group behaved in a manner more consistent to the expected permeability results, as only an average of 8% of the embryos tested were permeable to the tracer. If IgG2b embryos were treated as the reliable control group then both BV11 and BV12 had an increased incidence of permeability, at 27% and 37% respectively. However, due to the variation within each group the differences between the JAM-1 treated embryos and the IgG2b control embryos were not significantly different using a Student's T-test.

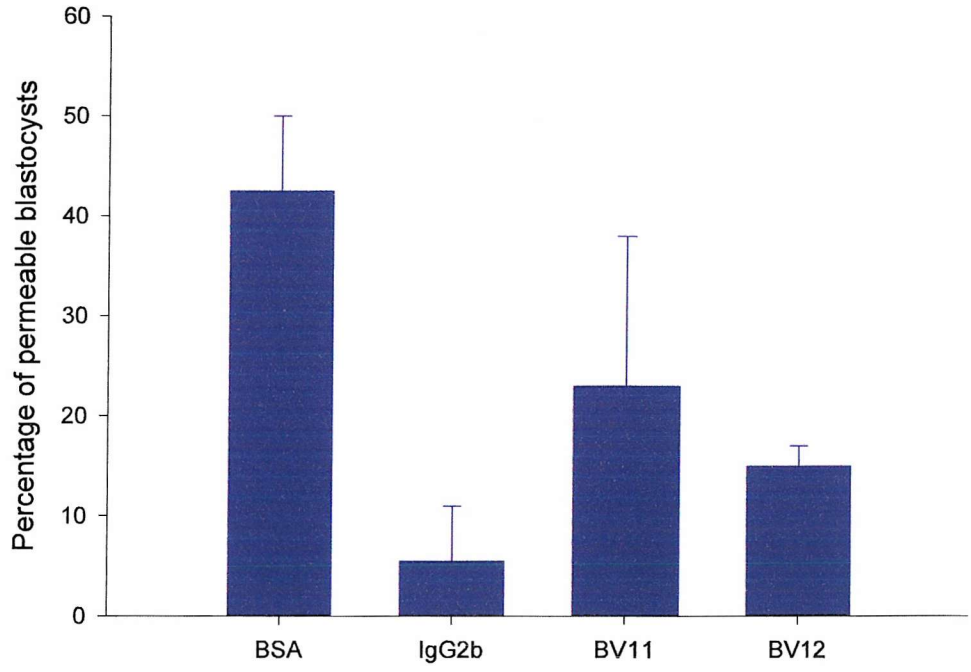

Figure 5.16 Permeability of blastocysts (cavity >20%total volume) to FITC-dextran (4kDa) following incubation in either medium only or medium plus antibody. n = 2 experiments

The assumptions on which these data were based, i.e. that the blastocysts should be categorised into two groups depending upon size, may be incorrect. Embryos collected in the study by Sheth *et al*, (2000a) were categorised purely by blastocoel size and not collected, as in this investigation, within a specified time post cavitation. Since all embryos collected for these permeability assays had cavitated within the past 2-hour, it may be correct to group all the embryos together as "nascent blastocysts" (Figure 5.17). If these data are examined as a whole then the IgG2b control does conform to the expected 25% permeability value. If only the IgG2b group is used as the control group then there is a 9% and 34% increase in permeability in embryos treated with BV11 and BV12 respectively. However, the T6-BSA only embryos are 16% more permeable to the FITC-dextran in comparison to the IgG2b control embryos. However, as seen in the previous data, there was a high degree of variation between these results and no group was shown to be significantly different from another when analysed with a Student's T-test.

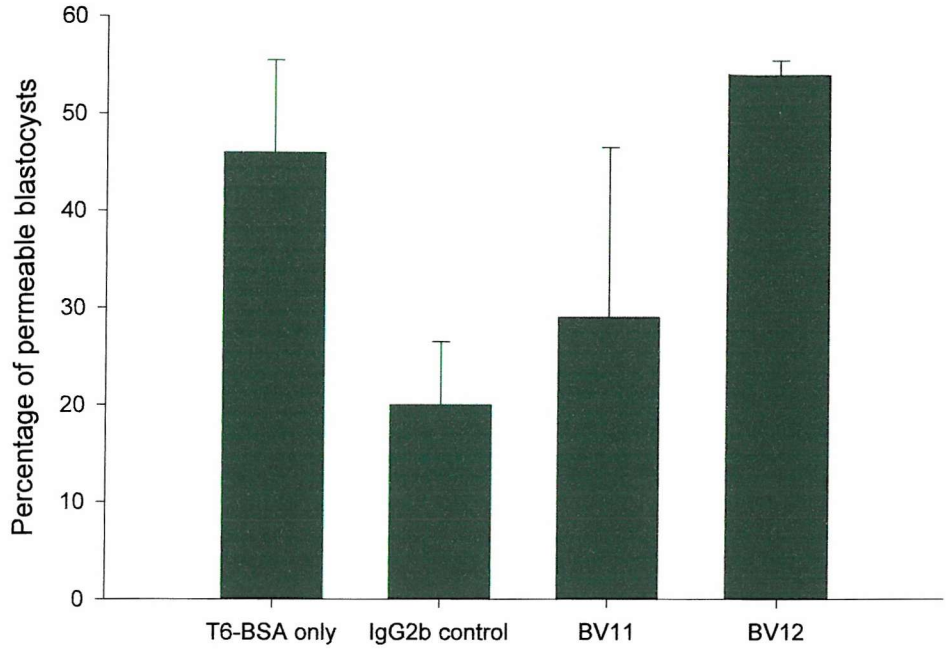

Figure 5.17 Permeability of 2-hour blastocysts to FITC-dextran (4kDa). n = 2 experiments

5.3.4 Effect of Cldn1-K15 treatment on mouse preimplantation embryos

5.3.4.1. Effect of Cldn1-K15 treatment on blastocyst recavitation after CCD treatment (method 1)

Cldn1-K15 peptide was first tested on zona intact, CCD-treated late blastocysts, at 20μM in T6-PVP (section 5.2.4, Figure 5.18). Using this method, Cldn-1-K15 treated embryos did not recavitate and subsequently arrested or lysed. Occludin peptide G (20μM), DMSO and medium control treated embryos did recavitate and did so at similar rates.

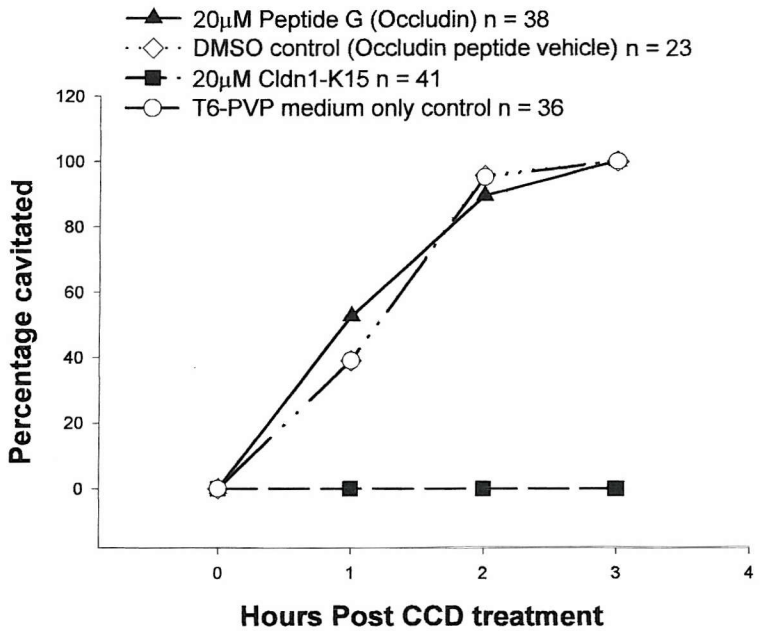

Figure 5.18 Effect of Cldn1-K15 on the recavitation of late blastocysts, cultured in T6-PVP medium, after disaggregation method 1.

Using the same approach (method 1), concentrations of Cldn1-K15 between 0.1μM and 20μM were tested upon early rather than late blastocysts (Figure 5.19). In the early blastocysts, control, 0.1μM and 1μM Cldn1-K15 treated embryos had similar recavitation rates. However, 10μM and 20μM Cldn1-K15 prevented recavitation and the embryos lysed or arrested development.

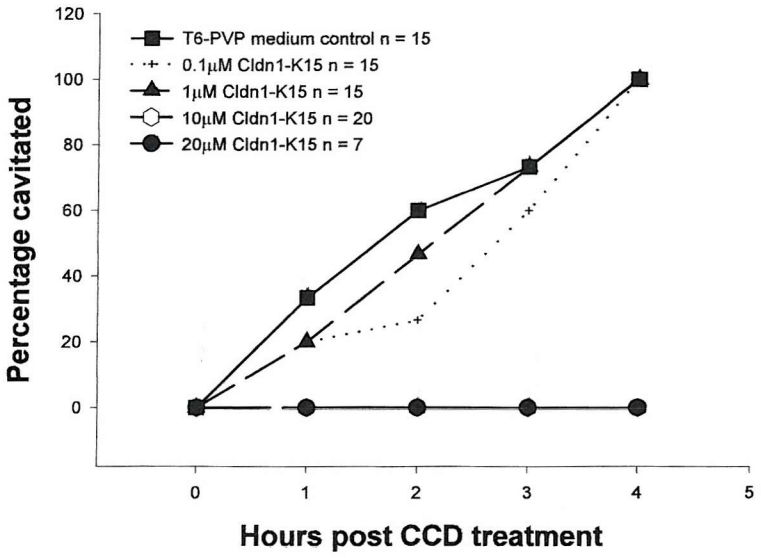

Figure 5.19 Effect of Cldn1-K15 on the recavitation of early blastocysts, cultured in T6-PVP, disaggregated using method 1.

The effect of different culture media containing Cldn1-K15 were also tested upon early and late blastocysts using method 1. In HEPES buffered medium (H6-PVP), control and 1μM Cldn1-K15 had similar recavitation rates (Figure 5.20, while 5μM Cldn1-K15 prevented recavitation of nearly all late blastocysts, which subsequently lysed or arrested.

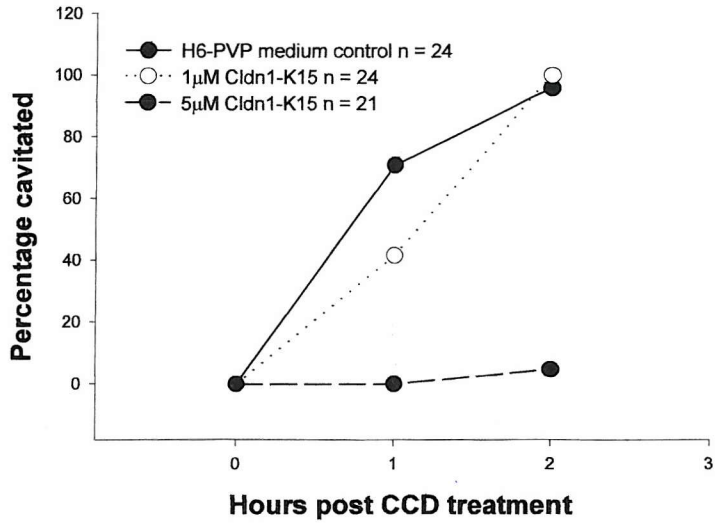

Figure 5.20 Effect of Cldn1-K15 on the recavitation of late blastocysts, cultured in H6-PVP, disaggregated using method 1.

The effect of Cldn1-K15 treatment on early blastocyst recavitation was investigated in H6-PVP and T6-PVP medium (Figure 5.21). Consistent with earlier experiments, 5μM Cldn1-K15 had an inhibitory/toxic effect upon CCD treated early blastocysts in both medium types while medium control embryos recavitated at a similar rate (100% recavitation by 4 hours). There was a large difference between 1μM Cldn1-K15 treated embryos in the two media. In H6-PVP, 77.8% of 1μM Cldn1-K15 treated embryos had recavited by 4 hours. However, in T6-PVP only 27.8% of Cldn1-K15 treated embryos had recavitated by 4 hours.

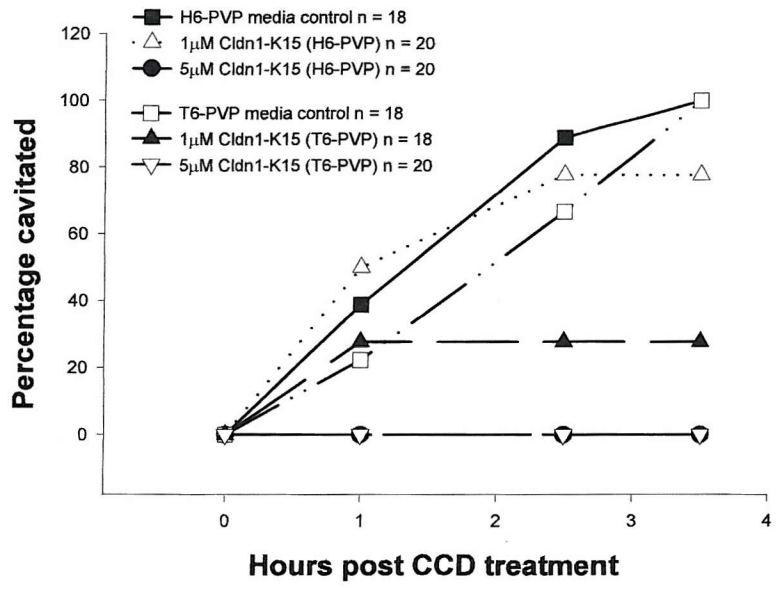

Figure 5.21 Effect of Cldn1-K15 on the recavitation of early blastocysts, cultured in H6-PVP or T6-PVP media, disaggregated using method 1.

These preliminary experiments using the method 1 strategy indicated that a) the rate of embryo recavitation was susceptible to Cldn1-K15 peptide from 1μM, and b) that incubation in T6 rather than H6 enhanced peptide effect. Similar results were seen for both early and late blastocysts, although groups of early blastocysts were slower to recavitate.

5.3.4.2. Effect of Cldn1-K15 on blastocyst recavitation after CCD treatment and mechanical disaggregation of the blastomeres (method 2)

Using zona free early blastocysts and disaggregation of embryos in CCD prior to Cldn1-K15 peptide treatment (method 2), the effect of Cld1-K15 upon recavitation rate was found to differ depending on medium used. Thus, 1μM Cldn1-K15 caused reduction in recavitation rate in T6-PVP but not in T6-BSA (Figure 5.22). However, in contrast to what was expected, T6-PVP control embryos had a better cavitation rate compared to T6-BSA control embryos.

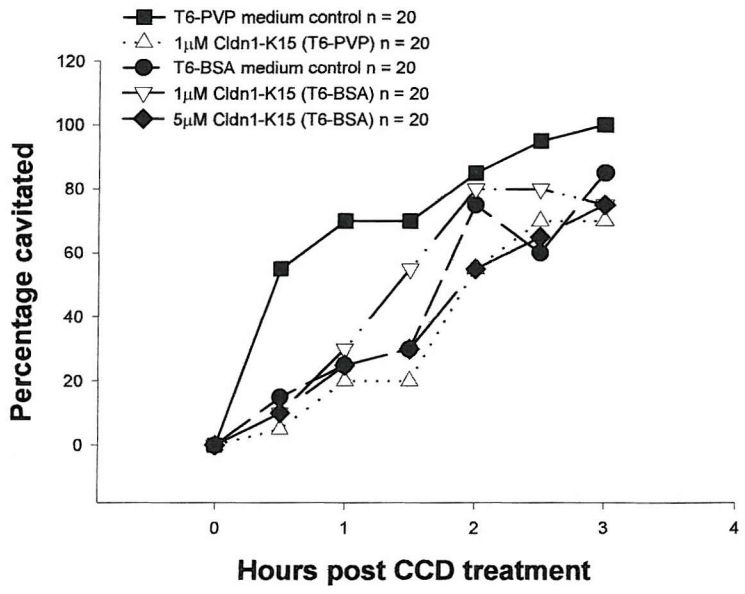

Figure 5.22 Effect of Cldn1-K15 on the recavitation of early blastocysts, cultured in either T6-PVP or T6-BSA medium, using disaggregation method 2.

5.3.4.3. Effect of Cldn1-K15 upon blastocyst recavitation after CCD treatment and mechanical disaggregation of the blastomeres (method 3)

Once again, using zona-free embryos but now disaggregating the blastomeres in CCD + Cldn1-K15 peptide (section 5.2.6), embryo recavitation was observed in culture media + Cldn1-K15 as described in the earlier experiments. As seen in section 5.3.4.2, 5μM Cldn1-K15 had little effect upon embryo recavitation, so higher concentrations of peptide were tested in T6-BSA medium. This new strategy was tested upon late blastocysts (Figure 5.23). In these experiments, 5μM peptide had an effect upon embryo recavitation rate, as did 10μM and 20μM. At 20μM, the embryos lysed or arrested.

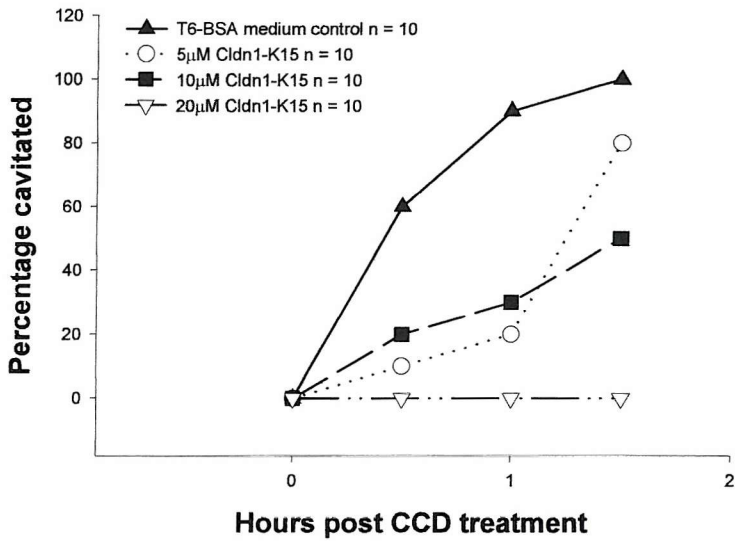

Figure 5.23 Effect of Cldn1-K15 on the recavitation of late blastocysts, cultured in T6-BSA medium, disaggregated using method 3.

Using the same experimental approach, recavitation of disaggregated late blastocysts was tested in the T6-BSA and T6-PVP medium in the presence or absence of Cldn1-K15 (Figure 5.24). T6-BSA control embryos recavitated fastest and by 3 hours 100% of the embryos had formed blastocysts. As seen in previous experiments, 5μM and 10μM Cldn1-K15 treated embryos recavitated at a slower rate compared to the control group. T6-PVP control and 1μM Cldn1-K15 treated embryos recavitated at a similar rate. However, embryos cultured in T6-PVP in the presence of 2μM Cldn1-K15 recavitated at a slower rate compared to the control group. However, in this experiment only 60% of the T6-PVP medium control treated embryos recavitated.

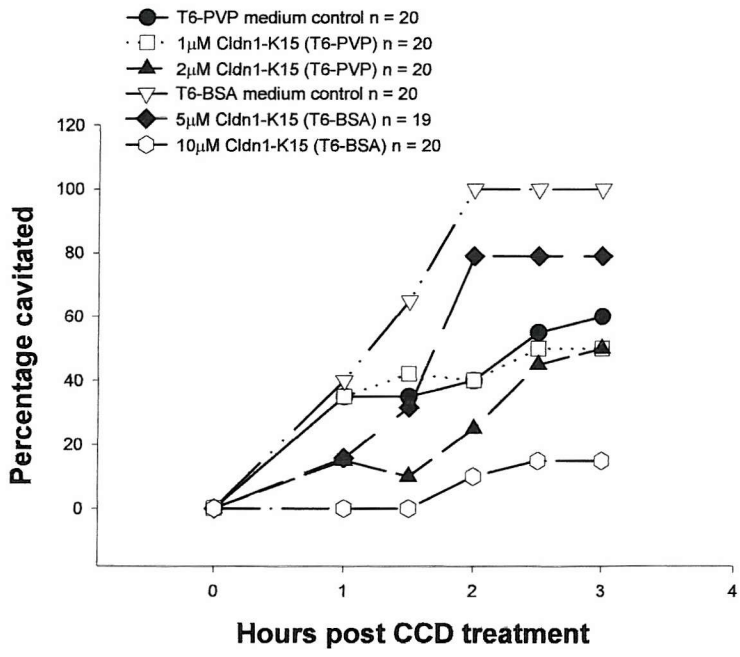

Figure 5.24 Effect of Cldn1-K15 on the recavitation of late blastocysts, cultured in T6-PVP or T6-BSA medium, disaggregated using method 3.

These experiments, using methods 2 and 3, confirm those for method 1 in that the rate of blastocyst recavitation is decreased in a concentration-dependent manner by exposure to Cldn1-K15 peptide. These experiments also showed that the presence of BSA in the medium suppressed the effect of peptide on recavitation rate. Once again, the results were similar in both early and late blastocysts.

5.3.4.4. Embryo recovery after removal from Cldn1-K15

The next experiments were designed to investigate whether blastocysts that fail to recavitate in the presence of Cldn1-K15 peptide were viable, and whether the peptide effect was specific for claudin-1 disruption.

Using the disaggregation strategy described in section 5.3.4.3 (method 3), early blastocysts were cultured in T6-BSA and then subsets of these embryos were then removed from the medium containing peptide and transferred to control (recovery) medium and their ability to recavitate examined (Figure 5.25). The first set of embryos were removed from 10μM Cldn1-K15 peptide after 2 hours (recovery 1)

and placed into T6-BSA medium. In the following hours, these embryos began to recavitate at a higher rate than those left in 10μM peptide. By the following day, all "recovery 1" embryos had recavitated. Another group of embryos (recovery 2) were removed from the culture media after 5 hours and by the following day 50% had recavitated. However, the 10μM Cldn1-K15 treated embryos, none of which had recavitated by 5 hours, 87.5% had recavitated overnight.

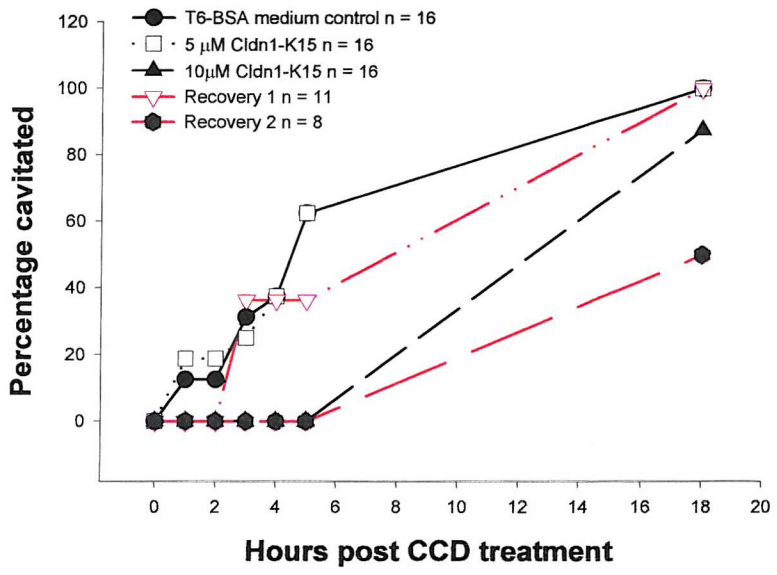

Figure 5.25 Recovery of <u>early blastocysts</u> after Cldn1-K15 treatment. Using embryo disaggregation method 3 as described earlier, early blastocysts were treated with Cldn1-K15 peptide in T6-BSA. A subset of 10μM treated embryos were removed from peptide after 2 hours (recovery 1) or after 5 hours (recovery 2) and placed in normal T6-BSA medium.

5.3.4.5 The effect of scrambled Cldn1-K15 on the recavitation of early blastocysts (method 3)

Once an effect had been established upon recavitating embryos treated with Cldn1-K15, a scrambled version of Cldn1-K15 was used. This peptide was used to verify whether the effects seen in previous experiments were specific or due to general toxicity of adding such a peptide (Figure 5.26). Unfortunately, use of the scrambled peptide did reveal that these effects were not specific and hence this approach to claudin-1 inhibition was abandoned.

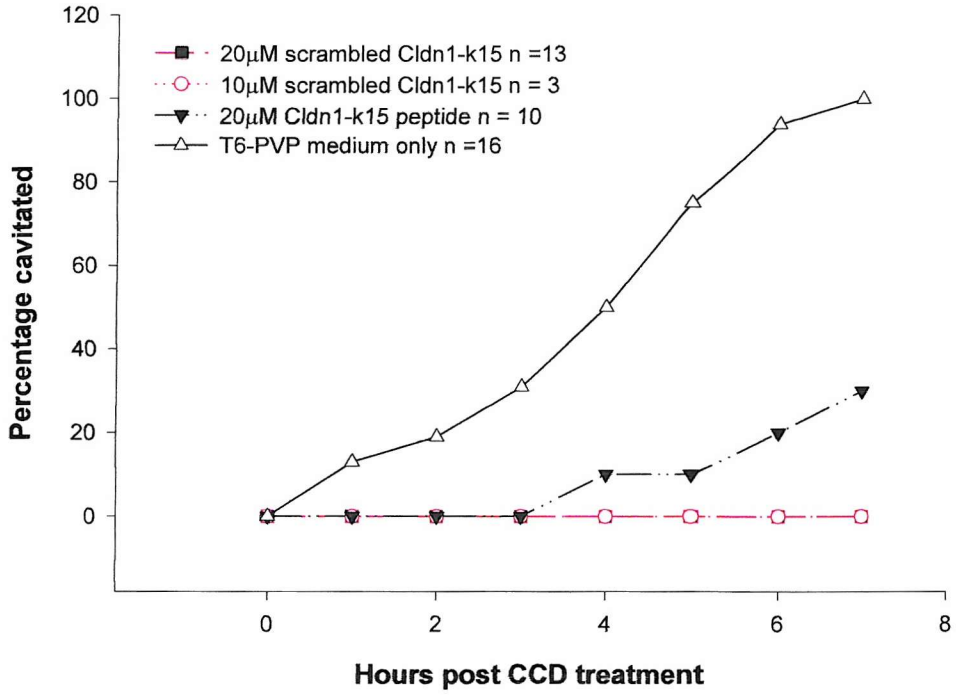

Figure 5.26 Effect of Cldn1-K15 and scrambled Cldn1-K15 peptides on the recavitation of early blastocysts, cultured in T6-PVP, disaggregated using method 3.

5.3.4.6 Effect of Cldn1-K15 on the electrical resistance of the mouse cell line CMT64

Prior to having access to the scrambled version of Cldn1-K15, a mouse epithelial cell line (CMT64) was used to examine the effects of Cldn1-K15 upon the TJ seal. Early experiments, examined the effect of Cldn1-K15 on pre-established monolayers. Initial results suggested that Cld1n-K15 impaired the electrical resistance of epithelial cells in a concentration dependant manner (Figure 5.27).

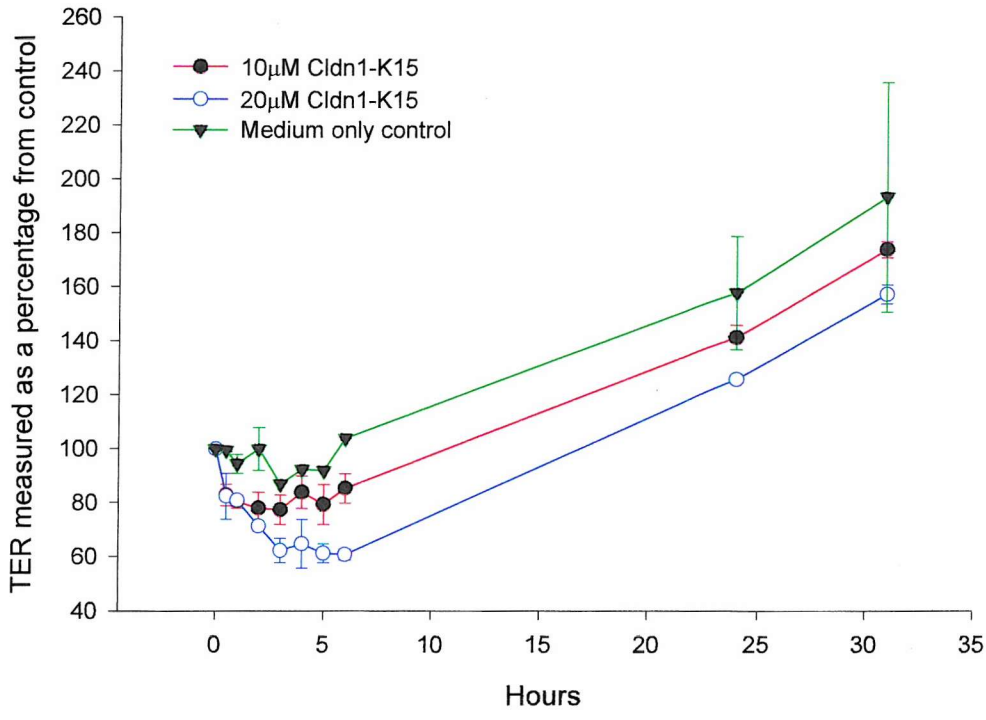

Figure 5.27 Effect of Cldn1-K15 on CMT64 cell monolayers. A baseline TER reading was taken prior to incubation of the cells in either medium containing peptide or control medium. At hourly timepoints TER readings were taken and the percentage difference from "time 0" was calculated.

Cldn1-K15 was also tested on CMT64 cell lines after Ca^{2+} switching (section 2.13.4), to disrupt the exisiting TJs. As seen with the embryo experiments, peptide concentrations, previously shown to have an apparent effect on the TJ were progressively less effective from one experiment to the next. Indeed in later cell line experiments, 20μM and even 100μM Cldn1-K15 showed little effect upon the TER (Figure 5.28).

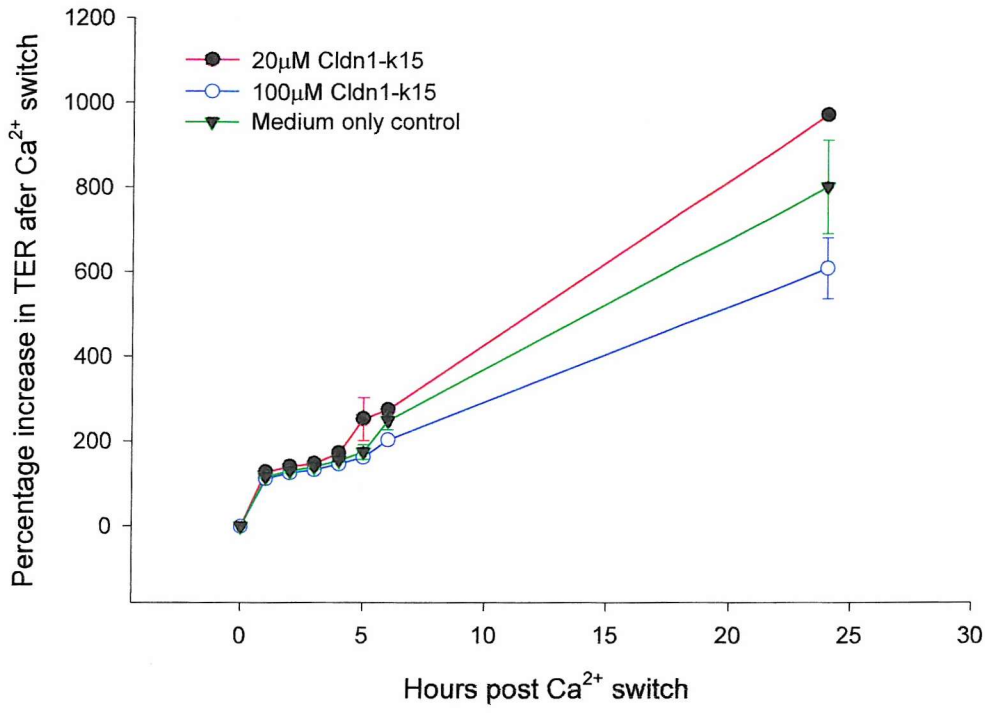

Figure 5.28 Effect of Cldn1-K15 on CMT64 cell monolayers after Ca^{2+}switch. A baseline TER reading was taken during cell incubation in the Ca^{2+} free medium. At hourly timepoints TER readings were taken and the percentage difference was calculated.

5.3.5 Microinjection of dsRNA into 1-cell embryos

dsRNA was synthesized to target either claudin-1 or JAM-1 specifically in RNA*i* experiments. While learning the microinjection technique, preliminary results were obtained for both claudin-1 and JAM-1 RNA*i*. The preliminary data obtained for claudin-1 RNA*i* did not indicate an obvious effect upon embryo development (Figure 5.29). The percentage of embryos arrested at any given stage did not vary greatly from between Tris-EDTA (TE) buffer injected embryos and claudin-1 dsRNA injected embryos. The number of embryos reaching blastocyst stage between injected and non-injected embryos did vary quite considerably, indicating that the microinjection technique needed improving. Claudin-1 RNA*i* was postponed until the claudin-1 (as opposed to claudin-3) could be confirmed as being expressed in mouse preimplantation embryos.

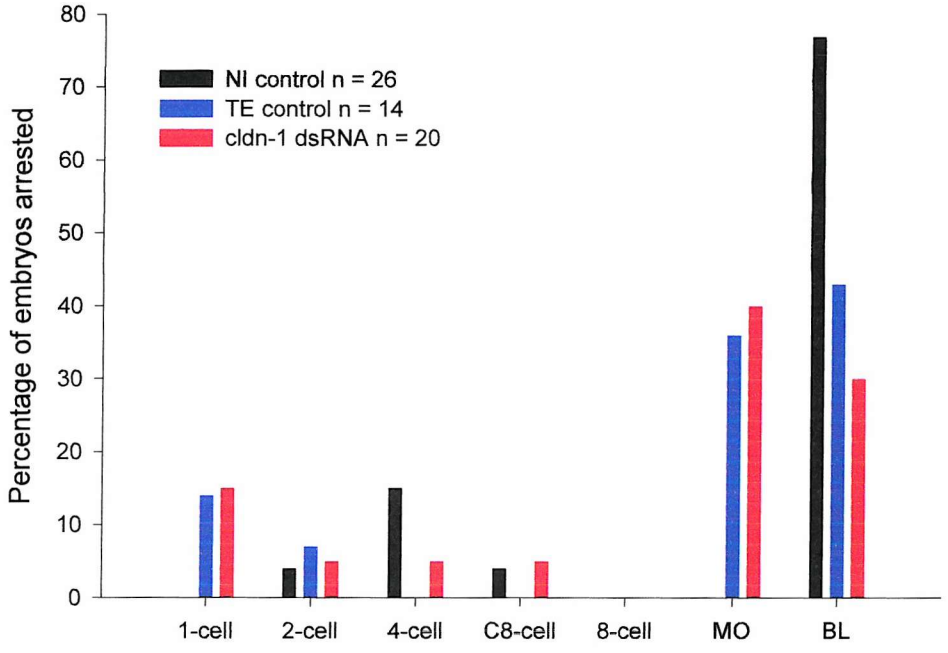

Figure 5.29 Comparison of embryo development after microinjection with claudin-1 dsRNA n = 1 experiment. Cldn-1 dsRNA or Tris-EDTA buffer only (TE) was injected into the male pronucleus of 1-cell embryos. Embryo development through cleavage up to blastocyst formation was assessed in comparison with non-injection (NI) embryos.

Preliminary data for JAM-1 RNA*i* also showed little obvious effects upon embryo development (Figure 5.30). The percentage of embryos arrested at any given stage did not vary greatly between TE buffer injected embryos and JAM-1 dsRNA injected embryos. However, a high degree of variation between the experimental replicates was observed and no statistically significant difference between the JAM-1 and TE buffer injected embryos was detected at any given developmental stage (Student's T-test). The non-injected and injected control groups gave comparable results suggesting that the microinjection technique had improved.

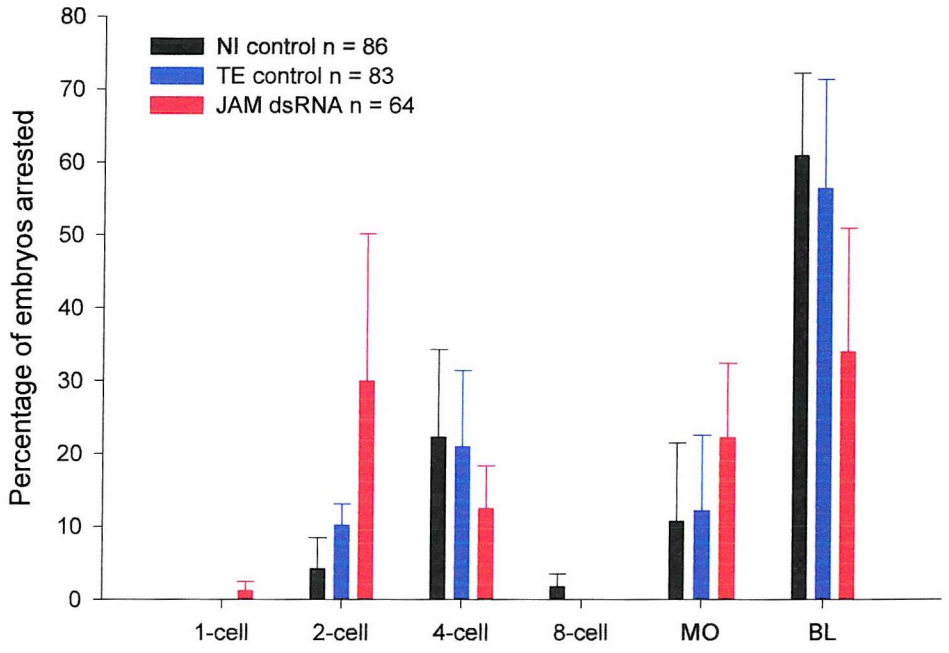

Figure 5.30 Comparison of embryo development after microinjection with JAM-1 dsRNA n = 4 experiements. JAM-1 dsRNA or Tris-EDTA buffer only (TE) was injected into the male pronucleus of 1-cell embryos. Embryo development through cleavage up to blastocyst formation was assessed in comparison with non-injection (NI) embryos.

5.4 Discussion

JAM-1 immunofluorescence data (Chapter 3) indicated that this protein might have an early role in TJ biogenesis. Indeed, JAM-1 is first detected before maturation of the ZA junction and may even have a role in early polarity events. However, preliminary experiments demonstrated that BV11 did not behave in a similar manner to the E-cadherin neutralising antibody, ECCD-1, because its presence in embryo culture medium did not cause embryo decompaction (Figures 5.10 and 5.11).

It is possible that although BV11 does not cause embryo decompaction, it may cause a delay in the onset of compaction. To examine this hypothesis, newly formed 8-cell embryos were observed at hourly intervals and the percentage of compacted embryos was recorded. The results of four experiments comprising a total of 89 embryos indicated that embryos treated with BV11, BV12, IgG2b control or medium only, all compacted at similar rates. Embryos from each treatment group were

morphologically indistinguishable from each other. This result is also consistent with an inhibition study in human epithelial cell lines (Liu *et al.*, 2000) where JAM-1 inhibition, using human JAM-1 neutralising antibodies, did not appear to effect AJ assembly after the transient removal of Ca^{2+} from the culture medium.

In view of JAM-1 originally being reported as a TJ protein and the inability of BV11 to affect embryo compaction, the early membrane localisation of JAM-1 indicates that it may have an important role in early adhesion events leading to cavitiation. Indeed, there have been reports with epithelial cell lines that JAM-1 is part of an early adhesion component of TJ assembly (Ebnet *et al.*, 2001). To examine the importance of JAM-1 to embryo cavitation, newly compacted 8-cell embryos were observed at 2-hourly intervals in the presence or absence of JAM-1 antibodies and the percentage of cavitated embryos was recorded. In comparison to the "true" experimental control (IgG2b antibody control) both BV11 and BV12 treated embryos showed a significant decrease in embryo cavitation ($p = <0.0001$ and $p = 0.004$, respectively). However, embryos incubated in only T6-BSA medium also showed a significant decrease in embryo cavitation in comparison to the IgG2b control treated embryos. These results indicate that addition of an IgG2b antibody to embryo culture medium may be advantageous to preimplantation embryo development. In which case, BV11 and BV12 antibodies can be concluded to delay embryo cavitation and therefore may play an important role in TJ assembly. However, JAM-1 inhibition can be compensated for, as embryo cavitation was not inhibited.

In human epithelial cell lines, JAM-1 antibodies have been shown to inhibit TER recovery after the transient removal of Ca^{2+} from the cell culture medium (Liu *et al.*, 2000). However, in conjunction with the embryo data in this study, the TER of the human epithelial cells was able to partially recover indicating that some components of the TJ are creating a permeability barrier, although the integrity of which appears to be reduced. It was proposed that BV11 could cause a reduction in blastocyst recavitation due to an increase in "leaky" TJs. To investigate further the effects of JAM-1 antibodies upon embryo development, a permeability assay was set up. Previous data in the laboratory, using FITC-dextran (4kDa), demonstrated that 25% of nascent blastocysts (deemed to have a cavity comprising <20% of the total

blastocyst) were still permeable to the FITC-dextran (Sheth *et al*, 2000a). However, 100% of blastocysts with a larger cavity were impermeable to the FITC-dextran tracer (Sheth *et al*, 2000a). In this study, neither the nascent nor the established blastocysts, cultured in T6-BSA control medium, conformed to the data in the study by Sheth *et al*., (2000a). However, despite the discrepancies in these results compared with previous data, there is a decrease in permeability between blastocysts with a small cavity (<20%) and those with a larger cavity (>20%) in all treatment groups.

Since all the blastocysts used in the dextran permeability assay had cavitated within the past 2 hours it may be more accurate to group all the embryos as "nascent blastocysts". Again, the T6-BSA only control embryos had an increased incidence of permeable blastocysts compared with data published by Sheth *et al*., (2000a). Moreover, T6-BSA control embryos were shown to be more permeable to the FITC-dextran than IgG2b control embryos. Again, as with the time course data (section 5.3.2 and Figure 5.14), IgG2b embryos appear to be the more appropriate control group and do conform with the expected incidence of permeability in a group of nascent blastocysts (compared with Sheth *et al*., 2000a).

Assuming the IgG2b treated embryos is the more appropriate control group then both BV11 and BV12 antibodies resulted in an increased incidence of permeable blastocysts to FITC-dextran (4kDa). However, the permeability data is hard to interpret in conjunction with the cavitation time course data (section 5.3.2), as the slowest embryo group to cavitate was BV11 treated embryos and not BV12. Indeed, T6-BSA embryos were faster to cavitate than BV11 but this group had a higher incidence of permeability to FITC-dextran. The fact that these permeability results do not correlate with the time course data, indicate that either more replicates are needed for both experiments or one or both of these assays needs improving.

Due to the asynchronous development of each cell comprising the blastocyst, more importantly the trophectoderm epithelium (TE), there may be transient periods during cell division where the integrity of the TE is disturbed. This may be the reason for some of the high variation in these results. The fact that the embryos in the study by Sheth *et al.,* (2000a) were grouped as nascent and established blastocysts

due to size and not necessarily an early time point post cavitation, as in this study, may be a reason for the discrepancies between the expected results and what was observed in this investigation. Although the presence and size of a blastocoel is indicative of the maturation of the TJ complex, the FITC-dextran procedure was not a quantitative assessment of the amount or rate of "leakage" of this tracer across the TE. It may be that the more subtle effects of embryos in these experiments are being overlooked. In order to assess the subtle effects of inhibiting JAM-1 in embryos these experiments should have incorporated immunofluorescent analysis of the changes in localisation for some important AJ and TJ proteins (e.g. E-cadherin, ZO-1, occludin and Cingulin). However, these experiments were not carried out and therefore should be a focus to any future inhibition studies.

Immunofluorescence data for claudin-1 (later discovered to be claudin-1/-3) indicate that this protein is expressed much later in embryo development compared with JAM-1. As claudin-1 is thought to be an important sealing component at the TJ (Furuse *et al.*, 1998b; Furuse *et al.*, 1999), a peptide (Cldn1-K15) was designed to bind the first extracellular loop of claudin-1 and its ability to prevent blastocyst recavitation was tested. The aim of these experiments was to disrupt claudin-1 in the trophectoderm cell layer by blocking claudin-1 interactions with neighbouring blastomeres. Blocking claudin-1 interactions between the cells of the trophectoderm may then disrupt the functionality of this epithelial layer thus inhibiting blastocyst development. Indeed, similar experiments using synthetic peptides to the first and second extracellular loop of occludin have previously been shown to disrupt epithelial integrity in cell lines (Wong and Gumbiner, 1997; Vieira *et al.*, 1999).

Preliminary experiments using the method 1 strategy indicated that the rate of embryo recavitation was susceptible to Cldn1-K15 peptide from 1μM and that incubation in T6 rather than H6 enhanced peptide effect. Improved experiments, using methods 2 and 3, confirmed that the rate of blastocyst recavitation decreased in a concentration-dependent manner by exposure to Cldn1-K15 peptide. Moreover, the presence of BSA in the medium suppressed the effect of peptide on recavitation rate, suggesting that some Cldn1-K15 peptide may have been binding to the BSA. Recovery experiments indicated that embryos remain viable during peptide treatment

and can recover if peptide is removed from the medium. It was apparent in most of the experiments that early blastocysts were more sensitive to the disruption technique than late blastocysts and control late blastocysts would often recavitate at a faster rate. Blastomeres from late blastocysts were harder to disaggregate than those from the early blastocysts and so the faster cavitation rate, in the former, was possibly due to incomplete blastomere disruption or less damage due to disaggregation.

The initial method of blastomere disruption of zona intact embryos treated with CCD was not easily reproducible. The length of time required for complete blastomere disaggregation varied from embryo to embryo. Because of the inconsistency in blastomere disaggregation, subtle effects upon embryo recavitation rates with some concentrations of the peptide may have been lost and consequently were also hard to reproduce. The later methods of embryo disaggregation, using a micropipette, appeared to help make the disaggregation state of each embryo comparable. However, there were still problems with reproducing the effects of Cldn1-K15 from one experiment to the next. These discrepancies are highlighted in the "recovery" experiments (section 5.3.2.4) where concentrations previously toxic to the embryos (10μM Cldn1-K15) were no longer fully inhibitory to embryo recavitation.

There were a number of concerns with the claudin-1 peptide data, as the embryos in the higher (inhibitory) concentrations of Cldn1-K15 embryos would turn brown and the outer blastomeres appeared disintegrated. A scrambled control peptide containing the same amino acids as Cldn1-K15, was tested on embryos alongside the experimental peptide to check that the inhibition of embryo recavitation was not a non-specific toxic effect. However, scrambled Cldn1-K15 was as toxic to the embryos as the original Cldn1-K15 peptide in the initial experiments (Figures 5.18-5.21). The apparent recovery of embryos in later experiments may have been as a result of the peptide quality deteriorating over time although the exact mechanism of this deterioration is not known.

The loss of inhibitory/toxic function of Cldn1-K15 was also seen in experiments with cell lines (section 5.3.4.6). Initially, differences between the

epithelial integrity of the mouse epithelial cell line (CMT64), measured by transepithelial electrical resistance (TER), were no longer observed in repeated experiments at a later date (Figures 5.27 and 5.28). In fact, even 100μM Cldn1-K15 did not greatly affect the TER values of mouse epithelial cells previously inhibited by 10μM of the same peptide. Therefore, despite the observations with embryos in the peptide "recovery" experiment (Figures 5.25) the observed inhibition results can only be attributed to a toxic effect unrelated to disruption of claudin-1 function, as shown with the scrambled Cldn1-K15 peptide experiments on embryos.

The non-specific toxicity was not as a result of a change in pH, as media containing the different concentrations of the peptide used for these experiments maintained pH 7.4. Indeed, toxicity of the peptides appeared to be due to the additional lysines added to the C-terminus to make these peptides soluble. Although addition of lysine residues to hydrophobic peptides had previously been successful without any apparent toxicity (Tomich *et al.*, 1998), it is possible that the length of both the hydrophobic peptide and the number of additional lysines caused the peptide to behave in a manner similar to that observed in antibacterial cell lytic peptides such as melittin (reviewed in Saberwal and Nagataj, 1994). Without the additional lysines the claudin-1 peptide would have been too hydrophobic to be soluble in the embryo culture medium. However, it appears that adding charge to the C-terminus of this peptide caused a non-specific lysis of the TE and later to all blastomeres of the embryo.

Due to the inconsistencies in the JAM-1 neutralising antibody data and the toxicity of Cldn1-K15, an alternative approach was explored to assess the functions of JAM-1 and claudin-1 in the preimplantation embryo. RNA*i*, which targets the destruction of a specific mRNA preventing its translation into protein, was deemed as a potentially useful technique for this study. Indeed, RNA*i* experiments for E-cadherin with mouse embryos demonstrated a phenotype similar to E-cadherin null mutant embryos (Wianny & Zernicka-Goetz, 2000; Larue *et al.*, 1994). Two pools of dsRNA were successfully produced from RT-PCR products, amplified from mouse tissue RNA extracts, to target either JAM-1 or claudin-1, respectively.

While the microinjection technique was being optimised, initial claudin-1 RNA*i* data did not demonstrate any adverse effects upon embryo development above those seen in control embryos. However, a high proportion of both TE buffer and dsRNA injected embryos compared to non-injected embryos did not develop to the blastocyst stage. It was clear from this experiment that the microinjection technique needed improving. Due to the lack of success in confirming the expression of claudin-1 mRNA in the mouse preimplantation embryo and that the claudin-1 antibody (71-7800) was now reported to detect both claudin-1 and claudin-3, claudin-1 RNA*i* experiments were postponed until its expression in the early embryo could be confirmed.

While expression data was being further examined for claudin-1, RNA*i* using dsRNA directed against JAM-1 mRNA was tested upon mouse preimplantation embryos. Once again there was no obvious effect upon embryo development after microinjection with JAM-1 dsRNA. However, there was huge variation from one experiment to the next. Some of this variation was also seen in the non-injected embryos and was, therefore, attributed to poor embryo quality. Once again, the RNA*i* experiments were postponed until the embryo culturing problems with non-injected embryos could be resolved. Unfortunately, due to the time constraints of this investigation the JAM-1 RNA*i* have not yet been continued to date.

Indeed, if the RNA*i* studies were resumed, more subtle measures of the effects of JAM-1 and claudin-1 inhibition need to be explored. Moreover, the inhibition of mRNA expression and translation need to be confirmed by RT-PCR and confocal microscopy. Once again, for this to be possible mRNA expression for claudin-1 needs to be confirmed in non-injected embryos and a more specific and reliable claudin-1 antibody needs to be optimised.

Since there are a growing number of transmembrane (TM) components comprising the TJ seal, it is unlikely that inhibiting one alone will cause a major effect upon the formation of a TJ seal in all epithelia. Indeed, it is possible that other TM proteins involved in the sealing of epithelial TJs will compensate for the loss of function from the one protein targeted. Moreover, knockout mice for both occludin and claudin-1 have both been shown to develop to term and only certain tissue

specific epithelia were shown to be affected, although the loss of epithelial integrity in particular organs were severe (Saitou *et al.*, 2000 and Furuse *et al.*, 2002). The effects of inhibiting the function of either JAM-1 or claudin-1 in the mouse preimplantation embryo is therefore most likely to show subtle differences in either the timing or co-localisation of TJ components during epithelial differentiation. In order to establish the roles of JAM-1 and claudins in the preimplantation embryo, more precise co-localisation studies and thorough quantitative analysis of mRNA and protein expression in the early embryo need to be investigated.

In conclusion, JAM-1 inhibition studies using BV11 and BV12 antibodies indicted that this protein is not vital for embryo compaction but may have an important role in embryo cavitation. Further confirmation of the apparent delay in cavitation still needs further investigation. Future experiments, in order to establishing the true effects of BV11 and BV12 on the preimplantation embryo, would require additional antibody control groups plus more repeats of the FITC-dextran permeability experiments. Although the strategies employed for the functional disruption of both JAM-1 and claudin-1 needed improving, expression data for Claudin-1 indicates that there is neither mRNA nor protein for this gene in the mouse preimplantation embryo. Indeed, the fact that the non-toxic doses of claudin-1 peptide had no effect upon embryo cavitation may also have been indicative of the absence of claudin-1 gene expression.

Chapter 6

General discussion

In summary, JAM-1 mRNA was not detected in unfertilised or fertilised eggs but was found from the 2-cell stage and all subsequent stages up to and including the late blastocyst. This expression pattern indicated that there was no maternal pool of JAM-1 mRNA and that it was first transcribed during the major phase of embryonic genome activation at the 2-cell stage. Although the mRNA analysis was not quantitative, there appeared to be a marked increase in JAM-1 mRNA at the 8-cell stage which increased further, at each stage, up to and including late blastocysts. The increase in detectable mRNA expression was consistent with the first detectable JAM-1 protein in immunofluorescence studies and a very interesting change in its pattern of localisation from cell-cell contacts to the apical pole.

Combining the findings from JAM-1 Western blotting and immunofluorescence experiments indicated that JAM-1 protein was first expressed in 8-cell embryos, where it was weakly localised at cell-cell contacts, with more intense staining post compaction, indicating that JAM-1 may play an early role in TJ biogenesis. Interestingly, JAM-1 had an unusual transient polar localisation pattern at compaction, not seen for other AJ or TJ proteins in the preimplantation embryo. Moreover, JAM-1 was not exclusively restricted to the TE lineage but was also found between cell-cell contacts in the ICM, suggesting that its role is not exclusive to providing an additional "barrier" component to the TJ. JAM-1 and actin double labelling in compact 8-cell embryos confirmed its localisation at the microvillous pole and indicated that its expression profile may be a reflection of actin-reorganisation during TE biogenesis.

As mentioned earlier, JAM-1 directly associates with ASIP/PAR-3 at TJs in epithelial cell lines (Ebnet *et al.*, 2001 and Itoh *et al.*, 2001). Originally discovered as cell polarity proteins in *C.elegans* and *Drosophila,* there is now growing evidence that the PAR-aPKC complex has a role in TJ biogenesis and hence epithelial polarity in mammals. Experiments with MDCK cells whereby a mutant for one aPKC

isoform (PKCι/λ) that lacked kinase activity, or another mutant of PAR-6 (lacking the aPKC- binding domain) were overexpressed demonstrated some important findings (Suzuki *et al.*, 2001; Yamanaka *et al.*, 2001). Firstly aPKC was found to be required for the correct localisation of the ASIP/PAR-3 and PAR-6 complex. Secondly, overexpression of either mutant resulted in the mislocalisation of TJ proteins (ZO-1, occludin and claudin-1) which in turn compromised the integrity of the entire TJ complex and its functions, although cell-cell contact was still maintained. Interestingly, the localisation of other membrane proteins was also affected. In fact, these proteins had previously been suggested to localize in the absence of TJs through their interaction with domain-specific membrane-cytoskeleton structures. All these defects were only seen in subconfluent cells, or cells that were in the process of redeveloping polarity (after transient removal of extracellular Ca^{2+} from the cell medium) suggesting that the aPKC-PAR complex is required for the establishment, but not the maintenance, of cell polarity.

Until recently, how the PAR-aPKC complex is recruited to the membrane and the TJ complex had not been elucidated. This question has begun to be answered by the direct association of JAM-1, but not claudins and occludin, with ASIP/PAR3 (Ebnet *et al.*, 2001; Itoh *et al,* 2001). More importantly, it was also shown that JAM-1 was required for the recruitment of ASIP/PAR-3 to cells establishing a polarised phenotype. Indeed, JAM-1 is the earliest member of the TJ to be recruited to cell contacts in wound healing assays, where cell polarity is being re-established, immediately prior to ASIP membrane assembly (Ebnet *et al.*, 2001). In the context of these findings, further investigation into JAM-1's unusual localisation patterns during mouse preimplantation development could provide some exciting insight into the *de* novo regulation of cell polarity formation in mammalian cells. Indeed, the preimplantation embryo is an excellent system to examine the establishment of cell polarity and has distinct advantages over artificially transformed mature cell lines. Moreover, the relatively long cell cycles enable analysis of the temporal pattern of the mechanisms and pathways involved in epithelial biogenesis to be easily observed.

Considering that PKCζ and PKCι/λ (two mammalian aPKC isoforms) appear to have different expression patterns in the mouse preimplantation embryo (personal communication with Dr. Judith Eckert), and that PKCζ is found apically polarised during compaction, a link between JAM-1 and the aPKC-PAR complex during the establishment of epithelial polarity seems likely. Investigating the binding partners of JAM-1 during preimplantation development could help in furthering our understanding of epithelial biogenesis. Indeed, double labelling of 8-cell and compacting 8-cell embryos for JAM-1 and both isoforms of aPKC could provide some interesting results. Furthermore, double labelling of JAM-1 with other components of both the AJ and the TJ in the preimplantation embryo could provide valuable spatial and temporal information, hopefully providing clues to the ever growing, dynamic puzzle of the *de novo* maturation of the TJ complex.

In addition to JAM-1 being found at the TJs of endothelial and epithelial cells it has been reported also as being constitutively expressed on circulating monocytes, neutrophils, platelets and some types of lymphocytes (Williams *et al.*, 1999). Indeed, it has been shown that JAM-1 is directly phosphorylated by cPKCs upon platelet activation (Ozaki *et al.*, 2000). Further studies into the interaction of various PKC isotypes, belonging to the three main PKC groups (cPKC, aPKC and nPKC), on JAM-1 could provide valuable information on how JAM-1 may be involved in TJ biogenesis. In addition to the double labelling experiments mentioned previously, it would be interesting to look at the expression of phosphorylated and non-phosphorylated JAM-1 in Western blots and if possible the localisation of these during preimplantation development. Immunofluorescence studies would require additional antibodies for JAM-1 that recognised either phosphorylated or non-phosphorylated JAM-1. Alternatively, a polyclonal anti-JAM-1 antibody used on Western blots may demonstrate multiple bands representing various forms of JAM-1 that may change in abundance during development. Unfortunately, a polyclonal JAM-1 antibody was not available when JAM-1 protein expression was examined in this study.

With the availability of a known JAM-1 neutralising antibody an alternative approach to understanding the role of this protein in TJ and epithelial biogenesis was

explored. These antibodies demonstrated that JAM-1 inhibition did not effect embryo compaction but did cause a delay in the onset of cavitation. Considering that in cell lines, disruption of the aPKC-PAR complex does not affect cadherin adhesion and that JAM-1 localisation in cell lines appears after E-cadherin, indicates that JAM-1 disruption should be specific to TJ assembly and not AJ assembly (which is consistent with the above mentioned time course data). However, in the preimplantation embryo there is a weak expression of JAM-1 prior to compaction that changes in localisation as compaction occurs. Again, it would be interesting to see whether this early expression is due to a non-functional form of JAM-1 and at what point ASIP/PAR-3 colocalises with this protein.

The apparent delay in blastocyst formation, after embryo culture in the presence of JAM-1 neutralising antibodies indicated that the integrity of the TJ might have been affected, although eventually blastocysts were able to develop. However, although FITC-dextran permeability assays indicated that this might be due to a compromised TJ seal the results were inconsistent with the time course data and therefore, not easy to conclude. In addition to using an alternative IgG2b control antibody and more experimental replicates, further confirmation of JAM-1 neutralisation is still necessary. Both BV11 and BV12 share overlapping epitopes that are thought to be important in JAM-1's function. Binding of these antibodies to endogenous JAM-1 in the embryo should therefore inhibit JAM-1 protein interactions between neighbouring blastocycsts. The best method to confirm that JAM-1 is indeed interacting with it's specified epitope would therefore be to use a JAM-1 antibody raised to the same epitope but in another species. However, such antibodies were not available and therefore complete neutralisation of JAM-1 in these experiments could not be confirmed. Alternatively, directly labelling the neutralising antibody would have been a useful approach to monitor the interaction of the antibody within the embryo during the inhibition timecourse experiments.

Confirmation of JAM-1's importance to embryo development and its role in epithelial biogenesis was examined using an additional method of inhibition, RNA*i*. RNA*i* in preimplantation embryos had been used successfully to disrupt E-cadherin expression in mouse preimplantation embryos (Wiany & Zernicka-Goetz, 1999).

Indeed, the phenotype of these embryos was consistent with that seen in E-cadherin knockout mice (Larue *et al.*, 1994; Riethmacher *et al.*, 1995). Knockout mice can provide important information about the requirement of particular genes to embryo development and whether its role is critical in the survival of an organism or the particular function of a particular tissue type. However, the establishment of pure breeding lines of animals with the required mutation can be an incredibly lengthy process. The reported success of RNA*i* in phenocopying knockout mice indicated that this might be a good technique for our functional inhibition studies.

JAM-1 dsRNA was successfully synthesised and preliminary experiments were carried out while the microinjection technique was being established. Consistent with the neutralising antibody data, embryos were able to compact and cavitate and were not significantly different from buffer injected embryos. However, the precise timing of these events were not examined, as seen in the previous time course data, and therefore a delay in cavitation was not thoroughly examined. Indeed, the numbers of embryos required to be able to select a synchronised pool of compacting and cavitating embryos were too large in order to carry out similar timed analysis. Unfortunately, there was not enough time to continue the RNA*i* experiments but the dsRNA and microinjection technique is ready for someone else in the lab to continue this study. Confirmation that the dsRNA is specifically interfering with endogenous JAM-1 mRNA and its translation into protein still needs investigation. In order to do this, RT-PCR and immunofluorescence techniques need to be used on dsRNA injected, buffer injected and non-injected embryos.

RNA*i* experiments could have been improved if the dsRNA had been injected into the cell cytoplasm rather than the pronucleus of the mouse oocyte. Although swelling of the pronuclei was a useful indicator of a successful injection, adding a fluorescent dye to the injection solution would have been sufficient to confirm the dsRNA had been injected. Indeed, Wianny and Zernicka-Goetz (1999) successfully interfered with E-cadherin gene function in early mouse development after microinjection of dsRNA into the cell cytoplasm. Moreover, although mRNA is synthesized in the nucleus it appears that RNA*i* primarily occurs in the cell cytoplasm prior to translation of the mRNA after binding to RISC protein (reviewed

in Bernstein *et al.*, 2001). Although there have been some studies in plants indicating that dsRNA can also induce gene silencing at the transcriptional level this has yet to be seen in animals. Therefore, if RNA*i* experiments were to be continued the efficiency of this technique could be improved by microinjecting it into the cytoplasm of the oocyte.

Claudin-1 mRNA and protein expression patterns were also examined in the preimplantation embryo but with limited success. Claudin-1 mRNA was detected in embryos on four occasions but could not be repeated after this, despite its amplification in mature mouse tissue. It was presumed that either low abundance or poor stability of this transcript might have been the cause. A combination of immunolocalisation and Western blot experiments using the first commercially available claudin-1 antibody (71-7800) indicated that claudin-1 protein was present in the preimplantation embryo from the 16-cell stage onwards. Moreover, double labelling experiments demonstrated that this protein co-localised with ZO-1α^{+} in late morulae and early blastocysts. However, this antibody was later reported to also cross react with claudin-3 and therefore the protein data for claudin-1 may have been in part, if not all, due to the presence of claudin-3 in preimplantation embryos. Claudin-3 RT-PCR confirmed the presence of claudin-3 mRNA from 2-cell embryos up to and including late blastocysts.

Upon the availability of more specific claudin antibodies, individual expression patterns of claudin-1 and claudin-3 were examined. However, although weak cell-contact staining was visible on tangential confocal images, typical junctional localisation was only weakly stained in the midplane images. In fact, with both antibodies the predominant staining was localised to within the nucleus of each blastomere. Unfortunately, Western blotting of preimplantation embryos was not successful but this might have been resolved if there had been time to collect fresh embryo samples rather than strip an existing blot (previously used for staining another protein). Confirmation of the nuclear staining needs further investigation as other transmembrane TJ proteins have not been seen localised within the nucleus and neither claudin had any known nuclear localisation signal (NLS) within its protein

sequence. However, neither the fact that claudins are transmembrane proteins, nor the lack of an NLS, is reason enough to dismiss this expression as real.

The nuclear localisation of claudin, which was most predominant with the specific claudin-1 and claudin-3 antibodies indicated a possible regulatory role for claudins. Indeed, both ZO-1 and ZO-2 have been found localised within the nucleus and may play a role in signalling between TJs and the nucleus, with the potential to influence cell growth, proliferation and differentiation (Balda & Matter, 2000; Gonzalez-Mariscal *et al.,* 2000; Islas *et al.*, 2002). The validity of the nuclear localisation pattern found with the two claudin antibodies needs further investigation, as the peptide sequence to which these antibodies was raised was not divulged by Zymed. Western blotting with nuclear extracts may help to validate these results. Moreover, if this staining is in fact attributed to claudin localisation then double labelling experiments with proteins that are known to localise to specific nuclear domains may aid in understanding the relevance of these results. Indeed, the nuclear localisation patterns appear similar to that found for ZO-2, which was shown to partially colocalise with a splicing factor SC35. Could claudin also be localised in spliceosomes and is its nuclear localisation due to its binding with ZO-2?

Interestingly, two transcription factors have been found localised at the TJ, ZONAB and ASH (Balda & Matter, 2000; Nakamura *et al.*, 2000). Fistly, ZONAB (a repressor of Erb-2 promoter) binds to ZO-1 and is localised at the TJ in confluent epithelial cells (Balda & Matter, 2000). Secondly, ASH has been shown to co-localise with ZO-1 and cingulin both at the TJ and within the cell nucleoplasm (Nakamura *et al.*, 2000). The *Drosophila* homologue of ASH has been shown to restrict the pattern of expression of homeotic genes. The biological relevance of the nuclear localisation of TJ components and the detection of transcription factors at the TJ still needs to be elucidated. However, the presence of high molecular weight bands in Western blots for both claudin-1 and claudin-3 antibodies indicate that the antibodies bind to other unrelated proteins. In which case, the nuclear staining may actually correspond to an unrelated protein to either of the claudins. This seems to be the most likely explanation for the unusual staining as the nuclear staining with the claudin-1 antibody indicates that this protein and therefore its mRNA should be in

abundance. However, claudin-1 mRNA could not be reliably amplified from the preimplantation embryo.

As mentioned earlier, Claudin-1/-3 protein localisation patterns in the mouse preimplantation embryo, with 71-7800 Zymed antibody, were similar to that found for occludin. Although claudins and occludin do not show sequence homology with each other, their structural similaries and ability to bind to similar TJ cytoplasmic proteins indicate that they may have similar roles within the TJ complex. Overexpression of each of these proteins have shown that both occludin and claudins are capable of increasing the TER in epithelial cell lines, indicating that they are both important in the barrier function of an epithelium. It is therefore, not suprising that either claudin-1, claudin-3 or both have a similar expression pattern in the preimplantation embryo.

Synthetic peptides, corresponding to the extracellular domains of occludin, have been shown to disrupt the TJ permeability barrier (Wong & Gumbiner *et al.*, 1997; Lacaz-Vieira *et al.*, 1999; Vietor *et al.*, 2001). It was thought that, considering the structural similarities between claudins and occludin that this might have been a useful approach to functionally disrupt claudins in the embryo. Unfortunately, claudin-1 inhibition studies were not successful as the only soluble form of this peptide was found to be toxic to the embryo. The synthesis of more peptides would have been very timely and expensive and thus this approach was not pursued further.

As mentioned previously, RNA*i* was seen as a potentially useful technique for further functional studies. Indeed, claudin-1 dsRNA was successfully synthesised and preliminary experiments were carried out. However, while RNA*i* and microinjection methods were being improved, doubt over the abundance and therefore, the importance of claudin-1 to the mouse preimplantation embryo were raised. RNA*i* for claudin-1 was therefore not continued until its specific expression in the embryo could be confirmed. Indeed, claudin-1 mice have been shown to develop post-implantation and, in fact, make it to term. However, they died within 24hrs after birth (Furuse *et al.*, 2002). Moreover, with the growing number of claudins, it seems important that, prior to further functional studies, embryonic

expression of more claudin members is examined. Indeed, RNA*i* for a number of claudins, including claudin-3, could provide valuable insight into the role of these proteins in epithelial polarity and TJ biogenesis. Considering the abundance of claudin-3 in the early embryo it would have been more appropriate to focus on this protein for the functional inhibition studies. However, the point in the study that the claudin-3 was obtained left no time to pursue such experiments. As mentioned earlier, future RNA*i* techniques would also need to be modified to improve the efficiency of this technique.

This study has therefore, established further insight into the spacial and temporal expression of JAM-1 during mouse preimplantation development and epithelial biogenesis. Moreover, this data indicates that JAM-1 has a fairly unique role in the early stages of epithelial polarity. Unfortunately, data obtained for claudin-1 and claudin-3 was not clear but has indicated that their role in TJ biogenesis is, at least in part, similar to what we know for occludin. Since the discovery of occludin, major advances have been made in understanding the molecular architecture of the TJ. Furthermore, investigation into the interactions between these proteins and their temporal and spatial patterns during the reestablishment of an epithelium and during its *de novo* biogenesis, have exposed the complexity of this junction. Understanding these interactions in the mouse preimplantation embryo will not only provide valuable information about normal processes during epithelial differentiation but also equip us with a basis to understand the diseases associated with this tissue.

Appendix I

Media components

Solution B (per 10ml, osmolarity 444±20mOsm)

0.2106g	$NaHCO_3$

Solution E (per 50 ml, osmolarity 354±20mOsm)

2.98785g	HEPES (pH7.4)

Solution F (per 100ml, osmolarity 2552±20mOsm)

4.72g	NaCl
0.11g	KCl
0.06g	$NaH_2PO_4H_2O$
0.1g	$MgCl_2.6H_2O$
2.9ml	70% sodium lactate syrup
1.0g	D-glucose

Solution G (per 10ml, osmolarity 60±10mOsm)

0.03g	sodium pyruvate
0.06g	penicillin
0.05g	streptomyosin

Solution H (per 10ml, osmolarity 415±20mOsm)

0.26	$CaCl_2.2H_2O$

Phenol red stock solution

Dissolve 0.13g phenol red in 10ml isotonic stock $NaHCO_3$

0.9% Saline

36g NaCl in 4L of Milli-Q water

Streptomycin

2ml isotonic stock $NaHCO_3$ to original vial of 1g (100 x conc stock). Take 0.1ml and make up to 10ml with 0.9% NaCl. Aliquot and store at ¯20°C.

Phosphate Buffered Saline (per 100ml; PBS)

0.8	NaCl
0.02	KCL
0.115	Na_2HPO_4*
0.020	KH_2PO_4

*or

0.286	$Na_2HPO_4.12H_2O$

Table 1

Components of H6+BSA and T6+BSA media

H6 BSA	T6 BSA	Component
1ml	1ml	B
0.1ml	0.1ml	E
0.84ml	N/A	F
0.16ml	1ml	G
0.1ml	0.1ml	H
40mg	40mg	Bovine serum albumin (BSA)
60mg	60mg	Poly-vinyl pyrolidone (PVP)
60mg	40mg	20% NaCl
7.8ml	7.8ml	H_2O
	*Plus 1 drop of phenol red	

Nb/ Solutions are sterile filtered and stored at 4°C

Hyaluronidase

20ml	PBS
0.2g	PVP
20mg	hyaluronidase (Sigma type II)

nb/ store at –20 in 1ml aliquots

Acidic Tyrodes solution (per 100ml, pH 2.3)

0.8g	NaCl
0.02g	KCL
0.0265g	$CaCl_2.2H_2O$
0.01g	$MgCl_2.2H_2O$
0.1g	D-glucose
0.4g	PVP*
	*or
0.02g	$CaCl_2$

nb/ store at –20 in 1ml aliquots

Pregnant mares serum (PMS; Folligon)

vial (1000 i.u.) diluted in 20ml 0.9% saline solution. Sterile filtered and aliquoted in 4ml samples. Stored at ¯20°C

Human chorionic gonadotropin (hCG; Chorulon)

1 vial (1500 i.u.) diluted in 30% 0.9% saline solution. Sterile filtered and aliquoted in 4ml samples. Stored at ¯20°C.

SOB and SOC medium

For 100ml of SOB weight out:

2g Bacto-Tryptone
0.5g Yeast extract
0.05g NaCl

and dissolve in 90ml mQ-H_20

Add 1ml of 250mM KCl . Adjust to pH 7 with 1M NaOH (~0.1ml). Make up the final volume to 100ml and autoclave. Before use add 25µl MgCl per 5ml 2M $MgCl_2$.
*SOC medium is identical to SOB except for 20mM glucose. Make 1M glucose and ass 100µl for every 5ml of SOB.

Appendix II

Recipes

1.5M Tris (pH 8.8)

Dissolve 45.41g of Tris base into ~200ml water and correct pH with ~10ml concentrated HCL. Make upto 250ml

0.5M Tris (pH6.8)

Dissolve 15.14g of Tris base into ~200ml water and correct pH with ~10ml concentrated HCL and make upto 250ml

Table 1

Gel solutions for SDS PAGE

	Stacking gel	Resolving gel		
	4%	10%	12%	15%
H_20	8.95ml	6.02ml	5.02ml	3.52ml
1.5M Tris (pH8.8)	3.75ml	3.75ml	3.75ml	3.75ml
30%Acryl 0.8% Bis	2ml	5ml	6ml	7.5ml
10% SDS	0.15ml	0.15ml	0.15ml	0.15ml
10% APS	0.75ml	0.75ml	0.75ml	0.75ml
TEMED	0.75ml	0.75ml	0.75ml	0.75ml

Running buffer for PAGE (pH 8.3)

3g	Tris base
14.4g	Glycine
1g	SDS
1L	Water

Transfer buffer for Western blotting (per 2L)

6.05g	Tris base
28.83g	Glycine
2g	SDS
400ml	Methanol

Coomassie stain for protein gels

0.625g Coomassie blue

250ml (50%) Methanol

50ml (10%) Acetic acid

Strong coomassie destain for protein gels

400ml (40%) Methanol

100ml (10%) Acetic acid

500ml H_2O

Stripping buffer

62.5mM Tris-Cl

2% SDS

100mM β-mercaptoethanol

100mM IPTG

1.2g IPTG

50ml mQ- H_20

50mg/ml X-gal

50mg x-gal

1ml N,N'-dimethyl formamide

*Cover with foil and store at ¯20°C

LB/agar/Ampicilin

8g LB

6g agar

400ml mQ-H_20

*autoclave to dissolve, cool to 55°C and transfer the bottle to 55°C water bath until use. Pour 2 plates with Ampicillin. Then add 0.4ml Ampicillin (100mg/ml stock) to the remaining LB/agar, mix well and pour the rest onto more plates.

LB/agar/Ampicillin/IPTG/x-gal

100µl 100m IPTG

20µl 50mg/ml x-gal

*add to centre of LB/agar/Ampicillin plate 30 minutes prior to use. Spread with a glas rod and incubate the plate up-side down at 37°C for 30 minutes

LB/Ampicillin

8g LB

400ml mQ-H_20

*autoclave and allow to cool to r.t. Transfer 50ml of autoclaved LB to a Falcon tube and add 50µl of Ampicillin.

Appendix III

Sequence information

A

```
1      MANAGLQLLG FILASLGWIG SIVSTALPQW KIYSYAGDNI VTAQAIYEGL WMSCVSQSTG
61     QIQCKVFDSL LNLNSTLQAT RALMVIGILL GLIAIFVSTI GMKCMRCLED DEVQKMWMAV
121    IGGIIFLISG LATLVATAWY GNRIVQEFYD PLTPINARYE FGQALFTGWA AASLCLLGGV
211    LLSCSCPRKT TSYPTPRPYP KPTPSSGKDY V
```

B

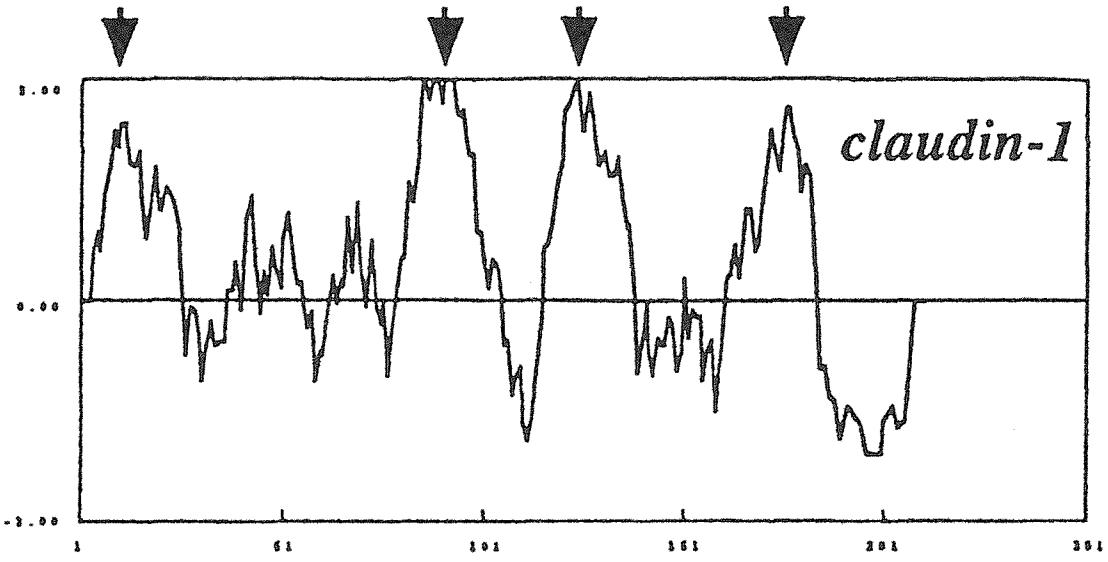

Amino acid sequence (A) and hydrophobicty plot (B) for claudin-1. Arrows depict the transmembane regions of the protein.

Cldn1-K15 peptide sequence

TALPQWKIYSYAGDNIVTAQAIYEGLWMSCVSQSTGQIQCKVFDSLLNLNST

Scrambled Cldn1-k15 peptide sequence

STSSLSYWSFQTWTVYQEQSIMCVDINKAGTVAQLPLNGYICGALDQAKNIL

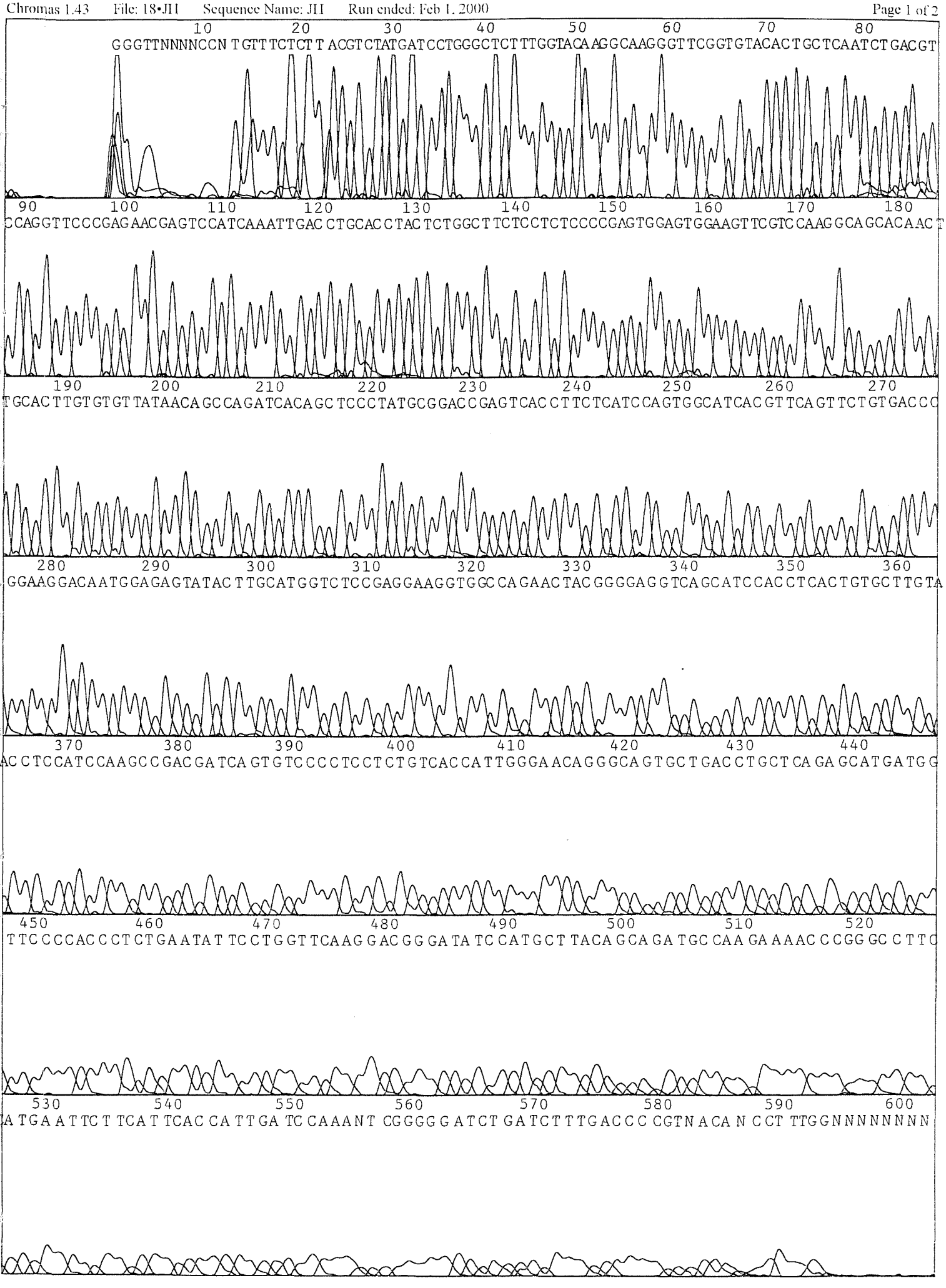
10 20 30 40 50 60 70 80
GGGTTNNNNCCN T GTT TCTCT T ACGTCTATGATCCTGGGCTCTTTGGTACAAGGCAAGGGTTCGGTGTACACTGCTCAATCTGACGT
90 100 110 120 130 140 150 160 170 180
CCAGGTTCCCGAGAACGAGTCCATCAAATTGAC CTGCACCTAC TCTGGCTTCTCCTCTCCCCGAGTGGAGTGGAAGTTCGTCCAAGGCAGCACAAC T
190 200 210 220 230 240 250 260 270
TGCACTTGTGTGTTATAACAGCCAGATCACAGCTCCCTATGCGGACCGAGTCACCTTCTCATCCAGTGGCATCACGTTCAGTTCTGTGACCC
280 290 300 310 320 330 340 350 360
GGAAGGACAATGGAGAGTATACTTGCATGGTCTCCGAGGAAGGTGGCCAGAACTACGGGGAGGTCAGCATCCACCTCACTGTGCTTGTA
370 380 390 400 410 420 430 440
ACCTCCATCCAAGCCGACGATCAGTGTCCCCTCCTCTGTCACCATTGGGAACAGGGCAGTGCTGACCTGCTCAGAGCATGATGG
450 460 470 480 490 500 510 520
TTCCCCACCCTCTGAATATTCCTGGTTCAAGGACGGGATATCCATGCTTACAGCAGATGCCAAGAAAACCCGGGCCTTC
530 540 550 560 570 580 590 600
CATGAATTCTTCATTCACCATTGATCCAAANT CGGGGGATCTGATCTTTGACCC CGTNACA N CCT TTGGNNNNNNNNN

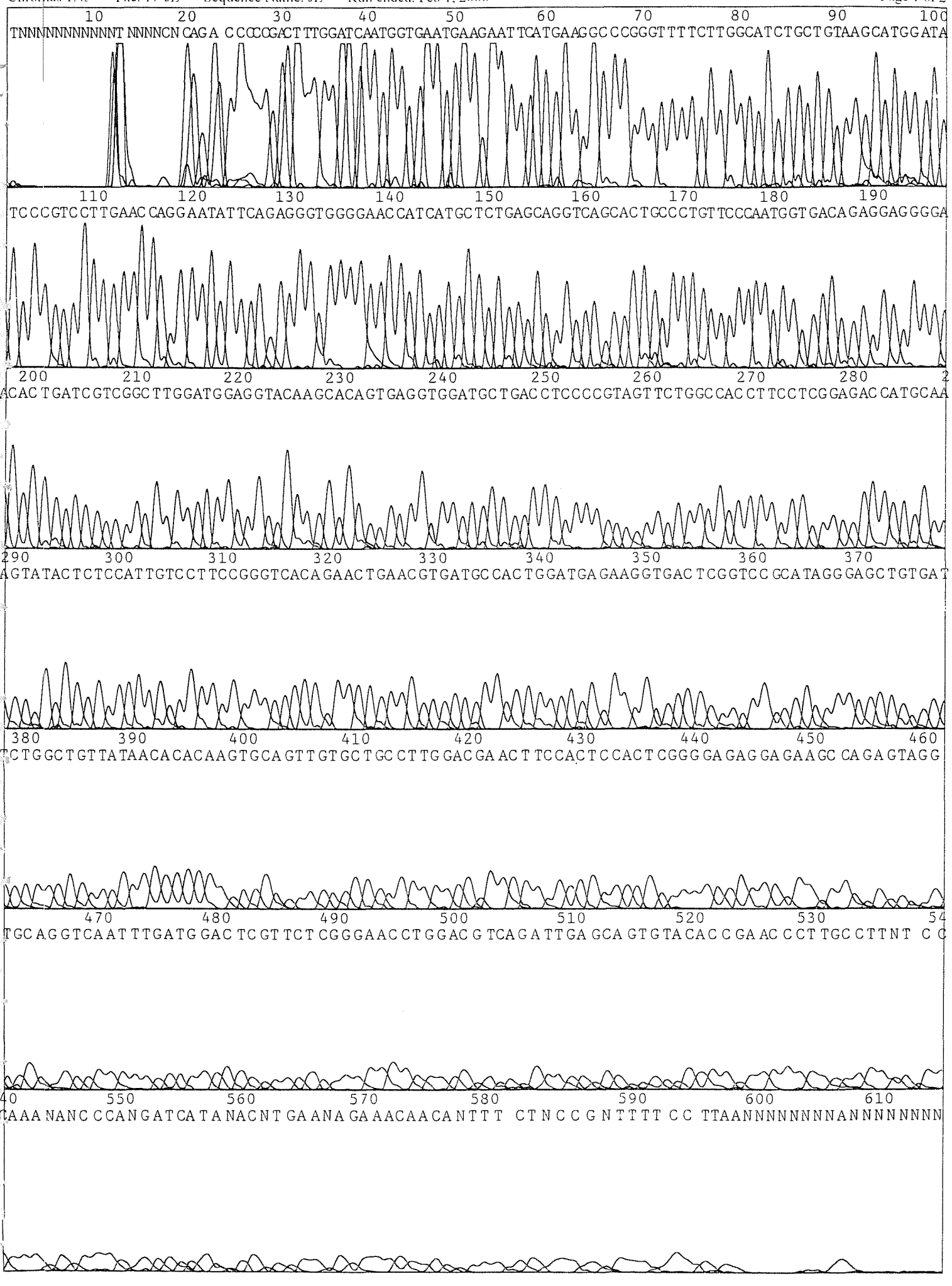
10 20 30 40 50 60 70 80 90 100
TNNNNNNNNNNNT NNNNCN CAGA C CCCCGACTTTGGATCAATGGTGAATGAAGAATTCATGAAGGCCCGGGTTTTCTTGGCATCTGCTGTAAGCATGGATA
110 120 130 140 150 160 170 180 190
TCCCGTCCTTGAACCAGGAATATTCAGAGGGTGGGGAACCATCATGCTCTGAGCAGGTCAGCACTGCCCTGTTCCCAATGGTGACAGAGGAGGGGA
200 210 220 230 240 250 260 270 280 2
ACACTGATCGTCGGCTTGGATGGAGGTACAAGCACAGTGAGGTGGATGCTGACCTCCCCGTAGTTCTGGCCACCTTCCTCGGAGACCATGCAA
290 300 310 320 330 340 350 360 370
AGTATACTCTCCATTGTCCTTCCGGGTCACAGAACTGAACGTGATGCCACTGGATGAGAAGGTGACTCGGTCCGCATAGGGAGCTGTGAT
380 390 400 410 420 430 440 450 460
TCTGGCTGTTATAACACACAAGTGCAGTTGTGCTGCCTTGGACGAACTTCCACTCCACTCGGGGAGAGGAGAAGCCAGAGTAGG
470 480 490 500 510 520 530 54
TGCAGGTCAATTTGATGGACTCGTTCTCGGGAACCTGGACGTCAGATTGAGCAGTGTACACCGAACCCTTGCCTTNT C C
40 550 560 570 580 590 600 610
CAAANANCCCANGATCATANACNTGAANAGAAACAACANTTT CTNCCGNTTTT CC TTAANNNNNNNNANNNNNNNN

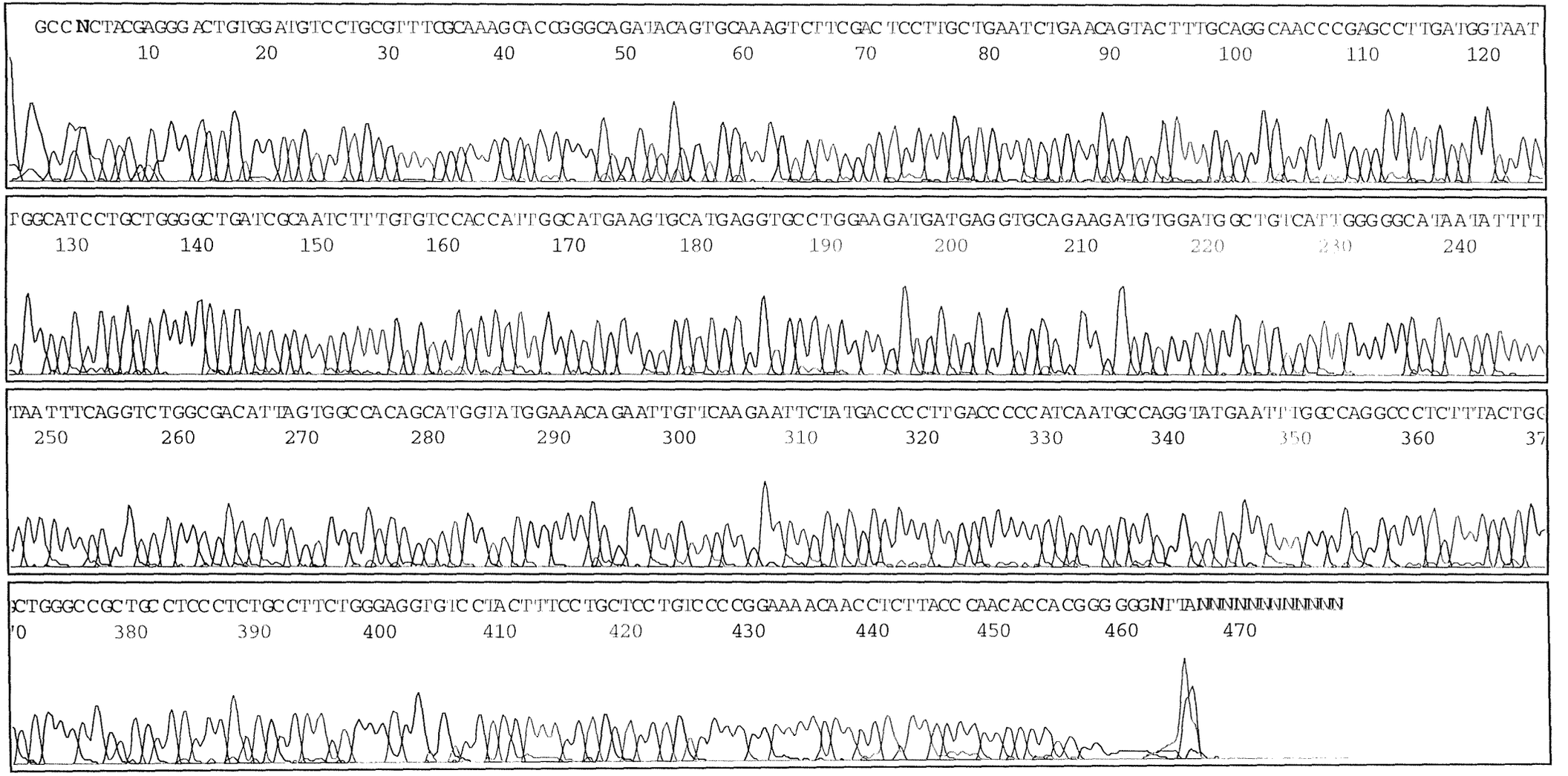
GCC NCTACGAGGG ACTGTGG ATGTCCTGCGTTTCGCAAAGCA CCGGGCAGATACAGTGCAAAGTCTTCGAC TCCTTGCTGAATCTGAACAGTACTTTGCAGG CAACCCGAGCCTTGATGGTAAT
10 20 30 40 50 60 70 80 90 100 110 120
TGGCATCCTGCTGGGGCTGATCGCAATCTTTGTGTCCACCATTGGCATGAAGTGCATGAGGTGCCTGGAAGATGATGAGGTGCAGAAGATGTGGATGGCTGTCATTGGGGGCATAATATTTT
130 140 150 160 170 180 190 200 210 220 230 240
TAATTTCAGGTCTGGCGACATTAGTGGCCACAGCATGGTATGGAAACAGAATTGTTCAAGAATTCTATGACCCCTTGACCCCCATCAATGCCAGGTATGAATTTGGCCAGGCCCTCTTTACTGC
250 260 270 280 290 300 310 320 330 340 350 360 37
CTGGGCCGCTGCCTCCCTCTGCCTTCTGGGAGGTGTCCTACTTTCCTGCTCCTGTCCCCGGAAAACAACCTCTTACC CAACACCACGGG GGGNTTANNNNNNNNNNNNN
0 380 390 400 410 420 430 440 450 460 470

ABI PRISM™

Model 377
Version 3.2
ABI100
Version 3.2

•02202*CLAUD-1C7613

02202*CLAUD-1C7613
Lane 40

Signal G:1790 A:1481 T:1080 C:1617
DT {BD Set Any-Primer}
newdye3-98
Points 1052 to 5758 Pk 1 Loc: 1052

Wed, Feb 3, 1999 10:00 am
Tue, Feb 2, 1999 4:06 pm
Spacing: 9.68{9.68}

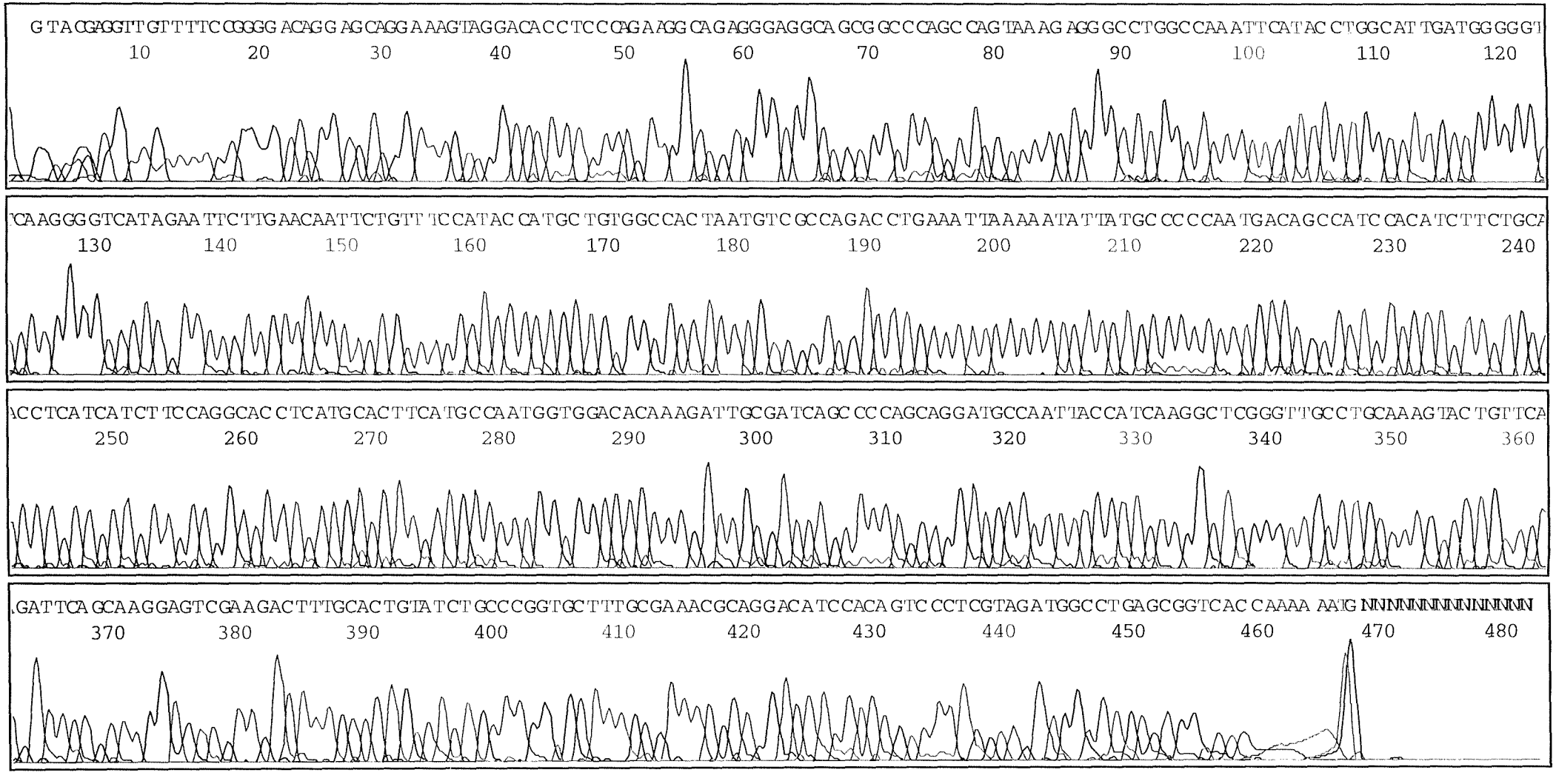

Appendix IV

Statistics

RNA*i* statistics for JAM-1

1-cell
UI vs TE

T value	NA
P value	NA
Degrees of Freedom	6

1-cell
UI vs JAM

T value	-1.0000000000
P value	0.3559176837
Degrees of Freedom	6

1-cell
TE vs JAM

T value	-1.0000000000
P value	0.3559176837
Degrees of Freedom	6

2-cell
UI vs TE

T value	-1.1628037995
P value	0.2890614838
Degrees of Freedom	6

2-cell
UI vs JAM

T value	-1.2472561409
P value	0.2587795761
Degrees of Freedom	6

2-cell
TE vs JAM

T value	-0.9674758904
P value	0.3706694286
Degrees of Freedom	6

FITC-dextran data for nascent blastocysts

BSA vs IgG2b

T value	-1.0293004709
P value	0.4115361076
Degrees of Freedom	2

BSA vs BV11

T value	1.1349906402
P value	0.3740885163
Degrees of Freedom	2

BSA vs BV12

T value	-1.2815364866
P value	0.3285077784
Degrees of Freedom	2

IgG2b vs BV11

T value	1.7143634650
P value	0.2285966168
Degrees of Freedom	2

IgG2b vs BV12

T value	-0.1118033989
P value	0.9211889594
Degrees of Freedom	2

FITC-dextan data for established blastocysts

BSA vs IgG2b

T value	3.9782646462
P value	0.0577643387
Degrees of Freedom	2

BSA vs BV11

T value	1.1627553483
P value	0.3649084406
Degrees of Freedom	2

BSA vs BV12

T value	3.5428614452
P value	0.0712585973
Degrees of Freedom	2

IgG2b vs BV11

T value	-1.0953557019
P value	0.3876588054
Degrees of Freedom	2

Established
IgG2b vs BV12

T value	-1.6232795497
P value	0.2460079994
Degrees of Freedom	2

FITC-dextan data for 2-hour blastocysts

BSA vs IgG2b

T value	0.87
P value	0.48
Degrees of Free	2.00

IgG2b vs BV11

T value	0.7499402176
P value	0.5315078630
Degrees of Freedom	2

IgG2b vs BV12

T value	2.0986887292
P value	0.1707115711
Degrees of Freedom	2

BSA vs BV11

T value	1.2052847063
P value	0.3513513514
Degrees of Freedom	2

BSA vs BV12

T value	2.4954011756
P value	0.1300006797
Degrees of Freedom	2

References

Aberle H, Schwartz H, Kemler R, 1996. Cadherin-catenin complex: protein interactions and their implications for cadherin function. *J Cell Biochem.* **61:**514-523.

Aghayan M, Rao L V, Smith R M, Jarett L, Charron M J, Thorens B and Heyner S, 1992. Developmental expression and cellular localisation of glucose transporter molecules during mouse preimplantation development. *Development* **115:**305-312.

Aghion J, Gueth-Hallonet C, Anthony C, Gros D and Maro B, 1994. Cell adhesion and gap junction formation in the early early embryo are induced prematurely by 6-DMAP in the absence of E-cadherin phosphorylation. *J.Cell.Sci.* **107:**1369-1379.

Alberts B, Bray D, Lewis J, Raff M, Roberts K and Watson JD, 1994. Molecular Biology of the cell. 3rd Edition, New York: Garland Publishing Inc.

Anderson J M and Van Itallie C M, 1995. Tight junctions and the molecular basis for regulation of the paracellular permeability. *The American Physiology Society.* **269:**G467-G475.

Anderson, J. M., B. R. Stevenson, L. A. Jesaitis, D. A. Goodenough, M. S. Mooseker. 1988. Characterization of ZO-1, a protein component of the tight junction from mouse liver and Madin-Darby canine kidney cells. *J Cell Biol.* 106: 1141-9.

Ando-Akatsuka Y, Saitou M, Hirase T, Kishi M, Sakakibara A, Itoh M, Yonemura S, Furuse M and Tsukita S, 1996. Interspecies diversity of the occludin sequence: cDNA cloning of human, mouse, dog and rat-kangaroo homologues. *J.Cell.Biol.* **133:**43-47.

Arrate, M. P., J. M. Rodriguez, T. M. Tran, T. A. Brock, S. A. Cunningham. 2001. Cloning of human junctional adhesion molecule 3 (JAM3) and its identification as the JAM2 counter-receptor. *J Biol Chem.* 276: 45826-32.

Bachavara R, De Leon V, Johnson A, Kapla G and Paynton B V, 1985. Changes in total RNA, Polyadenylated RNA , and actin mRNA during meiotic maturation of mouse oocytes. *Dev. Biol.* **109:**325-331.

Balda M S, Whitney J A, Flores C, Gonzalez S, Cereijido M and Matter K, 1996. Functional dissociation of paracellular permeability and transepithelial electrical resistance and disruption of the apical-basolateral intramembrane diffusion barrier by expression of a mutant tight junction membrane protein. *J.Cell.Biol.* **134:**1031-1049.

Balda M. S, and Anderson J.M, 1993. Two classes of tight junctions are revealed by ZO-1 isoforms. *Am. J. Physiol.* **264:** C918-C924.

Balda, M. S., K. Matter. 2000. The tight junction protein ZO-1 and an interacting transcription factor regulate ErbB-2 expression. *EMBO J.* 19: 2024-33.

Ballard S T, Hunter J H and Taylor A E, 1995. Regulation of tight junction permeability during nutrient absorption across the intestinal epithelium. *Ann.Rev.Nutr.* **15:**35-55

Barth AI, Nathke IS, Nelson WJ, 1997. Cadherins, catenins and APC protein: interplay between cytoskeletal complexes and signaling pathways. *Curr Opin Cell Biol.* **9:**683-690

Barth AI, Stewart DB, Nelson WJ, 1999. T cell factor-activated transcription is not sufficient to induce anchorage-independent growth of epithelial cells expressing mutant beta-catenin. *Proc Natl Acad Sci U S A* **96:**4947-4952.

Barton, E. S., J. C. Forrest, J. L. Connolly, J. D. Chappell, Y. Liu, F. J. Schnell, A. Nusrat, C. A. Parkos, T. S. Dermody. 2001. Junction adhesion molecule is a receptor for reovirus. *Cell.* 104: 441-51.

Batten B, Albertini, D and Ducibella T, 1987. Patterns of organelle distribution in mouse embryos during preimplantation development. *Amer.J.Anat.* **178:**204-213.

Bazzoni G, Martinez-Estrada O M, Orsenigo F, Cordenonsi M, Citi S and Dejana E, 2000a.Interaction of Junctioal Adhesion Molecule with the Tight Junction Components ZO-1, Cingulin and Occludin. *J.Biol.Chem.* **275:** 20520-20526.

Bazzoni G, Matinez-Estrada O M, Mueller F, Nelbroeck P, Schmid G, Bartfai T, Dejana E and Brockhaus M, 2000b. Homophilic interaction of Junctional Adhesion Moelcule. *J.Biol.Chem.* **274**:30970-30976

Beatch M, Jesaitis LA, Gallin WJ, Goodenough DA, Stevenson BR, 1996. The tight junction protein ZO-2 contains three PDZ (PSD-95/Discs-Large/ZO-1) domains and an alternatively spliced region. *J Biol Chem.* **271:**25723-25726.

Bensaude O, Babinet C Morange M and Jacob F, 1983. Heat shock proteins, first major products of zygotic gene activity in mouse embryo. *Nature* **305:**331-333.

Bernstein E, Denli AM and Hannon GJ, 2001. The rest is silence. *RNA* **7:**1509-1521.

Bernstein, E., A. A. Caudy, S. M. Hammond, G. J. Hannon. 2001. Role for a bidentate ribonuclease in the initiation step of RNA interference. *Nature*. 409: 363-6.

Berridge, M. J. 1993. Inositol trisphosphate and calcium signalling. *Nature*. 361: 315-25.

Bierkamp C, Mclaughlin KJ, Schwarz H, Huber O and Kemler R, 1996. Embryonic heart and skin defects in mice lacking plakoglobin. D*ev Biol* **180:**780-785.

Billy, E., V. Brondani, H. Zhang, U. Muller, W. Filipowicz. 2001. Specific interference with gene expression induced by long, double- stranded RNA in mouse embryonal teratocarcinoma cell lines. *Proc Natl Acad Sci U S A*. 98: 14428-33.

Blaschuk O W, Sullivan R, David S and Pouliot Y, 1990. Identification of a cadherin cell adhesion recognition sequence. *Dev.Biol* **139:**227-229.

Bogen S, Pak J, Garifallou, M, Deng X and Muller W A, 1994. Monoclonal antibody to murine PECAM-1 (CD31) blocks acute inflammation *in vivo*. *J.Exp.Medl* **179:**1059-1064.

Bouniol C, nguyen E and Debey P, 1995. Endogenous transciption occurs at the 1-cell stage in the mouse embryo. A human endothelial cell-restricted, externally disposed plasmalemal protein enriched in intercellular migration of leukocytes. *J.Exp.Med.* **170:**399-414.

Bowerman, B., C. A. Shelton. 1999. Cell polarity in the early Caenorhabditis elegans embryo. *Curr Opin Genet Dev.* 9: 390-5.

Braga, V. M., A. Del Maschio, L. Machesky, E. Dejana. 1999. Regulation of cadherin function by Rho and Rac: modulation by junction maturation and cellular context. *Mol Biol Cell.* 10: 9-22.

Braude P, Pelham H, Flach G and Lobatto R, 1979. Post-transcriptional control in the early mouse embryo. *Nature* **282:**102-105.

Briehl M.M, and Miesfeld, R.L, 1991. Isolation and characterisation of transcripts induced by androgen withdrawal and apoptotic cell death in the rat ventral prostate. *Mol. Endocrinol.* **5:**1381-1388.

Brison D R, Hewitson L C and Leese H J, 1993. Glucose, pyruvate, lactate concentrations in the blastocoel cavity of rat and mouse embryos. *Molec. Reprod.Dev.* **35:**227-232.

Butz s, Stappert J, Weissing H and Kemler R, 1992. Plakoglobin and β-catenin: distinct but closely related. *Science* **257:**1142-1144.

Cadigan, K. M., R. Nusse. 1997. Wnt signaling: a common theme in animal development. *Genes Dev.* 11: 3286-305.

Carroll, J. 2001. The initiation and regulation of Ca2+ signalling at fertilization in mammals. *Semin Cell Dev Biol.* 12: 37-43.

Cereijido M, Meza I and Martinez-Palomo A, 1981. Occluding junctions in cultured epithelial monolayers. *J.Am.Phys.* **240:**C96-C102.

Cereijido M, Ponce A and Gonzalez-Mariscal L, 1989.Tight junctions and apical/basolateral polarity. *J.Memb.Biol.* **110:**1-9.

Chavrier P, Goud B, 1999. The role of ARF and Rab GTPases in membrane transport. *Curr Opin Cell Biol.* **11:**466-75.

Chen Y, Merzdorf C, Paul D and Goodenough D A, 1997. COOH terminus of occludin is required for the tight junction barrier function in early *Xenopus* embryos. *J.Cell.Biol.* **4:**891-899.

Citi S, Sabanay H, Jakes R, Geiger B and Kendrick-Jones J, 1988. Cingulin, a new peripheral component of tight junctions. *Nature.* **333:**272-275.

Citi S, Sabanay H, Kendrick-Jones J and Geiger B, (1989). Cingulin: characterisation and localisation. *J.Cell. Sci.* **93**, 107-122.

Citi S, 1992.Protein kinase inhibitors prevent junction dissociation induced by low extracellular calcium in MDCK epithelial cells. *J.Cell. Biol.* **117:**169-178.

Claude P, 1978. Morphological factors influencing transepithelial permeability: A model for the resistance of the zonula occludens. *J.Memb.Biol.* **39:**219-232.

Clayton L, Stinchcombe S V and Johnson M H, 1993. Cell surface expression localisation and stability of uvomorulin during early mouse development. *Zygote* **1:**333-334.

Clayton L, McConnell JM and Johnson MH, 1995. Control of the surface of uvomorulin after activation of mouse oocytes. *Zygote* **3:**177-189.

Clayton L, Hall A and Johnson M H, 1999. A role for rho-like GTPases in the polarisation of mouse eight–cell blastomeres. *Dev.Biol* **205:**322-331

Coein P, Kapprell H, Franke W, Tamkun J and Hynes O, 1986. Plakoglobin: a protein common to different kinds of intercellular adhering junctions. *Cell* **46:**1063-1073.

Collins and Fleming 1995. Epithelial differentiation in the mouse preimplantation embryo: making adhesive cell contacts for the first time. *TIBS* **20:**307-312.

Collins J E, Lorimer J E, Garrod D R, Pidsley S, Buxton R and Fleming T P, 1995. Regulation of desmocollin transcription in mouse preimplantation embryos. *Development* **121:**743-753.

Collins JR, Rizzolo LJ, 1998. Protein-binding domains of the tight junction protein, ZO-2, are highly conserved between avian and mammalian species. *Biochem Biophys Res Commun.* **252:**617-622.

Collins, J. H., J. Leszyk. 1987. The "gamma subunit" of Na,K-ATPase: a small, amphiphilic protein with a unique amino acid sequence. *Biochemistry.* 26: 8665-8.

Cordenonsi N, Mazzon E, De Rigo L, Baraldo S, Meggio F and Citi S, 1997. Occludin dephosphorylation in early development of *Xenopus laevis*. *J.Cell.Biol.* **110:**3131-3139.

Cruz, Y. P., R. A. Pedersen. 1985. Cell fate in the polar trophectoderm of mouse blastocysts as studied by microinjection of cell lineage tracers. *Dev Biol.* 112: 73-83.

Cunningham S A, Arrate M P, Rodriguez J M, Bjercke R J, Vanderslice P, Morris A P and Brock T A, 2000. A novel protein with homology to the junctional Adhesion Molecule: Characterisation of Leukocyte Interactions. *J.Biol.Chem.* **275:**34750-34756.

Cuthbertson, K. S., P. H. Cobbold. 1985. Phorbol ester and sperm activate mouse oocytes by inducing sustained oscillations in cell $Ca2^{+}$. *Nature.* 316: 541-2.

D'atri F and Citi S, 2002. Molecular complexity of vertebrate tight junctions. *Mol Mem Biol.* **9:**103-112

Daniel JM, Reynolds AB, 1995. The tyrosine kinase substrate p120cas binds directly to E-cadherin but not to the adenomatous polyposis coli protein or alpha-catenin. *Mol Cell Biol.* **15:**4819-4824.

De Almeida J E, Holtzman E J, Peters P, Ercolani L, Ausiello D A and Stow J L, 1994.Targeting of chimeric $G\alpha_I$ proteins to specific membrane domains. *J.Cell. Sci.* **107:**507-515.

De Sousa P A, Watson A J, Schulltz G A, and Bilodeau-Goeseels S, 1998. Oogenetic and zygotic gene expression directing early bovine embryogenesis: A review. *Molec Repro and Dev.* **51:**112-121.

Del Maschio, A., A. De Luigi, I. Martin-Padura, M. Brockhaus, T. Bartfai, P. Fruscella, L. Adorini, G. Martino, R. Furlan, M. G. De Simoni, E. Dejana. 1999. Leukocyte recruitment in the cerebrospinal fluid of mice with experimental meningitis is inhibited by an antibody to junctional adhesion molecule (JAM). *J Exp Med.* 190: 1351-6.

Deng, M. Q., S. S. Shen. 2000. A specific inhibitor of p34(cdc2)/cyclin B suppresses fertilization- induced calcium oscillations in mouse eggs. *Biol Reprod.* 62: 873-8.

Denker B M, Saha C, Khawaja S, and Nigam S K, 1996. Involvement of a heteromeric G protein α subunit in tight junction biogenesis. *J.Biol.Chem.* **217:**25750-25753.

Diamond J, 1977. The epithelial bridge, gate and fence. *Physiologist **20:***10-18.

DiZio S M and Tasca R J, 1977. Sodium-dependent amino acid transport in preimplantation embryos III. Na^+, K^+-ATPase linked mechanism in blastocysts. *Dev.Biol.* **59:**198-205.

Dobrosotskaya, I., R. K. Guy, G. L. James. 1997. MAGI-1, a membrane-associated guanylate kinase with a unique arrangement of protein-protein interaction domains. *J Biol Chem.* 272: 31589-97.

Dobrosotskaya, I. Y., G. L. James. 2000. MAGI-1 interacts with beta-catenin and is associated with cell-cell adhesion structures. *Biochem Biophys Res Commun.* 270: 903-9.

Dodane, V., B. Kachar. 1996. Identification of isoforms of G proteins and PKC that colocalize with tight junctions. *J Membr Biol.* 149: 199-209.

Drenckhahn, D., R. Dermietzel. 1988. Organization of the actin filament cytoskeleton in the intestinal brush border: a quantitative and qualitative immunoelectron microscope study. *J Cell Biol.* 107: 1037-48.

Ducibella T and Anderson E, 1975. Cell shape and membrane changes in the 8-cell mouse embryo:prerequisites for morphogenesis of the blastocyst. *Dev.biol* **47:** 45-58.

Dyce, J., M. George, H. Goodall, T. P. Fleming. 1987. Do trophectoderm and inner cell mass cells in the mouse blastocyst maintain discrete lineages? *Development.* 100: 685-98.

Ebnet K, Schultz C U, Meyer zu Brickwedde M K, Pendi G G and Vestweber D, 2000. Junctional Adhesion Molecule Interacts with the PDZ Domain-containing Proteins AF-6 and ZO-1. *J.Biol.Chem.* **275:**27979-27988.

Ebnet, K., A. Suzuki, Y. Horikoshi, T. Hirose, M. K. Meyer Zu Brickwedde, S. Ohno, D. Vestweber. 2001. The cell polarity protein ASIP/PAR-3 directly associates with junctional adhesion molecule (JAM). Embo J. 20: 3738-48.

Eckert, J., H. Niemann. 1998. mRNA expression of leukaemia inhibitory factor (LIF) and its receptor subunits glycoprotein 130 and LIF-receptor-beta in bovine embryos derived in vitro or in vivo. Mol Hum Reprod. 4: 957-65.

Elbashir, S. M., W. Lendeckel, T. Tuschl. 2001. RNA interference is mediated by 21- and 22-nucleotide RNAs. Genes Dev. 15: 188-200.

Fagotto, F., U. Gluck, B. M. Gumbiner. 1998. Nuclear localization signal-independent and importin/karyopherin- independent nuclear import of beta-catenin. Curr Biol. 8: 181-90.

Fanning A S, Jameson B J, Jesaitis L A and Anderson J M, 1998. The tight junction protein ZO-1 establishes a link between the transmembrane protein occludin and the actin cytoskeleton. *J.Biol.Chem* **273:**29745-29720

Fissore, R. A., F. J. Longo, E. Anderson, J. B. Parys, T. Ducibella. 1999. Differential distribution of inositol trisphosphate receptor isoforms in mouse oocytes. Biol Reprod. 60: 49-57.

Flach G, Johnson M H, Braude P R, Taylor R A S and Bolton V N, 1982. The transition from maternal to embryonic control in the 2-cell mouse embryo. *EMBO* **1:**681-686.

Fleming T P and Pickering S J, 1985. Maturation and polarisation of the endocytic system in outside blastomeres during mouse preimplantation development. *J.Embryol.exp.Morph.* **89:**175-208

Fleming T P, Cannon P M and Pickering S J, 1986. The cytoskelton, endocytosis and cell polarity in the mouse preimplantation embryo. *Dev.Biol* **113:**406-419.

Fleming T P and Goodall H, 1986. Endocytic traffic in trophectoderm and polarised blastomeres of the mouse preimplantation embryo. *Anat.Rec.***216:**490-503.

Fleming T P and Johnson M H, 1988. From egg to epithelium. *Ann.Rev.Biol.* **4:**459-485.

Fleming T P, MC Connell J, Johnson M H and Stevenson B R, 1989. Development of tight junctions *de novo* in mouse early embryo: control of assembly of the tight junction-specific protein, ZO-1. *J.Cell.Biol.* **108:**1407-1418.

Fleming T P and Hay M H, 1991.Tissue specific control of expression of the tight junction polypeptide ZO-1 in the mouse early embryo. *Development* **113:**295-304.

Fleming T P, Hay M J, Javed Q and Citi S, 1993. Localisation of tight junction protein cingulin is temporally and spacially regulated during early mouse development. *Development* **117:**1135-1144.

Fleming T P, Butler E, Collins J, Sheth B and Wild A E, 1998. Cell polarity and mouse early development. *Advances in Molecular and Cell Biology.* **26:**67-94.

Fleming T.P, Pappenbrock T, Fesenko I, Hausen P and Sheth B, 2000. Assembly of tight junctions during early vertebrate development. *Cell Dev Biol.* **11:**291-9.

Fleming, T. P., B. Sheth, I. Fesenko. 2001. Cell adhesion in the preimplantation mammalian embryo and its role in trophectoderm differentiation and blastocyst morphogenesis. Front Biosci. 6: D1000-7.

Furuse M, Hirase T, Itoh M, Nagafuchi A, Yonemura S, Tsukita S and Tsukita S, 1993. Occludin: A novel integral membrane protein localising at tight junctions. *J.Cell.Biol.* **123:**1777-1788.

Furuse M, Itoh M, Hirase T, Nagafuchi A, Yonemura S, Tsukita Sa and Tsukita Sh, 1994. Direct association of occludin with ZO-1 and its possible involvement in the localisation of occludin at tight junctions. *J.Cell.Biol.* **127:**1617-1626.

Furuse M, Fujimoto K, Sato N, Hirase T, Tsukita Sa, and Tsukita Sh, 1996. Overexpression of occludin, a tight junction-associated integral membrane protein, induces the formation of intracellular multilamellar bodies bearing tight-junction like structures. *J.Cell.Sci.* **109:**429-435.

Furuse M, Fujita K, Hiiragi T, Fujimoto K and Tsukita Sh, 1998a. Claudin- 1 and –2:Novel integral membrane proteins localising at tight junctions with no sequence similarity to occludin. *J.Cell.Biol.* **141:**1539-1550.

Furuse M, Sasaki H, Fujimoto K and Tsukita Sh, 1998b. A single gene product, Claudin-1 or –2, reconstitutes tight junction strands and recruits occludin in fibroblasts. *J.Cell.Biol.* **143:**391-401.

Furuse M, Sasaki H and Tsukita, 1999. Manner of interaction of heterogeneous claudin species within and between tight junction strands. *J.Cell.Biol.* **147:**891-903.

Furuse, M., M. Hata, K. Furuse, Y. Yoshida, A. Haratake, Y. Sugitani, T. Noda, A. Kubo, S. Tsukita. 2002. Claudin-based tight junctions are crucial for the

mammalian epidermal barrier: a lesson from claudin-1-deficient mice. *J Cell Biol.* 156: 1099-111.

Gao, L., G. Joberty, I. G. Macara. 2002. Assembly of epithelial tight junctions is negatively regulated by Par6. *Curr Biol.* 12: 221-5.

Gardiner C S, Williams J S and Menino A R, 1990. Sodium/Potassium adenosine triphosphatase α- and β- subunit and α-subunit mRNA levels during mouse embryo development *in vitro Biol.Reprod.* **43:**788-794.

Garrod D R and Collins J E, 1992. Chapter 1 in "Epithelial organisation and development" edited by Fleming T P. Chapman and Hall, London.

Geering, K. 1991. The functional role of the beta-subunit in the maturation and intracellular transport of Na,K-ATPase. *FEBS Lett.* 285: 189-93.

Geiger, B. 1979. A 130K protein from chicken gizzard: its localization at the termini of microfilament bundles in cultured chicken cells. *Cell.* 18: 193-205.

Gonzalez-Mariscal L, Chavez De Ramirez B and Cereijido M, 1985. Tight junction formation I cultured epithelial cells (MDCK). *J.Menb.Biol.* **86:**113-125.

Gottardi, C. J., M. Arpin, A. S. Fanning, D. Louvard. 1996. The junction-associated protein, zonula occludens-1, localizes to the nucleus before the maturation and during the remodeling of cell-cell contacts. *Proc Natl Acad Sci U S A.* 93: 10779-84.

Gow A, Southwood CM, Li JS, Pariali M, Riordan GP, Brodie SE, Danias J, Bronstein JM, Kachar B, Lazzarini RA, 1999. CNS myelin and sertoli cell tight junction strands are absent in Osp/claudin-11 null mice. *Cell.* **99:**649-59.

Gumbiner B & Simons K, 1986. A functional assay for proteins involved in establishing an epithelial occluding barrier: Identification of a uvomorulin-like polypeptide. *J.Cell.Biol.* **102:**457-468.

Gumbiner B,Syevenson B and Grimaldi A, 1988. The role of the cell adhesion molecule Uvomorulin in the formation and maintenance of the epithelial junction complex. *J.Cell.Biol.* **107:**1575-1587.

Gumbiner B, Lowenkopf T and Apatira D, 1991. Identification of 160kDa polypeptide that binds to the tight junction protein ZO-1. *Proc.Natl.Acad.Sci.* USA **88:**345-57.

Gumbiner B, 1993. Breaking through he tight junction barrier. *J.Cell.Biol.* **123:**1631-1633.

Guth-Hallonet C and Maro B, 1992.Cell polarity and cell diversification during early mouse embryogenesis. *Trends.Genet.* **8:**274-279.

Haegel H, Larue L, Ohsugi M, Fedorou L, Herrenknecht K and Kemler R, 1995. Lack of β-catenin affects mouse development at gastrulation. *Dev.* **121:**3529-3537.

Hall, A. 1998. Rho GTPases and the actin cytoskeleton. *Science.* 279: 509-14.

Hamazaki, Y., M. Itoh, H. Sasaki, M. Furuse, S. Tsukita. 2002. Multi-PDZ domain protein 1 (MUPP1) is concentrated at tight junctions through its possible interaction with claudin-1 and junctional adhesion molecule. *J Biol Chem.* 277: 455-61.

Hamilton, A. J., D. C. Baulcombe. 1999. A species of small antisense RNA in posttranscriptional gene silencing in plants. *Science.* 286: 950-2.

Hammond, S. M., S. Boettcher, A. A. Caudy, R. Kobayashi, G. J. Hannon. 2001. Argonaute2, a link between genetic and biochemical analyses of RNAi. *Science*. 293: 1146-50.

Hancock JF, Cadwallader K, Paterson H, Marshall CJ, 1991. A CAAX or a CAAL motif and a second signal are sufficient for plasma membrane targeting of ras proteins. *EMBO J.***10:**4033-4039.

Haskins J, Gu L, Wittchen S, Hibbard J and Stevenson B R, 1998. ZO-3, a novel member of the MAGUK protein family found at the tight junction, interacts with ZO-1 and occludin. *J.Cell.Biol.* **141:**199-208.

Hazan, R B and Norton, L , 1998. The epidermal growth factor receptor modulates the interaction of E-cadherin with the actin cytoskeleton. *J.Biol.Chem.* **273:**9078-9084.

Heasman J, Crawford A, Goldstone K, Garner-Hamrick P, Gumbiner B, McCrea P, Kintner C, Noro CY, Wylie C, 1994. Overexpression of cadherins and underexpression of beta-catenin inhibit dorsal mesoderm induction in early Xenopus embryos. *Cell.* **79:**791-803.

Herrera, V. L., J. R. Emanuel, N. Ruiz-Opazo, R. Levenson, B. Nadal-Ginard. 1987. Three differentially expressed Na,K-ATPase alpha subunit isoforms: structural and functional implications. *J Cell Biol.* 105: 1855-65.

Hewitson L C and Leese H J, 1993. Energy metabolism of the trophectoderm and inner cell mass of the mouse late blastocyst. *J.Exp.Zool.* **267:**337-343.

Heyner, S., R. M. Smith, G. A. Schultz. 1989. Temporally regulated expression of insulin and insulin-like growth factors and their receptors in early mammalian development. *Bioessays.* 11: 171-6.

Hirano S, Nose A, Hatta K, Kawakami A, Takeichi M, 1987. Calcium-dependent cell-cell adhesion molecules (cadherins): subclass specificities and possible involvement of actin bundles. *J Cell Biol.* **105:**2501-2510.

Hirano S, Kimoto N, Shimoyama Y, Hirohashi S, Takeichi M, 1992. Identification of a neural alpha-catenin as a key regulator of cadherin function and multicellular organization. *Cell.* **70:**293-301.

Hogan B, Beddington R, Costantini F and Lacy E, 1994. Manipulating the mouse embryo. A laboratory manual, 2nd ed. Cold Spring Harbour Lab Press.

Hoschuetzky H, Aberle H, Kemler R, 1994. Beta-catenin mediates the interaction of the cadherin-catenin complex with epidermal growth factor receptor. *J Cell Biol.* **127:**1375-1380.

Howarth A G, Singer K L and Steveson B R, 1994.Analysis of the distribution and phosporylation state f ZO-1 in MDCK and non-epithelial cells.*J.Membr.Biol.* **137:**261-502.

Howlett S K, 1986. A set of proteins showing cell cycle dependent modification in the early mouse embryo. *Cell* **45:**387-396.

Hyafil , 1981. Cell-Cell interactions in early embryogenesis: A molecular approach to the role of calcium. *Cell* **26:**447-454.

Ide, N., Y. Hata, H. Nishioka, K. Hirao, I. Yao, M. Deguchi, A. Mizoguchi, H. Nishimori, T. Tokino, Y. Nakamura, Y. Takai. 1999. Localization of membrane-associated guanylate kinase (MAGI)-1/BAI- associated protein (BAP) 1 at tight junctions of epithelial cells. *Oncogene.* 18: 7810-5.

Inai T, Kobayashi J, Shibata Y, 1999. Claudin-1 contributes to the epithelial barrier function in MDCK cells. *Eur.J.Cell.Biol* **78:**849-855.

Islas S, Vega J, Pnce L and Gonzalez-Mariscal, 2002. Nuclear localisation of the tight junction protein ZO-2 in epithelial cells. *Exp.cell.Res.* **274:**138-148.

Itoh M, Furuse M, Morita K, Kubota K, Saitou M, Tsukita S, 1999. Direct binding of three tight junction-associated MAGUKs, ZO-1, ZO-2, and ZO-3, with the COOH termini of claudins. *J Cell Biol.* **147:**1351-63.

Itoh M, Nagafuchi A, Moroi S and Tsukita S, 1997. Involvement of ZO-1 in cadherin-based cell adhesion through its direct binding to α catenin and actin filaments. *J.Cell.Biol.* **138:**181-192.

Itoh, M., K. Morita, S. Tsukita. 1999. Characterization of ZO-2 as a MAGUK family member associated with tight as well as adherens junctions with a binding affinity to occludin and alpha catenin. *J Biol Chem.* 274: 5981-6.

Itoh, M., M. Furuse, K. Morita, K. Kubota, M. Saitou, S. Tsukita. 1999. Direct binding of three tight junction-associated MAGUKs, ZO-1, ZO-2, and ZO-3, with the COOH termini of claudins. *J Cell Biol.* 147: 1351-63.

Itoh, M., H. Sasaki, M. Furuse, H. Ozaki, T. Kita, S. Tsukita. 2001. Junctional adhesion molecule (JAM) binds to PAR-3: a possible mechanism for the recruitment of PAR-3 to tight junctions. *J Cell Biol.* 154: 491-7.

Izumi, Y., T. Hirose, Y. Tamai, S. Hirai, Y. Nagashima, T. Fujimoto, Y. Tabuse, K. J. Kemphues, S. Ohno. 1998. An atypical PKC directly associates and colocalizes at the epithelial tight junction with ASIP, a mammalian homologue of Caenorhabditis elegans polarity protein PAR-3. *J Cell Biol.* 143: 95-106.

Jaffe, L. F. 1983. Sources of calcium in egg activation: a review and hypothesis. *Dev Biol.* 99: 265-76.

Javed, Q., T. P. Fleming, M. Hay, S. Citi. 1993. Tight junction protein cingulin is expressed by maternal and embryonic genomes during early mouse development. *Development*. 117: 1145-51.

Joberty G, Tavitian A, Zahraoui A, 1993. Isoprenylation of Rab proteins possessing a C-terminal CaaX motif. *FEBS Lett.***330:**323-8.

Joberty, G., C. Petersen, L. Gao, I. G. Macara. 2000. The cell-polarity protein Par6 links Par3 and atypical protein kinase C to Cdc42. *Nat Cell Biol.* 2: 531-9.

Johansson A, Driessens M and Aspenstrom P, 2000. The mammalian homologue of Caenorhabditis elegans polarity protein in Par-6 links Par-3 partner to Rho GTPases Cdc42 and Rac1. *J. Cell Sci.* **113:**531-539.

Johnson M H and Ziomek C A, 1981. The foundation of two distinct cell lineages within the mouse morula. *Cell.* **24:**71-80.

Johnson M H, Maro B and Takeichi M, 1986. The role of adhesion in the synchronisation and orientation of polarisation in 8-cell blastomeres. *J.Embryol.morph.* **93:**239-255.

Jones, D. H., T. C. Davies, G. M. Kidder. 1997. Embryonic expression of the putative gamma subunit of the sodium pump is required for acquisition of fluid transport capacity during mouse blastocyst development. *J Cell Biol.* 139: 1545-52.

Kadowaki T, Shiozaki H, Inoue M, Tamura S, Oka H, Doki Y, Iihara K, Matsui S, Iwazawa T and Nagafuchi A, 1994. E-cadherin and alpha-catenin expression in human esophageal cancer. *Cancer Res.* **54:**291-296.

Katahira J, Sugiyama H, Inoue N, Horiguchi Y and Sugimoto N, 1997. *Clostridium perfringens enterotoxin* utilises two structurally related membrane proteins as functional receptors *in vivo*. *J.Biol.Chem.* **272:**26652-26658.

Keon B H, Schafer S, Kuhn C, Grund C and Franke W, 1996. Symplekin, a novel type of tight junction plaque protein. *J.Cell.Biol.* **134:**1003-1018.

Kidder G M and McLachlin J R, 1985. Timing of transcription and protein synthesis underlying morphogenesis in preimplantation mouse embryos. *Dev.Biol.***112:**265-275

Kiuchi-Saishin, Y., S. Gotoh, M. Furuse, A. Takasuga, Y. Tano, S. Tsukita. 2002. Differential expression patterns of claudins, tight junction membrane proteins, in mouse nephron segments. *J Am Soc Nephrol.* 13: 875-86.

Kline, D., J. T. Kline. 1992. Repetitive calcium transients and the role of calcium in exocytosis and cell cycle activation in the mouse egg. *Dev Biol.* 149: 80-9.

Knudsen KA, Wheelock MJ, 1992. Plakoglobin, or an 83-kD homologue distinct from beta-catenin, interacts with E-cadherin and N-cadherin. *J Cell Biol.* **118:**671-9.

Kurihara H, Anderson JM, Farquhar MG, 1992. Diversity among tight junctions in rat kidney: glomerular slit diaphragms and endothelial junctions express only one isoform of the tight junction protein ZO-1. *Proc Natl Acad Sci U S A.* **89:**7075-7059.

Kuriyama M, Harada N, Kurooda S, Yamamoto T, Nakafuku M, Iwamatsu A, Yamamoto D, Prasad R, Croce C, Canaani E and Kaibuchi K, 1996. Identification of AF-6 and canoe as putative targets for Ras. *J.Biol.Chem.***271:**207-210.

Lacaz-Vieira, F., A. P. Filho. 1999. An automatic temperature-control system for solutions in free flow. *Pflugers Arch.* 437: 285-8.

Lacaz-Vieira, F., M. M. Jaeger, P. Farshori, B. Kachar. 1999. Small synthetic peptides homologous to segments of the first external loop of occludin impair tight junction resealing. *J Membr Biol.* 168: 289-97.

Larue L, Ohsugi M, Hirchenhain and Kemler R, 1994. E-cadherin null mutant embryos fail to form a trophectoderm epithelium. *Proc.Natl.Acad.Sci, USA.* **91:**8263-8267.

Latham K E, Solter D and Schultz R M, 1992. Acquisition of a transcriptionally permissive state during the 1-cell stage of mouse embryos. *Dev.Biol* **149:**457-462.

Latham, K. E., R. M. Schultz. 2001. Embryonic genome activation. *Front Biosci.* 6: D748-59.

Le TL, Yap AS and Stow JL 1999. Recycling of E-cadherin: a potential mechanism for regulating cadherin dynamics. *J.Cell Biol.* **146:**219-232.

Le TL, Joseph S R, Yap A S and Stow J L, 2002. Protein kinase C regulates endocytosis and recycling of E-cadherin. *Am J Physiol Cell Physiol.* **283:**C489-C499.

Lechner F, Sahrbacher U, Frei K, Brockhaus M, Koedel U and Fontana A, 2000. Antibodies to the junctional adhesion molecule cause disruption of endothelial cells and do not prevent leukocyte influx into meninges after viral or bacterial infection. *J.Infect Dis.* **182:**978-982.

Lehtonen E, Ordonez G and Reima I, 1988. Cytoskeleton in preimplantation mouse development. *Cell Differentiation* **24:**165-178.

Levy J, Goodall H and Maro B, 1986. The timing of compaction: control of a major developmental transition in mouse early embryogenesis. *J.Embryol.Exp.Morphol.* **95:**213-237.

Lin Y, Nusrat A, Schnell FJ, Reaves TA, Walsh S, Pochet M and Pawson T, 2000. A mammalian Par-3 – Par-6 complex implicated in Cdc/Rac1 and aPKC signalling and cell polarity. *Nature cell Biol.* **2:**540-547.

Liu Y, Nusrat A, Schnell J F, Reaves T A, Walsh S, Pochet M and Parkos C, 2000. Human junction adhesion molecule regulates tight junction resealing in epithelia. *J.Cell.Sci.* **113:**2363-2374.

MacPhee D J, Holstead Jones D, Barr K J, Betts D H, Watson A J and Kidder G M, 2000. Differential involvement of Na^+, K^+ -ATPase Isozymes in Preimplantation development of the mouse. *Dev.Biol* **222:**486-498.

Madara, J. L., R. Moore, S. Carlson. 1987. Alteration of intestinal tight junction structure and permeability by cytoskeletal contraction. *Am J Physiol.* 253: C854-61.

Magnuson, T., J. B. Jacobson, C. W. Stackpole. 1978. Relationship between intercellular permeability and junction organization in the preimplantation mouse embryo. *Dev Biol.* 67: 214-24.

Maine, E. M. 2001. RNAi As a tool for understanding germline development in Caenorhabditis elegans: uses and cautions. *Dev Biol.* 239: 177-89.

Mandai K, Nakanishi A, Satoh A, Obaishi H, Walda M, Nishioka H, Itoh M, Mizoguchi A, Aoki T, Fujimoto T, Matsuda Y, Tsukita S, Takai Y, 1997. Afadin: Anovel actin filament binding-protein in with one PDZ domain localised at cadherin-based cell-cell adherens junction. *J.Cell.Biol.* 139:1061.

Manejwala and Schultz, 1989. Blastocoel expansion in the preimplantation mouse embryo: stimulation of sodium uptake by camp and possible involvement of camp-dependent protein kinase. *Dev.Biol* **136:**560-563.

Manejwala F M, Cragoe E J and Schultz R M, 1989. Blasotocoel expansion in the preimplantation embryo: role of extracellular sodium and chloride and possible apical routes of their entry. *Dev.Biol.* **133:**210-220.

Maro B, Johnson M H, Pickering S J and Louvard D, 1985. Changes in the distribution of membranous organelles during mouse early development. *IJ.Embryol.exp.Morph.* **90:**287-309.

Martinez-Palomo A, Meza I, Beaty G and Cereijido M, 1980.Experimental modulation of occluding junctions in a cultured transporting epithelium. *J.Cell.Biol.* **87:**736-745.

Martìn-Padura I, Lostaglio S, Schneemann M, Williams L, Romano M, Fruscella P, Panzeri C, Stoppacciaro A, Ruco L, Villa A, Simmons D and Elisabetta D, 1998. Junctional Adhesion Molecule, a novel member of the immunoglobulin superfamily that distributes at intercellular junctions and modulates monocyte transmigration. *J.Cell.Biol.* **142:**117-127.

Marzesco AM, Galli T, Louvard D, Zahraoui A, 1998. The rod cGMP phosphodiesterase delta subunit dissociates the small GTPase Rab13 from membranes. *J Biol Chem.* **273:**22340-22345.

Matsuyoshi N, Hamaguchi M, Taniguchi S, Nagafuchi A, Tsukita S, Takeichi M, 1992. Cadherin-mediated cell-cell adhesion is perturbed by v-src tyrosine phosphorylation in metastatic fibroblasts. *J Cell Biol.* **118:**703-14.

Matter K and Balda S, 1998. Biogenesis of tight junctions: the C-termina domain of occludin mediate basolateral targeting. *J.Cell.Sci.* **111:**511-519.

McCarthy K M, Skare I B, Stankewich M C, Furuse M and Tsukita Sh, Rogers R A, Lynch R D and Schneeberger E , 1996. Occludin is a functional component of the tight junction. *J.Cell.Sci.* **109:**2287-2298.

Mercer, R. W., D. Biemesderfer, D. P. Bliss, Jr., J. H. Collins, B. Forbush, 3rd. 1993. Molecular cloning and immunological characterization of the gamma polypeptide, a small protein associated with the Na,K-ATPase. J Cell Biol. 121: 579-86.

Merzdorf C S and Goodenough D A, 1997. Localisation of a novel 210 kDa protein in Xenopus tight junctions. *J.Cell.Sci.* **110:**1005-1012.

Merzdorf CS, Chen YH, Goodenough DA, 1998. Formation of functional tight junctions in Xenopus embryos. *Dev Biol.* **195:**187-203.

Morita K, Furuse M, Fujimoto K and Tsukita Sh, 1999. Claudin multigene family encoding four-transmembrane domain protein components of tight junction strands. *Proc.Natl.Acad. Sci.* USA. **96:**511-516.

Muller W A, Ratti C M, McDonnell S L and Cohn Z A, 1989.A human endothelial cell-restricted, externally disposed plasmalemal protein enriched in intercellular migration of leukocytes. *J.Exp.Med,* **170:**399-414.

Muller W A, Weigl S A, Deng X and Phillips D M, 1993. PECAM-1 Is required for Transendothelial Migration of Leukocytes. *J.Exp.Med.***178:**449-460.

Mumby SM, Casey PJ, Gilman AG, Gutowski S, Sternweis PC, 1990. G protein gamma subunits contain a 20-carbon isoprenoid. *Proc Natl Acad Sci U S A.* **87:**5873-7.

Nagafuchi A and Takeichi M, 1988. Cell binding function of E-cadherin is regulated by the cytoplasmic domain. *EMBO J* **7:**3679-3684.

Nakamura T, Bierchman J, Trada S, Rozouskaia T, Itoyama T, Bullrich F, Mazo A, Croce CM, Geiger B and Canaani E, 2000. huASH1 protein, a putative transcription factor encoded by a human homologue of the *Drosophila* ash1 gene, localises to both nuclei and cell-cell tight junctions. *Proc Nat Acad Sc U S A.* **97:**7284-7289.

Nicolson, G. L., R. Yanagimachi, H. Yanagimachi. 1975. Ultrastructural localization of lectin-binding sites on the zonae pellucidae and plasma membranes of mammalian eggs. J Cell Biol. 66: 263-74.

Nishikura, K. 2001. A short primer on RNAi: RNA-directed RNA polymerase acts as a key catalyst. *Cell.* 107: 415-8.

Nishimura M, Kakizaki M, Ono Y, Morimoto K, Takeuchi M, Inoue Y, Imai T and Takai Y, 2002. JEAP: A novel component of tight junctions in exocrine cells. *J.Biol.Chem.* **277:**5583-5587.

Novick P, Zerial M, 1997. The diversity of Rab proteins in vesicle transport. *Curr Opin Cell Biol.* **9:**496-504.

O'Sullivan D M, Johnson M H and McConnell, J.M.L, 1993. Staurosporine advances interblastomeric flattening of the mouse embryo. *Zygote* **1:**103-112.

Offenberg H, Barcroft L C, Caveney A, Viuff D, Thomsen P D and Watson A J, 2000. mRNAs encoding aquaporins are present during mouse preimplantation development. *Mol Rrepod.Dev.* **57:**323-330.

Ohsugi M, Hwang S Y, Bultz S, Knowles B B, Solter D and Kemler R, 1996. Expression and cell-membrane localization of catenins during mouse preimplantation development. *Dev.Dyn* **206:**391-402.

Ohsugi M, Butz S, Kemler R, 1999. β-catenin is major tyrosine-phosphorylated protein during mouse oocyte maturation and preimplantation development. *Dev.Dyn.* **216:**168-176.

Ohto H, Maeda H, Shibata Y, Chen R, Ozaki Y Higashihara M, Takeuchi A and Tohyama H, 1985. A novel leukocyte differentiation antigen: two monoclonal antibodies TM2 and TM3 define a 120 Kd molecule present on neutrophils, monocytes, platelets and activated lymphoblasts. *Blood* **66:**873-881.

Overduin M, Harvey TS, Bagby S, Tong KI, Yau P, Takeichi M, Ikura M, 1995. Solution structure of the epithelial cadherin domain responsible for selective cell

adhesion. *Science* **267:**386-389.

Ozaki H, Ishii K, Arai H, Horiuchi H, Kawamoto T, Suzuki H, Kita T, 2000. Junctional adhesion molecule (JAM) is phosphorylated by protein kinase C upon platelet activation. *Biochem Biophys Res Commun.* **276:**873-8.

Ozaki H, Ishii K, Horiuchi H, Arai H, Kawamoto, T, Okawa K, Iwamatsu A, Kita T, 1999. Combined treatment of TNF-α causes redistribution of junctional adhersion molecule in IFN-γ causes redistribution of junctional adhesion molecule in human endothelial cells. *J.Immmunol.* **163:**553-557.

Ozawa M, Baribault H and Kemler R, 1989. The cytoplasmic domain of cell adhesion molecule uvomorulin associates with three independent proteins structurally related in different species. *EMBO J.* **87:**4246-4250.

Palmer D, van Zante A, Huang C, Hemmerich S, and Rosen S D, 2000. Vascular Endothelial Junction-associated Molecule, a novel Member of the Immunoglobulin Superfamily, Is Localized to intercellular Boundaries of Endothelial Cells. *J.Biol.Chem.* **275:**19139-19145.

Pantaleon, M., M. B. Harvey, W. S. Pascoe, D. E. James, P. L. Kaye. 1997. Glucose transporter GLUT3: ontogeny, targeting, and role in the mouse blastocyst. Proc Natl Acad Sci U S A. 94: 3795-800.

Pantaleon, M., P. L. Kaye. 1998. Glucose transporters in preimplantation development. Rev Reprod. 3: 77-81.

Papaioannou V E, 1982. Lineage analysi of inner cell mass and trophectoderm using microsurgically reconstituted mouse blastocysts. *J.Embryol.exp.Morph* **68:**199-209.

Paria, B. C., H. Tsukamura, S. K. Dey. 1991. Epidermal growth factor-specific protein tyrosine phosphorylation in preimplantation embryo development. Biol Reprod. 45: 711-8.

Parrington, J., S. Brind, H. De Smedt, R. Gangeswaran, F. A. Lai, R. Wojcikiewicz, J. Carroll. 1998. Expression of inositol 1,4,5-trisphosphate receptors in mouse oocytes and early embryos: the type I isoform is upregulated in oocytes and downregulated after fertilization. Dev Biol. 203: 451-61.

Parrish, S., J. Fleenor, S. Xu, C. Mello, A. Fire. 2000. Functional anatomy of a dsRNA trigger: differential requirement for the two trigger strands in RNA interference. Mol Cell. 6: 1077-87.

Pauken C M and Capco D G, 1999. Regulation of cell adhesion during embryonic compaction of mammalian embryos: roles for PKC and β-catenin. *Mol.Reprod.Dev.***54:**135-144.

Pauken, C. M., D. G. Capco. 2000. The expression and stage-specific localization of protein kinase C isotypes during mouse preimplantation development. Dev Biol. 223: 411-21.

Paynton B V, Rempel R and Bachvarova R, 1988. Changes in state of adenylation and time course degredation of maternal mRNAs during oocyte maturation and early embryonic development in the mouse. *Dev.Biol.* **129:**304-314.

Pederson R A, Wu, K and Balakier H, 1986. Origin of the inner cell mass in mouse embryos: cell lineage analysis by microinjection. *Dev Biol* **117:**581-595.

Peifer M, McCrea PD, Green KJ, Wieschaus E, Gumbiner BM, 1992. The vertebrate adhesive junction proteins beta-catenin and plakoglobin and the Drosophila segment polarity gene armadillo form a multigene family with similar properties. *J Cell Biol.* **118:**681-91

Peifer, M. 1997. Beta-catenin as oncogene: the smoking gun. Science. 275: 1752-3.

Peifer, M., P. Polakis. 2000. Wnt signaling in oncogenesis and embryogenesis--a look outside the nucleus. Science. 287: 1606-9.

Pemble L B and Kaye P L, 1986. Whole protein uptake and metabolism by mouse blastocysts. *J.Reprod.Fert* **78:**149-157.

Peyeriéas N, Hyafil F, Louvard D, Ploegh H and Jacob F, 1983. Uvomorulin: A nonintegral membrane protein of early mouse embryo. *Proc.Natl.Acad.Sci.USA.***80:**6274-6277.

Piko, L., K. B. Clegg. 1982. Quantitative changes in total RNA, total poly(A), and ribosomes in early mouse embryos. Dev Biol. 89: 362-78.

Prasad R, Gu Y, Alder H, Nukamura T, Canaani O, Saito H, Huebner K, Gale R P, Nowell P C and Kuriyama K, 1993.Cloning of the ALL-1 fusion partner, the AF-6 gene, involved in acute myeloid leukemias with the T(6 11) chromosome-translocation. *Cancer Res* **53:**5624-5628.

Pratt H P M , 1985. Membrane organisatioon in the mouse preimplantation embryo. *J.Embryol.Exp.Morph.* **90:**101-121.

Qiu, R. G., A. Abo, G. Steven Martin. 2000. A human homolog of the C. elegans polarity determinant Par-6 links Rac and Cdc42 to PKCzeta signaling and cell transformation. *Curr Biol.* 10: 697-707.

Ranscht, 1994. Cadherins and catenins: interactions and functions in embryonic development. *Curr Opin Cell Biol.* **6:**740-6.

Reeve W J D and Kelly F, 1983. Nuclear position in cells of the early mouse embryo. *J.Embryo.exp.Morphol.* **75:**117-139.

Reeve W J D, 1981. Cytoplasmic polarity develops at compaction in rat and mouse embros.*J.Embryol.exp.Morph.* **62:**351-367.

Ridley, A. J. 1995. Rho-related proteins: actin cytoskeleton and cell cycle. *Curr Opin Genet Dev.* 5: 24-30.

Ridley, A. J., P. M. Comoglio, A. Hall. 1995. Regulation of scatter factor/hepatocyte growth factor responses by Ras, Rac, and Rho in MDCK cells. *Mol Cell Biol.* 15: 1110-22.

Riethmacher D, Brinkmann V and Birchmeier C, 1995. A targeted mutation in the mouse E-cadherin gene results in defective preimplantation development. *Proc.Natl.Acad.Sci USA.* **92:**855-859.

Rimm DL, Koslov ER, Kebriaei P, Cianci CD, Morrow JS, 1995. Alpha 1(E)-catenin is an actin-binding and -bundling protein mediating the attachment of F-actin to the membrane adhesion complex.*Proc Natl Acad Sci U S A.* **92:**8813-8817.

Rossant J, Vijh K M Siracusa L D and Chapman V M, 1983. Identification of embryonic cell linages in histological sections of M.musculus - M.caroli chimaeras. *J.Embryol.expMorph* **73:**179-191.

Rothstein, J. L., D. Johnson, J. A. DeLoia, J. Skowronski, D. Solter, B. Knowles. 1992. Gene expression during preimplantation mouse development. *Genes Dev.* 6: 1190-201.

Rubenfeld B, Souza B, Albert I, Muller O, Chamberlain S H, Masiart F R, Munemitsu S and Polarkis P, 1993. Association of the APC gene-product with beta-catenin. *Science* **262:**1731-1734.

Ruiz P, Brinkmann V, Ledermann B, Behrend M, Grund C, Thalhammer C, Vogel F, Birchmeier C, Gunthert U, Franke WW, Birchmeier W, 1996. Targeted mutation of plakoglobin in mice reveals essential functions of desmosomes in the embryonic heart. *J Cell Biol.* **135:**215-225.

Saberwal, G., R. Nagaraj. 1994. Cell-lytic and antibacterial peptides that act by perturbing the barrier function of membranes: facets of their conformational features, structure-function correlations and membrane-perturbing abilities. Biochim Biophys Acta. 1197: 109-31.

Saitou M, Fujimoto K, Doi Y Itoh M, Furuse M Takano H Noda T and Tsukita Sh, 1998. Occludin-deficient embryonic stem cells can differentiate into polarised epithelial cells bearing tight junctions. *J.Cell.Biol.* **141:**397-408.

Saitou M, Furuse M, Sasaki H, Schulzke Jörg-Dieter, Fromm M, Takano H, Noda T and Tsukita Sh, 2000. Complex phenotype of mice lacking occludin, a component of tight junction strands. *Mol.Biol.Cell.* **11:**4134-4142.

Sakakibara A, Furuse M, Saitou M, Ando-Akatsuka and Tsukita S, 1997. Possible involvement of phoshorylation of occludin in tight junction formation. *J.Cell.Biol.* **137:**1393-1401.

Satoh H, Zhong Y, Isomura H, Saitoh M, Enomoto K, Sawada N, Mori M, 1996. Localisation of 7H6 tight-junction associated antigen along the cell border of vascular endothelial cells correlates with paracellular barrier function against ions, large molecules, and cancer cells. *Exp.Cell.Res.* **222:**269-274.

Saunders C M, Larmen M G, Parrington J, Cox L J. Royse J, Blayney L M, Swam K and Lai F A, 2002. PLCζ: a sperm-specific trigger of Ca2+ oscillations in egg and embryo development. *Development* **129:**3533-3544.

Schultz R M, 1993. Regulation of zygotic gene activation in the mouse. *Bioessay* **15:**531-538.

Sefton M, Johnson M H and Clayton L, 1992. Synthesis and phosphorylation of uvomorulin during mouse early development. *Dev.***115:**313-318.

Sefton M, Johnson M H, Clayton L and McConnell J M, 1996. Experimental manipulations of compaction and their effects on the phosphorylation of uvomorulin. *Mol.Reprod.Dev* **44:**77-87.

Shapiro L, Fannon A M, Kwong P D, Thompson, A, Lehmann M S, Grübel G, Legrand J, Als-Nielson J, Coleman D R and Hendrickson W A, 1995. Structural basis of cell-cell adhesion by cadherins. *Nature* **374:**327-336

Sheth B, Fesenko I, Collins J E, Moran B, Wild A E, Anderson J M and Fleming T P, 1997. Tight junction assembly during mouse blastocyst formation i.e. regulated by the expression of ZO-1 α^{+} isoform. *Dev.* **124:**2027-2037.

Sheth B, Fontaine JJ, Ponza E, McCallum A, Page A, Citi S, Louvard D, Zahraoui A, Fleming TP, 2000a. Differentiation of the epithelial apical junctional complex during mouse preimplantation development: a role for rab13 in the early maturation of the tight junction. *Mech Dev. 2000* **97:**93-104.

Sheth B, Moran B, Anderson JM, Fleming TP, 2000b. Post-translational control of occludin membrane assembly in mouse trophectoderm: a mechanism to regulate timing of tight junction biogenesis and blastocyst formation. *Development.* **127:**831-40.

Simon DB, Lu Y,Choate KA, Velazquez H, Al-Sabbon E, 1999.Paracellin-1, a renal tight junction protein required for paracellular Mg^{2+} resorption. *Science* **285:**103-106.

Simpson E H, Suffolk R and Jackson I J, 1999. Multi-PDZ domain protein 1 contains 13 PDZ domains in tandem. *Genomics* **59:**102-104

Sirotkin H, Morrow B, Saint-Jore B, Puech A, Das Bupta R, Patanjali S R Lkoultchi A, Weissman S M, Kucherlapati R, 1997. Identification , characterisation, and precise mapping of a human gene encoding a novel membrane-spanning protein from the 22q11 region deleted in velo-cardio-facial syndrome. *Genomics* **42:**245-251.

Slager H G, Good M J, Schaart G, Groenewoud J S and Mummery C L, 1992. Organisation of non-muscle myosin during early embryonic differentiation. *Differentiation* **50:**47-56.

Sobel J S, 1983. Localisation of myosin in the preimplantation mouse embryo. *Dev.Biol.***95:**227-231.

Sonada N, Furuse M, Sasaki H, Yonemura S, Katahira J, Horiguchi Y, 1999. *Clostridium perfringens* enterotoxin fragment removes specific claudins form tight junction strands: evidence for direct involvement of claudins in tight junction barrier. *J.Cell.Biol.* **147:**195-204.

Staehelin L A, 1973. Further observations of the fine structure of freeze-cleaved tight junctions. *J.Cell.Sci* **13:**763-766.

Steinberg MS, Takeichi M, 1994. Experimental specification of cell sorting, tissue spreading, and specific spatial patterning by quantitative differences in cadherin expression. *Proc.Natl.Acad.Sci.USA.* **91:**206-209.

Stevenson B R, Siliciano J D, Mooseker M S and Goodenough D A, 1986. Identification of ZO-1: a high molecular weight polypeptide associated with the tight junction (zonula occludens) in a variety of epithelia. *J.Cell.Biol* **103:**755-766.

Stevenson B, Anderson J M, Goodenough D A and Mooseker M S, 1988. Tight junction structure and ZO-1 content are identical in two strains of Madin-Darby canine kidney cells which differ in transepithelial resistance. *J.Cell.Biol.* **107:**2401-2408.

Stockinger H, Gadd SJ, Eher R, Majdic O, Schreiber W, Kasinrerk W, Strass, B, Schnabl E, Knapp W, 1990. Molecular characterisation and functional analysis of the leukocyte surface protein CD31. *J.immunol.* **145:**3889-3897.

Su L K, Vogelstein B and Kinzler K W, 1993. Association of the APC tumour-supressor protein with catenins. *Science* **262:**1734-1737.

Suzuki, A., T. Yamanaka, T. Hirose, N. Manabe, K. Mizuno, M. Shimizu, K. Akimoto, Y. Izumi, T. Ohnishi, S. Ohno. 2001. Atypical protein kinase C is involved in the evolutionarily conserved par protein complex and plays a critical role in establishing epithelia- specific junctional structures. *J.Cell Biol.* 152: 1183-96.

Svoboda, P., P. Stein, H. Hayashi, R. M. Schultz. 2000. Selective reduction of dormant maternal mRNAs in mouse oocytes by RNA interference. *Development.* 127: 4147-56.

Tanaka M, Hemebold J D, Mactarlone J and Adash CY, 2001. A mammalian oocyte-specific linker histone gene H1a, has homology with the genes for the oocyte-specific cleavage stage histone (CS-H1) of sea Urchin and the B4/HIM histone of the frog. *Dev.* **128:**655-644.

Takeichi M, 1977. Functional correlation between cell adhesive properties and some surface proteins. *J.Cell.Biol* **75:**464-474.

Takeichi M, 1988. The caderins: cell-cell adhesion molecules controlling animal morphogenesis. *Development* **102:**639-655.

Takeichi M, 1990. Cadherins: a molecular family important in selective cell-cell adhesion. *Annu Rev Biochem.* **59:**237-252.

Telford N A, Watson A J and Schultz G A, 1990. Transition from maternal to embryonic control in early mammalian development: A comparison of several species. *Mole Repod and Dev.* **26:**90-100.

Temeles G L, Ram P T, Rothenstein J L and Shultz R M, 1994. Expression patterns of novel genes during mouse preimplantation embryogenesis. *Mol. Reprod. Dev.***37:**121-129.

Tomich, J. M., D. Wallace, K. Henderson, K. E. Mitchell, G. Radke, R. Brandt, C. A. Ambler, A. J. Scott, J. Grantham, L. Sullivan, T. Iwamoto. 1998. Aqueous

solubilization of transmembrane peptide sequences with retention of membrane insertion and function. *Biophys J.* 74: 256-67.

Tong, Z-B, L. M. Nelson. 1999. A mouse gene encoding an oocyte antigen associated with autoimmune premature ovarian failure. *Endocrinology.* 140: 3720-6.

Tong Z-B, Gold L, Pfeifer K E, Dorward H, Lee E, Bondy C A, Dean J and Nelson L M, 2000. Mater, a maternal effect gene required for early embryonic development in mice. *Nature genetics* **26:**267-268.

Torres M, Stoykova A, Huber O, Chowdhury K, Bonaldo P. Mansouri A, Butz S, kemler R, Gruss P (1997). An α-E-catenin gene trap mutantation defines its function in preimplantation development. *Proc.Natl.Acad. Sci.USA.***94:**901-906.

Tsukita S, Oishi K, Akiyama T, Yamanashi Y, Yamamoto T and Tsukita S, 1991. Specific proto-oncogenic tyrosine kinase of src family are enriched in cell-cell adherens junctions where the level of tyrosine phosphorylation is elevated. *J.Cell.Biol.* **113:**867-879.

Tsukita Sh and Furuse M, 2000a. Pores in the wall:Claudins constitute tight junction strands containing aqueous pores. *J.Cell.Biol.* **149:**13-16.

Tsukita, S., M. Furuse. 2000b. The structure and function of claudins, cell adhesion molecules at tight junctions. *Ann N Y Acad Sci.* 915: 129-35

Tsukita, S., M. Furuse, M. Itoh. 2001. Multifunctional strands in tight junctions. *Nat Rev Mol Cell Biol.* 2: 285-93.

Turksen, K., T. C. Troy. 2001. Claudin-6: a novel tight junction molecule is developmentally regulated in mouse embryonic epithelium. *Dev Dyn.* 222: 292-300.

Ullmer, C., K. Schmuck, A. Figge, H. Lubbert. 1998. Cloning and characterization of MUPP1, a novel PDZ domain protein. *FEBS Lett.* 424: 63-8.

Van Blerkom J, 1981. Structural relationship and posttranslational modification of stage-specific proteins synthesized during early preimplantation development in the mouse. *Proc.Natl.Acad..Sci.USA.* ***78:***7629-7633.

Vaporciyan A A, Delisser, H M Yan, Mendiguren I L, Thom S R, Jones M L, Ward P A and Albelda S M, 1993. Involvement of platelet endothelial celladhesion molecule-1 In neutrophil resruitment *in vivo*. *Science* **262:**1580-1582.

Vestweber D, Gossler A, Boller K and Kemler R, 1987. Expression and distribution of cell adhesion molecule uvomorulin in mouse preimplantation embryos. *Dev.Biol* **124:**451-456

Vietor, I., T. Bader, K. Paiha, L. A. Huber. 2001. Perturbation of the tight junction permeability barrier by occludin loop peptides activates beta-catenin/TCF/LEF-mediated transcription. EMBO Rep. 2: 306-12.

Volk, T., B. Geiger. 1984. A 135-kd membrane protein of intercellular adherens junctions. Embo J. 3: 2249-60.

Vorbrodt A, Konwinski M, Solter D and Koprowski H, 1977. Ultrstructural cytochemistry of membrane-bound phosphatases in preimplantation mouse embryos. *Dev.Biol* **55:**117-134.

Wahl JK, Sacco PA, McGranahan-Sadler TM, Sauppe LM, Wheelock MJ, Johnson KR, 1996. Plakoglobin domains that define its association with the desmosomal cadherins and the classical cadherins: identification of unique and shared domains.*J Cell Sci.* **109:**1143-54.

Wakelin MW, Sanz MJ, Dewar A, Albelda SM, Larkin SW, Boughton-Smith N, Williams TJ, Nourshargh S, 1996. An anti-platelet-endothelial cell adhesion molecule-1 antibody inhibits leukocyte extravasation from mesenteric microvessels in vivo by blocking the passage through the basement membrane. *J Exp Med* **184:**229-

39.

Watson A J and Kidder G M, 1988. Immunoflourescence assessment of the timing of appearance and cellular distribution of Na/K-ATPase during mouse embryogenesis. *Dev.Biol* **126:**80-90.

Watson A J, Pape C, Emanuel J R, Levenson R and Kidder G M, 1990. Expression of Na/K-ATPase α and β subunit genes during preimplantatin development of the mouse. *Dev.Genetics.* **11:**4-48.

Watson, A. J., L. C. Barcroft. 2001. Regulation of blastocyst formation. Front Biosci. 6: D708-30.

Whittingham D G, 1974. Fertilization, early development and storage of mammalian ova *in vitro*. In Balis, AE Wild (eds): "The early development of mammals". British Society for Developmental Biology Symposium, **Vol 2:**1-24. Cambridge: Cambridge University Press.

Wianny F and Zernika-Goetz M, 1999. Specific interference with gene function by double-stranded RNA in early mouse development. *Nature Cell Biol.* **2:**70-75.

Wiekowski M, Miranda M and DePamphilis M L, 1991. Regulation of gene expression in preimplantation mouse embryos; effects of the zygotic clock and the first mitosis on promoter and enhancer activities. *Dev.Biol* **147:**403-414.

Wieschaus E, Nusslein-Volhard C and Jugens G, 1984. Mutations affecting the pattern of the larval cuticle in *Drosophila melanogaster III.* Zygotic loci on the x-chromosome and fourth chromosome *Roux's Arch Dev Biol.* **193:**296-307.

Wiley L M, 1984. Cavitation in the mouse preimplanation embryo: Na/K – ATPase and the origin of nascent blastocoele fluid. *Dev.Biol* **105:**330-342.

Williams L A, Martin-Padura I, Dejana E, Hogg N and Simmons, 1999. Identification and characterisation of human junctional adhesion molecule (JAM). *Molecular immunology* **36:**1175-1188.

Willott E, Balda MS, Heintzelman M, Jameson B, Anderson JM, 1992. Localization and differential expression of two isoforms of the tight junction protein ZO-1. *Am J Physiol.* 262:C1119-1124.

Winkel G K, Ferguson J E, Takeichi M and Nuccitelli R, 1990. Activation of protein kinase C triggers premature compaction in the 4-cell stage mouse embryo. *Dev.Biol* **138:**1-15

Witcher LL, Collins R, Puttagunta S, Mechanic SE, Munson M, Gumbiner B, Cowin P, 1996. Desmosomal cadherin binding domains of plakoglobin. *J Biol Chem* **271:**10904-10909.

Wittchen, E. S., J. Haskins, B. R. Stevenson. 1999. Protein interactions at the tight junction. Actin has multiple binding partners, and ZO-1 forms independent complexes with ZO-2 and ZO-3. *J Biol Chem.* 274: 35179-85.

Wong V and B M Gumbiner, 1997. A synthetic peptide corresponding to the extracellular domain of occludin perturbs the tight junction permeability barrier. *J.Cell.Biol.* **136:**399-409.

Wong, V. 1997. Phosphorylation of occludin correlates with occludin localization and function at the tight junction. *Am J Physiol.* 273: C1859-67.

Wrenzycki, C., D. Herrmann, J. W. Carnwath, H. Niemann. 1998. Expression of RNA from developmentally important genes in preimplantation bovine embryos produced in TCM supplemented with BSA. *J Reprod Fertil.* 112: 387-98.

Wu X, Hepner K, Castelino-Prabhu S, Do D, Kaye M B, Yuan X J, Wood J, Ross C, Sawyers C L and Whang Y E, 2000. Evidence for regulation of the PTEN

tumour suppressor by a membrane-localised multi-PDZ domain containing scaffold protein. MAGI-2. *Proc Nat Achad Sci U S A.* **97:**4233-4238.

Wu Y, Dowbenko D, Spencer S, Laura R, Lee J, Gu O and Lasky L A, 2000. Interaction of tumour suppressor PTEN/MMAC with PDZ domain MAGI 3, a novel membrane associated guanylate kinase. *Journal Biol Chem.* **275:**21477-21485.

Yamamoto T, Harada N, Kano K, Taya S, canaani E, Matsuura Y, Mizoguchi A, Ide C and Kaibuchi K, 1997. The ras target AF-6 interacts with ZO-1 and serves as a peripheral component of tight junctions in epithelial cells. *J.Cell.Biol.* **139:**785-795.

Yamanaka, T., Y. Horikoshi, A. Suzuki, Y. Sugiyama, K. Kitamura, R. Maniwa, Y. Nagai, A. Yamashita, T. Hirose, H. Ishikawa, S. Ohno. 2001. PAR-6 regulates aPKC activity in a novel way and mediates cell-cell contact-induced formation of the epithelial junctional complex. *Genes Cells.* 6: 721-31.

Yap, A. S., W. M. Brieher, B. M. Gumbiner. 1997. Molecular and functional analysis of cadherin-based adherens junctions. *Annu Rev Cell Dev Biol.* 13: 119-46

Yap, A. S., W. M. Brieher, M. Pruschy, B. M. Gumbiner. 1997. Lateral clustering of the adhesive ectodomain: a fundamental determinant of cadherin function. *Curr Biol.* 7: 308-15.

Yokoya, F., N. Imamoto, T. Tachibana, Y. Yoneda. 1999. beta-catenin can be transported into the nucleus in a Ran-unassisted manner. *Mol Biol Cell.* 10: 1119-31.

Yonemura, S., M. Itoh, A. Nagafuchi, S. Tsukita. 1995. Cell-to-cell adherens junction formation and actin filament organization: similarities and differences between non-polarized fibroblasts and polarized epithelial cells. *J Cell Sci.* 108: 127-42.

Yoshida, C., M. Takeichi. 1982. Teratocarcinoma cell adhesion: identification of a cell-surface protein involved in calcium-dependent cell aggregation. *Cell.* 28: 217-24.

Zahraoui A, Joberty G, Arpin M, Fontaine J J, Hellio R, Tavitian A and Louvard D, 1994. A small rab GTPase is distributed in cytoplasmic vesicles in non polarised cells but colocalizes with the tight junction marker ZO-1 in polarised epithelial cells. *J.Cell.Biol.* **124:**101-115.

Zamore, P. D., T. Tuschl, P. A. Sharp, D. P. Bartel. 2000. RNAi: double-stranded RNA directs the ATP-dependent cleavage of mRNA at 21 to 23 nucleotide intervals. *Cell.* 101: 25-33.

Zhong Y, Enomoto K, Isomura H, Sawada N, Minase T, Oyamadaa M, Konishi Y and Mori M, 1994. Localisation of the 7H6 antigen at tight junctions correlates with the paracellualar barrier function of MDCK cells. *Exp.Cell.Res.* **214:**614-620.

Zhong Y, Saitoh T, Takashi M, Sawada N, Enomoto K and Mori M, 1993. Monoclonal antibody 7H6 reacts with a novel tight junction-associated protein distinct from ZO-1, cingulin and ZO-2. *J.Cell.Biol.* **120:**477-483.

Zhurinsky J, Shutman M and Ben-Ze'ev A, 2000. Plakoglobin and β-catenin: protein interactions, regulation and biological roles. *J cell Sci.* **113:**3127-3139.

Ziomek C A, Johnson M H and Handyside A H, 1982. The developmental potential of mouse 16-cell blastomeres. *J.Exp.Zool* **221:**345-355.